DETERMINISTIC AND STOCHASTIC MODELING OF CLINICAL AND NON-CLINICAL DYNAMICS OF HIV-HBV CO-INFECTION WITH OPTIMALITY

MIRGICHAN KHOBOCHA JAMES

A Thesis Submitted in Partial Fulfillment of Requirements for

Conferment of the Degree of Doctor of Philosophy in Mathematics

of Meru University of Science and Technology

2025

DECLARATION

This thesis is my original work and has not been presented for a degree in any other institution.

SC502/201386/20

Mirgichan Khobocha James

Signed ..... Date .....

This thesis has been presented with our authority as University Supervisors.

Signed ..... Date .....

Dr. Stephen Karanja, Ph.D

Meru University of Science and Technology, Kenya

Signed ..... Date .....

Dr. Cyrus Gitonga Ngari, Ph.D

Kirinyaga University, Kenya

Signed ..... Date .....

Dr. Robert Muriungi, Ph.D

Meru University of Science and Technology, Kenya

DEDICATION

To my dear wife Naomi Naminkin Nadesol.

To my sons; Jotham Hirlewa Mirgichan and Hanniel Kulmicha Mirgichan.

To my loving mum Elizabeth Leken Mirgichan.

ACKNOWLEDGMENT

First of all, I would like to express my deep appreciation to my family for their constant encouragement, inspiration, and support for the three years of education. Their sacrifice for time and finances have been valuable. They had all the confidence in my capability to complete my studies. I extend my sincere appreciation to my supervisors Dr.Stephen Karanja, Dr.Cyrus Ngari and Dr. Robert Muriungi for their wise direction, steadfast support and timely feedback during thesis write up. Their positive and constructive criticism have always enriched my research work. Their availability have been unconditional. Their commitment to this research work has been amazing. We have established good network and relations during this time. In addition, I express my gratitude to the faculty members of School of Pure and Applied Sciences and the academic staff of the Mathematics department for their moral support, encouragement and inputs to this research. Their positive and productive motivation has led me to conclude my research in time.

Furthermore, the academic journey would not have been what it is today if not for the co-operation of colleagues in the program and the invaluable discussions that we made. Employing their opinions and views has added great contributions, which helped to shape this thesis. I also give credit to my colleague teachers at Ruiga Girls Secondary school in Meru County for their moral support, understanding and tolerance during this research endeavor. Finally, my gratitude to the Higher Education Loans Board (HELB) for the scholarship that facilitated payment of my tuition fees. Not forgetting my friends who have stood with me in one way or the other in support of my studies.

TABLE OF CONTENTS

LIST OF TABLES

LIST OF FIGURES

LIST OF ABBREVIATIONS

Abbreviation	Definition
AHB	Acute Hepatitis B
AIDS	Acquired Immunodeficiency Syndrome
ART	Antiretroviral Therapy
BETA	Bottom-Up Economic Transformation Agenda xiv
cART	Combination Antiretroviral Therapy
CD4	Clusters of Differentiation 4
CFE	Co-infection Free Equilibrium
CHB	Chronic Hepatitis B
CTMC	Continuous Time Markov chain
CTL	Cytotoxic T Lymphocytes
DAA	Direct-Acting Antiviral
DNA	Deoxyribonucleic Acid
EFV	Efavirenz
HCV	Hepatitis C virus
HDV	Hepatitis Delta virus
HBeAg	Hepatitis B e Antigen
HBV	Hepatitis B virus
HIV	Human Immunodeficiency Virus
MTCT	Mother To Child Transmission
NACC	National AIDS Control Council
NGM	Next Generation Matrix
NVP	Nevirapine
PEP	Post-Exposure Prophylaxis
PLWHA	People Living With HIV/AIDS
PMP	Pontryagin's Maximum Principle
PRCC	Pearson Rank correlation coefficient
PrEP	Pre-Exposure Prophylaxis
RNA	Ribonucleic Acid
SDEs	Stochastic Differential Equations
SDGs	Sustainable Development Goals
SEI	Susceptible-Exposed Infectious
SI	Susceptible-Infectious
SIR	Susceptible-Infectious-Recovered
SIS	Susceptible-Infectious-Susceptible
SIRS	Susceptible-Infectious-Recovered-Susceptible
STI	Sexually Transmitted Infection
SSA	Sub-Saharan Africa
TB	Tuberculosis
UHC	Universal Health Coverage
UNAIDS	Joint United Nations Programme on HIV/AIDS
VCT	Voluntary Counseling and Testing
WHO	World Health Organization

OPERATIONAL DEFINITIONS OF TERMS

Term	Definition
Basic reproduction number	The number of infections that an index case is expected to cause in a population that is vulnerable.
Bifurcation theory	The change of steady state of a system when the parameters are varied.
Clinical intervention	Any procedure, practice or action designed to result to a health related outcome directed to the patient.
Co-infection	Two or more viruses or pathogen species invading a host at the same time. Co-infections may exist in various forms; co-infections by similar species or pathogens, co-infections by distinct species or even multiple infections.
Co-infection-Free Equilibrium Point	The solution to the differential equation system if the population as a whole is considered to be vulnerable and the disease is absent.
Control reproduction number	The mean number of contacts each case generates in the presence of interventions such as immunization, treatment, and public health interventions.
Drug Efficacy	A measure of the efficiency of a drug. When the efficacy is 0% then it is ineffective but when it reaches 100% then it means it is ideal.
Endemic	An epidemic disease which resides in the population for at least 10 to 20 years.
Endemic equilibrium point	The solution to the differential equation system when the infection is prevalent in the population. The result that begins in the interval $(0,k)$ and remains there forever.
Epidemiology	The study of rates, risks and changes in occurrence and characteristics of health events and states in specific population and the utilization of the findings to reduce and eliminate health disorders.
Force of infection	The rate of infection per unit of time among vulnerable people.
HIV-HBV co-infection	An infection with both HIV and HBV.
Infectious disease	An illness in which people contract pathogen micro-organisms, including bacteria, fungi, viruses, or other micro-parasites.

Term	Definition
Mathematica	A computational mathematical software that is commonly applied in numerous mathematical, scientific, engineering and computing disciplines.
Mathematical model	A mathematical abstraction and set of equations used to describe a physical occurrence.
MATLAB	A modern language for technical computing which is the building block of matrices.
Non-clinical intervention	Practices that do not necessarily provide any type of medical care, treatment, or testing to the patient.
Optimal control	An approach in mathematical sciences that comes from the calculus of variations.
Prevalence	The proportion of infected people in a certain population.
Sample path	A set of time-ordered data that explain the events of a single stochastic process.
Screening	Testing those who are not known to be at a higher risk of contracting HBV.
Stochastic process	A probability model representing the probable sample path that is comprised of a set of time-ordered random variables.
Susceptible population	Percentage of the population that is not yet infected but might get infected.
The law of Mass action	It assumes that the infection rate, β is proportional to the product of susceptible and infected individuals, $S * I$ (Kolokolnikov & Iron, 2021).
Vaccinated population	Percentage of the susceptible population that has had an HBV vaccination and is not infected with HBV but is nonetheless at a reduced risk of getting the virus.
Wiener process	A continuous-time stochastic process that has several important properties, including being Markovian, Gaussian, and having independent and stationary increments.

ABSTRACT

HIV and HBV infections are viral infections with the same route of transmission through sexual intercourse with an infected person and mother-to-child transmission among other means of transmission. Over the decades, these mono infections have led to the deaths of millions of people around the world despite increased access to prevention, diagnosis, treatment, and care. Yet, there have been no conclusive findings in the hunt for HIV/AIDS cure or vaccine. However, the hepatitis B vaccine is available, though not easily accessible. Consequently, HIV and HBV co-infection is equally a major global health burden that has attracted limited research interest. The interactions and synergistic relationship between these viruses are not well understood and documented. The co-infection presents complex transmission dynamics within a population. Few mathematical models of HIV and HBV co-infection are available that include risk factors and control measures. The effect of variability in predicting infection outcomes is also not captured in deterministic models. In addition, optimality conditions in co-infection models are not explored. This study sought to model HIV and HBV co-infection with optimal control interventions. This study set out to develop and examine a deterministic model of HIV-HBV co-infection, formulate an optimal control problem for the deterministic model and determine the optimal controls and finally convert the deterministic model into a stochastic model that accounts for variability and uncertainties in infection outcomes. The deterministic model formulation is based on SI and SIRS epidemic model framework. The theories of calculus are applied to analyze the deterministic model based on reproduction numbers. The threshold parameter; the basic and control reproduction number is obtained using the Jacobian NGM and survival function approaches. Co-infection-free and endemic equilibrium points are determined and it's local and global stability analysis established using Routh-Hurwitz criterion and Metzler matrix method respectively. The local sensitivity analysis of the model parameters on R_0 and A_0 are determined by use of forward normalized sensitivity index method. Using Pontryagin's Maximum Principle, an optimal control problem is formulated. The stochastic model is developed by extending the deterministic model using SDEs. The three models are implemented using MATLAB solver based on Runge-Kutta and Euler-Maruyama numerical schemes. The normalized sensitivity analysis of model parameters showed that co-infection transmission rate, β_4 and recruitment rate, π contribute the highest to R_0 and A_0. Numerical simulations of deterministic model revealed that the combined effect of clinical and non-clinical control interventions led to the reduction in infection rates with time. The effect of HIV and HBV viral loads on infection progression pointed out that the progression is faster at high levels of viral loads. Further, numerical results of optimal controls exhibited a gradual decrease in co-infection of HIV-HBV. The sample paths of SDEs showed variations in infection outcomes due to random noise transmission. Thus, this study recommends that focus should be directed towards reducing co-infection rate and vertical transmission to mitigate the co-infection, while reinforcing policies relating to both clinical and non-clinical control interventions at optimal conditions.

CHAPTER ONE: INTRODUCTION

1.1 Background Information

The co-infection of HIV and HBV is a frequent and severe infection because of overlapping modes of infection. It results in an accelerated progression of liver disease and needs combined, well co-ordinated antiretroviral therapy to keep both of the viruses at bay.

Deterministic models are employed in the cognition of the typical, anticipatory performance of the epidemic of a vast population, like that of HIV-HBV co-infection. They facilitate locating equilibrium points, challenge control mechanism at a population stage as well as give smooth, continuous framework on applying mathematical approaches of optimal control theory. Stochastic models are the ones that basically integrate randomness and probability which is important to model dynamics of small population or at the beginning of an epidemic. They have a robust ability to compute the probability of the disease extinction by itself, ability to accommodate heterogeneity as well as uncertainty and authenticate the finding of determinism through thousands of simulations. Deterministic model can give the outcome and determine the theoretically optimal method of population-wide control, whereas in stochastic models information about uncertainties and risks is given.

The control of a dynamic system by means of a combination of both models is combined with optimal control techniques to determine the most efficient method of controlling an enterprise, taking into consideration of cost constraints. Both models presented in conjunction with an optimal control strategy offer a broad approach evaluation, thus enabling the public health personnel to ensure they develop more robust, efficient and practical public health policies in order to deal with the obstructing problem of HIV-HBV co-infection.

1.1.1 HIV natural history and its epidemiology

HIV is a Ribonucleic Acid (RNA) virus that attacks the clusters of differentiation 4 (CD4) cells and makes the host progressively unhealthy over a period of time. In the process, all the white blood cells get destroyed thus making the immunity of a person to become weak against opportunistic infections such as Tuberculosis (TB), fungal infection, severe bacterial infection, STIs and some cancers. HIV exists as two strains: HIV 1 and HIV 2, HIV 1

is the most common in human beings. HIV 1 has been seen to be the most deadly virus by causing many fatalities. However, HIV 2 has also been discovered to cause Acquired Immunodeficiency Syndrome(AIDS) (Lasisi, 2020). There are three clinical stages of HIV; acute infection, asymptomatic or latency and AIDS stage. The first few weeks of infection are referred to as the acute stage, and the subsequent month or so is known as the latency stage. AIDS, the final stage of HIV infection is defined by the development of certain cancers, infections or other severe long-term clinical manifestations. Individuals that develop AIDS go through the successive stages of the HIV virus infection. The virus infection progresses with weakening the immune system and may culminate in the advanced and final stage of the HIV infection (R. Anderson, Medley, May, & Johnson, 1986). Depending on each person's immune system, this might take up to three years to happen if left untreated. The virus symptoms include; frequent coughing, skin infections, chronic illnesses and diarrhoea. HIV causes HIV infection and is transmitted primarily from human to human through; engaging in unprotected sexual activities with an infected individual, getting exposed to infected blood or blood products or receiving organ transplant of an infected mother, HIV-positive individuals exchanging syringes or needles, receiving infected blood transfusions or organ transplants, during pregnancy, birth, or breastfeeding.

HIV is a heterogeneous retrovirus that is capable of converting RNA to DNA and containing a viral enzyme reverse transcriptase. A human body has approximately 800-1000 CD4 T-cells$/\text{mm}^3$. When the CD4 T cell count reaches or falls below 200 cells $/\text{mm}^3$, an individual could possibly be diagnosed with AIDS. The CD4 count goes down with viral load increase levels and there is no evidence that this can generate a strong immune reaction. This further weakens the response from CTL and antibodies cannot be able to deal with the infection (Nowak & May, 1992). The CD4 cells count for the non-reacted and uninfected individuals is around $500 - 1500\text{cells}/\text{mm}^3$ of blood and slowly changes if the drugs are not consistently being taken or if the treatment is not professionalized.

The World Health Organization (WHO) advises people that are susceptible to HIV infection to seek for effective therapies in addition to testing and counseling services. HIV diagnosis and testing is done using simple and affordable rapid diagnostic tests as well

as self confidentially, counseling, correct results and reference to treatment and other services. Following a diagnosis, people with HIV must receive care and get prescription to ART as soon as possible and get periodically monitored by the use of medical and laboratory parameters, which include the check to degree the viral load. If ART is taken continuously, this treatment prevents HIV transmission to others. Further, ART improves health, prolongs life, and substantially reduces the viral load. However, a large number of HIV-positive individuals continue to pass away from AIDS, in part due to not taking their medications. Early therapy starts to inhibit the HIV, which lowers the chance that HIV will advance to AIDS. Early treatment of HIV infected individuals with ARV medicines lowers the viral load levels while life of the infected person is prolonged (Ho, 1995). As the most successful approach to combating the HIV/AIDS epidemic, prevention and control are currently being prioritized in non-clinical interventions including public health campaigns against new infections (Nannyonga, Mugisha, & Luboobi, 2011). Mukandavire, Gumel, Garira, and Tchuenche (2009) studied the effectiveness of condoms in combating HIV/AIDS infection and pointed out key nonclinical prevention and control interventions such as abstinence, commitment to a single sexual partner, and regular, appropriate condom usage and practicing male circumcision among others.

UNAIDS report of 2023, reported that globally by the end of 2023, 85.6 million people were HIV positive, 40.4 million people had died from AIDS-related diseases, and 86% of people living with HIV recognized their status. In 2022, 630,000 individuals lost their lives to AIDS related illnesses, and about 39 million people were HIV positive. Those under ART were reported as 29.8 million people proportionately consisting of 77% of adults who were 15 years and above, 57% of children aged $0-14$ years, 82% of women aged 15 years and older, 72% of men aged 15 years and older and 82% of pregnant women and out of this about 21 million have been averted. However, 9.2 million people had no access to ART. Further, from the report 1.3 million people contributed to new infections by the end of 2022. Women and girls between the ages of 15 and 24 made up 46% of the population worldwide, with Sub-Saharan Africa (SSA) having the largest percentage at 77% among this age group. Moreover, according to World Health Organization (2022), there were an

anticipated 37.7 million HIV-positive individuals worldwide, with the WHO African Region housing two thirds of those individuals (25.6 million). In 2021, 1.5 million new cases of HIV infection and 650000 deaths from HIV-related causes were reported. According to the data, Africa had the largest proportion of HIV/AIDS-positive people worldwide. According to the 2020 global estimates, there were about 1.5 million patients who had developed the first symptoms of the HIV infection and 680,000 people had died from the disease. New HIV infections had reduced worldwide by the year 2020 by 39% as compared to the year 2010, which was still short of the UN General Assembly's 75% reduction commitment in 2016. According to a research by Bert et al. (2018), more than 90% of people in SSA acquired HIV from unprotected sexual intercourse with HIV-positive partners. HIV services have over time been competed by unexpected pressures on public health systems, for instance measures that were put in place to combat the spread of COVID-19 have postponed and stalled other health targets (Sachs, Kroll, Lafortune, Fuller, & Woelm, 2022).

The NACC Kenya report for 2021 and 2022 states that despite efforts to lower its frequency, the HIV prevalence rate has remained startlingly high. One million three hundred and forty thousand Kenyans, or 4.8% of the country's population, are PLWHA, according to the research. From 5.9% in 2016, this rate has decreased dramatically and is still declining. A large number of initiatives that addressed HIV education, VCT nationwide, and ARV uptake are partially the reason for this decline. Most notably, Homa Bay County has the highest prevalence rate of 19.6%, while Garissa county has the lowest incidences of HIV/AIDS, with a rate of 0.01%. Additionally, 4.5% and 5.2% of men and women, respectively, are infected with HIV. The survey also showed that HIV prevalence is high at Kenyan universities (Owusu-Ansah et al., 2023).

HIV/AIDS has lived with the human population for five decades since it was identified in 1984 and remains one of the deadliest and most incurable infections in the world at the moment (Beyrer, 2021). It continues to be a major epidemic in the world, with the death toll at 40.1 million. However, there remains a very high demand for comprehensive HIV and AIDS management and also for treating opportunistic infections. AIDS has become

a chronic condition and People Living With HIV/AIDS (PLWHA) now require lifelong medication that enables them to live a normal, healthy and long life. This medication overburdens them as it is on daily use. So far, there exists no functional cure for HIV/AIDS. Clinical trials in search for cure for HIV/AIDS are still ongoing and no conclusive results have been realized. There exists disparities in implementing prevention, control and care for HIV/AIDS pandemic across the globe with countries forging efforts towards ending HIV/AIDS by the end of 2030. The attitude, knowledge, perception, treatment and viral load suppression of HIV/AIDS have increased substantially among the populations at risk.

1.1.2 Hepatitis B virus natural history and its epidemiology

Hepatitis B Virus (HBV) belongs to a class of hepatitis viruses which attacks the liver. Hepatitis *B* infection lasts for at least six months, for persons with compromised natural immunity after which the infection becomes chronic. Even though their symptoms are severe, the majority of adults with hepatitis B recover fully. Hepatitis B continued infection is a big risk especially in infants and children. Infectious particles containing the HBV can penetrate the skin and mucous membranes of another individual and thereby transmit the disease. Blood, seminal, or vaginal fluids infected with the virus can cause an infection in another person. With a possible half-life of seven days, the virus is moderately infectious. The following are ways that hepatitis B is spread: having multiple sexual partners, using a syringe contaminated with the virus, and having unprotected sexual intercourse with an infected person through the vaginal, anal or oral route. Additionally, during pregnancy, childbirth, or even breastfeeding, an infected woman might vertically transfer the hepatitis B virus to her foetus (*Global Hepatitis report 2022*, n.d.).

If left untreated, it usually does not have any specific symptoms in adults and lasts for several months. If the chronic infection is not promptly treated and adequate care is not given, children and adults may easily get severe illness and experience liver complications or even die. HBV infection is hard to fight for all generations. Hepatitis *B* vaccines are administered to babies and also to people who are vulnerable to the infection. Many individuals have been found to have hepatitis B, yet the symptoms are not usually obvious. They go unnoticed if no symptoms are seen until two or three months after infection. The

virus can still be transmitted at acute or asymptomatic stage. Acute infection shows symptoms similar to influenza such as; fatigue, fever, joint or muscle pain, general weakness or nausea, weight loss, loss of appetite, vomiting, diarrhoea, jaundice, dark brown urine, pale clay-colored stools. After six months individuals with acute infection progresses to chronic hepatitis *B* infection stage. These include children aged below five years, expectant mothers and people with immune deficient systems such as AIDS patients. Individuals suffering from chronic hepatitis B are more vulnerable to liver cancer, liver conditions, and liver failure.

Chevaliez, Roudot-Thoraval, Hezode, Pawlotsky, and Njouom (2021) emphasized that a rapid sample blood test should be carried out to show whether one has the virus or not. Liver function test may also be carried to check if the liver is damaged. A Hepatitis viral load test is also a crucial step for early treatment, but is expensive and takes a lot of time. It is advisable that even if one does not show symptoms a test should be done. One should also be tested for other STIs if infected with hepatitis B. Getting tested for and treating a hepatitis B infection is extremely crucial for someone who has had several sexual partners. The duration of the viral infection determines the treatment to administer on the patient with hepatitis B. An acute hepatitis B patient most often begins to recover in one to two months, but there are no specific treatments. If a patient experiences symptoms, then it is most likely to be treated at home, with enough rest and medicine where necessary. Thus, acute hepatitis B in the majority of cases is resolved by the phenomenon of natural immunity. Chronic hepatitis *B* requires a lifetime treatment, thus it is suggested that an individual who develops persistent hepatitis B, needs to receive treatment in order to manage a number of the signs and symptoms. This will further reduce the chance of unfavorable liver damage and delay the progression to liver cancer. The treatment only regulates the virus by putting it under control without curing the condition. Having STI tests regularly is the best control intervention for good sexual health. For people with many sexual partners, it is crucial to use condoms and get tested regularly, in the absence of any symptoms. Use of shared and unsafe injectables such as needles, razors and syringes or other items that may contaminate blood should be avoided. Body piercing, tattoos and acupuncture do not

transmit hepatitis *B* infection if new and sterile needles are used. Receiving hepatitis *B* vaccination is a protective intervention for individuals at risk of HBV infection (*Global Hepatitis report 2022*, n.d.).

Hepatitis B is a scary liver infection which can be fatal. It is an infection that lies on the silent level and, unfortunately, is one of the greatest global health problems. Chronic infection can be a constant threat and along with the risk of liver cancer and liver cirrhosis remains high. Almost 3000 people die from hepatitis B every day and almost 90% of people with viral hepatitis are unaware that they have it. The Eastern Mediterranean WHO region has the highest incidence of hepatitis B infection, with 60 million persons infected, followed by the South-East Asia WHO region (18 million), the European WHO region (14 million), and the American WHO region (5 million). Based on eligibility requirements and location, WHO estimated in 2021 that 12% to 25% of people with chronic hepatitis B infection could require treatment (*Global Hepatitis report 2022*, n.d.).

Abbas and Abbas (2021) estimated the number of individuals who contracted hepatitis B which was about 257 million people worldwide. It is also true that out of thousand, only 10% of them knew their condition. The primary reasons for the infection being transmitted from mother to child, is through nosocomial transmission, and in the course of sexual contact. Working towards the health improvement of the millions of people who are living in this state of ignorance should be a world-wide concern. HBV needs longer-term antiviral care, but it is not obvious to identify patients in need of treatment; therefore, it is difficult to develop such kind of protocol. To decrease the chance of contracting HBV infection during pregnancy, pregnant women should be tested and begin ART if the virus is reactive, from week 28 of pregnancy.

The plan of the elimination programme must include the following: implementation of birth dosage and neonatal immunization, monitoring of individuals at high risk following vaccination, catch-up vaccination, and carrier registration. WHO therefore gives a guideline that programs with a continuum of care are necessary to ensure there's a provision of prevention modalities (screening, treatment and referral). The program should be integrated with the existing local health care services and also incorporate HBV testing and

treatment services. According to WHO, establishing a proper ambiance, creating awareness, getting over the social stigma and screening those who are at a risk and treating those infected should be the goal too. A holistic policy on this which incorporates capacity development, funding and implementation strategies is favorable. The reduction strategies would complement the national elimination efforts. In addition, it is advised that the guidelines for diagnosis and treatment of patients infected by HBV are streamlined. Monitoring has to be done to track progress and to determine how much elimination program reduces the incidence and the death from the disease, and whether the gaps in the treatment/ care have been addressed.

As per the study by World Health Organization and others (2021), HBV contamination is considered a primary public health burden causing great harm all over the world. The WHO estimated that 296 million people were positive with chronic HBV, and 78,200 people died from HBV infection in 2021. Worldwide, the mortality resulting from chronic viral hepatitis has become higher than that caused by HIV, TB, and malaria together. Thus, the World Health Organization has stated their intention to eliminate chronic hepatitis B and C by the end of the 2030. The actual prevalence of chronic Hepatitis B infection among PLWHA is unknown because of intermittent HBV screening and monitoring that is prevalent in many parts of the world (Kim, 2020). In Kenya information on prevalence of HBV is poorly documented and majority of research has been dedicated to special groups such as blood donors and people living with HIV, therefore it is possible that the samples are not a good representation of population at large. Other studies have rigorous inclusion criteria, which means that the significant demographics groups are not taken into account. HBV testing is not among the list of common tests in hospitals, not even those for screening program for pregnant women. According to the Kenyan Ministry of Health, the triple hepatitis vaccine at the age of six weeks with each dose being delivered according to the WHO Expanded Programme for Immunization (EPI) is recommended as part of the national immunization programme. On the other hand, the ministry does not currently recommend the monovalent Hepatitis B vaccine at birth, because they think that the transmission of the virus in early life in Kenya is horizontal rather than vertical, and therefore the birth

dose vaccine will not provide any significant advantage over the vaccination that will be started at six weeks. Nevertheless, more of data should be gathered to justify the basis of legislation for this infection (Downs et al., 2022).

1.1.3 HIV and HBV co-infections

The dual activity of an infection is when the patient lives with two distinct or similar infections.The co-infections present complexities in their transmission, treatment and control. The cost of treatment of a co-infected patient is expected to be high and at the same time it becomes difficult for the medical practitioners to decide on the medication. The co-infection weakens much more, the immune status of a co-infected individual as compared to that of a mono-infected individual. Consequently, the co-infected patients' morbidity and fatality rate rise. For this reason, attention should be given to developing novel strategies in curbing this menace. Multiple infections are investigated in terms of their effect on the host's well-being and due to the possibility of changing the selective pressures upon pathogens.

Co-infections that commonly occur alongside HIV include respiratory illnesses that cause serious complications. In addition to causing serious disease on their own, co-infections or the medicines to treat them may interact with HIV or HIV medicines. The medications used in the treatment of the co-infections or the co-infections themselves are capable of having an interaction with HIV or the HIV medications other than the fact that they are so dangerous on their own. Moreover, HIV-positive status may increase one's vulnerability to concurrent infections, and conversely, some infections may in some situations augment HIV infection rates. The paper by World Health Organization and others (2017), examined the immuno-pathogenesis of the five most common infectious diseases; TB, cryptococcosis, HBV, HCV, and malaria that continue to significantly increase morbidity and death among individuals living with HIV worldwide.

A fatal global disease that receives less attention is hepatitis C. Prussing et al. (2015) projected that 399,000 people around the globe succumb to diseases related to HCV co-infection affects approximately 71 million people. Liver illnesses are a leading source of illness and mortality among PLWHA, accounting for about 2.3 million of the estimated

36.7 million persons living with HIV worldwide who are currently or have previously been infected with hepatitis C virus (HCV). Studies on distribution of viral hepatitis show that a minimum of 7 million individuals living with HIV have HCV or had contracted it at some point in time. In the two WHO's Southeast Asian and Western Pacific regions, 13.3 million people meet the criteria for HCV. Some of the highest co-infection rates of HIV-HCV are recorded in Eastern Europe and the Central Asian Region. While over 95% of patients with HCV infection can be cured using the new DAA medicines, there are many patients who have no reasonable access to these drugs.

HBV is another common co-infection that is quite notable among PLWHA. Approximately 2.7 million people of the global population were co-infected with HIV and HBV in 2015, and approximately 257 million individuals globally had chronic HBV infection. The WHO Western Pacific region had both the highest prevalence rate and the biggest population of HBV carriers overall. Indeed vaccination against HBV is very important for those who are suffering from HIV/AIDS. However, the utility of the hepatitis B vaccination could be affected by immunological suppression that is caused by HIV infection; which reduces the protective antibody response. And so, after organism overall rehabilitation, it might be necessary to re-vaccinate (World Health Organization and others, 2017). Cervical or anal cancer development is associated with HPV and this is a frequent co-infection among HIV positive patients. Thus, it may be said that patients with HIV are more likely to have persistent HPV infections and acquire these cancers than people who are HIV-negative. Even though HPV vaccines have been developed, barriers exist toward their use in the WHO Western Pacific region.

According to Bruchfeld, Correia-Neves, and Källenius (2015), another prevalent co-infection that leads to one of the main causes of mortality for PLWHA globally is TB. WHO approximates suggest that, compared to the rest of the population, HIV-positive individuals have a 16-27 fold risk of acquiring tuberculosis(TB). The infection in its latent form has a high chance of turning into active illnesses among people with weakened immune systems due to poorly controlled HIV. To create novel approaches for the best possible treatment and prevention, it is essential to comprehend the intricate relationships that exist between HIV,

these co-infections, and the host immune system. Despite the increasing availability of cART, HIV contributed, nearly 1.5 million deaths in 2010. The immunodeficiency as a result of persistent HIV contamination increases the danger of co-infection with pathogens which might be controllable some of which can be controlled by phagocytic antibody responses, through both innate and adaptive cell immunological responses. Furthermore, it is typically not possible to return the pathogen-specific immune response to normal levels while managing cART in the context of HIV co-infection (World Health Organization and others, 2017).

The complexity of overseeing the treatment of a patient infected with HBV increases in a variety of unique circumstances. Primary care physicians are in the best position to identify and address these circumstances, as well as to coordinate treatment and refer patients to specialized services in order to optimize the health and well-being of those with chronic HBV. Global public health is seriously threatened by the HBV shared pathways of transmission with HIV, HCV, and hepatitis D viruses (HDV). Depending on the endemicity of HBV and HDV as well as the primary means of transmission of HIV and HCV, the incidence of co-infections varies greatly around the world. After a suitable pre-test conversation, testing for the existence of all these co-infections should be made available to all CHB patients. Every virus modifies the CHB infection's normal course and makes treatment strategies more challenging. Due to the complexity of co-infection management, collaborative care with a specialist physician is typically necessary (Kourtis, Bulterys, Hu, & Jamieson, 2012).

HDV is a virus that causes inflammation of the liver, and the type of hepatitis is caused by the HDV which depends on the HBV in order to replicate. In individuals who have chronic infection of HBV, the prevalence is close to 5 percent, but populations that are at risk of co-infection include indigenous populations, those that receive the withdrawal of haemodialysis and those that use drugs. Chronic HDV infection is also taken as the worst chronic viral hepatitis as it develops very fast as well as leads to death of the liver including hepatocellular carcinoma. HDV has been determined to be carcinogenic to human beings in the same category as hepatitis B and C. An estimate published in 2020 suggests that

close to 5 percent of worldwide individuals, with a persistent infection of HBV, are living with HDV, and co-infection may contribute to an estimated one in every five cases of liver disease and liver cancer in individuals with an HBV infection. HDV co-infection can be prevented by vaccination to HBV, and the spread of HBV immunization in childhood has led to reduction of hepatitis D in most of the world. Simultaneous infection of HDV with HBV can cause the symptoms causing mild-to-severe hepatitis, with full recovery occurring as a rule, and development of chronic hepatitis D symptoms being a rare case (World Health Organization, 2024).

HDV has been an issue of serious concern and its diagnostics and treatment are not an easy issue because of its low supply and unstandardized nature. Pegylated interferon 3 alpha (PEG-IFN3 alpha) is the only form of treatment, but this has been limited because it does not work well and has undesirable side effects. Nevertheless, novel drugs such as Bulevirtide have demonstrated good performance. The hepatitis B treatments with nucleoside analogues have not directly resulted in the control of HDV. The services should aim at preventing the HBV transmission by HBV immunization such as birth doses, antiviral prophylaxis on pregnant women, blood safety, injection safety, and harm reduction services. The Global Health Sector Strategies (GHSS) 2022-2030 developed by the WHO directs the health sector in carrying out strategic responses to end AIDS, hepatitis, and sexually transmitted infections by 2030. In 2024 the WHO has published revised guidance on the prevention, diagnosis, care, and treatment of all individuals with chronic hepatitis B infection, as well as official guidance on tests and confirmatory diagnosis.

HIV and HBV are contagious blood borne viruses that are transmitted from one individual to another by semen, blood or other liquid secretions. Beside these, the primary route of HIV and HBV are similar. These include, for example, having sex without a condom and injected drug use, among others. According to research by Zaongo, Ouyang, Chen, Jiao, and Wu (2022), between 10% and 28% of HIV-positive individuals also carry the HBV virus. The cases of HBV infections among HIV infected people around the world is reported to be around 7.4%. Since 2015 WHO has recommended treatment for all those who are diagnosed with HIV infection, whether in the early or the late stage. One of

the medications in the combination regimen recommended as the first-line treatment for HIV infection, tenofovir, is also effective against HBV. Chronic Hepatitis B (CHB) disease should be conducted to a known positively co-infected patient applied during appropriate pre-test discussion. Patients prone to constant comorbidity of co-infection can be referred for repeat screening especially when their conditions worsen.

HCV co-infected patients should be given the opportunity to be receive DAA therapy and the requirement for HBV treatment should be re-evaluated before HCV therapy is started. Consequently, there is need for close monitoring of HBV-infected patients not receiving the antiviral therapy in parallel to DAA therapy. Taking into account the fact that co-infection takes much longer and may predispose patients to worse health states in case of the worsening of either of the infections. Any patient who is undergoing a significant immune suppression needs to be tested for HBV infection as the virus can reactivate and the associated flare of hepatitis can be fatal. While administering HBV vaccine to all people susceptible to HIV goes against Centre for Disease control (CDC) recommendation, this explanation clarifies that CDC supports HBV vaccination of all people with HIV to prevent HBV infection in them (Schillie et al., 2018).

1.1.4 Optimal control strategies

Several clinical and non-clinical control measures to curb HIV and HBV mono-infections are in use. These measures include but are not limited to abstinence, condom promotion and use, health education and campaigns, Voluntary counseling and testing (VCT), use of treatment such Anti-retroviral (ArVs), Pre-exposure prophylaxis (PreP), Post-exposure prophylaxis (PEP), and vaccination among others (Radix, Gonzalez, & Hoffmann, 2022). Despite the benefits realized from these measures, it is important to design the best optimal control strategy that will arrest the co-existence between these viral infections.

An optimal control model is therefore necessary to study the interaction between these viruses. Thus, if a mathematical model for a certain system is developed, there are several approaches to determine the best control. For instance using Pontryagin's maximum

principle one is able to find out the optimal control given some constraint for a model system of general differential equations. Gaff and Schaefer (2009) discovered variations of Pontryagin's maximum principle for several model types, such as partial differential and difference equations. Utilizing these techniques on illness models yields significant results and useful insights into the most effective ways to lower the burden of disease. To determine the optimal vaccination schedule that balances the cost of the vaccine and the cost of the disease burden, for instance, a mathematical model of the specific disease can be utilized (Hethcote, 1988). Determining the disease's epidemic structure is one of the first steps in employing optimum surveillance to recommend intervention methods for a particular condition.

Control is co-ordinated in a dynamic system to accomplish a goal in optimal control problems. State variables and control restrictions are included in the fundamental optimum control issue. Differential equations that rely on the control variables are satisfied by the state variables. The differential equation's solution varies as the control function does. Therefore, the relationship between control and state is expressed as a mapping of control variables and state variables. State variables are functions of independent variables. Finding a piecewise continuous control, $u(t)$ and the matching state variable, $x(t)$ to maximize or minimize a given objective function is the primary goal of an optimal control problem. The underlying system may hold a wide range of equations such as; discrete, stochastic, integral difference, partial, and ordinary differential equations. Lenhart and Workman (2007) emphasized the use of an optimal control theory is a very powerful form of mathematics to make decision making in complex biological settings. Neilan and Lenhart (2010) stated that modeling the situation using an ODE system, choosing the form and bounds of control, building the corresponding objective function, and proving the existence of optimal

control are the fundamental steps in setting up and solving an optimal control problem. We demonstrate, derive the required conditions for optimal control, characterize optimal control, and compute optimal control numerically.

In addition, there may also be a desire to demonstrate the uniqueness of optimal control. The analysis of the changes of the optimal control depending on the model parameters is necessary. We must first understand how the parameters affect the uncontrolled model and then consider the control case. Stochastic optimum control issues arise when systems defined by Stochastic Differential Equations (SDEs) are taken into consideration using the optimal control theory. Enhancing system performance through the determination of the best control and stochastic parameter values is the goal of optimal stochastic control issues. Most control theories result in the computation of time derivatives; a feature that stochastic processes do not conform with regular calculus. This makes the stochastic optimal control problem a difficult problem to solve. This means that it is necessary to utilize techniques that would enable one to differentiate and integrate stochastic processes using the Ito's lemma (Dixit, Dixit, & Pindyck, 1994).

Simulations allow us to find theoretically optimal vaccination strategies. The age groups that should receive vaccinations first in order to reduce expenditures or death during an influenza pandemic were determined by Longini Jr, Ackerman, and Elveback (1978) using an epidemic model. The ideal age for measles immunization was determined by Hethcote (1988) using a modeling technique. These findings primarily mean that to mine the ideal age for vaccination, more precise data on age-specific vaccine efficacy are required. Thus, the use of epidemiological modeling can help determine what information should be gathered.

1.1.5 Deterministic and stochastic models

The frequent use of epidemic models to analyze HIV and HBV mono-infection and its dynamics has long been appreciated. Numerous research studies have been done on the transmission of HIV / AIDS infection and Hepatitis B at both population and in-host scales (Shahriar et al., 2022). Since reality is complex, certain assumptions are postulated to develop a model from a real life phenomenon. Models are built on various premises; the question a model tries to answer or the problem it seeks to address. Generally, mathematical models are classified as deterministic or stochastic (Martcheva, 2015). Deterministic models do not contain any elements of randomness, uncertainty and chance in detecting future conditions of the system. They merely explain the average tendency of an infection and possibilities are not taken into account estimates and average results are obtained based on initial conditions. Deterministic models are applicable to large populations. To formulate them, ordinary differential equations are employed. However, stochastic models include randomness, having uncontrolled data with uncertainties and variations. They generate a wide range of results based on the actual values of the random variables. Stochastic models are applicable for small populations and are more realistic compared to deterministic models.

Mathematical models have been applied extensively in many areas of science ad technology across the natural sciences and the social sciences. One of the essential areas is the use of the approaches in the mathematical description of complex systems and, in particular, living things. Actual experiments sometimes cannot be carried out on live subjects for some practical reasons such as the complexity of the organism or for the lack of some equipment in certain situations. This type of experiment is normally of a chronic nature, raises a lot of funds, and is highly susceptible to ethical concerns. The concepts of mathematical models include some characteristic features of the described phenomena and estimate the potential development of the processes without actual experiments(Kapur, 2023).

In contrast to the modeling of physico-mechanical systems, it is necessary to point out the specifics of the difference between living and the dead matter for scientists who work

with biological systems. As is known, the concern of systems, which concern inert matter, can be analyzed by using the invariance principles and the conservation laws and the interaction of their constituent components obeys the laws of Newton or quantum mechanics. On the other hand, these laws cannot be applied for living organisms in the same way as above considerations. Due to the kind of existence that living things have and in an attempt to survive they have a high internal differentiation. They feed, resuscitate, in order to fend off pests and predators, and, essentially, many transformations of substances and energy occur. From the perspective of several centuries when organisms have been learning, while adjusting to various circumstances, such adaptation has been elaborated which makes possible altering the ways of operation of the structural components with subsequent reproduction or elimination according to these circumstances. Several diseases including- Cancer, Infectious diseases, auto-immune diseases, Cardiovascular diseases, Neuro-degenerative diseases and several more have been described using mathematical models (Brauer, Castillo-Chavez, & Feng, 2019).

Mathematical modeling facilitates the comprehension of real-world issues, their formulation into mathematical models, and the interpretation of the results in relation to the real world. Creating a mathematical model is the process of mathematical modeling. It is a system interpretation made possible by a variety of packages and notions. History demonstrates that the use of mathematics in biology dates back to the 12th century (Vinothini & Kavitha, 2020). In the study of biology, mathematical modeling develops into an interdisciplinary field that learns about both biology and mathematics. These days, research is favouring trans-disciplinary and interdisciplinary studies. Mathematical modeling is now used in different areas of medicine, dynamics, population biology, ecology, bio-statistics, and molecular biology. In biology, botanists, zoologists, and chemists along with mathematicians build up models of a definite structure. Modeling can be easily understood when done in forms of diagrams. Thus, the use of modeling in research assists in enhancing understanding of the role of outstanding factors in different biological activities and occurrences, like various diseases in medicine, the reform of existing and appearance of new medications, treatment regimens, hospital technology, and successful health care manage-

ment system. The advancement of computing techniques and mathematical theories may be influenced by the uses of mathematical models in biology and medicine (Banerjee, 2021).

Epidemiological classical models in a way base most of their frameworks on the assumption that every individual within the prevailing population has the same susceptibility to an infection and probability of passing it on to other beings. Nevertheless, these assumptions are not always realistic for directly transmitted infectious diseases which exhibit a high level of variability in percentage of infection. According to classical epidemiological models, within a particular population, there exists several kinds of individuals: susceptible (S), exposed (E), infected (I), and recovered (R). The people are segregated into partitions or sections commonly referred to as compartments depending on their level of infection or diseases. Among the most widely used classical models are; SIR, SIRS, SI, SIS and SEI. The SI model represents illnesses for which infection with the disease does not confer immunity, whereas the SIR model represents illnesses for which infection with the disease confers immunity.

The epidemics models are done for the diseases that persists for a very short time while models for an endemic situation are done with a view of looking at the implications of 'herd immunity' on vaccination of specific disease (Hethcote & Levin, 1989). The above mentioned classical epidemic models are subject to further extension or alteration to incorporate demographic aspects of the populations, or both the pharmaceutical and non-pharmaceutical interventions. For this reason, these models differ from one disease or infection to another. Furthermore, deterministic or stochastic processes are used for building mathematical models. There is no randomness in a deterministic model, people get solutions that is an average, there is no room for one possibility or the other. Ordinary differential equations are utilized to formulate the deterministic models. On the other hand, stochastic models, which are created using SDEs and CTMC among other methods, permit unpredictability.

The methods employed by pathogens and host organisms are complex; the interactions between the micro-organisms that attack cells, and the bodily defense systems of the host,

can be primary where both the infectious agents are in the cell or extracellular wherein each of the infectious agents provokes immunological or inflammatory response. According to Derouin et al. (1998) numerous studies have demonstrated the advantageous impact of co-infections; many studies of bacterial, protozoal, and fungal infections have been done to prove multiple infection models, proving that infection by one germ may be protective against a second pathogen. In other cases, protective immunity or a close match to other bacterial antigens would provide the protection. This paves the path for the delivery of vaccines utilizing non-virulent organisms, or hetero-immunization. On another occasion, the protection can come from related or unrelated organisms, indicating that the non-specific immunity might also be implicated. Although co-infection models with viruses have proven to be very useful for researching the patho-physiology of opportunistic infections and how they interact with the development of a viral disease, few pharmacological applications have been developed to assess the efficacy of drugs that target the virus or the pathogen in order to prevent illness. The primary goal for the development of the models for acute and chronic co-infections was to research treatment approaches to stop opportunistic infections. This strategy was considered to be appropriate with the occurrences of multiple diseases in individuals having a compromised immune system (especially HIV patients), effectiveness of certain drugs against different pathogens as well as the possibility that in vivo experiments better represent real clinical scenario as compared to the commonly used in vitro models.

Co-infection models introduce additional complexity by including a co-infected host class other than the mono infected classes. Previous studies have considered several mathematical models for HIV and HBV co-infections with multiple specific diseases such as ; HIV-TB co-infection model by Bruchfeld et al. (2015), HIV-Pneumonia co-infection model by Teklu and Mekonnen (2021), HIV/AIDS- COVID19 co-infection model by Ringa et al. (2022), HIV-malaria co-infection model by Amwata (2015), HIV-gonorrhea co-infection model by Mushayabasa, Tchuenche, Bhunu, and Ngarakana-Gwasira (2011) among many other studies that have focused modeling in this direction. The existing HBV co-infection models include HBV-HCV, HBV/HDV (Packer, Forde, Hews, & Kuang, 2014), TB/HBV

(Bowong & Kurths, 2010), HIV-HBV (Yusuf & Idisi, 2020). These models were developed and analyzed in the previous studies with different considerations.

The national and global health aspirations are envisaged in sustainable development goals (SDGs), Kenya Vision 2030, the Big Four Agenda, BETA and the Kenyan constitution. Among the SDG is goal No.3, that targets progress towards supporting the promotion of healthy lives and well-being for all, through prioritizing and working toward decreasing the burden of the total health expenditure to attain the necessary level of UHC. The approach followed was the global implementation of the 2030 Agenda for Sustainable Development; the assessment of this was provided by the SDG Report 2022, using the most updated estimations and data. While tracking regional and worldwide progress towards the 17 Goals, it has a breakdown of specific indicators for each Goal. According to the Report by Sachs et al. (2022), a range of closely connected and escalating issues pose a threat to the 2030 Agenda for Sustainable Development and human existence. The Report pays specific attention to the importance and extent of the issues societies and nations grapple with.

COVID-19, climate change, and conflicts are unfolding crises that impact all the SDG and have subsequent impacts on health, learning, food and nutrition, environment and peace and security. The report outlines how the gains of several years in several aspects of life such as in the provision of basic services, health and education, alleviation of hunger and poverty, among others were all undone. It also defines the sectors for which, by 2030, much needs to be done to preserve the Sustainable Development Goals and make the necessary changes for people and the environment's progress.

The SDG report by Sachs et al. (2022) indicated that COVID-19 pandemic is a persistent reality that affects people's health and increases barriers to reaching Goal No.3. Some of the improvements that had been observed before the pandemic affected overall health in reproductive, maternal, and child health; immunization coverage; and the treatment of communicable diseases, but they had massive inequalities across the regions. The COVID-19 outbreak significantly affected the fundamental health interventions, increased the prevalence of anxiety and depression, reduced global life expectancy, interrupted the fight against HIV, TB, and malaria and threatened universal health coverage, which was

promised to be achieved in 20 years. As a result, vaccination reach actually declined for the first time in 10 years, while the numbers of people perishing from malaria and tuberculosis went up. For a system shift towards the achievement of Goal 3, increased and collaborative efforts are needed in the shortest time possible.

The Kenya Vision 2030 is a long-term development strategic plan that seeks to alter the country's economic structure and status to middle income status by the year 2030. According to this vision, Kenya is to be a prosperous and competitively ranked country globally where citizens' quality of life is significantly enhanced. The above blueprint has been premised on three major factors that include; the economic, the social and the political factors. Projects of the development in the social pillar of the Vision are outlined for the nation's social change. Under the social pillar of the vision there is a noble quest of attaining a just and coherently developed society with emphasis on social sectors such as health care, education, water and environment, housing, youth sports and culture, gender, and youth. The extension of social services and the integration of society's most vulnerable segments will accomplish this. For instance, a suggestion is made to shift the paradigm of the development of the emphasis of the healthcare system which is primarily on preventive than on curative care. with focus on increasing utilization and reducing costs to the population particularly the most vulnerable.

The long term goal of the health sector for 2030 is to make quality healthcare more accessible to the general public. The first stage of this five-year medium range plan is to revitalize health centers, focusing more on preventive services than on curative ones. The sector also plans to decentralize more authorities and resources through direct funding of hospitals rather than district headquarters to reduce bureaucratic setbacks of government. This would also include a disconnection of the Ministry of health from from policy formulation rather than service provision. With an objective of increasing the efficiency of health care management through operationalizing decentralization at district, provincial and national levels to support institutions to offer quality health care. Also there is a proposed Social Health Insurance Fund (SHIF) so as to enhance equity in access to health for everybody. Some of the directional proposals will entail enacting of laws, and therefore, involving

parliament (Mwenzwa & Misati, 2014).

In a study on the challenges of the vision 2030 strategy implementation, Moyare (2012) acknowledged that the Kenya government has experienced several challenges. The study shows that one of the major areas of challenge was leadership since there was a lack of commitment and agreement on a common goal among the leaders who were steering the 2030 strategy plan. Organizational culture was recognized as a challenge as it has been associated with people's refusal to change their roles as assigned to them by the government during the part of the fine-tuning of vision 2030 strategy. The second focus was about the inadequacy of capital mobilization which could be attributed to the increase in cost of capital and the low trend of savings in the country. The study also found that were are three types of resources that had been a problem, namely financial, physical and human. Furthermore the analysis identified other difficulties such as the failure of creation of the public-private partnership which was intended to play a key role in financial mobilization, limited resources, lack of effective communication between stakeholders and lack of skills among civil servants in the community. Ultimately, the study showed a deficiency of the Kenyan Government in establishing reward and support channels for all the policymakers and practitioners who contribute to the implementation of Vision 2030 strategy.

The "Big Four Agenda", a Kenyan transformative agenda initiated in 2017, prioritized four main areas: for instance, investments in Universal Health Coverage (UHC) to enhance access to quality and affordable health care for all the citizens in Kenya; Quality and affordable housing; Food security to feed every citizen in Kenya and industrialization for adding value to its products; as well as to create job opportunities for the country's population by 2022 as emphasized by M. James (2019). This transformative agenda was meant to tackle the key challenges that Kenyans were facing and to provide the right environment that would foster growth of Socioeconomic development. With regard to health, intentions are made to finalize NHIF reforms, to increase the number of county's health facilities, and to improve the health professional training in order to develop the quality and affordability of the health care across the country. The government then had shown what seemed to be a very solid commitment in the last time allotted to the agenda of the so-called Big Four

reforms. However, the following problems soluble continue to arise which hampered the implementation of this strategy. Such issues as financial constraints, the lack of public knowledge concerning the Big Four and corruption, early campaigns in early 2022, and conflicts between the federal and the state governments were some of the issues that were discussed. A legislative push was launched in response to these difficulties to help realize the Big Four goal. A legislative foundation for ongoing health research was one of these, and it was developed through the National Research/Health Bill.

The Constitution of Kenya 2010 accords every citizen of Kenya the following economic and social rights; right to health care, education, right to food and right to a decent quality of life. The devolved county administration is in charge of a number of operations in the following areas: markets, county public works, water and sanitation services, early childhood education services, agriculture and health (Kenya, 2013). The Big Four Agenda was finally abandoned and replaced with Bottom-up Economic Transformation Agenda (BETA) which adopts many of the Big Four Agenda proposals especially in health matters. The Kenya Kwanza Government development blueprint, BETA, 2023-2027 road-map intends to raise Kenyans' standard of living by providing an effective, integrated, high-quality, reasonably priced healthcare system that meets all the requirements. Increasing the number of people receiving healthcare and developing a single basic health benefit package that would provide access to primary healthcare services among other services are the two key goals of the strategy.

1.2 Statement of the Problem

Among those with HIV, HBV is a major cause of death. The co-infection brings complexities in designing control and prevention strategies for HIV-HBV co-infected individuals. According to WHO, the HIV-HBV co-infection morbidity and mortality rates are high especially among pregnant women, children aged below 5 years, with disparities in regional spread, management and care. Further, the predisposing factors of these co-infections are not well known. Clinical trials are ongoing to understand the association between these viruses and adverse effects of treatment regimens on the co-infected patients. Both clinical and nonclinical interventions have been employed in managing HIV and HBV single viral infections. Since co-infection increases fear and death beyond what would be expected from either infection alone, HIV and HBV co-infection have not received enough attention. As a result, the co-infection of HIV and HBV complicates the dynamics of transmission and increases the risk of death, malignancy, and persistent infection. Current treatments cannot completely remove either virus. World Health Organization (2024) report indicate that a large of population are unaware of their HIV, HBV as well as its co-infection status with many countries across the world having no information about this co-infection. Although there are some mathematical models of HIV-HBV co-infection in the literature, there exist evidence that there is an interaction between the two infections.

Previous studies by Bowong and Kurths (2010), Yusuf and Idisi (2020) considered a deterministic model of HIV and HBV co-infection. Few compartments representing infection differences were considered. The authors' intention was solely to prevent HBV infection; they did not take into account treating other infections. Endashaw and Mekonnen (2022) focused on how treatment and immunization affected the dynamics of HBV-HIV co-infection transmission. An analysis of the impact of HBV and HIV MTCT on the co-infection's transmission patterns was conducted by Endashaw, Gebru, Alemneh, et al. (2022) so the significance of screening in the dynamics of HIV/AIDS-HBV co-infection was pointed out to have been overlooked in their research. In order to influence the dynamics of HIV/AIDS-HBV co-infection transmission in a population, screening and testing are essential. Other factors such as viral load saturation, optimal control interventions and un-

certainties were not considered in these studies. This is the focus and consideration of the current study.

Screening and testing of susceptible populations for HIV and HBV as well as viral load test in co-infected individuals are required to select the optimal control interventions. A mathematical model is needed to assess whether screening is a risk factor for HIV-HBV co-infection and establish the optimal control strategies. Screening and testing are key components in planning for treatment as well as a prevention measure. There are hazards associated with screening tests. The majority of screening tests carry dangers, and not all of them are beneficial. It's critical to understand the test's hazards and whether it has been shown to lower the risk of dying from a disease. This work presents a deterministic model to describe HIV-HBV co-infection in Sub-Saharan Africa (SSA) taking into account risk factors and optimal control measures with a view of ascertaining its transmission trends and health implication. The deterministic model is extended to stochastic model to predict infection outcomes and uncertainties in infection spread.

1.3 Objectives of the Study

1.3.1 Main objective

The broad objective of this study was to model the impact of clinical and nonclinical optimal control strategies on the dynamics of HIV-HBV co-infection using deterministic and stochastic approach.

1.3.2 Specific objectives

The specific objectives of this study were to;

i. Formulate a deterministic model of HIV and HBV co-infection.
ii. Analyze and simulate the deterministic model based on reproduction number and strength number.
iii. Establish the optimal control strategies for the developed model using Pontryagin's Maximum Principle.
iv. Convert the deterministic model to a stochastic model using Stochastic differential equations.

v. Simulate SDEs numerically.

1.4 Justification and Significance of the Study

1.4.1 Justification of the study

The study of HIV-HBV co-infection is essential because it has a large effect on infection development, higher mortality, and the possible development and risks of liver disease. It may also cause an immune dysfunction, which makes treatment even more complicated. The combined infection of HIV and HBV predisposes to the development of liver cirrhosis, hepatocellular cancer and mortality related to liver disease (Gopalappa, Farnham, Chen, & Sansom, 2017). It also causes a higher morbidity and mortality rate and can coincidentally weaken the immune system against HBV. Possible toxicities of drugs and drug resistance can be treated with complications. HIV might hide HBV diagnosis hence its management becomes challenging. According to Mayaphi et al. (2012), People Living with HIV (PLWHIV) live longer due to increased access to antiretroviral therapies, but are still susceptible to opportunistic infections and co-infections, especially with the HBV. Co-infections occur due to shared transmission modes, HIV infection, and side effects of HIV drugs. Those with HBV/HIV co-infection are more likely to die due to hematological problems, organ failure, and chronic liver disease (Abatenh, Asmamaw, Hiluf, & Mohammed, 2018). Studies should focus on coming up with viable therapeutics of HBV in HIV co-infection situations. Thus, this study focuses on formulation of deterministic, optimal and stochastic mathematical HIV-HBV co-infection models that incorporates clinical and non-clinical control interventions.

1.4.2 Significance of the study

The findings of this study will assist policy makers and healthcare practitioners to identify patterns of HIV-HBV co-infection and the process in which to apply clinical and non-clinical control interventions. Since ignorance forms an obstacle to HIV testing, prevention, and care as well as HBV and its co-infection, the government should come up with programs that directs the targeted population to access such information so that early screening and treatment can be done. Additional considerations should also be made to

boost activities aimed at the elaboration of the treatment regimens for co-infected patients. This is an essential step in lowering the morbidity and death from HIV and chronic hepatitis B. Ignorance is rife in many people who do not know their status ad hence do not seek treatment. This not only constitutes a likelihood of succumbing to fatal liver disease or perhaps liver cancer as one gets older, but it might also result in people passing the infection to other individuals without knowing it. The outcomes of this investigation would be relevant to the maternity clinics, Voluntary Counseling Treatment centers, medical laboratories, government research centres and NGOs by placing importance on the coordinated factors of HIV-HBV co-infection. The research findings of this study also add to knowledge in the content area and future studies of mathematical modeling of HIV-HBV co-infection. Further, this study helps in realization of the health targets envisaged in SDG goal No.3, Africa Agenda 2063, Kenya vision 2030, and the BETA Agenda.

1.5 Scope of the Study

The study formulated both deterministic and stochastic models of HIV and HBV co-infection focusing on optimal control interventions to mitigate HIV and HBV infections. Secondary data and published parameters from the literature were taken from Sub-Saharan Africa and further used to validate the models. Other possible co-infections with HIV and HBV such as TB, malaria, COVID-19, pneumonia and other STIs are not considered in this study. Population resistant to HIV and HBV treatments is not captured in the model. The progression of chronic Hepatitis B to cancer stage is also not considered in the model. HIV-2 strain and other hepatitis strains are ignored. At the same time, the differences in individuals health status and transmission of HIV and hepatitis B infections is not taken into account.

CHAPTER TWO: LITERATURE REVIEW

2.1 Introduction

Most of the developed mathematical models concentrated on determining the parameters that contribute to HIV and HBV mono infections and assessed their sensitivity. A few HIV-HBV co-infection models exist and included the clinical intervention strategies such as treatment and vaccination. Non-clinical control strategies such condom use, health education, mass media campaign among others are not taken into account. The developed models also assumed vertical transmission of HIV and HBV through MTCT. Screening component has also been ignored in these models. The different phases of Hepatitis B is also not taken into consideration. Furthermore, few studies have been dedicated to illustrating the impact of HBV on HIV infection. This chapter begins with a review of interaction between HIV and HBV, existing co-infection models of HIV-HBV with or without control interventions and etiological factors and finally focuses on the current research.

HBV and HIV are blood-borne viruses transmitted primarily through sexual intercourse, injection-drug use, mother to child during pregnancy, delivery or breastfeeding. Because of these shared routes of transmission, a high proportion of adults are at risk of HIV and HBV infections. People with HIV who become infected with HBV are at increased risk of liver-related morbidity and mortality (Spradling et al., 2010). To prevent HBV infection in people with HIV, universal hepatitis B vaccination for all susceptible people infected with HIV is recommended (Bellini et al., 2009). People with HIV who test positive for HBV should receive HIV antiviral medication such as tenofovir and entecavir which are active against HBV. However, it has been observed that although HAART can limit the progress of HIV infection to a certain point, HIV infection can further magnify the harm for HBV infected patients. The mechanisms by which this happens are still relatively unknown (Y.-J. Li, Wang, & Li, 2012). Sun et al. (2014) noted that HIV infection and low CD4 count are common in all the HBV phases including reverse seroconversion, viral disease progression, development of hepatic fibrosis, HCC and reactivation and in chronicity. Other factors also found to be independently related to 1ow CD4 count in treatment naive HIV-HBV co-infected patients include high HBV DNA level as well as low clearance rate of

HBeAg. The directionality of the relationship is, however, not fully understood although, on one side the evidence sustains the concept that CD4 + T cell is important for the immune response against HBV and for the early clearance of the virus, thus, low CD4 count in HIV infection may predispose one to uncontrolled HBV replication while, on the other hand, HBV may contribute to the decline of CD4 count through immune activation .

Clinical research indicated that patients with both HBV and HIV showed lower base count of CD4 and considerably higher base levels of HIV load they obtained before they started HAART. The study has also pointed out that HIV can increase the rate of progression of disease in HBV due to the suppression of innate immunity thereby suggesting that the subjects' natural history of HIV was altered to some extent due to HBV infection. So, the issue regarding microbial translocation as well as the process of immune activation in the case of co-infected patients with HBV/HIV remains an enigma. Similarly, another study by Singh, Crane, Audsley, and Lewin (2017) noted that HIV co-infection also affects the natural course of chronic HBV, having higher HBV DNA level, more aggressive liver disease and higher liver related morbidity and mortality than HBV mono infection. Early HBV-ART commencement prior to the onset of hepatic events has resulted in notable alterations to the natural history of individuals co-infected with HIV and HBV, but the burden of liver disease still remains higher among the co-infected patients than mono-infected counterparts. Therefore, the study argued that research to enhance the development of cure for HIV and HBV is necessary since the outcome will affect co-infected people.

2.2 HIV-HBV Mathematical Models

This section covers HIV, HBV mono-infection and co-infection models related to the current research.

Saha and Samanta (2019) developed structured models that included the transmission of HIV/AIDS, and treatment as well as usage of pre-exposure prophylaxis (PrEP). It also takes into consideration the impact of a person's behavioural reaction to PrEP information.. PrEP use by uninfected individuals really be the primary factor preventing HIV infection from spreading. The analysis of the model has offered details about the local and global stability of the points along with the structure of the model. Besides, the problem of

optimal control has been formulated which incorporates target function of treatment cost and fatality in the context of treatment choice and PrEP information effect. Based only on PrEP knowledge, the therapy is more effective for long-term management, but it will be more cost-effective in the short term. This is demonstrated by the numerical analysis. Additionally, using two control therapies voluntarily would be more preferable than using just one. It also greatly reduces the number of infectious persons with the goal of completely eliminating the illness, minimizing the financial costs associated with both its burden and management. According to the suggested model, the population's acceptance of PrEP reduces the number of new sexual transmissions, which can enhance the HIV prevention mechanism. Furthermore, it was discovered that the combined impact of the two control measures was more cost-effective than the use of one strategy throughout the duration of the epidemic.

Yusuf and Idisi (2020) looked at a mathematical model on the co-epidemic of HIV and HBV that was simplified and consisted of four non-linear ODEs. The basic reproduction number, or R_0 of the model was used to determine the necessary conditions for the stability of the model equilibrium. It was demonstrated that for the corresponding HBV-sub model, HIV-sub model, and complete model, each of the three disease-free equilibrium E_{0B}, E_{0H}, and E_0 is locally asymptotically stable when $R_0 < 1$ (i.e., $R_B < 1, R_H < 1$). Additionally, the proper Lyapunov functions were used to complete the global stability study of the HIV-sub model and the HBV-sub model. Furthermore, a sensitivity analysis was conducted on R_0 concerning all model parameters. The results indicated that HIV transmission rate, τ and HBV transmission rate, γ were the factors that R_0 was most sensitive to. This means that if the two parameters are to be predicted with the use of the model, then estimation of each of them has to be precise. It also implies that in an attempt to mitigate the spread of the two diseases, control actions that reduces each of these factors would be useful. However, the numerical solution of the suggested model was performed using the Runge-Kutta method of order four, and MATLAB R2016a was used for this purpose. According to the findings of their mathematical investigations, their numerical result simulations agree with their conclusions. The simulations showed that although the co-epidemic could not

be eradicated completely, if the co-epidemic of HIV and HBV is to be contained in such a population, control measures that would reduce the basic reproduction number below one must be implemented. Since failing to do so could result in an alarming co-epidemic of both diseases, it is advised that proactive and effective control measures be effected in any society where either HIV or HBV disease is endemic in order to stop the other disease from spreading. Starting programmes that would enable prompt identification of sick people could help achieve this, and patients who have been found to be infected should receive sustained counseling and start treatment right away.

In another study, Endashaw and Mekonnen (2022) introduced and contrasted a deterministic model for assessing the effect of immunization and treatment on the transmission of co-infection between HBV and HIV/AIDS. The HBV-HIV/AIDS co-infection model's pre-intervention estimate was R_0^{BH}, and its post-intervention estimate, which included treatment and vaccine, was R_{eff}^{BH}. They were able to evaluate the numerical values of the basic and effective reproduction numbers in order to ascertain the effectiveness of their intervention by applying their methodology to the used data. The basic reproduction number $R_0^{BH} = 4.2$ and the effective reproduction number $R_{\text{eff}}^{BH} = 0.94$ are represented numerically. This suggests that if an intervention mechanism is not put in place, one sick person will infect at least four healthy people during their infectious period. However, after combining vaccination and treatment strategies into a single model that decreases the impact of the co-infected person with both HBV-HIV/AIDS, the effective reproductive number is found to be $R_{\text{eff}}^{BH} = 0.94$ which indicates it is below the threshold value, which is one. This implies that the illness will vanish from the community and that, should individuals follow the vaccination and treatment recommendations, the possibility of the illness infecting others will be eliminated. The stability of the endemic equilibrium points of the sub and full models when $R_{\text{eff}}^{B}, R_{\text{eff}}^{H} > 1$ and $R_{\text{eff}}^{BH} < 1$ was demonstrated, as was the local and global asymptotic stability of the disease-free equilibrium points of the sub and full models when the reproduction numbers $R_{\text{eff}}^{B}, R_{\text{eff}}^{H} > 1$ and $R_{\text{eff}}^{BH} < 1$ were demonstrated using that dynamical system analysis.

Despite the aforementioned observation, the sensitivity analysis that was carried out to

demonstrate the effect of parameter variability on the effective reproduction number of the HIV and TB has been the only source of information available regarding the general profiles of parameters of infection and; the most sensitive factors are the HBV co-infection model, ω_B and ω_H, which represent the effective contact rates for HIV and HBV transmission, respectively. According to the simulation results, the number of HBV infectious individuals, the number of HIV infectious individuals, and the number of HBV and HIV/AIDS co-infectious individuals decrease significantly and even eventually fall to zero if the effective contact rates ω_B and ω_H are less than 0.42 and 0.58 for HBV and HIV transmission, respectively, the proportion of immune individuals following vaccination to HBV infection is greater than 0.14, the treatment rate for chronic HBV. Therefore, it is determined that in order to prevent the spread of both the Hepatitis B Virus and HIV/AIDS infection, it is imperative to reduce the effective contact rates for HBV and HIV transmission and to utilize vaccination and treatment at the highest possible rate. From the numerical outcomes they advised public policy makers and other concerned bodies should concentrate on boosting up the vaccination against HBV infection, treating HIV/AIDS and hepatitis B to reduce the prevalence of this unusual co-infection. This study did not explore the distribution pattern of HBV and HIV co-infection in a population due to screening reasons. It could change how HIV/AIDS and HBV co-infection propagate within a community. This was left for future consideration.

Endashaw et al. (2022) investigated how HIV-HBV co-infection dynamics were affected by mother-to-child transmission in order to develop a proposal that the public health community, policy makers, and programme implementers can use. Based on numerical modeling results, it was found that while a decrease in these rates decreased the number of cases, an increase in MTCT rates of both HBV and HIV exacerbated the co-infection, helped the spread to be limited, and assisted in the eradication of co-infection of HIV and HBV. Additionally, they advised that besides the policy that the study presented by Endashaw and Mekonnen (2022), the policy makers and other relevant parties should also support the suggested approach to lower the rate of multiplication of concurrent MTCT of HIV/AIDS and hepatitis B infections.

A susceptible (S), exposed (E), acute infection individuals (I), chronic HBV carriers (C) and recovered (R) model of hepatitis B virus infection was presented by Kamyad, Akbari, Heydari, and Heydari (2014) and included vaccination and treatment as two controls. Initially, they carried out a dynamic analysis of the system, fully controlling all of the parameters and maintaining constant values. They calculated the chance of discovering the infectious equilibrium and the critical reproduction number in the constant controls condition. The population cannot exist at one side of the system; instead, it has two non-negative equilibrium which includes DFE and the EE points. Furthermore, it was seen that there was both local stability of the stable endemic equilibrium and a disease-free equilibrium, which only existed in as much as the long-run equilibrium $R_0 > 1$ with regard to the disease-free equilibrium and $R_0 < 1$ with respect to the endemic equilibrium. The dynamic properties of the system with constant controls, which had been previously obtained for producing different results, were then used to construct an optimal control problem when the controls are time variable. This problem was then solved using Pontryagin's maximum principle. Several kinds of option control are being used and effectiveness is rated through simulation indicators. Further, from the information presented here it becomes clear that a given set of control activities done in a coordinated manner produce far better results compared to the use of a single control measure. As people have pointed out the work is still at the preliminary level only. The characteristics are never homogeneous because characteristics are formulated by the environmental impacts. Hence, it is possible to argue that there are rather limited studies concerning the specific connection between these variables and numerous environmental factors. This needs a time lag because the susceptible individuals do not get infected at once and also the susceptible population cannot be immune at one go.

Additionally, J. Y. James, Garba, Habila, and Bororo (2022) attempted to stop the spread of HBV by incorporating immigration, vaccination, on-the-sport treatment, and sanatorium into the pre-existing SEIR model using the deterministic framework. From an epidemiological point of view, this suggests that the illness will persist if the HBV infection brought about by immigration is not controlled. The local stability of the disease-free equilib-

rium of the dynamic system in the absence of HBV infective immigrants has a reproductive number less than one, making it locally asymptotically stable, as is evident from the coefficient of the polynomial characteristics satisfying the Routh-Hurwitz criterion. The disease-free equilibrium of the model was shown to have global stability, indicating stickily positive matrix entries for the infected compartment $G(X,Z)$. The global stability that is free of disease is hence stable. In order to calculate numerical values and assess the effectiveness of vaccine, sanatorium, or a combination of both control measures in combating HBV, they set baseline values for the parameters and begged for the use of MATLAB codes. According to the findings, the population that is infected is much larger than the other population densities, even in cases where vaccinations are administered in tiny quantities. A 0.9 vaccination rate resulted in a significant drop in the impacted population, and vice versa.

The risk factors reported to be common for Hepatitis B virus infection among HIV/AIDS patients were investigated by Musafili, Hadisaputro, and Sofro (2022). This created analytical observational design where case control test was conducted on the 68 (34 cases and 34 controls) participants. Using the data collected from all the HIV patients enrolled in the study, the sample was arrived at from a positive test for the HBsAg factor. The dependent variable is whether or not a HIV/AIDS patient tests positive for the hepatitis B virus and the independent variable is CD 4 count of 100 or less, age of 30 or more, male gender, single/married status, education level, MSM. Thus, univariate, bivariate (using the chi square test) and multivariate (using logistic regression) analysis were used to analyze the data. Afterwards several tests were performed to affect the results. The goal of this paper was to determine the factors that led to the incidence of Hepatitis B virus infection among HIV/AIDS patients. The results which included the following variables were obtained $CD4 \leq 100$, men who had sex with other men (MSM). When these risk factors are present, patients with HIV/AIDS have an 88.18% chance of also having the Hepatitis B virus. Age, gender, marital status, and educational attainment were among the other variables that did not affect the frequency of Hepatitis B virus in HIV/AIDS patients. They hypothesized that MSM and a CD4 count of less than 100 were two of the several factors

that have been shown to influence the prevalence of the hepatitis B virus in AIDS patients. Volinsky (2022) introduced a mathematical model of Hepatitis B virus treatment by supporting the immune system. The model categorizes the points of equilibrium and approximates effects of right hand side dislocations on solution patterns. This trial examines regulation where both upper- and lower-bound limits of integrals delay introducing a time frame that has the IL-2 supporting treatment. Hepatitis B is a life threatening and is a chronic disease that has afflicted 240 million people worldwide causing death of 350,000 people annually. Interferon and similar interferon-nucleoside combination therapies are widely adopted as the solution to treating the chronic HBV type of cases. The immune response to the antibody cells however quickly fades within a period of time and the fusion of these two methods clearly show a lot of potential in a way of reducing the rate at which viruses grow. The IL-2 therapy was introduced as characterized by a mathematical model and proved to be highly successful.

Yu et al. (2020) in their study aimed to determine the prevalence of Hepatitis B and Hepatitis C (HBV) and/or HCV co-infection in HIV-positive patients in China through a systematic review and meta-analysis. The Chinese Center for Disease Control and Prevention estimated that there were approximately 500,000 people infected with HIV by the end of 2014, and at the end of June 2017, this number had changed to 660,000, including 41.7% of whom were already AIDS patients. China is also one of the countries with the greatest number of chronic HCV infections, with an estimate of 9.8 million chronic HCV infections. The researchers searched databases like Medicine, Web of Science, Chinese Web of Knowledge, and Wanfang to identify relevant cohort or cross-sectional studies published up to April 2019. The meta-analysis included 66 studies, with the pooled HBV-HCV co-infection prevalence being 3.5%, with variations found in terms of age and geographic region. The study concluded that due to the high burden of HBV and HCV co-infections in HIV-positive patients, the incorporation of comprehensive screening, treatment, prevention, and vaccination programs into general HIV management in China is imperative.

Boyd, Melin, and Lacombe (2022) investigated the co-infection with HBV and HDV in PLWHA. The risk of contracting hepatitis Delta virus (HDV) is over six times higher

in HIV-infected patients co-infected with hepatitis B (HBV) compared to those infected with HBV alone. HIV-induced immunosuppression decreases seroconversion, fibrosis, and immunological response, all of which are detrimental to the hepatitis D virus (HDV) course. HIV exacerbation or AIDS-related events are not increased by co-infection with HDV. Currently, immunocompromised individuals receive anti-retroviral medication with tenofovir as a treatment, along with HDV vaccination.

The study by Bowong and Kurths (2010) proposed a theoretical basis that was aimed at explaining the similar transmission dynamics of co-infection of tuberculosis (TB) and hepatitis B virus (HBV). The model has thirteen different epidemiological states which are represented by thirteen classes susceptible, vaccinated, latent TB, active TB, acute or chronic HBV, recovered and co-infected. The main characteristics in the model are the exogenous TB reinfection, HBV vertical transmission, waning vaccine immunity, varying disease progression form, and the outcome of treatment of TB and HBV. This all showed that the disease-free equilibrium (DFE) was globally stable with a unique endemic equilibrium being locally stable. The condition of coexistence has the two partial reproduction numbers to be above one. HBV immunization, TB chemoprophylaxis, and interventions in treatment can only be integrated to realize effective control. Furthermore, the presence of co-infection increases the burden of the disease by causing immune suppression and high rate of development illustrating the need to have combined public health measures.

In their work, Singh and Lewin (2020) brought attention to the fact that HIV-HBV co-infection is widespread, little understood, and a major problem for some of the world's poorest nations. The distribution of infection and, in particular, the frequency of HBV in PLWHA in Eastern Europe and Central Asia as well as in important susceptible populations are among the many unknowns they pointed out. People with HIV and HBV have been known for almost 20 years to have disproportionately high rates of morbidity and death. This is true even in the presence of suppressive antiretroviral therapy (ART). Perhaps the time has come to create a fresh international plan that focuses on HIV/HBV co-infection.

2.3 Deterministic Model Extended to Optimal Control Model

Nampala, Luboobi, Mugisha, Obua, and Jablonska-Sabuka (2018) developed a mathematical model and used numerical simulations to study the therapeutic as well as toxic effect of the currently used HIV-HBV therapy, and consequently derived an optimal combination in treating the co-infection. They considered Hepatic necrosis. Their findings showed that disease-free equilibrium of the HIV-HBV model was locally asymptotically stable when the basic reproduction number was below unity and unstable when above unity. However, the disease-free equilibrium was globally asymptotically stable only if there were no hepatocytes that were co-infected with both viruses at the same time. It was concluded that global stability depended on the number of cells that were infected by the first virus before the second would infect them. Their study showed that 3TC+TDF is the best baseline NRTI for HBV while FTC+TDF is best for HIV in either regimen. The combination that is most effective in reducing HIV load is at the same time the most toxic in either regimen. PIs are more effective in reducing HIV and HBV load in the liver. Generally, NVP was highly toxic while EFV was highly efficacious in reducing HIV/HBV load in the liver. The therapy that is so good in reducing HIV load is the one that is most toxic. The drug combination that optimizes efficacy and toxicity in HIV/HBV co-infection was FTC+ TDF + EFV.

A mathematical model of the interactions between hepatocytes and concurrent HBV and HIV infection was developed by Nampala, Jablonska-Sabuka, and Singull (2021). The model included a time delay to illustrate the time interval between the viral entrance into the host cell as shown in the matrix column and the time the delay occurred when the cell was able to reproduce the virus. Determining how the latency time affected the HIV-HBV infection dynamics was the primary objective of the investigation. Analytical, bound, and

constructive judgements were drawn on the model solutions. The fundamental reproduction number, or R_0, could be found by computing the disease free equilibrium, or DFE. If R_0 is less than 1, a locally asymptotically stable disease-free equilibrium point is found, and if it is greater than 1, an endemic equilibrium is obtained. Data demonstrated the impossibility for the HBV to have dominance over the HIV since the latter, circulating from other cells, will certainly find its way into the liver cells. Therefore, there cannot be any equilibrium point in which HBV is the predominant hepatitis virus. According to the optimum control problem results with varying delay durations, HIV and Hepatitis B virus loads develop best with longer delays. In the context of cART, HIV and HBV copies rise, hence, the latency period indicates that viral latency hampers medication administration and virus control. The research provided evidence that latent inhibitors need to be unique to CD4 cells, as there is proof that other cells might serve as viral reservoirs. The liver, where HIV viral reservoirs hides, is significantly affected through the HIV long-term silent infection (latency) in patients who are co-infected by HIV/HBV. In these cases, the HBV may multiply in the liver through an indirect approach.

In their paper, Ayele, Goufo, and Mugisha (2021) developed a mathematical model of HIV/AIDS that incorporates the main compartments: people with HIV infections that are diagnosed with and without symptoms of AIDS, people who are unaware of their susceptibility, people who have not been diagnosed with HIV, and people who are receiving treatment for the disease. The model, being a function of media campaign, was evaluated in respect to increase of rates of awareness and decline of rates of lack of awareness, although rates of screening and treatment remain consistent. The reproductive infective number, equilibrium and the grounds on which they can be stable were indicated. Additionally, when the effective reproduction number equals one, the bifurcation occurs.

Additionally, a new systems model based on interventions like screening, treatment, or preventive measures was integrated with it. By using Pontryagin's Maximum Principle, the optimal control problem in this model was solved.

Campos, Silva, and Torres (2019) in their paper provided a study on numerical methods to deal with modeling and optimal control of epidemic problems. Simple but effective Octave/MATLAB code was fully provided for a recent model proposed. The given numerical procedures were robust with respect to the parameters, nevertheless, the code is highly flexible with respect to the other models and can be used for other parameter settings. The control measure calculated from the control equation as given by the Pontryagin's maximum principle and calculated numerically using the Octave code indicated that the incidence of HIV/AIDS infected and the chronic population reduces and hence the susceptible population improves. These findings pointed out how optimal control theory could be applied in the medical field and the uses of scientific computing systems such as GNU Octave. Their study should be of great importance to a practitioner in the area of disease control. In fact, the numerous letters they have received requesting the software code for their research publications on the applications of optimal control theory in epidemiology have served as the driving force behind this endeavor.

Aghdaoui, Alaoui, Nisar, and Tilioua (2021) extended all incidence function forms found in the literature by proposing a SEIRI model with relapse and a generic nonlinear incidence function represented as a function of three variables: S, I, and R. Two equilibrium points were detected by the two authors in the first preliminary analysis about the model under examination without control: DFE and EE points. Both points of equilibrium are locally asymptotically stable as shown by the local stability analysis. Next, the first model has three control terms which control the S, E, I, and R compartments' dynamics. This model

has been proposed to incorporate different immunization treatment procedures to determine the effects on the disease's behavior. They used the Pontryagin's maximum principle to find the best possible control. In addition, the adjoint equations have been derived and the explicit expression of the optimal controls obtained. Theoretical results are illustrated through numerical simulations that showed the effectiveness of the applied controls and their impact on the dynamics of the different classes.

Bassey (2020) formulated a penultimate 7-Dimensional mathematical dynamic HIV-HBV model using ODEs, which was then transformed to an optimal control problem, following the introduction of multi-therapies in the presence of dual adaptive immune system and time delay lags. Applying classical Pontryagin's maximum principle, the system was analyzed, leading to the derivation of the model optimality system and uniqueness of the system. Specifically, following the dual role of the adaptive immune system, which culminated into triple-dual application of multi-therapies, the investigation was characterized by dual delayed HIV-HBV virions decays from infected double-lymphocytes in a bi-phasic manner, accompanied by more complex decay profiles of infectious dual HIV-HBV virions. The result further led to significant tri-phasic maximization of susceptible double-lymphocytes and dual adaptive immune system (cytotoxic T-lymphocytes and humeral immune response) achieved under minimal systemic cost. Therefore, the model is comparatively a monumental and intellectual accomplishment, worthy of emulation for related and future dual infectivity.

Lenhart and Workman (2007) provided the basic framework of formulating an optimal control problem applied to biological models. The Pontryagin's maximum principle is used to establish the conditions required to solve an optimal control problem. However, it was noted that there may be some problems in applying this approach. The required

circumstances may provide a spectrum of solution sets and out of these some may even be imaginary control solutions. However, one needs to recall that when specifying the essential conditions in the derivation of the formulation, existence of an optimum control was postulated in advance. In turn, if the nature of the primitives of the optimum control problem remains undefined, the above conditions can be met as well. With regard to the objective function, the latter is expected to yield only a finite response at the ideal state as well as at control. If in the evaluation of the objective function the value is found to be ∞ or $-\infty$, then it was concluded that no solution could be obtained in solving the optimization problem.

Okongo, Okelo Abonyo, Kioi, Moore, and Nnaemeka Aguegboh (2024) developed a mathematical model for the transmission of the monkeypox virus in human and rodents with the interaction of the environment. Regarding the control factors, five time-based factors are considered as a means of dealing with the condition. The optimality criteria are derived from the validity of the Pontryagin's Maximum Principle for the given system to prove the existence of optimal control. The solutions for both the state and co-state systems are obtained through Runge-Kutta fourth-order that functions in both forward and backward time. It also gives profiles of different control variable values showing the monkeypox infection rates. The findings of the study provide directions for physicians and policy makers interested in designing the best and optimal prevention measures to halt the monkeypox epidemic.

2.4 Conversion of Deterministic to Stochastic Model

Selvan and Kumar (2023) investigated deterministic as well as stochastic model with two epidemics and transmission mechanisms of SIR and SIRS accompanied with saturation incidence rate. Saturation contact rate is considered since the time the vulnerable persons

come into contact with infected persons is limited. The model thresholds are defined for both models. Statistical evidence was assumed to differentiate between the circumstances of the illnesses' extinctions and persistence. It became stochastic when incidence rates with a white noise that can be defined by a Brownian motion was included in the deterministic model.

Ouaro, Traoré, et al. (2013) developed an ODE deterministic model and a corresponding SDE model for schistosomiasis. The model considered four sub-populations; susceptible human, infected human, susceptible snails and infected snails. The SDE model was derived by computing different probabilities of change of state variables using Poisson processes technique. The change of state was assumed to be normally distributed. The SDE model was solved by using the Euler-Maruyama method taking a sample of 1000. The analysis showed the basic reproduction number, R_0 under the given conditions and computational simulations were provided. A performance comparison is made between the deterministic model and stochastic analogous model. It was shown that there was almost no difference in the behaviour of the deterministic and comparable stochastic models.

Olabode et al. (2021) attempted to investigate the COVID-19 transmission patterns through the use of data from Wuhan, China, in their deterministic and stochastic models. Based on the fundamental SEIR model, the system of ODEs defines the deterministic model. The constant parameter obtained from the ODE model yields the Continuous Time Markov Chain (CTMC), which describes the stochastic process. A nonlinear CTMC model of the infectious disease process is replaced with a multi-type branching process to derive an analytical expression for the probability of occurrence of an epidemic. The local and global dynamics of the disease are analyzed by using the deterministic model with constant parameters, and the result indicates that the basic reproduction number R_0 serves as a sharp disease threshold: this disease disappears if $R0 \leq 1$ while it continuously circulates if $R_0 > 1$. The second aspect of the deterministic dynamics in contrast to the stochastic dynamics was that the disease may not last when $R_0 > 1$. Fitting of the ODE model is done by estimating and validating the parameters in order to approach the public reported data. From their findings, therefore, exposed and infected classes are all seen to

have an influence on the epidemic dynamics of COVID-19 in Wuhan China. Additionally, mathematical modeling predicted that if preventive and control measures are not applied correctly, there will be a second wave of the current pandemic.

MacIndoe (2019) focused on the HIV virus specifically using the Susceptible-Infected-Virus (SIV) model. The inside-host dynamics of viral infections were explained by the SIV mathematical model. The deterministic model which presupposes that the constants are precisely known and the stochastic model, generates a random variable that will represent the healthy cell death rate. As for the two of the deterministic model's simplified conditions, analytical solutions were derived. The two deterministic and stochastic systems have been discussed using numerical characteristics. As there was no therapy administered to the patients, the results provided insights toward the progression of the HIV in-host population. They also explained how randomness can influence the development of the infection. Despite the fact that the estimates based on those approximations were not very precise, the study described the roles of infection rate, viral production rate, and infected cell death in the SIV model. The two numerical approaches that can be used to calculate approximate solutions of the entire SIV model are the stochastic version, where the healthy cell death rate is represented by a random variable, and the deterministic form, where all the parameters are known. The findings demonstrated that the inclusion of the randomness element made the progression of HIV in the system without treatment seem more plausible.

In their study also, Maliyoni, Chirove, Gaff, and Govinder (2017) used a stochastic epidemic model of a continuous-time Markov chain to explain the dynamics of tick-borne disease transmission in a single population. Based on the deterministic meta population tick-borne disease model that is present currently the stochastic model is developed. To determine the impact of randomness in the disease dynamics of ticks, disease dynamics of Stochastic and Deterministic models are compared. The Galton-Watson branching process of multiple types and numerical estimate represent the probability of a large outbreak and the extinction of the disease, respectively. Several noticeable differences were identified between the analysis of the deterministic and stochastic models' results of a set of analyt-

ical and numerical calculations. Consequently, they further ascertained that an infection disseminates with greater ease via infected deer compared to the infected ticks. Therefore, these results draw focus on the migration of the host as the cause of invasion of the tick borne diseases to new areas.

2.5 Research Gap

Previous models of HIV-HBV co-infection did not take into account the factors of screening, viral load and randomness in the process of transmission of deterministic HIV/AIDS-HBV in a population of individuals. Since screening can influence the dynamic behaviour of HIV/AIDS-HBV co-infection transmission in a population, enhancing the availability of voluntary HIV testing and counseling for persons infected with HBV is crucial. In the literature, HIV-HBV co-infection model incorporating optimal control interventions was not found. At the same time, a co-infection model with HBV vaccinated individuals with HIV was not found. More attention has been geared towards therapeutic measures for HIV and HBV mono infections across the globe and the cost of medication and management is high. The effective prevention and control measures for the co-infection has been neglected despite the cART which has been reported to have detrimental effects. Moreover, previous researchers have adopted deterministic models to study disease dynamics, ignoring the stochastic effects. Subsequently, numerical simulations of deterministic models show only average dynamics of the infections in the population. However, stochastic simulations of models can account for dynamic behaviors that are introduced by the noisy nature of the systems but not revealed by deterministic simulations. Thus, converting an existing model from the most common deterministic formulation to an equivalent stochastic simulation enables further investigation of uncertainties in infection outcomes.

The current study incorporates the risk factors and investigates a combination of control measures into the developed deterministic co-infection model. At the same time, the bounds to which the parameters affect the control reproduction number were also be investigated. With vertical transmission in consideration, the births are divided into six proportions and a compartmental class of HBV vaccinated group infected with HIV is incorporated in the model based on the shortcomings and recommendations of past studies.

CHAPTER THREE: RESEARCH METHODOLOGY

3.1 Introduction

This chapter describes the methodology used in conducting this study to achieve the objectives in Section 1.5, namely to formulate a model for HIV-HBV co-infection incorporating screening and viral load saturation function as a risk factor of transmission and control variables, to determine model thresholds and perform stability analysis, sensitivity analysis, backward bifurcation analysis so as to establish the conditions for the spread of the infection, to estimate numerical results of model using secondary data as well as to evaluate normalized sensitivity indices for the reproduction numbers and to perform numerical simulations to validate analytical results of the developed models.

Optimal control problem is formulated for the deterministic co-infection model and the optimal control functions established. Further, the deterministic co-infection model is converted to equivalent stochastic model to determine the probability transition rates so as to predict the outcomes of the infection.

3.2 Model Development Using Classical Epidemic Models

According to R. M. Anderson (1991), the epidemic models are formulated as compartmental models, in which human population is partitioned into compartments, and there are assumptions about the nature and rate of change in transferring infections between the compartments. Pathogen is diseases that can cause immunity have a different compartmental structure from the diseases without immunity.

The SIR is used to identify passage from the susceptible class, S , to the infectious class, I , and ultimately to the removed class, R , as well as to characterize a sickness that makes the host immune and incapable of contracting it again and vice versa. The SIS model describes a disease in which the hosts have no immunity against the disease, and shows the movement from the susceptible class S to infective class I and again to the susceptible class, S. Other possibilities include SEIR, susceptible, exposed, infective and recovered compartments and SEIS models, where there's a time interval between the onset of infection and the time an individual is capable of spreading the disease and SIRS models, where

there is even temporary immunity for those recovering from infection. In compartmental models the independent variable is time, t and the state variable is the dependent variable and the rates of transfer between compartments are shown mathematically with the help of derivatives of compartment sizes and models which are originally presented in the form of differential equations for the rate of change of states with time. To model such an epidemic using the SIR model, for example, the population under study is classified into three classes, assigned S, I, and R.$S(t)$ represents the number of individuals susceptible to the disease but not yet infected at time t;$I(t)$ represents the number of individuals infected and presumed infectious, able to spread the disease through contact with susceptible individuals; and $R(t)$ represents the number of individuals infected and removed from the possibility of contracting the disease again or of spreading it to other people.

An individual can be eliminated from a system in a few different ways, such as by dying from the illness, acquiring immunity against the disease after recovering, or being isolated from the general population to stop the sickness from spreading. From an epidemiological perspective, these descriptions of the removed people differ, but from a modeling perspective that just takes into account each individual's status in relation to the epidemic, they are similar. To derive the models in terms of derivatives of sizes of each compartment, we have adopted the following assumptions; that the simplification can be made in terms of an integer, where the number of individuals belonging to a particular condition is differential with time. This may be reasonably accurate if there are a large number of people in a compartment, although it has to be questionable in all other circumstances. When using differential equations to formulate models, we suppose that epidemic process is a deterministic one, meaning that the population behaviour depends solely on its past and on the model's rules. On other hand, stochastic models where the probabilistic concepts are used and the distribution of possible behaviour by inserting random noise is also described. There is a series of models with the following hierarchy that address the elementary description of the distribution of communicable diseases; the McKendrick, Anderson, and Kermack classical sequence of models dating from 1927, 1932, and 1933 (Kermack & McKendrick, 1927). The general framework relied on the individual's age of infection, which is the duration of

their infection. Interestingly though, in their additional models that included demographic characteristics, Kermack and McKendrick did not go into further detail about this circumstance. Age of infection models are therefore important in HIV/AIDS research. The case when the influx of susceptible is constant and when there is no recovery, which was first studied by Kermack and McKendrick (1927), is considered to be the basis of compartmental epidemic models. These models are further modified and adopted for a particular case of infection being modeled with inclusion such as demographic factors, births and deaths and control strategies among others.

3.2.1 Formulation of deterministic HIV-HBV co-infection model

The classical Susceptible-Infectious (SI) and Susceptible-Infectious-Recovered-Susceptible (SIRS) models are adopted to formulate the deterministic co-infection model. The human population is categorized into 12 compartments based on their infection status. The populations are all functions of time t. Thus, we denote susceptible population at any time as $S(t)$, the HBV vaccinated as $V(t)$, HIV infected $I_H(t)$, mild HBV infected $I_B(t)$, severe HBV infected $I_{cB}(t)$, HBV treatment class $T_B(t)$, HIV-HBV vaccinated $V_H(t)$, HIV acute HBV co-infected $I_{HB}(t)$, HIV chronic HBV co-infected $I_{HCB}(t)$, HIV-HBV treatment class $T_{HB}(t)$, AIDS class $A(t)$ and $R(t)$ represents the hep B population at time t which recovers either due to natural immunity or treatment. As a result, $N(t)$ represents the whole human population at a specific time t as given in table 3.1. The compartments are connected with continuous line representing the movement between the compartments being the transition rates. The recruitment rate into the model is given by $\pi = bN$, where b is the birth rate. This entry is divided proportionately and distributed into five compartments defined in the table 3.2 in terms of $\theta\pi$. Screening regarded as a function of treatment seeking behaviour and viral load saturation functions are also incorporated in the model as ϕ, τ, D_H and D_B respectively as described in table 3.2. Both deterministic and stochastic methods are used in the constructed mathematical models in this study to characterize the co-dynamics of HIV and HBV infections.

3.2.2 Description of the model state variables and parameters

The following variables and parameters are used to define the populations and transition rates. Table 3.1 describes the state variables which represents the human populations in different states of the HIV and HBV.

Table 3.1
Definition of state variables

Variable	Description
$S(t)$	Susceptible Individuals at time t
$I_H(t)$	People with HIV who exhibit symptoms of AIDS at a given time,t
$A(t)$	People who have complete AIDS symptoms at a given period
$I_{HB}(t)$	Co-infected individuals with HIV and AHB at time, t
$I_{HcB}(t)$	Co-infected individuals with HIV and CHB at time, t
$T_{HB}(t)$	Co-infected individuals under HIV-HBV treatment at time, t
$I_B(t)$	Individuals with AHB infection at any time, t
$I_{cB}(t)$	Individuals with CHB infection at any time, t
$T_B(t)$	HBV Treated individuals at any time, t
$R(t)$	Persons who recover from AHB through treatment or natural immunity
$V(t)$	Vaccinated individuals against HBV
$V_H(t)$	HIV infected individuals vaccinated against HBV
$N(t)$	The total population at time, t

Source: Researcher (2025)

Table 3.2 gives the definitions of the model parameters which describes the transition between the compartments.

Table 3.2
Definition of model parameters

Parameters	Description
λ	Force of infection
π	Recruitment rate
β	Infection rate
μ	Natural mortality rate
δ_1	Mortality rate due to HIV/AIDS
δ_2	Death caused by Hepatitis B Virus infection
δ_3	Death brought on by HBV therapy
δ_4	Induced HIV-HBV co infection mortality
θ_1	Proportion of births infected with HIV
θ_2	Proportion of births infected with HBV
θ_3	Proportion of births vaccinated with HBV
θ_4	Proportion of births infected with HIV and vaccinated with HBV
θ_5	Proportion of susceptible births
ε_1	Efficacy of HIV drugs
ε_2	Efficacy of HBV drugs
σ	Treatment rate of HIV-HBV co-infected individuals
α	Hep B recovery rate due to natural immunity
ω	Drug/immunity waning rate
φ	Recovery rate of Hep B infected individuals due to treatment
τ	Treatment rate for mild Hep B to seek treatment
ϕ	Treatment rate of Acute Hep B infectious individuals
ψ	Progression rate of acute to chronic Hep B
γ	Progression rate of acute to chronic HIV-HBV co infection
D_H	HIV viral load saturation function
D_B	HBV viral load saturation function
Γ	Progression rate of Hep B vaccinated to HIV
v	Progression rate of HIV vaccinated to HIV-HBV co infected
ρ	Proportion of HIV-HBV births
λ_1	HIV force of infection
λ_2	HBV force of infection
λ_3	HIV-HBV force of infection

Source: Researcher (2025)

3.2.3 Assumptions of the deterministic co-infection model

The model assumes that both HIV and HBV is transmitted vertically (or mother to child) and horizontally (between individuals). The population is also uniformly and randomly mixed in compartments and observed to interact homogeneously conforming to the law of mass action and frequency-dependent transmission (FDT) in the spread of the HIV and HBV infection. Every individual has a natural mortality rate that is constant irrespective of the disease condition. Antiretroviral treatment lowers the mortality among individuals on

treatment and also makes them less infectious to other people. This is the reason why the AIDS cases with symptoms take part in transmission in λ_1 and λ_4. Treatment is accessed only by those who are screened since people will not self-refer to treatment on the basis of infection. The patient that recovers by natural immunity or by the treatment of acute HBV infection once again finds himself or herself back in the vulnerable category and never attains permanent immunity. There is a specific percentage of the newborns who are vaccinated against HBV in their infancy. Immunized individuals will not be susceptible to HBV unless the infection interference of HIV destroys their immunity. The viruses have no immunity or resistance to people of the different age categories as they all are potential candidates to the infections.

3.3 Methods for Deterministic Co-infection Model Analysis

The theories of ordinary differential equations are applied to obtained the analytical solutions of the deterministic co-infection model.

3.3.1 Boundedness and positivity of solutions

Using the theories of ODEs, the positivity of solutions to the deterministic co-infection model without the control variables is examined. The positivity of each compartments are investigated since the model deals with human populations. The values of these biological compartments are expected to be positive and remain positive for all time $t \geq 0$ in the feasible region. A theorem to test the positivity of the model solutions is postulated, followed by a proof using integration techniques such as separation of variables and integrating factor among others. Initial conditions are used in the proof of the theorem to show that all the state variables stay positive. In this case, the temporal rate of change of the entire population is obtained to demonstrate the boundedness of solutions in the feasible region.. Also integration techniques are used. Macías-Díaz (2017) stated that the assumption used is from the fact that all the model solution should lie within the domain of non-negative and restricted within the required domain and provided the epidemiologically well-posed or simply known as biologically and mathematically acceptable model.

3.3.2 Determination of co-infection free and endemic equilibrium point

The co-infection free equilibrium point represents the state at which the system is free of co-infection while the endemic equilibrium point is where the co-infection is present in the population. Setting the infectious classes to zero yields the Co-infection-Free Equilibrium point (CFE). The resulting algebraic equations are evaluated at $I_H = A = I_B = I_{HB} = I_{cB} = I_{HcB} = T_B = T_{HB} = V_H = 0$. We denote the HIV-HBV co-infection free equilibrium point as

$E^0_{HB} = \left(S^0, I^0_H, A^0, I^0_B, I^0_{HB}, I^0_{cB}, I^0_{HcB}, T^0_B, T^0_{HB}, V^0, V^0_H, R^0\right)$.

The uniqueness and existence theorem is used to determine conditions in which endemic equilibrium for which the co-infection is present in the population, exists. The endemic co-infection state is defined as E^*_{HB}.

This state exists in a population if $I^*_H, A^*, I^*_B, I^*_{HB}, I_{cB}, I_{HcB}, T_B, T, V_H$ are non zero. At E^*_{HB}, the equations $S(t)$ and $V(t)$ are solved in terms of the force of infection λ^*.

3.3.3 Determination of model threshold parameters

The most significant parameter in an epidemic model is the basic reproduction number. It enables us to determine whether the infection is going extinct or not. Diekmann and Heesterbeek (2000) and Van den Driessche and Watmough (2002) defined R_0 as the number of secondary infections that an infectious host will generate in a large population of vulnerable hosts during the course of its infectious life. It also provides a stability threshold requirement for the co-infection-free equilibrium point. If the value of this parameter is less than 1, then the infection will not sustain in the involving population and conversely if the value is more than 1 then the infection will remain in the involved population. Thus, the current study's objective is to employ the Jacobian based NGM approach introduced by Diekmann, Heesterbeek, and Roberts (2010) and Van den Driessche and Watmough (2002) to identify the basic and control reproduction numbers for the two illnesses in the framework of co-infection.

In the absence of any controls, R_0, the basic reproduction number, is calculated, and R_c, the control reproduction number is obtained when the control interventions are taken into

consideration. The Jacobian based Next Generation Matrix (NGM) approach involves identifying the infectious classes that contribute directly to the infection, identifying the gains and losses of the infectious individuals from the infectious compartments. The new infections are taken as gains whereas the transfer of infections count as losses. The Jacobian of matrices of new infections F and transfers V are then obtained and assessed at the CFE point. The product of the Jacobian of matrix of new infections and the inverse of Jacobian of matrix of transfers yields the NGM, FV^{-1}. The eigenvalues of Next-Generation Matrix are obtained. As the spectral radius of NGM, the basic reproduction number, commonly represented as R_0, is derived, which is the dominant eigenvalue of FV^{-1}. The estimated number of secondary HIV/AIDS infections caused by a single HIV/AIDS infectious individual during their infectious phase when introduced into a population that is fully susceptible to HIV/AIDS is indicated by the reproduction number, R_H. Comparably, when a single HBV infectious individual is put into a population that is entirely susceptible to HBV, the reproduction number, R_B indicates the anticipated number of secondary HBV infections that individual will create over his or her infectious time. In the presence of control interventions, the control reproduction number, R_C^{HB} is therefore represented in terms of pertinent infection rates owing to HBV and HIV.

3.3.4 Investigating the stability of co-infection free equilibrium point

To determine the local and global stability of the co-infection free equilibrium (CFE) point, stability theorems are utilized. The Routh-Hurwitz criterion presented by DeJesus and Kaufman (1987) is used to examine the local stability of the CFE point whereas the Castillo-Chavez method is applied for performing the global stability of CFE point utilized by Roeger, Feng, and Castillo-Chavez (2009). The Routh-Hurwitz criterion states that the number of roots of the characteristic polynomial with positive real parts (unstable) is equal to the number of changes of sign of the coefficients in the first column of the Routh array. Applying the criterion entails creating the Routh array table and determining the characteristic equation of the Jacobian matrix of the system of ODEs. The sign shifts of the coefficients of the characteristic polynomial in the Routh-array are used to assess the local stability of the CFE point without seeking to determine the roots of the polynomial. A CFE

point is stable if all the elements in the first column of the array are completely positive and the constant term is greater than zero, otherwise the system is unstable. The criterion provides an analytical means for testing the stability of a linear system of any order (Edelstein-Keshet, 1988) and (Soares & Bassanezi, 2020). The Castillo-Chavez method entails the use of the Metzler matrix under two conditions. These conditions are proved for a CFE point to be globally asymptotically stable (GAS) using a theorem. The theorem asserts necessary and sufficient condition for a CFE to be GAS.

3.3.5 Bifurcation analysis

Bifurcation arises when there is a change in the stability of the system or emergence of new state. The Centre Manifold Theory is used for the bifurcation analysis (Castillo-Chavez & Song, 2004) and (Hassard & Wan, 1978). When a DFE and EE points co-exist, then the model exhibits either a forward or backward bifurcation. The Center Manifold theory is a technique used in determining the stability of a system exhibiting bifurcation. It also determines the direction of the bifurcation at the critical value of the bifurcation parameter. The theory encompasses linearizing the system of equations in section 3.3 by change of variables, finding the Jacobian of the system's matrix at CFE point, evaluating the bifurcation parameter at the control reproduction number equal to unity, finding the eigenvalues and the associated eigenvectors of the Jacobian of the linearized system and calculations are eventually made for the coefficients, which are the system's non-zero partial derivatives. This establishes whether the system will show the presence of backward or forward bifurcation.

3.3.6 Sensitivity analysis

Martcheva (2015) defined the sensitivity of a parameter with respect to control reproduction number as the behavior of the model to small changes in the parameter values. The forward normalized sensitivity index method is utilized in local sensitivity index analysis. The method includes differentiating the model with respect to each parameter to yield an additional system of the same size as the initial one, the result of which is the solution sensitivity. A variable's normalized forward sensitivity index to a parameter is determined by dividing the relative change in the state variable by the relative change in the parameter.

The sensitivity index is defined using partial derivatives. According to Chitnis, Hyman, and Cushing (2008), the sensitivity index in this case is provided as follows, taking the parameter as ξ and the basic reproduction number as R_0, then

$$\Lambda_{\xi}^{R_0} = \frac{\partial R_0}{\partial \xi} \times \frac{\xi}{R_0} \tag{3.4.1}$$

By plugging in the initial values for the parameters, each parameter's sensitivity index for the control reproduction number is calculated. These indices can assume both positive and negative values. The indices presented in the previous section can be also represented visually and that is why these variables are plotted with the help of MATLAB program. Sensitivity analysis tells us how important each parameter is to the spread of the illness. Such data is useful for the selection of experimental design as well as for the minimization of multiple non-linear methods and the requirement for data fitting (Powell, Fair, LeClaire, Moore, & Thompson, 2005). Since there are tendencies for errors during data compilation and assumption of basic parameter values, the sensitivity analysis is often used to analyze how similar the model's forecasts are to the parameter values. It is utilized in establishing values that are crucial in affecting the control variable and thus should be addressed through intervention. The impact of every investigated parameter on the control variable is subsequently ascertained using the indices. It is clear that compared to the other negative indices, the positive indices have a greater influence on reproduction number.

3.3.7 Numerical simulations of deterministic co-infection model

The values for the state variables and parameters are collected from the literature to perform the numerical simulations for the deterministic co-infection model to analyze the co-dynamics pattern. For the deterministic model, the ODE solver of Runge-Kutta order 45, which is an embedded numerical Scheme included in the MATLAB package, has been used. Fourth-order Runge Kutta is an approximate numerical solution to first order ordinary differential equation for a certain initial state. It involves four stage approximations and each of these approximations is again broken down into four stages. The general formulation of the method is described as follows; For an I.V.P. of a first-order ODE,

$\frac{dy}{dx} = f(x,y)$ with initial condition, $y(x_0) = y_0$, the basic fourth-order Runge formula for single ODE is;

$$y_{n+1} = y_n + \frac{1}{6}(k_1 + 2k_2 + 2k_3 + k_4)$$
$$\text{where, } k_1 = hf(x_n, y_n), k_2 = hf\left(x_n + \frac{h}{2}, y_n + \frac{k_1}{2}\right), k_3 = hf\left(x_n + \frac{h}{2}, y_n + \frac{k_2}{2}\right),$$

$k_4 = hf(x_n + h, y_n + k_3)$ and h is the step size. This formula can be generalized to a system of ODEs.

Akinsola (2023) pointed that the fourth order Runge-Kutta gives more accurate, more stable and easier to be implemented for the solution of the nonlinear differential equations. As it is clearer and built specifically for the various types of the categories of differential equations, and it presents improved accuracy. The approach is less affected by the initial conditions and the choice of the step size and hence it is more robust. This makes it more reliable particularly in solving hard problems such as the optimization of neural networks problems. Hence, it is used preferably as the other two owing to its accuracy and steadiness while approximating nonlinear differential equations.

3.4 Derivation of an Optimal Control Problem

A deterministic co-infection model is extended to an optimal control model.. The model is formulated by adding the control functions $U = (u_1, u_2, u_3, u_4, u_5)$ where u_1, u_2, u_3, u_4, u_5 are the specific control variables. These variables are also functions of time. Using an optimal control theory, the deterministic co-infection model is optimized to identify the best mitigation method that reduces the number of infected persons over time while effectively balancing the control techniques included in the model. The deterministic model's time-dependent optimal control problem is formulated by the application of Pontryagin's Maximum Principle (Joshi, Lenhart, Li, & Wang, 2006). Our optimization task is to minimize the objective function J while taking control of the variables. Since the study is focused on models of HIV-HBV co-infection and the optimal strategy for prevention and control, the $U(t)$ control function is integrated. When quantifying the state variables dynamics under constraints new control variables $u_1(t), u_2(t), u_3(t), u_4(t)$, and $u_5(t)$ are added to the

deterministic model. It is assumed that the values u_1, u_2, u_3, u_4 and u_5 lie between 0 and 1. If these values equal to zero, then it implies no efforts are being placed in these controls. Similarly, optimal effort infers to these values being 1.

The control function $U(t)$ is defined as follows; u_1 represents the contact control, u_2 is the treatment control, u_3 is the viral load control, u_4 the vaccination control and u_5 represents the effort to control the recovery rate. The contact control, $u_1(t)$, means the ability to prevent the vulnerable persons from becoming the infected persons. Measures like isolation, sensitization, health education and other campaigns, the use of condoms among others not under the clinical form of treatment are related to $u_1(t)$. The treatment control, $u_2(t)$, represents the early diagnosis, detection and testing of susceptible individuals, screening of high-risk exposed individuals. This approach is a first step towards creating treatment plans for those who are affected, such as those with acute HBV infection. The likelihood that an acute HBV infection would develop into a chronic infection is greatly decreased by treatment. Given that some populations have a very high risk of contracting HIV or HBV after exposure, the screening control effort is a critical step for HIV and HBV management care program. Such individuals who do not know their infection status are screened and those identified with the infection are further directed to seek treatment. In this context, the term $u_3(t)$ of "viral load control" depicted the efforts that are required to begin as well as to complete the treatment of the infected individuals. The process also includes the use of government subsidies and other procedures that ensure that people take the drugs as required until the illness is eradicated permanently.

In our model, the level of acute HBV cases is directly dependent on the control variable $u_3(t)$, and the number of infection cases depends on it indirectly. With higher $u_3(t)$, we can reduce both the number of exposed persons and the number of infectious ones. Therefore, it is possible to state that further focus should be made on the reduction of treatment failure. In the HIV-HBV co-infection dynamic system, reducing the treatment failure rate is the control function $u_2(t)$, while control function $u_1(t)$ is responsible for lowering the transmission rate β. On the other hand, the treatment control, $u_2(t)$, contributes to raising the rate of HIV infection and acute HBV infection screening and treatment.

The necessary conditions for optimality is established by Lagrangian and Hamiltonian polynomials. Further, the uniqueness of the optimality conditions is obtained by partial differentiation of the Hamiltonian polynomial with relation to state variables along the transversality requirements. The optimal controls, u_1^*, u_2^*, u_3^*, u_4^*, and u_5^*, are obtained by solving the optimality conditions.

3.4.1 Simulation of the optimal control model numerically

An optimal control solution is obtained through forward and backward Runge-Kutta numerical scheme as explained for the deterministic case using MATLAB (R2017a). Under the control measures, the pattern of infection is demonstrated graphically to ascertain the best control strategy to curb the co-infection. The simulation of each control strategy is also displayed graphically at a time with and without the controls. In addition, the numerical simulation of the implementation of combined control strategies is illustrated on the same axes with and without controls. Further, the percentage reduction in infection outcomes of each control is accounted for.

3.5 SDE Co-infection Model Formulation

While SDEs are used to create the stochastic model from the deterministic model, the formulation of a SDE entails introducing randomness or stochasticity into the deterministic equations that explain the development of the infections. Because it represents the intrinsic unpredictability in the transmission process, such as the coincidence of interactions between susceptible and infected people, stochasticity is essential to epidemiological models. We incorporate stochasticity into the transmission rates of both HIV and HBV, considering factors such as the frequency and randomness of sexual contacts, sharing of needles or other drug paraphernalia, and perinatal transmission. We also consider the existing or potential positive relations between HIV and HBV in regard to disease development and progression. Stochastic components are included to explain the efficacy of treatment and control strategies like antiretroviral therapy (ART) for HIV and anti-HBV therapy (ART), as well as vaccination campaigns and behavioral interventions. We take into account for individual-level heterogeneity in contact patterns, susceptibility, and other factors that influence disease transmission, which may introduce additional stochasticity into the model.

By formulating an SDE for an epidemic model, researchers can better capture the complex and dynamic nature of co-epidemics, including the effects of stochasticity on infection spread and the potential impact of interventions on epidemic dynamics (L. J. Allen, 2010). The study by Farnoosh and Parsamanesh (2017) applied a general SDE to a susceptible-infected-susceptible epidemic model incorporating immigration and vaccination. The Ito stochastic differential equations from transition probabilities technique, which is predicated on the diffusion process, was developed by E. Allen (2007). The stochastic differential equation used by E. Allen (2007) and Farnoosh and Parsamanesh (2017) has the following generic form:

$$dX = H(t,X(t))dt + J(t,X(t))dW(t) \tag{3.6.1}$$

where $X = [X_n]^T = \{S, I_H, A, I_{HB}, T_{HB}, I_{HcB}, V, V_H, I_B, I_{cB}, T_B, R\}^T$ is the population vector of each compartments while $W_t = [W_n(t)]^T$ denotes an nth-dimensional vector of the Wiener process. Vector H and 12×12 matrix S are drift or deterministic part and diffusion coefficients or stochastic terms, respectively. The functions H and J are defined as follows; $H(t,X(t)) = E(\Delta X/\Delta t)$ and $J(t,X(t)) = \sqrt{E\left[\Delta X(\Delta X)^T\right]/\Delta t}$.

The Wiener process, W_t has the following properties;

i) It has a convenient starting point, $t = 0, W_0 = 0$

ii) Continuous function in time, that is, W_t is continuous, jagged at any proximity but still finite.

iii) The increments are distributed independently with a normal distribution with variance, σ^2, and μ zero.

iv) it is independent of what happened before.

According to Ditlevsen and Samson (2013), continuous time processes are the focus of deterministic models, which are frequently represented by ODEs. These theories pre-assume that internal and deterministic mechanisms are the only ones driving the observable dynamics. Nevertheless, there will always be impacts on genuine biological systems that are poorly understood or impractical to formally represent. The analysis of the biological systems under study may suffer if these events are ignored in the modeling. As a

result, there is a growing demand to include more intricate dynamical variability so as to expand the deterministic models. Adding noise or random effects is one method of modeling these components. A system of SDEs is a logical extension of a deterministic differential equations model, in which key parameters are either considered as appropriate random processes or additional random processes are introduced to the governing system of equations. This method makes the assumption that noise contributes to the dynamics.

It is assumed in this section that the state variables

$S(t), I_H(t), I_{HB}(t), A(t), I_B(t), I_{cB}(t), I_{HcB}(t), T_B(t), T_{HB}(t), V(t), V_H(t)$ and $R(t)$ are continuous random state variables, and that $t \in [0, \infty]$, the time parameter, is continuous, that is, $S(t), I_H(t), I_{HB}(t), A(t), I_B(t), I_{cB}(t), I_{HcB}(t), T_B(t), T_{HB}(t), V(t), V_H(t)$ and $R(t) \in [0, N]$, and their corresponding changes are denoted as follows;

$\Delta S = S(t+\Delta t) - S(t)$

$\Delta I_H = I_H(t+\Delta t) - I_H(t)$

$\Delta A = A(t+\Delta t) - A(t)$

$\Delta I_{HB} = I_{HB}(t+\Delta t) - I_{HB}(t)$

$\Delta T_{HB} = T_{HB}(t+\Delta t) - T_{HB}(t)$

$\Delta I_{HcB} = I_{HcB}(t+\Delta t) - I_{HcB}(t)$

$\Delta V = V(t+\Delta t) - V(t)$

$\Delta V_H = V_H(t+\Delta t) - V_H(t)$

$\Delta I_B = I_B(t+\Delta t) - I_B(t)$

$\Delta I_{cB} = I_{cB}(t+\Delta t) - I_{cB}(t)$

$\Delta T_B = T_B(t+\Delta t) - T_B(t)$

$\Delta R = R(t+\Delta t) - R(t)$

Additionally, it is also assumed that the change or transition of random state variables $S(t), I_H(t), A(t), I_{HB}(t), T_{HB}(t), I_{HcB}(t), V(t), V_H(t), I_B(t), I_{cB}(t), T_B(t), R(t)$ is approximately normally distributed,

$\Delta S(t) \sim N\left(\mu(s)\Delta t, \sigma^2(s)\Delta t\right), \Delta I_H(t) \sim N\left(\mu\left(I_H\right)\Delta t, \sigma^2\left(I_H\right)\Delta t\right),$

$\Delta A(t) \sim N\left(\mu(A)\Delta t, \sigma^2(A)\Delta t\right), \Delta I_{HB}(t) \sim N\left(\mu\left(I_{HB}\right)\Delta t, \sigma^2\left(I_{HB}\right)\Delta t\right),$

$\Delta T_{HB}(t) \sim N\left(\mu\left(T_{HB}\right)\Delta t, \sigma^2\left(T_{HB}\right)\Delta t\right), \Delta IHcB(t) \sim N\left(\mu(IHcB)\Delta t, \sigma^2(IHcB)\Delta t\right),$

$\Delta V(t) \sim N\left(\mu(V)\Delta t, \sigma^2(V)\Delta t\right), \Delta V_H(t) \sim N\left(\mu\left(V_H\right)\Delta t, \sigma^2\left(V_H\right)\Delta t\right),$

$\Delta I_B(t) \sim N\left(\mu\left(I_B\right)\Delta t, \sigma^2\left(I_B\right)\Delta t\right),$

$\Delta I_{cB}(t) \sim N\left(\mu\left(I_{cB}\right)\Delta t, \sigma^2\left(I_{cB}\right)\Delta t\right), \Delta T_B(t) \sim N\left(\mu\left(T_B\right)\Delta t, \sigma^2\left(T_B\right)\Delta t\right),$

$\Delta R(t) \sim N\left(\mu(R)\Delta t, \sigma^2(R)\Delta t\right)$

for small time interval Δt.

3.5.1 Numerical method for SDE

Since the explicit solutions of SDEs are rare, solving the system of SDEs obtained above by direct integration techniques is not possible analytically. Thus, we solve the SDEs numerically using Euler-Maruyama numerical method as described in the study by L. J. Allen (2017) and Bonnet (2010). This study utilizes a discrete-time approximations. Euler-Maruyama numerical technique is an extension of the explicit Euler method for solving an I.V.P, demonstrated as follows; given $\frac{dy}{dt} = f(y,t)$ is a first-order ordinary differential equation, then the discretized form using Euler formula becomes,

$\frac{\Delta y}{\Delta t} = \frac{y_{i+1}-y_i}{\Delta t} = f(y,t) \Rightarrow y_{i+1} = y_i + \Delta t f\left(y_i, t_i\right)$, where $i = 0, y_i = y_0$ and $t_i = i\Delta t$

The Euler-Maruyama method is utilized to simulate sample paths of SDEs. The Euler-Maruyama technique stems directly from the derivation of an SDE and has an order of Δt. The Euler-Maruyama method is chosen because of it provides computationally efficient approach to approximate the solution paths of an SDE. The method has order $\frac{1}{2}$ for strong convergence for approximating solution of SDEs (Sauer, 2011).

In general, a system of SDEs follows the Ito's lemma as stated below;

Lemma 1. Suppose that the value of a variable X_t follows an Ito process, then a SDE of X_t in differential form is given by

$$dX_t = H(X(t),t) + J(X(t),t)dW(t) \tag{3.6.2}$$

with initial conditions, $X(0) = X0$ and $0 \leq t \leq T$, where dW is a Wiener process, H and J are both functions of X and t. The finite difference approximation used in the Euler-Maruyama method has the following form:

$$X(t+\Delta t) = X(t) + H(X(t),t)\Delta t + J(X(t),t)\eta\sqrt{\Delta t} \tag{3.6.3}$$

and $\Delta W(t) = W(t+\Delta t) - W(t) \sim \text{Normal}(0, \Delta t)$, where Δt is chosen sufficiently small to ensure a strong convergence of the solution but with a fixed length. In the context of k independent Wiener processes $W(t) = (W_1(t), W_2(t), \ldots\ldots W_k(t))^T$, k independent standard normal random numbers may be found in the vector $\eta = (\eta_1, \eta_2, \ldots.\eta_k)$ where $\eta \in \text{Normal}(0,1)$.

The numerical simulations of SDEs is implemented in MATLAB (R2017a). Independent realizations are obtained for each SDE for three sample paths. Deterministic solution is presented together with stochastic solution. For comparison purposes, descriptive statistics are determined for both stochastic and deterministic trajectories. The related Matlab codes for these numerical scheme are provided in the appendix C .

CHAPTER FOUR: RESULTS AND DISCUSSIONS

4.1 Introduction

In order to determine the conditions for the spread of infection, this chapter explains how each of the specific objectives in section 3.1 are achieved, including the formulation of an HIV and HBV co-infection model, model threshold determination and stability analysis, sensitivity analysis, and backward bifurcation analysis. Thus, solving three models, numerical results are derived from secondary data collected from existing literature. Normalized sensitivity indices are calculated on each of the model parameters and numerical solutions are carried out in order to compare the analytical solutions of the model. The control functions are therefore obtained from the objective function and dynamics under each control evaluated on the population.

4.2 Deterministic Co-infection Model Results

In this section the analytical and numerical solution of the deterministic model is obtained as follows.

4.2.1 Deterministic HIV-HBV co-infection model framework

Based on the above descriptions and assumptions, a deterministic model of co-infection of HIV and HBV is established as shown by the flowchart in figure 4.1 below.

Figure 4.1
HIV and HBV co-infection model schematic diagram

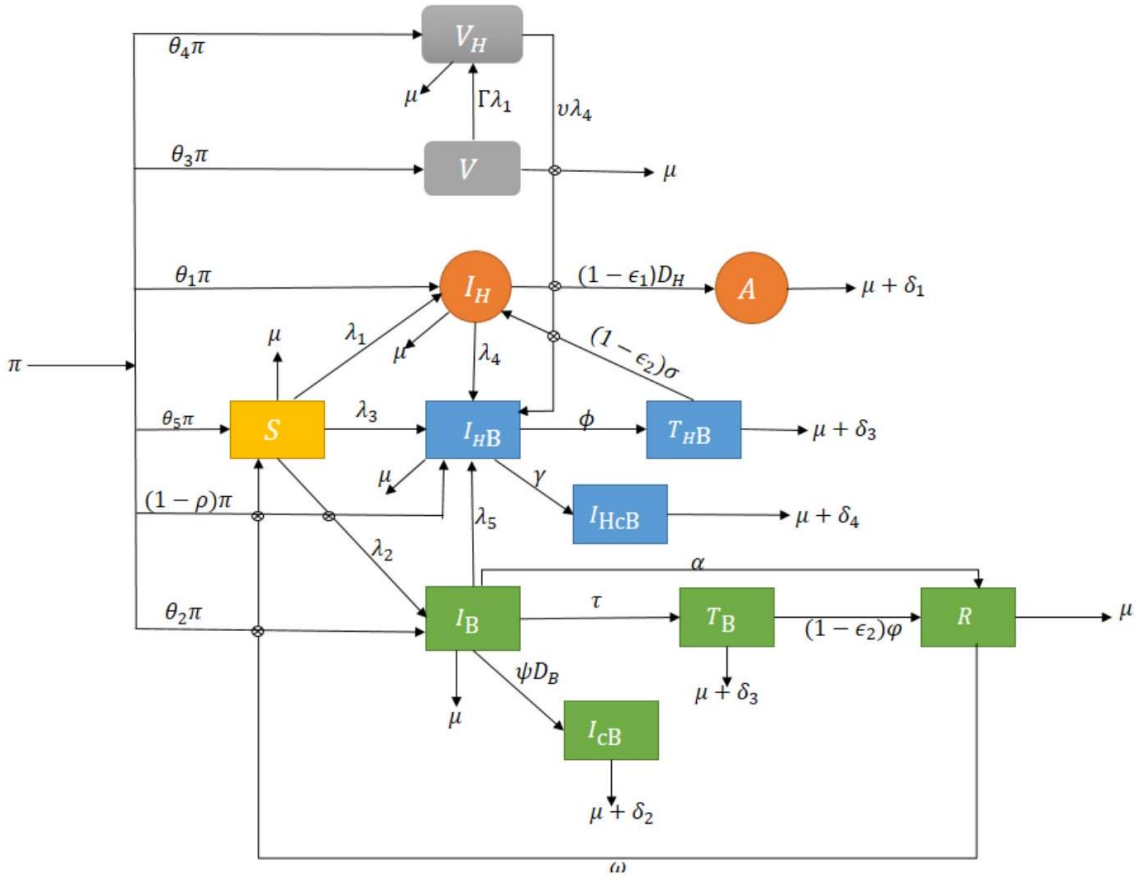

Source: Researcher (2025)

4.2.2 Deterministic co-infection model equations

The model is governed by the following system of non-linear ordinary differential equations derived from the schematic diagram in figure 4.1.

$$\frac{dS}{dt} = \theta_5\pi - (\lambda_1+\lambda_2+\lambda_3+\mu)S + \omega R. \tag{4.2.1}$$

$$\frac{dI_H}{dt} = \theta_1\pi + \lambda_1 S + (1-\varepsilon_2)\sigma T_{HB} - (\lambda_4+\mu+(1-\varepsilon_1)D_H)I_H. \tag{4.2.2}$$

$$\frac{dA}{dt} = (1-\varepsilon_1)D_H I_H - (\delta_1+\mu)A. \tag{4.2.3}$$

$$\frac{dI_{HB}}{dt} = (1-\rho)\pi + \lambda_3 S + (I_H+v)\lambda_4 + \lambda_5 I_B - (\phi+\gamma+\mu)I_{HB}. \tag{4.2.4}$$

$$\frac{dT_{HB}}{dt} = \phi I_{HB} - (\mu+\delta_3+(1-\varepsilon_2)\sigma)T_{HB}. \tag{4.2.5}$$

$$\frac{dI_{HcB}}{dt} = \gamma I_{HB} - (\mu+\delta_4)I_{HcB}. \tag{4.2.6}$$

$$\frac{dV}{dt} = \theta_3\pi - (\mu + \Gamma\lambda_1)V. \tag{4.2.7}$$

$$\frac{dV_H}{dt} = \theta_4\pi + \Gamma\lambda_1 V - (\mu + v\lambda_4)V_H. \tag{4.2.8}$$

$$\frac{dI_B}{dt} = \theta_2\pi + \lambda_2 S - (\mu + \lambda_5 + \alpha + \tau + \psi D_B)I_B. \tag{4.2.9}$$

$$\frac{dI_{cB}}{dt} = \psi D_B I_B - (\mu + \delta_2)I_{cB}. \tag{4.2.10}$$

$$\frac{dT_B}{dt} = \tau I_B - (\mu + \delta_3 + (1-\varepsilon_2)\varphi)T_B. \tag{4.2.11}$$

$$\frac{dR}{dt} = \alpha I_B + (1-\varepsilon_2)\varphi T_B - (\omega + \mu)R. \tag{4.2.12}$$

where $\rho = \theta_1 + \theta_2 + \theta_3 + \theta_4 + \theta_5$, $\lambda_1 = \frac{\beta_1(I_H + \eta_1 I_{HB} + \eta_2 I_{HcB} + \eta_3 A + \eta_4 T_{HB})}{N}$, where $\eta_1 > \eta_2 > \eta_3 > \eta_4$ and $\eta_1 < 1, \eta_2 < 1, \eta_3 < 1, \eta_4 < 1$, $\lambda_2 = \frac{\beta_2(I_B + \chi_1 I_{cB} + \chi_2 I_{HB} + \chi_3 I_{HcB} + \chi_4 T_B + \chi_5 T_{HB})}{N}$, where $\chi_1 > \chi_2 > \chi_3 > \chi_4$, and $\chi_1 < 1, \chi_2 < 1, \chi_3 < 1, \chi_4 < 1$, $\lambda_3 = \frac{\beta_3(I_{HB} + \Psi_1 I_{HcB} + \Psi_2 T_{HB})}{N}$, where, $\Psi_1 > \Psi_2$, and $\Psi_1 < 1, \Psi_2 < 1$, $\lambda_4 = \frac{\beta_4(I_H + \Lambda_1 I_{HB} + \Lambda_2 I_{HCB} + \Lambda_3 A + \Lambda_4 T_{HB} + \Lambda_5 V_H)}{N}$, where $\Lambda_1 > \Lambda_2 > \Lambda_3 > \Lambda_4 > \Lambda_5$ and $\Lambda_1 < 1, \Lambda_2 < 1, \Lambda_3 < 1, \Lambda_4 < 1, \Lambda_5 < 1$

$\lambda_5 = \frac{\beta_5(I_B + \Upsilon_1 I_{HB} + \Upsilon_2 I_{cB} + \Upsilon_3 I_{HCB} + \Upsilon_4 T_B + \Upsilon_5 T_{HB})}{N}$,

where $\Upsilon_1 > \Upsilon_2 > \Upsilon_3 > \Upsilon_4 > \Upsilon_5$ for $\Upsilon_1 < 1, \Upsilon_2 < 1, \Upsilon_3 < 1, \Upsilon_4 < 1, \Upsilon_5 < 1$

and $\Gamma \leq 1$ and $v \leq 1$.

Hence the total number of humans at any given time, t, is determined by

$$N(t) = S(t) + I_H(t) + A(t) + V(t) + V_H(t) + I_{HB}(t) + I_{HcB}(t) \tag{4.2.13}$$

$$+ T_{HB}(t) + I_B(t) + I_{cB}(t) + T_B(t) + R(t)$$

4.2.3 Positivity of state variables

For all times $t \geq 0$, the governing differential equations' solution is non-negative, since in the human population under consideration there are sub-populations co-infected with HIV, HBV and other infections. This is a necessary condition for the model to be biologically realistic and mathematically acceptable in analysis. Techniques of differential and integral

calculus are applied for the analysis in the following theorems.

Theorem 1. Let $S(0) \geq 0, I_H(0) \geq 0, A(0) \geq 0, I_B(0) \geq 0, I_{cB}(0) \geq 0, T_B(0) \geq 0, R(0) \geq 0, I_{HB}(0) \geq 0, I_{HcB}(0), T_{HB}(0) \geq 0, V(0) \geq 0, V_H(0) \geq 0$

be the solution to the differential equations 4.2.1 to 4.2.12.

Proof. From equation (4.2.2.1) $\frac{dS}{dt} = \theta_5\pi - (\lambda_1 + \lambda_2 + \lambda_3 + \mu)S + \omega R$ and since $\theta_5\pi + \omega R \geq 0$ it follows that

$$\frac{dS}{dt} \geq -(\lambda_1 + \lambda_2 + \lambda_3 + \mu)S \tag{4.2.14}$$

By separation of variables, equation (4.2.14) becomes

$$\frac{dS}{S} \geq -(\lambda_1 + \lambda_2 + \lambda_3 + \mu)\,dt \tag{4.2.15}$$

and integrating both sides of (4.2.15) with respect to t, we get

$\ln S(t) \geq \frac{d}{dt}\left[\int_0^t -(\lambda_1(s) + \lambda_2(s) + \lambda_3(s) + \mu)\,dt + K\right]$,

where K is a constant of integration

$S(t) \geq \frac{d}{dt}\left[\text{K}\exp\int_0^t (-(\lambda_1(s) + \lambda_2(s) + \lambda_3(s) + \mu)\,dt)\right]$

At $t = 0, K = S_0$ hence $S(t) \geq \left[S_0 \exp\int_0^t (-(\lambda_1(s) + \lambda_2(s) + \lambda_3(s) + \mu)\,dt)\right]$

As $t \to \infty, S(t) \geq \left[S_0 \exp\int_0^t (-(\lambda_1(s) + \lambda_2(s) + \lambda_3(s) + \mu)\,dt)\right] \geq 0$, thus $S(t)$ stays positive for all time $t \geq 0$

Similarly by the same technique, it follows that

$I_H(t) \geq I_H(0)\exp\int_0^t (-(\lambda_4(s) + \mu + (1-\varepsilon_1)D_H)\,dt) \geq 0,$

$A(t) \geq A_0 \exp(-(\delta_1 + \mu)t) \geq 0,$

$I_B(t) \geq I_{B0}\exp\int_0^t (-(\mu + \lambda_5(s) + \alpha + \tau + \psi D_B)\,dt) \geq 0\,,$

$I_{cB}(t) \geq I_{cB0}\exp(-(\mu + \delta_2)t) \geq 0,$

$T_B(t) \geq T_{B0}\exp(-(\mu + \delta_3 + (1-\varepsilon_2)\varphi)t) \geq 0\,,$

$R(t) \geq R_0 \exp(-(\omega+\mu)t) \geq 0,$

$I_{HB}(t) \geq I_{\text{HBo}} \exp(-(\phi+\gamma+\mu)t) \geq 0,$

$T_{HB}(t) \geq T_{HB0} \exp\left(-\left(\mu+\delta_3+(1-\varepsilon_2)\,\sigma\right)t\right) \geq 0,$

$I_{HcB}(t) \geq I_{HcB0} \exp\left(-\left(\mu+\delta_4\right)t\right) \geq 0\,,$

$V(t) \geq V_0 \exp \int_0^t \left(-\left(\mu+\Gamma\lambda_1(s)\right)dt\right) \geq 0$ and

$V_H \geq V_{H0} \exp \int_0^t \left(-\left(\mu+v\lambda_4(s)\right)dt\right) \geq 0.$

Thus $S(t), I_H(t), A(t), I_B(t), I_{cB}(t), T_B(t), R(t), I_{HB}(t), I_{HcB}(t), T_{HB}(t), V(t),$ and $V_H(t)$ also stays positive for all time $t \geq 0$.

4.2.4 Boundedness of solutions and feasible region

The feasible region is the region of convergence to the solution of the system of equations 4.2.1 to 4.2.12. The solution stays within this region throughout, that is, positively invariant. This is implemented with the rate of change of the total population, N, with respect to time, denoted as $\frac{dN}{dt}$. This is done to signify that the solution to the problem lies strictly in the feasible region.

Theorem 2. The required region Ω given by

$\Omega = \{S(t), I_H(t), A(t), I_B(t), I_{CB}(t), T_B(t), R(t), I_{HB}(t), I_{HCB}(t), T_{HB}(t), V(t), V_H(t) \in$

$R_+^{12}, N \leq \frac{\pi}{\mu}\Big|$

$S(0) \geq 0, I_H(0) \geq 0, A(0) \geq 0, I_B(0) \geq 0, I_{CB}(0) \geq 0, T_B(0) \geq 0, R(0) \geq 0, I_{HB}(0) \geq$

$0, I_{HcB}(0), T_{HB}(0) \geq 0, V(0) \geq 0, V_H(0) \geq 0\}$

is positively invariant and attracting the solutions of the system of equations 4.2.1-4.2.12 to Ω.

Proof. We consider equation 4.2.13 from the system of equations in section 4.2.2

$N(t) = S(t) + I_H(t) + A(t) + V(t) + V_H(t) + I_{HB}(t) + I_{HcB}(t) + T_{HB}(t) + I_B(t) + I_{cB}(t) +$

$T_B(t) + R(t)$

differentiating both sides with respect to t yields

$$\frac{dN}{dt} = \frac{dS}{dt} + \frac{dI_H}{dt} + \frac{dA}{dt} + \frac{dV}{dt} + \frac{dV_H}{dt} + \frac{dI_{HB}}{dt} + \frac{dI_{HcB}}{dt} + \frac{dT_{HB}}{dt} + \frac{dI_B}{dt} + \frac{dI_{cB}}{dt} + \frac{dT_B}{dt} + \frac{dR}{dt} \tag{4.2.16}$$

Substituting equations 4.2.1 to 4.2.12 into 4.2.16 we have,

$$\begin{aligned}
\frac{dN}{dt} &= \theta_5\pi - (\lambda_1+\lambda_2+\lambda_3+\mu)S + \omega R + \theta_1\pi + \lambda_1 S + (1-\varepsilon_2)\sigma T_{HB} - \\
&(\lambda_4+\mu+(1-\varepsilon_1)D_H)I_H + (1-\varepsilon_1)D_H I_H - (\delta_1+\mu)A + \theta_3\pi - (\mu+\Gamma\lambda_1)V \\
&+ \theta_4\pi + \Gamma\lambda_1 V - (\mu+\nu\lambda_4)V_H + (1-\rho)\pi + \lambda_3 S + (I_H+\nu)\lambda_4 + \lambda_5 I_B - \\
&(\phi+\gamma+\mu)I_{HB} + \gamma I_{HB} - (\mu+\delta_4)I_{HcB} + \phi I_{HB} - (\mu+\delta_3+(1-\varepsilon_2)\sigma)T_{HB} \\
&+ \theta_2\pi + \lambda_2 S - (\mu+\lambda_5+\alpha+\tau+\psi D_B)I_B + \psi D_B I_B - (\mu+\delta_2)I_{cB} + \tau I_B \\
&- (\mu+\delta_3+(1-\varepsilon_2)\varphi)T_B + \alpha I_B + (1-\varepsilon_2)\varphi T_B - (\omega+\mu)R
\end{aligned}$$

Expanding and simplifying we obtain

$$\begin{aligned}
\frac{dN}{dt} &= \pi - (A+S+V+V_H+I_B+I_{cB}+I_{HcB}+T_B+T_{HB}+R)\mu - \\
&A\delta_1 - I_{cB}\delta_2 - T_B\delta_3 - T_{HB}\delta_3 - I_{HcB}\delta_4 - \omega R + (1-V_H)\nu\lambda_4
\end{aligned} \tag{4.2.17}$$

but $N = A+S+V+V_H+I_B+I_{cB}+I_{HcB}+T_B+T_{HB}+R$, (4.2.17) reduces to

$$\frac{dN}{dt} + \mu N = \pi - A\delta_1 - I_{cB}\delta_2 - (T_B+T_{HB})\delta_3 - I_{HcB}\delta_4 - \omega R + (1-V_H)\nu\lambda_4 \tag{4.2.18}$$

Therefore by comparison theorem (4.2.18) reduces to

$$\frac{dN}{dt} + \mu N \leq \pi + (1-V_H)\nu\lambda_4 \tag{4.2.19}$$

Integrating (4.2.19) using integrating factor (I.F.), $\exp(\int \mu dt) = K\exp(\mu t)$ and multiply-

ing I.F on both sides of (4.2.19), we have

$$K\exp(\mu t)\left(\frac{dN}{dt}+\mu N\right)\leq K\exp(\mu t)\left(\pi+(1-V_H)\,v\lambda_4\right) \tag{4.2.20}$$

Integrating both sides of (4.2.20) with respect to t gives

$$K\exp(\mu t)N(t)\leq\frac{K\pi}{\mu}\exp(\mu t)+\int_0^t k\exp(\mu t)\left(1-V_H(s)\right)v\lambda_4(s)dt+H \tag{4.2.21}$$

Dividing I.F on both sides of (4.2.21), we obtain

$$N(t)\leq\frac{\pi}{\mu}+\frac{1}{K}\exp(-\mu t)\int_0^t K\exp(\mu t)\left(1-V_H(s)\right)v\lambda_4(s)dt+\frac{H}{K}\exp(-\mu t) \tag{4.2.22}$$

At $t=0$, (4.2.22) becomes

$N(0)=\frac{\pi}{\mu}+\frac{H}{K},\Longleftrightarrow H=K\left(N_0-\frac{\pi}{\mu}\right)$, substituting for H in (4.2.22), we obtain,

$N(t)\leq\frac{\pi}{\mu}+\frac{1}{K}\exp(-\mu t)\int_0^t k\exp(\mu t)\left(1-V_H(s)\right)v\lambda_4(s)dt+\left(N_0-\frac{\pi}{\mu}\right)\exp(-\mu t)$

As $t\to\infty$,

$\frac{1}{K}\exp(-\mu t)\int_0^t k\exp(\mu t)\left(1-V_H(s)\right)v\lambda_4(s)dt=0,\left(N_0-\frac{\pi}{\mu}\right)\exp(-\mu t)=0$, thus

$\lim_{t\to\infty}N(t)\leq\frac{\pi}{\mu}$.

This demonstrates that the solutions inside of $\mathbb{R}$ are bounded. It follows from this that any solution to the system of equations 4.2.1 to 4.2.12 that begins in $\mathbb{R}$ ends up staying in $\mathbb{R}$ forever. The dynamics of the system of equations in $\mathbb{R}_+^{12}$ can be adequately taken into consideration as $\mathbb{R}$ is positively invariant and attractive.

4.2.5 HIV-HBV co-infection free equilibrium point

This is a solution to the system of equations 4.2.1-4.2.12, where the population is considered susceptible and neither HIV nor HBV infection is present. In the absence of HIV

and HBV infections, the co-infection-free equilibrium point (CFE) of the system of equations 4.2.1 to 4.2.12 is achieved by setting infectious classes to zero, $I_H = 0, A = 0, I_{HB} = 0, I_{HcB} = 0, T_{HB} = 0, I_B = 0, I_{cB} = 0, T_B = 0, R = 0$, and $V_H = 0$ and the equations 4.2.1 to 4.2.12 consist of two compartment classes; the susceptible, S and vaccinated, V. The vaccination of the population implies absence of HIV and HBV infections as well as co-infection. Thus, we let the CFE point as $E^0_{HB} = \left(S^0, I^0_H, A^0, I^0_{HB}, I^0_{HcB}, T^0_{HB}, I^0_B, I_{cB}, T^0_B, R^0, V^0, V^0_H\right)$. By setting equation (4.2.1) to (4.2.12) to zero it follows that $S^0 = \frac{\theta_5 \pi}{\mu}, V^0 = \frac{\theta_3 \pi}{\mu}$, hence $E^0_{HB} = \left(\frac{\theta_5 \pi}{\mu}, 0, 0, 0, 0, 0, 0, 0, 0, 0, \frac{\theta_3 \pi}{\mu}, 0\right)$.

4.3 Computation of Model Threshold Parameters

In epidemic models, the basic reproductive rate is the most significant of all the parameters regarded as a threshold (Ma, 2020). It is used to study the pattern of prevalence and tendency of an infection within a given population as well as helping understand the patterns of infection spread. The magnitude of the basic reproduction number varies for different infections or diseases. Various methods are available for determining the basic reproduction number. These include; Next Generation Matrix (NGM), survival function method and method of characteristics. In this study, NGM and survival function methods are employed to find $R_{0,N}$ and $R_{0,S}$ as used by Agarwal, Nieto, Ruzhansky, Torres, et al. (2021). Further, the strength number is also computed using the NGM method.

4.3.1 Basic reproduction number using the next generation matrix

This is the number of secondary infections that one infective host individual will produce in an entirely susceptible population during its lifespan as infective. It is conventionally denoted as R_0 in nearly all epidemic models. Van den Driessche and Watmough (2002) initially introduced and used the Next-Generation Matrix technique, which we employ to determine the basic reproduction number. The basic reproduction number R_{HB} is then de-

fined as the spectral radius of the NGM. The NGM is defined as the matrix that relates the number of newly infected individuals in the various categories in consecutive generations. The method involves the following; identification of infectious compartments, defining the infection transfer matrix as g and the matrix of new infections as f, determination of Jacobian of matrix of f and g as F and G respectively evaluated at CFE point, finding the inverse of matrix G as G^{-1}. The NGM is defined as the product of FG^{-1} and $R_{HB} = \rho\left(FG^{-1}\right)$, where $\rho(A)$ denotes the spectral radius of A. The spectral radius of a matrix A is defined as the maximum of the absolute values of the eigenvalues of A. Based on these procedures, we compute the R_H, R_B and R_{HB} as follows.

The infectious classes are identified as ($I_H, A, I_B, I_{HB}, I_{cB}, I_{HcB}, T_B, T_{HB}, V_H$)

The identification of matrix of new infections and transfer of infections were guided by the work of Nthiiri, Lavi, and Manyonge (2015) as follows;

Matrix of new infections $f = \begin{pmatrix} \theta_1\pi + \lambda_1 S \\ 0 \\ \theta_2\pi + \lambda_2 S \\ (1-\rho)\pi + \lambda_3 S + (I_H + v)\lambda_4 + \lambda_5 I_B \\ 0 \\ 0 \\ 0 \\ 0 \\ \theta_4\pi + \Gamma\lambda_1 V \end{pmatrix}$

and matrix of transfer of infections

$$g = \begin{pmatrix} (\lambda_4 + \mu + (1-\varepsilon_1) D_H) I_H - (1-\varepsilon_2) \sigma T_{HB} \\ (\delta_1 + \mu) A - (1-\varepsilon_1) D_H I_H \\ (\mu + \lambda_5 + \alpha + \tau + \psi D_B) I_B \\ (\phi + \gamma + \mu) I_{HB} \\ (\mu + \delta_2) I_{cB} - \psi D_B I_B \\ (\mu + \delta_4) I_{HcB} - \gamma I_{HB} \\ (\mu + \delta_3 + (1-\varepsilon_2) \varphi) T_B - \tau I_B \\ (\mu + \delta_3 + (1-\varepsilon_2) \sigma) T_{HB} - \phi I_{HB} \\ (\mu + v\lambda_4) V_H \end{pmatrix}$$

The Jacobian matrix of f and g at the equilibrium point where co-infection is absent is obtained as,

$$E^0_{HB} = \left(\frac{\theta_5 \pi}{\mu}, 0, 0, 0, 0, 0, 0, 0, 0, \frac{\theta_3 \pi}{\mu}, 0 \right)$$

$$F = \begin{pmatrix} f_{11} & f_{12} & 0 & f_{14} & 0 & f_{16} & 0 & f18 & 0 \\ 0 & 0 & 0 & 0 & 0 & 0 & 0 & 0 & 0 \\ 0 & 0 & f_{33} & f_{34} & f_{35} & f_{36} & f_{37} & f_{38} & 0 \\ f_{41} & f_{42} & 0 & f_{44} & 0 & f_{46} & 0 & f_{48} & f_{49} \\ 0 & 0 & 0 & 0 & 0 & 0 & 0 & 0 & 0 \\ 0 & 0 & 0 & 0 & 0 & 0 & 0 & 0 & 0 \\ 0 & 0 & 0 & 0 & 0 & 0 & 0 & 0 & 0 \\ 0 & 0 & 0 & \phi & 0 & 0 & 0 & 0 & 0 \\ f_{91} & f_{92} & 0 & f_{94} & 0 & f_{96} & 0 & f_{98} & 0 \end{pmatrix}$$

where,

$$f_{11} = \frac{\theta_5 \pi \beta_1}{\mu}, f_{12} = \frac{\theta_5 \pi \beta_1 \eta_3}{\mu}, f_{14} = \frac{\theta_5 \pi \beta_1 \eta_1}{\mu}, f_{16} = \frac{\theta_5 \pi \beta_1 \eta_2}{\mu}, f_{18} = \frac{\theta_5 \pi \beta_1 \eta_4}{\mu}$$

$$f_{33} = \frac{\theta_5 \pi \beta_2}{\mu}, f_{34} = \frac{\theta_5 \pi \beta_2 \chi_2}{\mu}, f_{35} = \frac{\theta_5 \pi \beta_2 \chi_1}{\mu}, f_{36} = \frac{\theta_5 \pi \beta_2 \chi_3}{\mu}, f_{37} = \frac{\theta_5 \pi \beta_2 \chi_4}{\mu}$$

$$f_{38} = \frac{\theta_5 \pi \beta_2 \chi_5}{\mu}, f_{41} = \beta_4 v, f_{42} = \beta_4 v \Lambda_3, f_{44} = \frac{\theta_5 \pi \beta_3}{\mu} + \beta_4 v \Lambda_1$$

$$f_{46} = \frac{\theta_5 \pi \beta_3 \Psi_1}{\mu} + v \beta_4 \Lambda_2, f_{48} = \frac{\theta_5 \pi \beta_3 \Psi_2}{\mu} + v \beta_4 \Lambda_4, f49 = v \beta_4 \Lambda_5$$

$$f_{91} = \frac{\theta_3 \pi \Gamma \beta_1}{\mu}, f_{92} = \frac{\theta_3 \pi \eta_3 \Gamma \beta_1}{\mu}, f_{94} = \frac{\theta_3 \pi \eta_1 \Gamma \beta_1}{\mu}$$

$f_{96} = \frac{\theta_3 \pi \eta_2 \Gamma \beta_1}{\mu}, f_{98} = \frac{\theta_3 \pi \eta_4 \Gamma \beta_1}{\mu}$ are elements of matrix F.

and

$$\mathrm{G} = \begin{pmatrix} G_{11} & 0 & 0 & 0 & 0 & 0 & 0 & G_{18} & 0 \\ G_{21} & G_{22} & 0 & 0 & 0 & 0 & 0 & 0 & 0 \\ 0 & 0 & G_{33} & 0 & 0 & 0 & 0 & 0 & 0 \\ 0 & 0 & 0 & G_{44} & 0 & 0 & 0 & 0 & 0 \\ 0 & 0 & G_{53} & 0 & G_{55} & 0 & 0 & 0 & 0 \\ 0 & 0 & 0 & -\gamma & 0 & G_{66} & 0 & 0 & 0 \\ 0 & 0 & -\tau & 0 & 0 & 0 & G_{77} & 0 & 0 \\ 0 & 0 & 0 & -\phi & 0 & 0 & 0 & G_{88} & 0 \\ 0 & 0 & 0 & 0 & 0 & 0 & 0 & 0 & \mu \end{pmatrix}$$

where;

$G_{11} = \mu + D_H (1 - \varepsilon_1), G_{18} = (-1 + \varepsilon_2) \sigma,$

$G_{21} = (\varepsilon_1 - 1) D_H, G_{22} = \delta_1 + \mu,$

$G_{33} = \alpha + \mu + \tau + \psi D_B, G_{44} = \phi + \gamma + \mu,$

$G_{53} = -\psi D_B, G_{55} = \mu + \delta_2, G_{66} = \mu + \delta_4, G_{77} = \mu + \delta_3 + (1 - \varepsilon_2) \varphi,$

$G_{88} = \mu + \delta_3 + (1 - \varepsilon_2) \sigma$, are the elements of matrix G .

With the aid of Mathematica software, the inverse of G is obtained as

$$G^{-1} = \begin{pmatrix} W_1 & 0 & 0 & W_2 & 0 & 0 & 0 & W_3 & 0 \\ W_4 & W_5 & 0 & W_6 & 0 & 0 & 0 & W_7 & 0 \\ 0 & 0 & W_8 & 0 & 0 & 0 & 0 & 0 & 0 \\ 0 & 0 & 0 & W_9 & 0 & 0 & 0 & 0 & 0 \\ 0 & 0 & W_{10} & 0 & W_{11} & 0 & 0 & 0 & 0 \\ 0 & 0 & 0 & W_{12} & 0 & W_{13} & 0 & 0 & 0 \\ 0 & 0 & W_{14} & 0 & 0 & 0 & W_{15} & 0 & 0 \\ 0 & 0 & 0 & W_{16} & 0 & 0 & 0 & W_{17} & 0 \\ 0 & 0 & 0 & 0 & 0 & 0 & 0 & 0 & W_{18} \end{pmatrix} \tag{4.2.23}$$

where

$$W_1 = \frac{1}{\mu + D_H(1-\varepsilon_1)}, W_2 = \frac{\sigma\phi(1-\varepsilon_2)}{(\gamma+\mu+\phi)(\mu+D_H(1-\varepsilon_1))(\mu+\delta_3+(1-\varepsilon_2)\sigma)},$$
$$W_3 = \frac{\sigma(1-\varepsilon_2)}{(\mu+D_H(1-\varepsilon_1)(\mu+\delta_3+(1-\varepsilon_2)\sigma)}, W_4 = \frac{D_H(1-\varepsilon_1)}{(\mu+\delta_1)(\mu+D_H(1-\varepsilon_1))},$$
$$W_5 = \frac{1}{\mu+\delta_1}, W_6 = \frac{\sigma\phi D_H(\varepsilon_1-1)(\varepsilon_2-1)}{(\gamma+\mu+\phi)(\mu+\delta_1)(\mu+D_H(1-\varepsilon_1))(\mu+\delta_3+(1-\varepsilon_2)\sigma)},$$
$$W_7 = \frac{\sigma D_H(\varepsilon_1-1)(\varepsilon_2-1)}{(\gamma+\mu+\phi)(\mu+\delta_1)(\mu+D_H(1-\varepsilon_1))(\mu+\delta_3+(1-\varepsilon_2)\sigma)},$$
$$W_8 = \frac{1}{\alpha+\mu+\tau+\psi D_B},$$
$$W_9 = \frac{1}{\phi+\gamma+\mu}, W_{10} = \frac{\psi D_B(\mu+\varphi+\delta_3-\varphi\varepsilon_2)}{(\alpha+\mu+\tau+\psi D_B)(\mu+\delta_2)(\mu+\delta_3+(1-\varepsilon_2)\varphi)},$$
$$W_{11} = \frac{1}{\mu+\delta_2}, W_{12} = \frac{\gamma}{(\phi+\gamma+\mu)(\mu+\delta_4)},$$
$$W_{13} = \frac{1}{\mu+\delta_4}, W_{14} = \frac{1}{(\alpha+\mu+\tau+\psi D_B)(\mu+\delta_3+(1-\varepsilon_2)\varphi)},$$
$$W_{15} = \frac{\phi}{\mu+\delta_3+(1-\varepsilon_2)\varphi}, W_{16} = \frac{1}{(\phi+\gamma+\mu)(\mu+\delta_3+(1-\varepsilon_2)\sigma)},$$
$$W_{17} = \frac{1}{\mu+\delta_3+(1-\varepsilon_2)\sigma} \text{ and } W_{18} = \frac{1}{\mu}$$

The eigenvalues of NGM, FG^{-1} is given by,

$$FG^{-1}-PI=\begin{pmatrix} a_{11}-P & a_{12} & 0 & a_{14} & 0 & a_{16} & 0 & a_{18} & 0 \\ 0 & -P & 0 & 0 & 0 & 0 & 0 & 0 & 0 \\ 0 & 0 & c_{33}-P & c_{34} & c_{35} & c_{36} & c_{37} & c_{38} & 0 \\ d_{41} & d_{42} & 0 & d_{44}-P & 0 & d_{46} & 0 & d_{48} & d_{49} \\ 0 & 0 & 0 & 0 & -P & 0 & 0 & 0 & 0 \\ 0 & 0 & 0 & 0 & 0 & -P & 0 & 0 & 0 \\ 0 & 0 & 0 & 0 & 0 & 0 & -P & 0 & 0 \\ 0 & 0 & 0 & 0 & 0 & 0 & 0 & -P & 0 \\ I_{91} & I_{92} & 0 & I_{94} & 0 & I_{96} & 0 & I_{98} & -P \end{pmatrix} \tag{4.2.24}$$

whose elements are represented as below

$$a_{11} = \frac{\pi\beta_1\theta_5}{\mu\left(\mu + D_H\left(1-\varepsilon_1\right)\right)} + \frac{\pi D_H\beta_1\eta_3\theta_5\left(1-\varepsilon_1\right)}{\mu\left(\mu+\delta_1\right)\left(\mu + D_H\left(1-\varepsilon_1\right)\right)}, a_{12} = \frac{\pi\beta_1\eta_3\theta_5}{\mu\left(\delta_1+\mu\right)}$$

$$a_{14} = \frac{\pi\beta_1\eta_1\theta_5}{\mu(\phi+\gamma+\mu)} - \frac{\pi\beta_1\theta_5\sigma\phi\left(\varepsilon_2-1\right)}{\mu\left(\mu + D_H\left(1-\varepsilon_1\right)\right)(\phi+\gamma+\mu)\left(\mu+\delta_3+\left(1-\varepsilon_2\right)\sigma\right)}$$

$$+ \frac{\pi\gamma\beta_1\eta_2\theta_5}{\mu(\phi+\gamma+\mu)\left(\mu+\delta_4\right)} + \frac{\pi\phi\beta_1\eta_4\theta_5}{\mu(\phi+\gamma+\mu)\left(\mu+\delta_3+\left(1-\varepsilon_2\right)\sigma\right)}$$

$$- \frac{\pi D_H\beta_1\eta_3\theta_5\sigma\phi\left(\varepsilon_1-1\right)\left(\varepsilon_2-1\right)}{\mu(\gamma+\mu+\phi)\left(\mu+\delta_1\right)\left(\mu + D_H\left(1-\varepsilon_1\right)\right)\left(\mu+\delta_3+\left(1-\varepsilon_2\right)\sigma\right)}$$

$$a_{16} = \frac{\pi\beta_1\eta_2\theta_5}{\mu\left(\mu+\delta_4\right)},$$

$$a_{18} = \frac{\pi\beta_1\eta_4\theta_5 + \mu\sigma\left(1-\varepsilon_2\right)}{\mu\left(\mu+\delta_3+\left(1-\varepsilon_2\right)\sigma\right)}$$

$$+ \frac{\pi D_H\beta_1\eta_3\theta_5\sigma\left(\varepsilon_1-1\right)\left(\varepsilon_2-1\right)}{\mu(\gamma+\mu+\phi)\left(\mu+\delta_1\right)\left(\mu + D_H\left(1-\varepsilon_1\right)\right)\left(\mu+\delta_3+\left(1-\varepsilon_2\right)\sigma\right)}$$

$$- \frac{\pi\beta_1\theta_5\sigma\left(\varepsilon_2-1\right)}{\mu\left(\mu + D_H\left(1-\varepsilon_1\right)\right)\left(\mu+\delta_3+\left(1-\varepsilon_2\right)\sigma\right)}$$

$$c_{33} = \frac{\pi\beta_2\theta_5}{\mu\left(\alpha+\mu+\tau+\psi D_B\right)} + \frac{\pi\beta_2\theta_5\chi_4\tau}{\mu\left(\alpha+\mu+\tau+\psi D_B\right)\left(\mu+\delta_3+\left(1-\varepsilon_2\right)\varphi\right)}$$

$$+ \frac{\pi\beta_2\theta_5\chi_1\psi D_B}{\mu\left(\alpha+\mu+\tau+\psi D_B\right)\left(\mu+\delta_2\right)},$$

$$c_{34} = \frac{\pi\beta_2\chi_2\theta_5}{\mu(\gamma+\mu+\phi)} + \frac{\pi\gamma\beta_2\chi_3\theta_5}{\mu(\gamma+\mu+\phi)\left(\mu+\delta_4\right)} + \frac{\pi\phi\beta_2\chi_5\theta_5}{\mu(\gamma+\mu+\phi)\left(\mu+\delta_3+\left(1-\varepsilon_2\right)\sigma\right)},$$

$$c_{35} = \frac{\pi\beta_2\chi_1\theta_5}{\mu\left(\mu+\delta_2\right)}, c_{36} = \frac{\pi\beta_2\chi_3\theta_5}{\mu\left(\mu+\delta_4\right)}, c_{37} = \frac{\pi\beta_2\chi_4\theta_5}{\mu\left(\mu+\delta_3+\left(1-\varepsilon_2\right)\varphi\right)},$$

$$c_{38} = \frac{\pi\beta_2\chi_5\theta_5}{\mu\left(\mu+\delta_3+\left(1-\varepsilon_2\right)\sigma\right)},$$

$$d_{41} = \frac{v\beta_4}{\left(\mu + D_H\left(1-\varepsilon_1\right)\right)} - \frac{D_H\beta_4 v\Lambda_3\left(\varepsilon_1-1\right)}{\left(\mu+\delta_1\right)\left(\mu + D_H\left(1-\varepsilon_1\right)\right)},$$

$$d_{42} = \frac{v\beta_4\Lambda_3}{\mu+\delta_1},$$

$$d_{44} = \frac{v\beta_4\sigma\phi\left(1-\varepsilon_2\right)}{\left(\mu + D_H\left(1-\varepsilon_1\right)\right)(\phi+\gamma+\mu)\left(\mu+\delta_3+\left(1-\varepsilon_2\right)\sigma\right)} +$$

$$D_H\beta_4 v\Lambda_3\sigma\phi\left(\varepsilon_1-1\right)\left(\varepsilon_2-1\right)$$

$$\overline{(\phi+\gamma+\mu)\left(\mu+\delta_1\right)\left(\mu + D_H\left(1-\varepsilon_1\right)\right)\left(\mu+\delta_3+\left(1-\varepsilon_2\right)\sigma\right)}$$

$$+ \frac{\pi\beta_3\theta_5 + \beta_4\mu v\Lambda_1}{\mu(\gamma+\mu+\phi)} + \frac{\gamma(\mu v\beta_4\Lambda_2 + \beta_3\theta_5\pi\Psi_1)}{\mu(\phi+\gamma+\mu)\left(\mu+\delta_4\right)} + \frac{\phi\left(\beta_4\Lambda_4\mu v + \beta_3\theta_5\pi\Psi_2\right)}{\mu(\phi+\gamma+\mu)\left(\mu+\delta_3+\left(1-\varepsilon_2\right)\sigma\right)}$$

$$d_{46} = \frac{v\mu\beta_4\Lambda_2 + \beta_3\theta_5\pi\Psi_1}{\mu\left(\mu+\delta_4\right)},$$

$$d_{48} = \frac{v\mu\beta_4\Lambda_4 + \beta_3\theta_5\pi\Psi_2}{\mu\left(\mu+\delta_3+(1-\varepsilon_2)\sigma\right)} + \frac{D_H\beta_4 v\Lambda_3\sigma\left(\varepsilon_1-1\right)\left(\varepsilon_2-1\right)}{\left(\mu+\delta_1\right)\left(\mu+D_H\left(1-\varepsilon_1\right)\right)\left(\mu+\delta_3+(1-\varepsilon_2)\sigma\right)} - \frac{\beta_4 v\sigma\left(\varepsilon_2-1\right)}{\left(\mu+D_H\left(1-\varepsilon_1\right)\right)\left(\mu+\delta_3+(1-\varepsilon_2)\sigma\right)},$$

$$d_{49} = \frac{v\beta_4\Lambda_5}{\mu},$$

$$I_{91} = \frac{\theta_3\pi\Gamma\beta_1}{\mu\left(\mu+D_H\left(1-\varepsilon_1\right)\right)} - \frac{\pi\Gamma D_H\beta_1\eta_3\theta_3\left(\varepsilon_1-1\right)}{\mu\left(\mu+\delta_1\right)\left(\mu+D_H\left(1-\varepsilon_1\right)\right)},$$

$$I_{92} = \frac{\theta_3\pi\eta_3\Gamma\beta_1}{\mu\left(\delta_1+\mu\right)},$$

$$I_{96} = \frac{\theta_3\pi\eta_2\Gamma\beta_1}{\mu\left(\mu+\delta_4\right)},$$

$$I_{94} = \frac{\theta_3\pi\eta_1\Gamma\beta_1}{\mu(\gamma+\mu+\phi)} + \frac{\pi\Gamma\beta_1\phi\eta_4\theta_3}{\mu(\gamma+\mu+\phi)\left(\mu+\delta_3+(1-\varepsilon_2)\sigma\right)} + \frac{\pi\Gamma D_H\beta_1\eta_3\theta_3\sigma\phi\left(\varepsilon_1-1\right)\left(\varepsilon_2-1\right)}{\mu(\gamma+\mu+\phi)\left(\mu+\delta_1\right)\left(\mu+D_H\left(1-\varepsilon_1\right)\right)\left(\mu+\delta_3+(1-\varepsilon_2)\sigma\right)} + \frac{\gamma\pi\Gamma\beta_1\eta_2\theta_3}{\mu(\gamma+\mu+\phi)\left(\mu+\delta_4\right)} - \frac{\pi\Gamma\beta_1\theta_3\sigma\phi\left(\varepsilon_2-1\right)}{\mu(\gamma+\mu+\phi)\left(\mu+D_H\left(1-\varepsilon_1\right)\right)\left(\mu+\delta_3+(1-\varepsilon_2)\sigma\right)},$$

$$I_{98} = \frac{\theta_3\pi\eta_4\Gamma\beta_1}{\mu\left(\mu+\delta_3+(1-\varepsilon_2)\sigma\right)} + \frac{\pi\Gamma\sigma D_H\beta_1\eta_3\theta_3\left(\varepsilon_1-1\right)\left(\varepsilon_2-1\right)}{\mu\left(\mu+\delta_1\right)\left(\mu+D_H\left(1-\varepsilon_1\right)\right)\left(\mu+\delta_3+(1-\varepsilon_2)\sigma\right)} - \frac{\pi\Gamma\sigma\beta_1\theta_3\left(\varepsilon_2-1\right)}{\mu\left(\mu+D_H\left(1-\varepsilon_1\right)\right)\left(\mu+\delta_3+(1-\varepsilon_2)\sigma\right)}$$

The determinant of 4.2.24 is obtained by reducing $FG^{-1} - PI$ to upper triangular matrix T and using Gaussian elimination method as follows, where I is a 12×12 identity matrix and P is a scalar.

$R_4 \to d_{41}R_1 - (a_{11} - P)R_4$

$$J = \begin{pmatrix} a_{11}-P & a_{12} & 0 & a_{14} & 0 & a_{16} & 0 & a_{18} & 0 \\ 0 & -P & 0 & 0 & 0 & 0 & 0 & 0 & 0 \\ 0 & 0 & c_{33}-P & c_{34} & c_{35} & c_{36} & c_{37} & c_{38} & 0 \\ 0 & J_{42} & 0 & J_{44} & 0 & J46 & 0 & J48 & J49 \\ 0 & 0 & 0 & 0 & -P & 0 & 0 & 0 & 0 \\ 0 & 0 & 0 & 0 & 0 & -P & 0 & 0 & 0 \\ 0 & 0 & 0 & 0 & 0 & 0 & -P & 0 & 0 \\ 0 & 0 & 0 & 0 & 0 & 0 & 0 & -P & 0 \\ I_{91} & I_{92} & 0 & I_{94} & 0 & I_{96} & 0 & I_{98} & -P \end{pmatrix}$$

where

$J_{42} = d_{41}a_{12} - (a_{11}-P)\,d_{42}, J_{44} = d_{41}a_{14} - (a_{11}-P)\,(d_{44}-P),$

$J_{46} = d_{41}a_{16} - (a_{11}-P)\,d_{46}, J_{48} = d_{41}a_{18} - (a_{11}-P)\,d_{48},$

$J_{49} = -(a_{11}-P)\,d_{49}.$

$$R_9 \to I_{91}R_1 - (a_{11}-P)\,R_9$$

$$X = \begin{pmatrix} a_{11}-P & a_{12} & 0 & a_{14} & 0 & a_{16} & 0 & a_{18} & 0 \\ 0 & -P & 0 & 0 & 0 & 0 & 0 & 0 & 0 \\ 0 & 0 & c_{33}-P & c_{34} & c_{35} & c_{36} & c_{37} & c_{38} & 0 \\ 0 & X_{42} & 0 & X_{44} & 0 & X_{46} & 0 & X_{48} & X_{49} \\ 0 & 0 & 0 & 0 & -P & 0 & 0 & 0 & 0 \\ 0 & 0 & 0 & 0 & 0 & -P & 0 & 0 & 0 \\ 0 & 0 & 0 & 0 & 0 & 0 & -P & 0 & 0 \\ 0 & 0 & 0 & 0 & 0 & 0 & 0 & -P & 0 \\ 0 & X_{92} & 0 & X_{93} & 0 & X_{95} & 0 & X_{98} & X_{99} \end{pmatrix}$$

where;

$$X_{42} = d_{41}a_{12} - (a_{11} - P)\, d_{42}, X_{44} = d_{41}a_{14} - (a_{11} - P)\,(d_{44} - P)\,,$$

$$X_{46} = d_{41}a_{16} - (a_{11} - P)\, d_{46}, X_{48} = d_{41}a_{18} - (a_{11} - P)\, d_{48},$$

$$X_{49} = -\,(a_{11} - P)\, d_{49}, X_{92} = I_{91}a_{12} - (a_{11} - P)\, I_{92},$$

$$X_{93} = I_{91}a_{14} - (a_{11} - P)\, I_{94}, X_{95} = I_{91}a_{16} - (a_{11} - P)\, I_{96},$$

$X_{98} = I_{91}a_{18} - (a_{11} - P)\, I_{98}, X_{99} = P\,(a_{11} - P)$ are the elements of matrix X.

$R_4 \rightarrow (d_{41}a_{12} - (a_{11} - P)\, d_{42})\, R_2 + PR_4$

$$Y = \begin{pmatrix} a_{11}-P & a_{12} & 0 & a_{14} & 0 & a_{16} & 0 & a_{18} & 0 \\ 0 & -P & 0 & 0 & 0 & 0 & 0 & 0 & 0 \\ 0 & 0 & c_{33}-P & c_{34} & c_{35} & c_{36} & c_{37} & c_{38} & 0 \\ 0 & 0 & 0 & Y_{44} & 0 & Y_{46} & 0 & Y_{48} & Y_{49} \\ 0 & 0 & 0 & 0 & -P & 0 & 0 & 0 & 0 \\ 0 & 0 & 0 & 0 & 0 & -P & 0 & 0 & 0 \\ 0 & 0 & 0 & 0 & 0 & 0 & -P & 0 & 0 \\ 0 & 0 & 0 & 0 & 0 & 0 & 0 & -P & 0 \\ 0 & Y_{92} & 0 & Y_{94} & 0 & Y_{96} & 0 & Y_{98} & Y99 \end{pmatrix}$$

where;

$Y_{44} = P\,(d_{41}a_{14} - (a_{11} - P)\,(d_{44} - P))\,, Y_{46} = P\,(d_{41}a_{16} - (a_{11} - P)\, d_{46})\,,$

$Y_{48} = P\,(d_{41}a_{18} - (a_{11} - P)\, d_{48})\,, Y_{49} = -\,(a_{11} - P)\, Pd_{49}, Y_{92} = a_{12}I_{91} - (a_{11} -$

$P)I_{92},$

$Y_{94} = I_{91}a_{14} - (a_{11} - P)\, I_{94}, Y_{96} = a_{16}I_{91} - (a_{11} - P)\, I_{96},$

$Y_{98} = I_{91}a_{18} - (a_{11} - P)\, I_{98}, Y_{99} = P\,(a_{11} - P)$ are the elements of matrix Y.

$$R_9 \to (a_{12}I_{91} - (a_{11} - P)\, I_{92})\, R_2 + PR_9$$

$$N = \begin{pmatrix} a_{11}-P & a_{12} & 0 & a_{14} & 0 & a_{16} & 0 & a_{18} & 0 \\ 0 & -P & 0 & 0 & 0 & 0 & 0 & 0 & 0 \\ 0 & 0 & c_{33}-P & c_{34} & c_{35} & c_{36} & c_{37} & c_{38} & 0 \\ 0 & 0 & 0 & N_{44} & 0 & N_{46} & 0 & N_{48} & N_{49} \\ 0 & 0 & 0 & 0 & -P & 0 & 0 & 0 & 0 \\ 0 & 0 & 0 & 0 & 0 & -P & 0 & 0 & 0 \\ 0 & 0 & 0 & 0 & 0 & 0 & -P & 0 & 0 \\ 0 & 0 & 0 & 0 & 0 & 0 & 0 & -P & 0 \\ 0 & 0 & 0 & N_{94} & 0 & N_{96} & 0 & N_{98} & N_{99} \end{pmatrix}$$

where;

$$N_{44} = P\left(d_{41}a_{14} - (a_{11} - P)\left(d_{44} - P\right)\right), N_{46} = P\left(d_{41}a_{16} - (a_{11} - P)\, d_{46}\right),$$

$$N_{48} = P\left(d_{41}a_{18} - (a_{11} - P)\, d_{48}\right), N_{49} = -\left(a_{11} - P\right) P d_{49},$$

$$N_{94} = P\left(I_{91}a_{14} - (a_{11} - P)\, I_{94}\right), N_{96} = P\left(a_{16}I_{91} - (a_{11} - P)\, I_{96}\right),$$

$$N_{98} = P\left(I_{91}a_{18} - (a_{11} - P)\, I_{98}\right), N_{99} = P^2\left(a_{11} - P\right)$$

are the elements of matrix N.

$$R_9 \to \left(P\left(I_{91}a_{14} - (a_{11} - P)\, I_{94}\right)\right) R_4 - P\left(d_{41}a_{14} - (a_{11} - P)\left(d_{44} - P\right)\right) R_9$$

$$M = \begin{pmatrix} a_{11}-P & a_{12} & 0 & a_{14} & 0 & a_{16} & 0 & a_{18} & 0 \\ 0 & -P & 0 & 0 & 0 & 0 & 0 & 0 & 0 \\ 0 & 0 & c_{33}-P & c_{34} & c_{35} & c_{36} & c_{37} & c_{38} & 0 \\ 0 & 0 & 0 & m_1 & 0 & m_2 & 0 & m_3 & -(a_{11}-P)Pd_{49} \\ 0 & 0 & 0 & 0 & -P & 0 & 0 & 0 & 0 \\ 0 & 0 & 0 & 0 & 0 & -P & 0 & 0 & 0 \\ 0 & 0 & 0 & 0 & 0 & 0 & -P & 0 & 0 \\ 0 & 0 & 0 & 0 & 0 & 0 & 0 & -P & 0 \\ 0 & 0 & 0 & 0 & 0 & m_4 & 0 & m_5 & m_6 \end{pmatrix}$$

where;

$m_1 = P\left(d_{41}a_{14} - (a_{11}-P)(d_{44}-P)\right), m_2 = P\left(d_{41}a_{16} - (a_{11}-P)d_{46}\right),$

$m_3 = P\left(d_{41}a_{18} - (a_{11}-P)d_{48}\right)$

$m_4 = P^2\left(a_{16}d_{41} + (P-a_{11})d_{46}\right)\left(a_{14}I_{91} + (P-a_{11})I_{94}\right)$

$-P^2\left(a_{14}d_{41} - (P-a_{11})(P- \ d_{44})\left(a_{16}I_{91} + (P-a_{11})I_{96}\right)\right),$

$m_5 = P^2\left(I_{91}a_{14} - (a_{11}-P)I_{94}\right)\big)\left(d_{41}a_{18} - (a_{11}-P)d_{48}\right)$

$-P^2\left(d_{41}a_{14} - (a_{11}- \ P)(d_{44}-P)\right)\left(I_{91}a_{18} - (a_{11}-P)I_{98}\right)$

$m_6 = -P^2\left(I_{91}a_{14} - (a_{11}-P)I_{94}\right)\big)(a_{11}-P)d_{49}$

$-P^3\left(d_{41}a_{14} - (a_{11}-P)(d_{44}- \ P)\right)(a_{11}-P)$ are the elements of matrix M.

$R_9 \to m_4R_6 + PR_9$

$$W = \begin{pmatrix} a_{11}-P & a_{12} & 0 & a_{14} & 0 & a_{16} & 0 & a_{18} & 0 \\ 0 & -P & 0 & 0 & 0 & 0 & 0 & 0 & 0 \\ 0 & 0 & c_{33}-P & c_{34} & c_{35} & c_{36} & c_{37} & c_{38} & 0 \\ 0 & 0 & 0 & W_{44} & 0 & W_{46} & 0 & W_{48} & W_{49} \\ 0 & 0 & 0 & 0 & -P & 0 & 0 & 0 & 0 \\ 0 & 0 & 0 & 0 & 0 & -P & 0 & 0 & 0 \\ 0 & 0 & 0 & 0 & 0 & 0 & -P & 0 & 0 \\ 0 & 0 & 0 & 0 & 0 & 0 & 0 & -P & 0 \\ 0 & 0 & 0 & 0 & 0 & 0 & 0 & W_{98} & W_{99} \end{pmatrix}$$

where ;

$W_{44} = P\left(d_{41}a_{14} - (a_{11}-P)(d_{44}-P)\right), W_{46} = P\left(d_{41}a_{16} - (a_{11}-P)d_{46}\right),$

$W_{48} = P\left(d_{41}a_{18} - (a_{11}-P)d_{48}\right), W_{49} = -(a_{11}-P)Pd_{49}$

$W_{98} = P^3\left(I_{91}a_{14} - (a_{11}-P)I_{94}\right)\left(d_{41}a_{18} - (a_{11}-P)d_{48}\right)$

$-P^3\left(d_{41}a_{14} - (a_{11}- \ P)(d_{44}-P)\right)\left(I_{91}a_{18} - (a_{11}-P)I_{98}\right),$

$W_{99} = -P^3\left(I_{91}a_{14} - (a_{11}-P)I_{94}\right)(a_{11}-P)d_{49}$

$-P^4\left(d_{41}a_{14} - (a_{11}-P)(d_{44}- \ P)\right)(a_{11}-P)$ are the elements of matrix W.

$R_9 \to w_1R_8 + PR_9$

and finally the upper triangular matrix, T becomes

$$T = \begin{pmatrix} a_{11}-P & a_{12} & 0 & a_{14} & 0 & a_{16} & 0 & a_{18} & 0 \\ 0 & -P & 0 & 0 & 0 & 0 & 0 & 0 & 0 \\ 0 & 0 & c_{33}-P & c_{34} & c_{35} & c_{36} & c_{37} & c_{38} & 0 \\ 0 & 0 & 0 & T_{44} & 0 & T_{46} & 0 & T_{48} & T_{49} \\ 0 & 0 & 0 & 0 & -P & 0 & 0 & 0 & 0 \\ 0 & 0 & 0 & 0 & 0 & -P & 0 & 0 & 0 \\ 0 & 0 & 0 & 0 & 0 & 0 & -P & 0 & 0 \\ 0 & 0 & 0 & 0 & 0 & 0 & 0 & -P & 0 \\ 0 & 0 & 0 & 0 & 0 & 0 & 0 & 0 & T_{99} \end{pmatrix}$$

where;

$T_{44} = P\left(d_{41}a_{14} - (a_{11}-P)(d_{44}-P)\right), T_{46} = P\left(d_{41}a_{16} - (a_{11}-P)d_{46}\right),$

$T_{48} = P\left(d_{41}a_{18} - (a_{11}-P)d_{48}\right), T_{49} = -(a_{11}-P)Pd_{49}$

$T_{99} = -P^4\left(I_{91}a_{14} - (a_{11}-P)I_{94}\right)\left(a_{11}-P\right)d_{49} - P^5\left(d_{41}a_{14} - (a_{11}-P)(d_{44}- P)(a_{11}-P)\right.$

are the components of matrix T, which is triangular whose determinant is determined by multiplying the primary diagonal's elements;

$$-P^5(a_{11}-P)(c_{33}-P)T_{44}T_{49} = 0 \tag{4.2.25}$$

substituting for T_{44} and T_{49} into (4.2.25) and simplifying yields the characteristic polynomial

$$P^5(a_{11}-P)(c_{33}-P)\left(k_1P^3 - k_2P^2 - k_3P + k_0\right) = 0 \tag{4.2.26}$$

where $k_2 = a_{11} + d_{44}, k_3 = a_{14}d_{41} - a_{11}d_{44} + d_{49}I_{94}$ and $k_0 = a_{11}d_{49}I_{94} - a_{14}d_{49}I_{91}$

solving 4.2.26, gives the eigenvalues of the reduced form of NGM as ;

$P_1 = P_2 = P_3 = P_4 = P_5 = 0, P_6 = c_{33}, P_7 = a_{11},$

$$P_8 = \frac{k_2}{3} + \frac{\sqrt[3]{2}\left(k_2^2+3k_3\right)}{3\left(2k_2^3-27k_0+9k_2k_3+\sqrt{-4\left(k_2^2+3k_3\right)^3+\left(2k_2^3-27k_0+9k_2k_3\right)^2}\right)^{\frac{1}{3}}} +$$

$$\frac{\left(2k_2^3-27k_0+9k_2k_3+\sqrt{-4\left(k_2^2+3k_3\right)^3+\left(2k_2^3-27k_0+9k_2k_3\right)^2}\right)^{\frac{1}{3}}}{3\sqrt[3]{2}}$$

$$\frac{\left(1+i\sqrt{3}\right)\left(-k_2^2-3k_3\right)}{}$$

$$P_9 = \frac{k_2}{3} + \frac{3\times 2^{\frac{2}{3}}\left(2k_2^3-27k_0+9k_2k_3+\sqrt{-4\left(k_2^2+3k_3\right)^3+\left(2k_2^3-27k_0+9k_2k_3\right)^2}\right)^{\frac{1}{3}}}{\left(-1+i\sqrt{3}\right)\left(2k_2^3-27k_0+9k_2k_3+\sqrt{-4\left(k_2^2+3k_3\right)^3+\left(2k_2^3-27k_0+9k_2k_3\right)^2}\right)^{\frac{1}{3}}}$$

$$P_{10} = \frac{k_2}{3} + \frac{\left(1-i\sqrt[3]{2}\right)\left(-k_2^2-3k_3\right)}{3\times 2^{\frac{2}{3}}\left(2k_2^3-27k_0+9k_2k_3+\sqrt{-4\left(k_2^2+3k_3\right)^3+\left(2k_2^3-27k_0+9k_2k_3\right)^2}\right)^{\frac{1}{3}}} +$$

$$\frac{\left(1+i\sqrt{3}\right)\left(2k_2^3-27k_0+9k_2k_3+\sqrt{-4\left(k_2^2+3k_3\right)^3+\left(2k_2^3-27k_0+9k_2k_3\right)^2}\right)^{\frac{1}{3}}}{6\sqrt[3]{2}}$$

$$\frac{}{6\sqrt{3}}$$

The complex eigenvalues P_9 and P_{10} are ignored since the solution to the model exists and bounded within the positive real domain $\mathbb{R}$. By inspection, it is evident from the above expressions that P_6 corresponds to basic reproduction number to the case of HBV infection, P_7 to the case of HIV and P_8 contains the components of HIV-HBV co-infection. Thus, setting parameters representing the control interventions $\theta_3 = \theta_4 = \varepsilon_1 = \varepsilon_2 = \tau = \phi = 0$, the corresponding basic reproduction numbers for HBV and HIV-HBV co-infection case is given by;

$$R_{0,N}^{H} = \frac{\pi\beta_1\theta_5}{\mu\left(\mu+D_H\right)} + \frac{\pi D_H\beta_1\eta_3\theta_5}{\mu\left(\mu+\delta_1\right)\left(\mu+D_H\right)} \tag{4.2.27}$$

$$R_{0,N}^{B} = c_{33} = \frac{\pi\beta_2\theta_5}{\mu\left(\alpha+\mu+\psi D_B\right)} + \frac{\pi\beta_2\theta_5\chi_1\psi D_B}{\mu\left(\alpha+\mu+\psi D_B\right)\left(\mu+\delta_2\right)} \tag{4.2.28}$$

$$R_{0,N}^{HB} = \frac{k_2}{3} + \frac{\sqrt[3]{2}\left(k_2^2+3k_3\right)}{3\left(2k_2^3-27k_0+9k_2k_3+\sqrt{-4\left(k_2^2+3k_3\right)^3+\left(2k_2^3-27k_0+9k_2k_3\right)^2}\right)^{\frac{1}{3}}} + \frac{\left(2k_2^3-27k_0+9k_2k_3+\sqrt{-4\left(k_2^2+3k_3\right)^3+\left(2k_2^3-27k_0+9k_2k_3\right)^2}\right)^{\frac{1}{3}}}{3\sqrt[3]{2}} \tag{4.2.29}$$

and like most co-infection models, the maximum for the HIV-HBV co-infection model is included in the basic reproduction number and is expressed as $R_{0,N}^{HB} = \max\left\{P_7, R_{0,N}^{H}, R_{0,N}^{B}\right\}$. However, the spectral radius of the Jacobian matrix for the full model is ascertained in numerical simulation. Eigenvalues describes the stability of a system. In epidemic models, complex eigenvalues are often avoided due to their complexity and applicability. These eigenvalues are not directly meaningful in the context of epidemic modeling. Instead, researchers should focus on real eigenvalues, which correspond to exponential growth or decay in the population of infected individuals. This approach simplifies the analysis and interpretation of the model (Hitzer, 2002). The maximum values for $R_{0,N}^{HB}$ is confirmed numerically in section 4.5.3.

The reproduction numbers calculated in 4.2.27, 4.2.8 have the interpretation that they can be used to account for the contribution of each infection to HIV-HBV co-infection in 4.2.29. They can also be used to ascertain the spread, persistence and endemicity of the co-infection. In essence, in co-infection models, the concept of R_0 now becomes much more complicated since the infection may have an effect on the spread of another. The presence of one infection may cause the immune system of the host to be weak, which would further increase the R_0 of the second infection. On the other hand, a protective

immune response against one might be provoked by the other or they may both require similar resources in the host; resulting in reduced value of R_0 of the second infection. In other instances, co-infections may result in a more severe disease outcome and possible changes to the transmission dynamics which can change the R_0 values of both the infections. Consequently, in the co-infection models, the R_0 of each organism must be considered in conjunction with others circulating in the population where they may interact and affect transmission levels and severity of the diseases they cause.

4.3.2 Control reproduction numbers

Control reproduction number was defined by Brauer et al. (2019) as the average number of susceptible individuals that an infected individual can infect once control measures; treatment, vaccination and natural immunity are taken into account. This is given by the dominant eigenvalue known as the spectral radius ζ of the Jacobian matrix represented as $\zeta\left(FG^{-1}\right)$. We use the notation R_C for the control reproduction number estimated when control interventions are in place. Therefore, the control reproduction numbers for each of the cases are as follows;

$$R_C^H = \frac{\pi\beta_1\theta_5}{\mu\left(\mu + D_H\left(1-\varepsilon_1\right)\right)} + \frac{\pi D_H\beta_1\eta_3\theta_5\left(1-\varepsilon_1\right)}{\mu\left(\mu+\delta_1\right)\left(\mu + D_H\left(1-\varepsilon_1\right)\right)} \tag{4.2.30}$$

$$R_C^B = \frac{\pi\beta_2\theta_5}{\mu\left(\alpha+\mu+\tau+\psi D_B\right)} + \frac{\pi\beta_2\theta_5\chi_4\tau}{\mu\left(\alpha+\mu+\tau+\psi D_B\right)\left(\mu+\delta_3+\left(1-\varepsilon_2\right)\varphi\right)} + \frac{\pi\beta_2\theta_5\chi_1\psi D_B}{\mu\left(\alpha+\mu+\tau+\psi D_B\right)\left(\mu+\delta_2\right)} \tag{4.2.31}$$

$$R_C^{HB} = \frac{k_2}{3} + \frac{\sqrt[3]{2}\left(k_2^2+3k_3\right)}{3\left(2k_2^3-27k_0+9k_2k_3+\sqrt{-4\left(k_2^2+3k_3\right)^3+\left(2k_2^3-27k_0+9k_2k_3\right)^2}\right)^{\frac{1}{3}}} + \frac{\left(2k_2^3-27k_0+9k_2k_3+\sqrt{-4\left(k_2^2+3k_3\right)^3+\left(2k_2^3-27k_0+9k_2k_3\right)^2}\right)^{\frac{1}{3}}}{3\sqrt[3]{2}} \tag{4.2.32}$$

The numerical values for control reproduction numbers given by 4.2.30, 4.2.31 and 4.2.32 are obtained numerically obtained in section 4.5.3.

4.3.3 Computation of basic reproduction using the survival function method

The survival function defines the number of new infections due to an initial case and comprises of three components;

(i) the rate at which an individual in a particular class causes new infections, $k_t b_t$

(ii) the probability, P that an individual is still in the class at time, t.

(iii) the probability that an initial case will enter that class (Shaw & Kennedy, 2021).

Thus, the basic reproduction number based on this approach is defined by the integral of the product of the first two terms (i) and (ii) multiplied by the third term (iii) derived from the contagious classes and following the study by J. Li, Blakeley, et al. (2011), the reproductive number by method of survival function is given by

$$R_{0,S} = \int_0^\infty (kb \times P) dt \tag{4.2.33}$$

where kb is the number of new susceptible individuals that the infected individual infects in unit time when infected for total time t and P is probability that the newly infecting individual develops an infection that persists for at least time t.

Casting 4.2.33 to all the infectious classes and integrating, we have

$R_{0,I_H} = \beta_1 S^0 \int_0^\infty \exp\left(-\left(\mu + (1-\varepsilon_1) D_H\right) t\right) dt = \frac{\beta_1 S^0}{\mu + (1-\varepsilon_1) D_H}$

$R_{0,A} = 0 \int_0^\infty \exp\left(-\left(\delta_1 + \mu\right) t\right) dt = \frac{0}{\mu + \delta_1} = 0$

$R_{0,I_B} = \beta_2 S^0 \int_0^\infty \exp\left(-\left(\mu + \alpha + \tau + \psi D_B\right) t\right) dt = \frac{\beta_2 S^0}{\mu + \alpha + \tau + \psi D_B}$

$R_{0,I_{cB}} = 0 \int_0^\infty \exp\left(-\left(\mu + \delta_2\right) t\right) dt = \frac{0}{\mu + \delta_2} = 0$

$R_{0,I_{HB}} = \beta_3 S^0 \int_0^\infty \exp(-(\phi + \gamma + \mu) t) dt = \frac{\beta_3 S^0}{\phi + \gamma + \mu}$

$R_{0,I_{HCB}} = 0\int_0^\infty \exp\left(-\left(\mu+\delta_4\right)t\right)dt = \frac{0}{\mu+\delta_4} = 0$

$R_{0,T_B} = 0\int_0^\infty \exp\left(-\left(\mu+\delta_3+\left(1-\varepsilon_2\right)\varphi\right)t\right)dt = \frac{0}{\mu+\delta_3+(1-\varepsilon_2)\varphi} = 0$

$R_{0,T_{HB}} = 0\int_0^\infty \exp\left(-\left(\mu+\delta_3+\left(1-\varepsilon_2\right)\sigma\right)t\right)dt = \frac{0}{\mu+\delta_3+(1-\varepsilon_2)\sigma} = 0$

$R_{0,V_H} = \Gamma\beta_1 V^0\int_0^\infty \exp\left(-\left(\mu+v\beta_4\Lambda_5\right)t\right)dt = \frac{\Gamma\beta_1 V^0}{\mu+v\beta_4\Lambda_5}.$

Hence 4.2.33 becomes

$$R_{0,S} = R_{0,I_H} + R_{0,A} + R_{0,I_B} + R_{0,I_{cB}} + R_{0,I_{HB}} + R_{0,I_{HcB}} + R_{0,T_B} + R_{0,T_{HB}} + R_{0,V_H} \quad (4.2.34)$$

Substituting for S^0 and V^0 as previously obtained into 4.2.34 yields

$$R_{0,S} = \frac{\pi}{\mu}\left(\frac{\beta_1\theta_5}{\mu+(1-\varepsilon_1)D_H} + \frac{\beta_2\theta_5}{\mu+\alpha+\tau+\psi D_B} + \frac{\beta_3\theta_5}{\phi+\gamma+\mu} + \frac{\Gamma\beta_1\theta_3}{\mu+v\beta_4\Lambda_5}\right) \quad (4.2.35)$$

Equation 4.2.34 gives the sum of individual reproduction numbers of the infectious compartments; $I_H, A, I_B, I_{cB}, I_{HB}, I_{HcB}, T_B, T_{HB}$, and V_H from an index case respectively. The $R_{0,S}$ in 4.2.35 accounts for the reproduction number from each of the infectious classes in the presence of control interventions at CFE point, E^0_{HB}. Thus, it represents the control reproduction number R_C. Unlike the NGM, the survival function has the advantage that it always produces the average number of secondary individuals infected by a single infected individual, in the same class. It is a generalized method of calculating the basic reproductive ratio that is not restricted to ODEs. However, determining the individual probabilities can be cumbersome, especially if multiple states are involved as in co-infection models. Accordingly, although this method always gives the correct R_0 in practice, it is rather ineffective. This is particularly the case for models of sufficient complexity and these are usually the most common types of models encountered.

4.3.4 Determination of strength number

The study by Atangana and İğret Araz (2021), among many epidemic models indicated that while some success has been achieved, great limitations have also been experienced in terms of the basic reproduction number. While this concept has been employed to determine whether the spread will be severe or not, some great weaknesses have been pointed out by some researchers. For instance, they realized that such value is not unique as it can be obtained using different methods. Another issue is that, this number should have been a function of time not a constant value. Additionally, it was also noticed that a reproductive number cannot be used to indicate whether a model will predict waves or not (Hussien, Genawi, Hagabdulla, & Ahmed, 2025). As a result of these shortcomings, recently an alternative number called strength number is suggested and it is still under several investigation to establish whether it can be used to help detect some complexities in the infection spread or at least it can help detect waves in a spread (Farman, Shehzad, Akgül, Baleanu, & Sen, 2023).

The value is derived using the NGM by taking the second derivative of infectious classes. The evaluation of the signs of the strength number helps to quantify the complexities in the spread or waves. If the second derivatives of the infection is zero, then there is no complexity or wave in the infection spread. A positive second derivative implies that there are more than one wave or complexities involved in the spread while a negative value shows that there is one single wave in the spread. The concept of Frequency-Dependent Transmission (FDT) is applied for the force of infection, which asserts that the per capita contact rate between susceptible (S) and infected (I) people in FDT is independent of population density (Ecology, 2013). Therefore, density has no effect on transmission rates. Here we discuss about the strength number A_0 related to the co-infection model as follows.

Applying the quotient rule, the associated second derivatives of the contagious classes $I_H, A, I_B, I_{cB}, I_{HB}, I_{HcB}, T_B, T_{HB}$ and V_H are;

$\frac{\partial^2}{\partial I_H^2}\left(\frac{\beta_1 S^0 I_H}{N}\right) = \beta_1 S^0 \frac{\partial^2}{\partial I_H^2}\left(\frac{I_H}{N}\right) = \beta_1 S^0 \frac{\partial}{\partial I_H}\left(\frac{(N - I_H \cdot N')}{N^2}\right) = -\frac{\beta_1 S^0}{N^2}$

$\frac{\partial^2}{\partial I_B^2}\left(\frac{\beta_2 S^0 I_B}{N}\right) = \beta_2 S^0 \frac{\partial^2}{\partial I_B^2}\left(\frac{I_H}{N}\right) = \beta_2 S^0 \frac{\partial}{\partial I_H}\left(\frac{(N - I_B \cdot N')}{N^2}\right) = -\frac{\beta_2 S^0}{N^2}$

$\frac{\partial^2}{\partial I_{HB}^2}\left(\frac{(\beta_3 S^0 + \beta_4 v\Lambda_1) I_{HB}}{N}\right) = (\beta_3 S^0 + \beta_4 v\Lambda_1)\frac{\partial^2}{\partial I_B^2}\left(\frac{I_{HB}}{N}\right)$

$= (\beta_3 S^0 + \beta_4 v\Lambda_1)\left(\frac{(N - I_{HB} \cdot N')}{N^2}\right) = -\frac{(\beta_3 S^0 + \beta_4 v\Lambda_1)}{N^2}$

The second derivatives of $A, I_{cB}, I_{HcB}, T_B, T_{HcB}, T_{HB}$ and V_H are zero. Therefore, the Jacobian of the matrix of new infections and transfer of infections for the second derivatives of the infectious classes are found as

$$F_A = \begin{pmatrix} -\frac{\beta_1 S^0}{N^2} & 0 & 0 & 0 & 0 & 0 & 0 & 0 & 0 \\ 0 & 0 & 0 & 0 & 0 & 0 & 0 & 0 & 0 \\ 0 & 0 & -\frac{\beta_2 S^0}{N^2} & 0 & 0 & 0 & 0 & 0 & 0 \\ 0 & 0 & 0 & -\frac{(\beta_3 S^0 + \beta_4 v\Lambda_1)}{N^2} & 0 & 0 & 0 & 0 & 0 \\ 0 & 0 & 0 & 0 & 0 & 0 & 0 & 0 & 0 \\ 0 & 0 & 0 & 0 & 0 & 0 & 0 & 0 & 0 \\ 0 & 0 & 0 & 0 & 0 & 0 & 0 & 0 & 0 \\ 0 & 0 & 0 & 0 & 0 & 0 & 0 & 0 & 0 \\ 0 & 0 & 0 & 0 & 0 & 0 & 0 & 0 & 0 \end{pmatrix}$$

and G_A^{-1} is the same as G^{-1} as earlier obtained in 4.2.23.

The det $\left(\left|F_A G_A^{-1} - \lambda I\right|\right) = 0$, gives the strength numbers related to I_H, I_B and I_{HB} given as

$$A_{0,I_H} = -\frac{\pi\beta_1\theta_5}{N^2\mu\left(\mu + D_H\left(1-\varepsilon_1\right)\right)} < 0 \tag{4.2.36}$$

$$A_{0,I_B} = -\frac{\pi\beta_2\theta_5}{N^2\mu\left(\alpha+\mu+\tau+\psi D_B\right)} < 0 \tag{4.2.37}$$

$$A_{0,I_{HB}} = -\frac{\pi\beta_3\theta_5}{N^2\mu(\gamma+\mu+\phi)} < 0 \tag{4.2.38}$$

From 4.2.36, 4.2.37 and 4.2.38 above, it follows that the strength numbers are all negative for ε_1 is greater than or equal to zero in equation 4.2.36. This is an indication that the HIV-HBV co-infection model will have a single magnitude or wave, which implies a single, forceful surge that does not renew itself at once, although further analysis is required to confirm at what point the infections will increase, decrease or even resurge.

4.4 Co-infection-Free-Equilibrium Point Stability Analysis

The local and global stability of Co-infection-Free-Equilibrium Point is established using the Routh-Hurwitz criterion and Castillo-Chavez technique respectively.

4.4.1 Investigating local stability of CFE point, E^0_{HB}

Here, we use the Routh-Hurwitz stability criterion to establish the local stability of E^0_{HB}. The necessary and sufficient conditions for every root of the characteristic polynomial (with real coefficients) to be on the left half of the complex plane are provided by significant criteria by Routh-Hurwitz. In other words, if and only if the determinants of every Hurwitz matrix are positive, then every polynomial root is negative or has negative real roots (DeJesus & Kaufman, 1987). We prepare the Routh table and determine whether the system is stable or not since it is not easy to find the roots of the characteristic equation of a matrix with symbolic representation.

The system of ordinary differential equations (ODE) can be called linearized when a non-linear system is approximated with a linear one near a specific point, usually an equilibrium point. This does not break local behaviour and simplifies the analysis. Linearization reduces a nonlinear system and approximates it to a linear system and is one powerful method to study the local behaviour of the nonlinear system around an equilibrium point. This is by finding the eigenvalues of the Jacobian matrix at the equilibrium point and consequently finding the stability of the equilibrium point (Cheng, Hu, & Shen, 2010). Thus, the system of equations 4.2.1 to 4.2.12 are linearized as follows:

$$f_1(S,I_H,A,I_{HB},I_{HCB},T_{HB},I_B,I_{CB},T_B,R,V,V_H) = \theta_5\pi - (\lambda_1+\lambda_2+\lambda_3+\mu)S + \omega R$$

$$f_2(S,I_H,A,I_{HB},I_{HCB},T_{HB},I_B,I_{CB},T_B,R,V,V_H) = \theta_1\pi + \lambda_1 S + (1-\varepsilon_2)\sigma T_{HB}$$

$$-(\lambda_4+\mu+(1-\varepsilon_1)D_H)I_H$$

$$f_3(S,I_H,A,I_{HB},I_{HcB},T_{HB},I_B,I_{cB},T_B,R,V,V_H) = (1-\varepsilon_1)D_H I_H - (\delta_1+\mu)A$$

$$f_4(S,I_H,A,I_{HB},I_{HcB},T_{HB},I_B,I_{cB},T_B,R,V,V_H) = (1-\rho)\pi + \lambda_3 S + (I_H+v)\lambda_4 + \lambda_5 I_B - (\phi+$$

$$\gamma+\mu)I_{HB}$$

$$f_5(S,I_H,A,I_{HB},I_{HcB},T_{HB},I_B,I_{cB},T_B,R,V,V_H) = \gamma I_{HB} - (\mu+\delta_4)I_{HcB}$$

$$f_6(S,I_H,A,I_{HB},I_{HCB},T_{HB},I_B,I_{CB},T_B,R,V,V_H) = \phi I_{HB} - (\mu+\delta_3+(1-\varepsilon_2)\sigma)T_{HB}$$

$$f_7(S,I_H,A,I_{HB},I_{HcB},T_{HB},I_B,I_{cB},T_B,R,V,V_H) = \theta_2\pi + \lambda_2 S - (\mu+\lambda_5+\alpha+\tau+\psi D_B)I_B$$

$$f_8(S,I_H,A,I_{HB},I_{HcB},T_{HB},I_B,I_{cB},T_B,R,V,V_H) = \psi D_B I_B - (\mu+\delta_2)I_{cB}$$

$$f_9(S,I_H,A,I_{HB},I_{HCB},T_{HB},I_B,I_{CB},T_B,R,V,V_H) = \tau I_B - (\mu+\delta_3+(1-\varepsilon_2)\varphi)T_B$$

$$f_{10}(S,I_H,A,I_{HB},I_{HcB},T_{HB},I_B,I_{cB},T_B,R,V,V_H) = \alpha I_B + (1-\varepsilon_2)\varphi T_B - (\omega+\mu)R$$

$$f_{11}(S,I_H,A,I_{HB},I_{HcB},T_{HB},I_B,I_{cB},T_B,R,V,V_H) = \theta_3\pi - (\mu+\Gamma\lambda_1)V$$

$$f_{12}(S,I_H,A,I_{HB},I_{HcB},T_{HB},I_B,I_{cB},T_B,R,V,V_H) = \theta_4\pi + \Gamma\lambda_1 V - (\mu+v\lambda_4)V_H$$

where $f_1, f_2, ...f_{12}$ denotes the derivatives of the state variables in equation 4.2.1-4.2.12.

The Jacobian matrix J of the above system at E^0_{HB} is given by $J\left(E^0_{HB}\right)$

$$J\left(E^0_{HB}\right) = \begin{pmatrix} -\mu & -L_{12} & -L_{13} & -L_{14} & -L_{15} & -L_{16} & -L_{17} & -L_{18} & -L_{19} & \omega & 0 & 0 \\ 0 & -L_{22} & -L_{23} & -L_{24} & -L_{25} & L_{26} & 0 & 0 & 0 & 0 & 0 & 0 \\ 0 & L_{32} & -L_{33} & 0 & 0 & 0 & 0 & 0 & 0 & 0 & 0 & 0 \\ 0 & L_{42} & L_{43} & L_{44} & L_{45} & L_{46} & 0 & 0 & 0 & 0 & 0 & L_{49} \\ 0 & 0 & 0 & \gamma & -L_{55} & 0 & 0 & 0 & 0 & 0 & 0 & 0 \\ 0 & 0 & 0 & \phi & 0 & -L_{9} & 0 & 0 & 0 & 0 & 0 & 0 \\ 0 & 0 & 0 & L_{74} & L_{75} & L_{76} & L_{77} & L_{78} & L_{79} & 0 & 0 & 0 \\ 0 & 0 & 0 & 0 & 0 & 0 & \psi D_B & L_{88} & 0 & 0 & 0 & 0 \\ 0 & 0 & 0 & 0 & 0 & 0 & \tau & 0 & L_{99} & 0 & 0 & 0 \\ 0 & 0 & 0 & 0 & 0 & 0 & \alpha & 0 & L_{109} & L_{1010} & 0 & 0 \\ 0 & L_{112} & L_{113} & -L_{114} & -L_{115} & -L_{116} & 0 & 0 & 0 & 0 & -\mu & 0 \\ 0 & L_{122} & L_{123} & L_{124} & L_{125} & L_{126} & 0 & 0 & 0 & 0 & 0 & L_{1212} \end{pmatrix}$$

where

$$L_{12} = S^0\beta_1, L_{13} = S^0\beta_1\eta_3, L_{17} = S^0\beta_2, L_{18} = S^0\beta_2\chi_1, L_{19} = S^0\beta_2\chi_4$$

$$L_{14} = S^0\left(\beta_3 + \beta_1\eta_1 + \beta_2\chi_1\right), L_{15} = S^0\left(\beta_1\eta_2 + \beta_2\chi_3 + \beta_3\Psi_1\right)$$

$$L_{16} = S^0\left(\beta_1\eta_4 + \beta_2\chi_5 + \beta_3\Psi_2\right), L_{23} = S^0\beta_1\eta_3, L_{24} = S^0\beta_1\eta_1$$

$$L_{25} = S^0\beta_1\eta_2, L_{22} = S^0\beta_1 + \mu + D_H\left(1-\varepsilon_1\right), L_{26} = \sigma\left(1-\varepsilon_2\right) + S^0\beta_1\eta_4$$

$$L_{32} = D_H\left(1-\varepsilon_1\right) L_{33} = \left(\mu + \delta_1\right), L_{44} = S^0\beta_3 + v\beta_4\Lambda_1 - \left(\gamma + \mu + \phi\right)$$

$$L_{42} = v\beta_4, L_{43} = v\beta_4\Lambda_3, L_{49} = v\beta_4\Lambda_5$$

$$L_{45} = v\beta_4\Lambda_2 + S^0\beta_3\Psi_1, L_{46} = v\beta_4\Lambda_4 + S^0\beta_3\Psi_2, L_{55} = \left(\mu + \delta_4\right)$$

$$L_{66} = \mu + \delta_3 + \sigma\left(1-\varepsilon_2\right), L_{74} = S^0\beta_2\chi_2, L_{75} = S^0\beta_2\chi_3, L_{76} = S^0\beta_2\chi_5$$

$$L_{77} = S^0\beta_2 - \left(\alpha + \mu + \tau + \psi D_B\right), L_{78} = S^0\beta_2\chi_1, L_{79} = S^0\beta_2\chi_4$$

$$L_{88} = -\left(\mu + \delta_2\right), L_{99} = -\mu - \delta_3 - \varphi\left(1-\varepsilon_2\right)$$

$$L_{109} = \left(1-\varepsilon_2\right)\varphi, L_{1010} = -(\omega + \mu)$$

$$L_{112} = -V^0\Gamma\beta_1, L_{113} = -V^0\Gamma\beta_1\eta_3, L_{114} = V^0\Gamma\beta_1\eta_1, L_{115} = V^0\Gamma\beta_1\eta_2$$

$$L_{116} = V^0\Gamma\beta_1\eta_4, L_{122} = V^0\Gamma\beta_1 - v\beta_4, L_{123} = V^0\Gamma\beta_1\eta_3 - v\beta_4\Lambda_3$$

$$L_{124} = V^0\Gamma\beta_1\eta_1 - v\beta_4\Lambda_1, L_{125} = V^0\Gamma\beta_1\eta_2 - v\beta_4\Lambda_2, L_{126} = V^0\Gamma\beta_1\eta_4 - v\beta_4\Lambda_4$$

$$L_{1212} = -\mu - v\beta_4\Lambda_5$$

The eigenvalues of $J\left(E^0_{HB}\right)$ are obtained by reducing $J\left(E^0_{HB}\right)$ to $J - zI$, an upper triangular matrix by applying the Gaussian elimination process. The process involves row operation by addition, subtraction and multiplication. By subsequent row operations, nine eigenvalues are obtained as follows;

$$z_1 = -\mu,$$

$$z_2 = L_{14} = -\left(S^0\beta_1 + \mu + D_H\left(1-\varepsilon_1\right)\right),$$

$$z_3 = U_1 = -\left(S^0\beta_1\eta_3 D_H\left(1-\varepsilon_1\right) - \left(S^0\beta_1 + \mu + D_H\left(1-\varepsilon_1\right)\right)\left(\mu+\delta_1\right)\right),$$

$$z_4 = U_4U_2 - U_1U_5,$$

$$z_5 = H_1 = \gamma\left(U_4U_3 - U_1U_6\right) + \left(U_4U_2 - U_1U_5\right)\left(\mu+\delta_4\right),$$

$$z_6 = H_3H_2 - H_1H_4,$$

$$z_7 = P_1,$$

$$z_8 = \psi D_B P_2 + P_1\left(\mu+\delta_2\right), \text{ and}$$

$$z_9 = G_1.$$

where,

$$U_1 = -S^0\beta_1\eta_3 D_H(1-\varepsilon_1) - L_{14}(\mu+\delta_1), U_2 = -S^0\beta_1\eta_1 D_H(1-\varepsilon_1),$$

$$U_3 = -S^0\beta_1\eta_2 D_H(1-\varepsilon_1),$$

$$U_4 = -S^0\beta_1\eta_3 v\beta_4 + L_{14}v\beta_4\Lambda_3, U_5 = -S^0\beta_1\eta_1 v\beta_4 + L_{14}L_{16}$$

$$U_6 = -S^0\beta_1\eta_2 v\beta_4 + L_{14}L_{17}, U_7 = v\beta_4 L_{15} + L_{14}L_{18}, U_8 = L_{14}v\beta_4\Lambda_5,$$

$$T_1 = S^0\beta_1\eta_3 V^0\Gamma\beta_1 - L_{14}V^0\Gamma\beta_1\eta_3$$

$$T_2 = S^0\beta_1\eta_1 V^0\Gamma\beta_1 - L_{14}V^0\Gamma\beta_1\eta_1$$

$$T_3 = S^0\beta_1\eta_2 V^0\Gamma\beta_1 - L_{14}V^0\Gamma\beta_1\eta_2, T_4 = -V^0\Gamma\beta_1 L_{15} - L_{14}V^0\Gamma\beta_1\eta_4, T_5 = -L_{14}\mu,$$

$$D_1 = -S^0\beta_1\eta_3\left(V^0\Gamma\beta_1 - v\beta_4\right) + L_{14}\left(V^0\Gamma\beta_1\eta_3 - v\beta_4\Lambda_3\right)$$

$$D_2 = -S^0\beta_1\eta_1\left(V^0\Gamma\beta_1 - v\beta_4\right) + L_{14}\left(V^0\Gamma\beta_1\eta_1 - v\beta_4\Lambda_1\right)$$

$$D_3 = -S^0\beta_1\eta_2\left(V^0\Gamma\beta_1 - v\beta_4\right) + L_{14}\left(V^0\Gamma\beta_1\eta_2 - v\beta_4\Lambda_2\right)$$

$$D_4 = \left(V^0\Gamma\beta_1 - v\beta_4\right)L_{15} + L_{14}\left(V^0\Gamma\beta_1\eta_4 - v\beta_4\Lambda_4\right)$$

$$D_5 = -L_{14}(\mu + v\beta_4\Lambda_5)$$

$$H_1 = \gamma(U_4U_3 - U_1U_6) + (U_4U_2 - U_1U_5)(\mu+\delta_4)$$

$$H_2 = \gamma(U_4D_H(1-\varepsilon_1)L_{15} - U_1U_7)$$

$$H_3 = \phi(U_4U_3 - U_1U_6)$$

$$H_4 = \phi(U_4D_H(1-\varepsilon_1)L_{15} - U_1U_7) + (U_4U_2 - U_1U_5)L_{19}$$

$$H_5 = S^0\beta_2\chi_2(U_4U_3 - U_1U_6) - (U_4U_2 - U_1U_5)S^0\beta_2\chi_3$$

$$H_6 = S^0\beta_2\chi_2(U_4D_H(1-\varepsilon_1)L_{15} - U_1U_7) - (U_4U_2 - U_1U_5)S^0\beta_2\chi_5$$

$$H_7 = -(U_4U_2 - U_1U_5)(L_{1010} - z)$$

$$H_8 = -(U_4U_2 - U_1U_5)S^0\beta_2\chi_1$$

$$H_9 = -(U_4U_2 - U_1U_5)S^0\beta_2\chi_4$$

$$H_{10} = (T_1U_2 - U_1T_2)(U_4U_3 - U_1U_6) - (U_4U_2 - U_1U_5)(T_1U_3 - U_1T_3)$$

$$H11 = (T_1U_2 - U_1T_2)(U_4D_H(1-\varepsilon_1)L_5 - U_1U_7) -$$

$$(U_4U_2 - U_1U_5)(T_1D_H(1-\varepsilon_1)L_{15} - U_1T_4)$$

$$H12 = (U_4U_2 - U_1U_5)U_1T_5$$

$$H13 = (D_1U_2 - U_1D_2)(U_4U_3 - U_1U_6) - (U_4U_2 - U_1U_5)(D_1U_3 - U_1D_3)$$

$$H14 = (D_1U_2 - U_1D_2)(U_4D_H(1-\varepsilon_1)L_5 - U_1U_7) -$$

$$(U_4U_2 - U_1U_5)(D_1D_H(1-\varepsilon_1)L_{15} - U_1D_4)$$

$$H15 = -(D_1U_2 - U_1D_2)U_1U_8 + (U_4U_2 - U_1U_5)U_1D_5$$

$$P_1 = (H_3H_2 - H_1H_4)H_1H_7$$

$$P_2 = (H_3H_2 - H_1H_4)H_1H_8$$

$$P_3 = (H_3H_2 - H_1H_4)H_1H_9$$

$$P_4 = -U_1U_8\gamma H_3(H_5H_2 - H_1H_6) + (H_3H_2 - H_1H_4)U_1U_8\gamma H_5$$

$$P_5 = (H_3H_2 - H_1H_4)H_1H_{12}$$

$$P_6 = -U_1U_8\gamma H_3(H_{10}H_2 - H_1H_{11}) + (H_3H_2 - H_1H_4)U_1U_8\gamma H_{10}$$

$$P_7 = -U_1U_8\gamma H_3(H_{13}H_2 - H_1H_{14}) - (H_3H_2 - H_1H_4)(U_1U_8\gamma H_{13} + H_1H_{15})$$

$$\text{and } G_1 = (\psi D_B)^2 P_2P_3 - (\psi D_BP_2 + P_1(\mu+\delta_2))(\tau P_3 - P_1L_{12})$$

$$G_2 = (\psi D_B)^2 P_2P_4 - (\psi D_BP_2 + P_1(\mu+\delta_2))\tau P_4$$

$$G_3 = \alpha P_2\psi D_BP_3 - (\psi D_BP_2 + P_1(\mu+\delta_2))(\alpha P_3 - P_1(1-\varepsilon_2)\varphi)$$

$$G_4 = -P_1(\psi D_BP_2 + P_1(\mu+\delta_2))(\omega+\mu)$$

$$G_5 = \alpha P_2\psi D_BP_4 - (\psi D_BP_2 + P_1(\mu+\delta_2))\alpha P_4$$

The Jacobian matrix J finally reduces to a 3×3 upper triangular matrix $J - zI$ given as

$$\begin{pmatrix} -G_1G_4 - z & 0 & G_3G_2 - G_1G_5 \\ 0 & P_5 - z & P_6 \\ 0 & 0 & P_7 - z \end{pmatrix} \tag{4.2.39}$$

Thus, the eigenvalues of 4.2.39 are obtained by $\det(J - zI) = 0$ given by

$-(G_1G_4 + z)(P_5 - z)(P_7 - z) = 0$

On expansion it yields a characteristic polynomial of degree 3 of the form

$P(z) = a_1z^3 + a_2z^2 + a_3z + a_0$

which is equivalent to

$$z^3 + (G_1G_4 - P_5 - P_7)z^2 + (P_5P_7 - G_1G_4P_5 - G_1G_4P_7)z + G_1G_4P_5P_7 = 0$$

The signs of the remaining 3 eigenvalues of 4.2.39 are predicted using the Routh-Hurtwitz criterion (Patil, 2021) as shown in the proof of theorem 3.

where $a_1 = 1 > 0, a_2 = G_1G_4 - P_5 - P_7, a_3 = P_5P_7 - G_1G_4P_5 - G_1G_4P_7$ and $a_0 = G_1G_4P_5P_7 > 0$

Theorem 3. E^0_{HB} is locally asymptotically stable if and only if all the elements in the first column of the Routh array are completely positive and $a_1 > 0$ otherwise E^0_{HB} is unstable.

Proof. The Routh array for $P(z)$ is constructed as follows

z^3	a_1	a_3
z^2	a_2	a_0
z	b_1	b_2
z^0	a_0	

The b_1 and b_2 are the Hurwitz matrices obtained as

$$b_1 = \frac{a_2 a_3 - a_1 a_0}{a_2}$$
$$= \frac{(G_1 G_4 - P_5 - P_7)(P_5 P_7 - G_1 G_4 P_5 - G_1 G_4 P_7) - G_1 G_4 P_5 P_7}{G_1 G_4 - P_5 - P_7}$$

$$b_2 = 0$$

At this point, it is not possible to ascertain the signs of a_2 and b_1 due to their symbolic representation. But numerical simulation will give a confirmation of this realization.

4.4.2 Investigating global stability of CFE point E^0_{HB}

We apply the Castillo-Chavez technique by Brauer et al. (2019) to assess the global stability of E^0_{HB}. According to this method, the conditions that must be met in order for the system to be globally asymptotically stable are;

C1: $\frac{dX}{dt} = F(X^*, 0), X^*$ is globally asymptotically stable

C2: $M(X,Z) = AZ - \widehat{M}(X,Z)$, where $\widehat{M}(X,Z) \geq 0$ for $(X,Z) \in \Omega$, where

$A = D_Z M(X^*, Z)$ is a Metzler matrix whose off diagonal entries are positive and Ω is the feasible region.

Thus, if $\widehat{M}(X,Z) \geq 0$, then the CFE point E^0_{HB} is globally asymptotically stable if the parameters of the model are positive otherwise it is unstable.

Theorem 4. If the CFE point E^0_{HB} satisfies C 1 and C 2 whenever $R^*_C < 1$, then, it is globally asymptotically stable.

Proof. The model (4.2.2) is written as $\frac{dX}{dt} = F(X,Z)$ and $\frac{dZ}{dt} = M(X^*, Z)$, where the components of X stand for the quantity of susceptible, immunized, and recovered non-infectious individuals, that is $X = \{S, V, R\}$ and the components of Z denote the number of individuals capable of transmitting the infection given as,

$Z = \{I_H, A, I_B, I_{cB}, I_{HB}, I_{HcB}, T_B, T_{HB}, V_H\}$. In our case,

$$(X,0) = F(S,V,0,0,0,0,0,0,0,0,0,0) = \begin{pmatrix} \theta_5\pi - (\lambda_1+\lambda_2+\lambda_3+\mu)S + \omega R \\ \theta_3\pi - (\mu+\Gamma\lambda_1)V \\ 0 \\ 0 \\ 0 \\ 0 \\ 0 \\ 0 \\ 0 \end{pmatrix} \tag{4.2.41}$$

and the Jacobian of (4.2.4.1) denoted as

$$D_X F(X,0) = \begin{pmatrix} -\beta_1\mu & 0 & 0 & 0 & 0 & 0 & 0 & 0 & 0 & 0 & 0 & 0 \\ 0 & -\mu V & 0 & 0 & 0 & 0 & 0 & 0 & 0 & 0 & 0 & 0 \\ 0 & 0 & 0 & 0 & 0 & 0 & 0 & 0 & 0 & 0 & 0 & 0 \\ 0 & 0 & 0 & 0 & 0 & 0 & 0 & 0 & 0 & 0 & 0 & 0 \\ 0 & 0 & 0 & 0 & 0 & 0 & 0 & 0 & 0 & 0 & 0 & 0 \\ 0 & 0 & 0 & 0 & 0 & 0 & 0 & 0 & 0 & 0 & 0 & 0 \\ 0 & 0 & 0 & 0 & 0 & 0 & 0 & 0 & 0 & 0 & 0 & 0 \\ 0 & 0 & 0 & 0 & 0 & 0 & 0 & 0 & 0 & 0 & 0 & 0 \\ 0 & 0 & 0 & 0 & 0 & 0 & 0 & 0 & 0 & 0 & 0 & 0 \\ 0 & 0 & 0 & 0 & 0 & 0 & 0 & 0 & 0 & 0 & 0 & 0 \\ 0 & 0 & 0 & 0 & 0 & 0 & 0 & 0 & 0 & 0 & 0 & 0 \\ 0 & 0 & 0 & 0 & 0 & 0 & 0 & 0 & 0 & 0 & 0 & 0 \end{pmatrix} \tag{4.2.42}$$

From the above matrix 4.2.42, since all of the eigenvalues are evidently negative, E_{HB}^0 is asymptotically stable globally. Thus, Condition C1 satisfied.

$$M(X,Z) = \begin{pmatrix} \theta_1\pi + \lambda_1 S + (1-\varepsilon_2)\,\sigma T_{HB} - (\lambda_4 + \mu + (1-\varepsilon_1)\,D_H)\,I_H \\ (1-\varepsilon_1)\,D_H I_H - (\delta_1 + \mu)A \\ \theta_2\pi + \lambda_2 S - (\mu + \lambda_5 + \alpha + \tau + \psi D_B)\,I_B \\ \psi D_B I_B - (\mu + \delta_2)\,I_{cB} \\ (1-\rho)\pi + \lambda_3 S + (I_H + v)\,\lambda_4 + \lambda_5 I_B - (\phi + \gamma + \mu)I_{HB} \\ \gamma I_{HB} - (\mu + \delta_4)\,I_{HcB} \\ \tau I_B - (\mu + \delta_3 + (1-\varepsilon_2)\,\varphi)\,T_B \\ \phi I_{HB} - (\mu + \delta_3 + (1-\varepsilon_2)\,\sigma)\,T_{HB} \\ \theta_4\pi + \Gamma\lambda_1 V - (\mu + v\lambda_4)\,V_H \end{pmatrix}$$

The Metzler Matrix A is obtained as

$$A = D_Z M(X,Z) = \begin{pmatrix} A_{11} & A_{12} & 0 & 0 & A_{15} & A_{16} & 0 & A_{18} & 0 \\ A_{21} & -A_{22} & 0 & 0 & 0 & 0 & 0 & 0 & 0 \\ 0 & 0 & A_{33} & A_{34} & A_{35} & A_{36} & A_{37} & A_{38} & 0 \\ 0 & 0 & \psi D_B & -(\mu+\delta_2) & 0 & 0 & 0 & 0 & 0 \\ v\beta_4 & v\beta_4\Lambda_3 & 0 & 0 & A_{55} & A_{56} & 0 & A_{58} & A_{59} \\ 0 & 0 & 0 & 0 & \gamma & -A_{66} & 0 & 0 & 0 \\ 0 & 0 & \tau & 0 & 0 & 0 & A_{77} & 0 & 0 \\ 0 & 0 & 0 & 0 & \phi & 0 & 0 & A_{78} & 0 \\ A_{91} & A_{92} & 0 & 0 & A_{95} & A_{96} & 0 & A_{98} & -\mu \end{pmatrix}$$

where

$$A_{11} = \beta_1 S^0 - \mu - (1-\varepsilon_1) D_H, A_{12} = \beta_1 \eta_3 S^0, A_{15} = \beta_1 \eta_1 S^0, A_{16} = \beta_1 \eta_2 S^0,$$

$$A_{18} = \beta_1 \eta_4 S^0 + (1-\varepsilon_2)\sigma, A_{21} = (1-\varepsilon_1) D_H, A_{22} = (\delta_1 + \mu), A_{34} = \beta_2 \chi_1 S^0,$$

$$A_{33} = \beta_2 S^0 - (\mu + \alpha + \tau + \psi D_B), A_{35} = \beta_2 \chi_2 S^0, A_{36} = \beta_2 \chi_3 S^0, A_{37} = \beta_2 \chi_4 S^0,$$

$$A_{38} = \beta_2 \chi_5 S^0, A_{55} = \beta_3 S^0 + v\beta_4 \Lambda_1 - (\phi + \gamma + \mu), A_{56} = \beta_3 S^0 \Upsilon_1 + v\beta_4 \Lambda_2,$$

$$A_{58} = \beta_3 S^0 \Upsilon_2 + v\beta_4 \Lambda_4, A_{59} = v\beta_4 \Lambda_5, A_{66} = (\mu + \delta_4),$$

$$A_{77} = -(\mu + \delta_3 + (1-\varepsilon_2)\varphi), A_{78} = -(\mu + \delta_3 + (1-\varepsilon_2)\sigma)$$

$$A_{91} = \Gamma \beta_1 V^0, A_{92} = \Gamma \beta_1 V^0 \eta_3, A_{95} = \Gamma \beta_1 V^0 \eta_1, A_{96} = \Gamma \beta_1 V^0 \eta_2,$$

$$A_{98} = \Gamma \beta_1 V^0 \eta_4$$

and

$$AZ = \begin{pmatrix} A_{11} & A_{12} & 0 & 0 & A_{15} & A_{16} & 0 & A_{18} & 0 \\ A_{21} & -A_{22} & 0 & 0 & 0 & 0 & 0 & 0 & 0 \\ 0 & 0 & A_{33} & A_{34} & A_{35} & A_{36} & A_{37} & A_{38} & 0 \\ 0 & 0 & \psi D_B & -(\mu+\delta_2) & 0 & 0 & 0 & 0 & 0 \\ v\beta_4 & v\beta_4\Lambda_3 & 0 & 0 & A_{55} & A_{56} & 0 & A_{58} & A_{59} \\ 0 & 0 & 0 & 0 & \gamma & -A_{66} & 0 & 0 & 0 \\ 0 & 0 & \tau & 0 & 0 & 0 & A_{77} & 0 & 0 \\ 0 & 0 & 0 & 0 & \phi & 0 & 0 & A_{78} & 0 \\ A_{91} & A_{92} & 0 & 0 & A_{95} & A_{96} & 0 & A_{98} & -\mu \end{pmatrix} \begin{pmatrix} I_H \\ A \\ I_B \\ I_{CB} \\ I_{HB} \\ I_{HCB} \\ T_B \\ T_{HB} \\ V_H \end{pmatrix}$$

$$= \begin{pmatrix} A_{11}I_H + A_{11}A + A_{15}I_{HB} + A_{16}I_{HcB} + A_{18}T_{HB} \\ A_{21}I_H - A_{22}A \\ A_{33}I_B + A_{34}I_{cB} + A_{36}I_{HcB} + A_{37}T_B + A_{38}T_{HB} \\ \psi D_B I_B - (\mu+\delta_2) I_{cB} \\ v\beta_4 I_H + v\beta_4\Lambda_3 A + A_{55}I_{HB} + A_{56}I_{HcB} + A_{58}T_{HB} + A_{59}V_H \\ \gamma I_{HB} - A_{66}I_{HcB} \\ \tau I_B - A_{77}T_B \\ \phi I_{HB} - A_{78}T_{HB} \\ A_{91}I_H + A_{92}A_{95}I_{HB} + A_{96}I_{HcB} + A_{98}T_{HB} - \mu V_H \end{pmatrix}$$

But $\widehat{M}(X,Z) = AZ - (X,Z)$

$$
\begin{pmatrix}
I_H A_{11} + A_{12} A + A_{15} I_{HB} + A_{16} I_{HcB} + A_{18} T_{HB} \\
I_H A_{21} - A_{22} A \\
A_{33} I_B + A_{34} I_{cB} + A_{35} I_{HB} + A_{36} I_{HcB} + A_{37} T_B + A_{38} T_{HB} \\
\psi D_B I_B - (\mu + \delta_2) I_{cB} \\
\nu \beta_4 I_H + \nu \beta_4 \Lambda_3 A + A_{55} I_{HB} + A_{56} I_{HcB} + A_{58} T_{HB} + A_{59} V_H \\
\gamma I_{HB} - A_{66} I_{HcB} \\
\tau I_B - A_{77} T_B \\
\phi I_{HB} - A_{78} T_{HB} \\
A_{91} I_H + A_{92} A + A_{95} I_{HB} + A_{96} I_{HcB} + A_{98} T_{HB} - \mu V_H
\end{pmatrix}
$$

$$
\begin{pmatrix}
\theta_1 \pi + \lambda_1 S + (1 - \varepsilon_2) \sigma T_{HB} - (\lambda_4 + \mu + (1 - \varepsilon_1) D_H) I_H \\
(1 - \varepsilon_1) D_H I_H - (\delta_1 + \mu) A \\
\theta_2 \pi + \lambda_2 S - (\mu + \lambda_5 + \alpha + \tau + \psi D_B) I_B \\
\psi D_B I_B - (\mu + \delta_2) I_{cB} \\
(1 - \rho) \pi + \lambda_3 S + (I_H + \nu) \lambda_4 + \lambda_5 I_B - (\phi + \gamma + \mu) I_{HB} \\
\gamma I_{HB} - (\mu + \delta_4) I_{HcB} \\
\tau I_B - (\mu + \delta_3 + (1 - \varepsilon_2) \varphi) T_B \\
\phi I_{HB} - (\mu + \delta_3 + (1 - \varepsilon_2) \sigma) T_{HB} \\
\theta_4 \pi + \Gamma \lambda_1 V - (\mu + \nu \lambda_4) V_H
\end{pmatrix}
$$

$$\widehat{M}(X,Z) = \begin{pmatrix} \widehat{M}11(X,Z) \\ 0 \\ \widehat{M}31(X,Z) \\ 0 \\ \widehat{M}51(X,Z) \\ 0 \\ 0 \\ 0 \\ \widehat{M}91(X,Z) \end{pmatrix}.$$

where

$$\widehat{M}11(X,Z) = I_{11H}^2\beta_4 + I_{HB}\beta_1\eta_1\left(S^0 - S\right) + I_{HcB}\beta_1\eta_2\left(S^0 - S\right) + A\beta_1\eta_3\left(S^0 - S\right)$$

$$+ T_{HB}\beta_1\eta_4\left(S^0 - S\right) + I_H T_{HB}\Lambda_4\beta_4$$

$$+ I_H\left[\left(S^0 - S\right)\beta_1 + \beta_4\left(I_{HB}\Lambda_1 + \Lambda_2 I_{HcB} + \Lambda_3 A + \Lambda_5 V_H\right)\right] - \theta_1\pi$$

$$\widehat{M}31(X,Z) = I_B^2\beta_5 + I_B\left(\left(S^0 - S\right)\beta_2 + \beta_5\left(\Upsilon_1 I_{HB} + \Upsilon_2 I_{CB} + \Upsilon_3 I_{HCB} + \Upsilon_4 T_B + \Upsilon_5 T_{HB}\right)\right)$$

$$+ \beta_2\left(\left(2S^0 - S\right)\chi_1 I_{CB} + \left(S^0 - S\right)\left(\chi_2 I_{HB} + \chi_3 I_{HCB} + \chi_4 T_B + \chi_5 T_{HB}\right)\right) - \theta_2\pi$$

$$\widehat{M}51(X,Z) = \beta_3\left(S^0\left(\Upsilon_1 + I_{HB} + \Upsilon_1 I_{HcB} + \Upsilon_2 T_{HB}\right) - S\left(I_{HB} + \Psi_1 I_{HcB} + \Psi_2 T_{HB}\right)\right)$$

$$- \pi(1-\rho) - I_H\lambda_4 - I_B\lambda_5$$

$$\widehat{M}91(X,Z) = I_H\Gamma\beta_1\left(V^0 - V\right) + vV_H I_H\beta_4 + I_{HB}\Gamma\beta_1\eta_1\left(V^0 - V\right)$$

$$+ I_{HcB}\Gamma\beta_1\eta_2\left(V^0 - V\right) + + A\Gamma\beta_1\eta_3\left(V^0 - V\right) + T_{HB}\Gamma\beta_1\eta_4\left(V^0 - V\right)$$

$$+ v\beta_4 V_H\left(I_{HB}\Lambda_1 + I_{HcB}\Lambda_2 + A\Lambda_3 + T_{HB}\Lambda_4 + V_H\Lambda_5\right) - \theta_4\pi.$$

From the above analysis, it follows that $\widehat{M}_{11}(X,Z) \geq 0, \widehat{M}_{31}(X,Z) \geq 0, \widehat{M}_{51}(X,Z) \geq 0,$ $\widehat{M}_{91}(X,Z) \geq 0$, since there is a limit to the number of susceptible and immunized, then $S \leq S^0$ and $V \leq V^0$. It is also evident that $\widehat{M}_{21}(X,Z) = \widehat{M}_{41}(X,Z) = \widehat{M}_{61}(X,Z) = \widehat{M}_{71}(X,Z) = \widehat{M}_{81}(X,Z) = 0$. Hence $\widehat{M}(X,Z) \geq 0$, implying that CFE point is GAS when $R_C^{HB} < 1$.

Condition 2 is also satisfied. This completed the prove of the theorem.

4.4.3 Existence of co-infection endemic equilibrium point, E^*_{HB}

Three possible endemic equilibrium points that can be established are; HIV endemic equilibrium point, E^*_H, HBV endemic equilibrium point, E^*_B and co-infection endemic equilibrium point, E^*_{HB} but we only investigate the existence of co-epidemic endemic equilibrium point. We denote $E^*_{HB} = (S^*, V^*, V^*_H, R^*, I^*_H, A^*, I^*_B, I^*_{cB}, T^*_B, I^*_{HB}, I^*_{HcB}, T^*_{HB})$ to be the co-infection endemic equilibrium point for the system of equations (4.2.1 to 4.2.12). Equating the rates of change of equations 4.2.1 to 4.2.12 to zero, the expressions for endemic states are obtained as;

$$S^* = \frac{\theta_5\pi + \omega R^*}{\lambda_1^* + \lambda_2^* + \lambda_3^* + \mu}$$

$$V^*_H = \frac{\theta_4\pi + \Gamma\lambda_1^* V^*}{\mu + \nu\lambda_4^*}$$

$$V^* = \frac{\theta_3\pi}{\mu + \Gamma\lambda_1^*}$$

$$R^* = \frac{\alpha I^*_B + (1-\varepsilon_2)\varphi T^*_B}{\omega + \mu}$$

$$I^*_B = \frac{\theta_2\pi + \lambda_2^* S^*}{\mu + \lambda_5^* + \alpha + \tau + \psi D_B}$$

$$I^*_{cB} = \frac{\psi D_B I^*_B}{\mu + \delta_2}$$

$$T^*_B = \frac{\tau I^*_B}{\mu + \delta_3 + (1-\varepsilon_2)\varphi}$$

$$I^*_H = \frac{\theta_1\pi + \lambda_1^* S^* + (1-\varepsilon_2)\sigma T^*_{HB}}{\lambda_4^* + \mu + (1-\varepsilon_1)D_H}$$

$$A^* = \frac{(1-\varepsilon_1)D_H I^*_H}{\delta_1 + \mu}$$

$$I^*_{HB} = \frac{(1-\rho)\pi + \lambda_3^* S^* + (I^*_H + \nu)\lambda_4^* + \lambda_5^* I^*_B}{\phi + \gamma + \mu}$$

$$I^*_{HcB} = \frac{\gamma I^*_{HB}}{\mu + \delta_4}$$

$$T^*_{HB} = \frac{\phi I^*_{HB}}{\mu + \delta_3 + (1-\varepsilon_2)\sigma}$$

and $\lambda_1^* = \frac{\beta_1\left(I_H^*+\eta_1 I_{HB}^*+\eta_2 I_{HcB}^*+\eta_3 A^*+\eta_4 T_{HB}^*\right)}{N^*}$, $\lambda_2^* = \frac{\beta_2(I_B+\chi_1 I_{cB}+\chi_2 I_{HB}+\chi_3 I_{HcB}+\chi_4 T_B+\chi_5 T_{HB})}{N^*}$,

$\lambda_3^* = \frac{\beta_3\left(I_{HB}^*+\Psi_1 I_{HcB}^*+\Psi_2 T_{HB}^*\right)}{N^*}$, $\lambda_4^* = \frac{\beta_4\left(I_H^*+\Lambda_1 I_{HB}^*+\Lambda_2 I_{HCB}^*+\Lambda_3 A^*+\Lambda_4 T_{HB}^*+\Lambda_5 V_H^*\right)}{N^*}$,

$\lambda_5^* = \frac{\beta_5\left(I_B^*+\Upsilon_1 I_{HB}^*+\Upsilon_2 I_{cB}^*+\Upsilon_3 I_{HCB}^*+\Upsilon_4 T_B^*+\Upsilon_5 T_{HB}^*\right)}{N^*}$, where

$N^* = S^* + I_H^* + A^* + I_B^* + I_{HB}^* + I_{cB}^* + I_{HcB}^* + T_B^* + T_{HB}^* + V^* + V_H^* + R^*$.

Even though it was challenging to find an analytical solution for the endemic states in terms of model parameters, it was nevertheless possible to establish the necessary conditions for the endemic equilibrium point to exist. In order to determine the conditions for the existence of E_{HB}^*, we thus formulate and demonstrate theorem 5.

Theorem 5. There exists a positive and unique endemic equilibrium point E_{HB}^*

if $R_{0,HB} > 1$ otherwise does not exist.

Proof. A co-infection endemic equilibrium point exists when each component of E_{HB}^* is positive and the corresponding rates of change are equal to zero, that is $\frac{dS^*}{dt} = 0, \frac{dV^*}{dt} = 0, \frac{dV_H^*}{dt} = 0, \frac{dR^*}{dt} = 0, \frac{dI_H^*}{dt} = 0, \frac{dA^*}{dt} = 0, \frac{dI_B^*}{dt} = 0, \frac{dI_{cB}^*}{dt} = 0, \frac{dT_B^*}{dt} = 0\ , \frac{dI_{HB}^*}{dt} = 0, \frac{dI_{HcB}^*}{dt} = 0, \frac{dT_{HB}^*}{dt} = 0$, and the infectious classes; $I_H \neq 0, I_{HB} \neq 0, I_B \neq 0, I_{HcB} \neq 0, T_{HB} \neq 0$.

From section 4.2.2, we have the following equations for the co-infected cases

$$\frac{dI_{HB}^*}{dt} = (1-\rho)\pi + \lambda_3^* S^* + (I_H^* + v)\,\lambda_4^* + \lambda_5^* I_B^* - q_1 I_{HB}^* = 0 \tag{4.2.43}$$

$$\frac{dI_{HcB}^*}{dt} = \gamma I_{HB}^* - q_2 I_{HcB}^* = 0 \tag{4.2.44}$$

$$\frac{dT_{HB}^*}{dt} = \phi I_{HB}^* - q_3 T_{HB}^* = 0 \tag{4.2.45}$$

where $q_1 = \phi + \gamma + \mu, q_2 = \mu + \delta_4, q_3 = \mu + \delta_3 + (1 - \varepsilon_2\sigma)$

Solving 4.2.43, 4.2.44 and 4.2.45 for $I^*_{HB}, I^*_{HcB}, T^*_{HB}$, we obtain

$$I^*_{HB} = \frac{(1-\rho)\pi + \beta_3 S^* (I^*_{HB} + \Psi_1 I^*_{HcB} + \Psi_2 T^*_{HB}) + \beta_4 v (\Lambda_1 I^*_{HB} + \Lambda_2 I^*_{HcB} + \Lambda_4 T^*_{HB})}{q_1} \tag{4.2.46}$$

$$I^*_{HcB} = \frac{\gamma I^*_{HB}}{q_2} \tag{4.2.47}$$

$$T^*_{HB} = \frac{\phi I^*_{HB}}{q_2} \tag{4.2.48}$$

Substituting I^*_{HcB}, T^*_{HB} into 4.2.46 we get

$$I^*_{HB} = \frac{(1-\rho)\pi + \beta_3 S^* \left(I^*_{HB} + \Psi_1 \frac{\gamma I^*_{HB}}{q_2} + \Psi_2 \frac{\phi I^*_{HB}}{q_2}\right) + \beta_4 v \left(\Lambda_1 I^*_{HB} + \Lambda_2 \frac{\gamma I^*_{HB}}{q_2} + \Lambda_4 \frac{\phi I^*_{HB}}{q_2}\right)}{q_1} \tag{4.2.49}$$

canceling I^*_{HB} on both sides of 4.2.49, we obtain

$$1 = \frac{(1-\rho)\pi + \beta_3 S^* \left(1 + \Psi_1 \frac{\gamma}{q_2} + \Psi_2 \frac{\phi}{q_2}\right) + \beta_4 v \left(\Lambda_1 + \Lambda_2 \frac{\gamma}{q_2} + \Lambda_4 \frac{\phi}{q_2}\right)}{q_1} \tag{4.2.50}$$

From equation 4.2.50 it follows that

$$1 = \frac{(1-\rho)\pi}{q_1} + \frac{\beta_3 S^*}{q_1}\left(1 + \Psi_1 \frac{\gamma}{q_2} + \Psi_2 \frac{\phi}{q_2}\right) + \frac{\beta_4 v}{q_1}\left(\Lambda_1 + \Lambda_2 \frac{\gamma}{q_2} + \Lambda_4 \frac{\phi}{q_2}\right) \tag{4.2.50*}$$

Consequently, from equation 4.2.34, it implies that $R^*_{0,HB} = \frac{\beta_3 S^*}{q_1}$

Hence, 4.2.50* becomes

$$1 = \frac{(1-\rho)\pi}{q_1} + R^*_{0,HB}\left(1 + \Psi_1 \frac{\gamma}{q_2} + \Psi_2 \frac{\phi}{q_2}\right) + \frac{\beta_4 v}{q_1}\left(\Lambda_1 + \Lambda_2 \frac{\gamma}{q_2} + \Lambda_4 \frac{\phi}{q_2}\right) \tag{4.2.50**}$$

By letting, $A = \left(1 + \Psi_1 \frac{\gamma}{q_2} + \Psi_2 \frac{\phi}{q_2}\right)$, $B = \frac{\beta_4 v}{q_1}\left(\Lambda_1 + \Lambda_2 \frac{\gamma}{q_2} + \Lambda_4 \frac{\phi}{q_2}\right)$, and $C = \frac{(1-\rho)\pi}{q_1}$ equa-

tion 4.2.50** reduces to $R^*_{0,HB} = \frac{1-B-C}{A}$.

Since A and B contain positive model parameters, $R^*_{0,HB} > 1$, if and only if $\frac{1-B-C}{A} > 1$ or $1-B-C > A$ and $A < B+C$. Therefore, HIV-HBV co-infection model has a unique co-infection endemic equilibrium point E^*_{HB} if ad only if $R^*_{0,HB} > 1$. Thus theorem 5 is proved.

4.4.4 Existence of bifurcation and stability analysis of endemic equilibrium point E^*_{HB}

According to Hirsch, Smale, and Devaney (2013), bifurcation is defined as a shift in a system's structure or behavior that takes place at particular parameter values and can result in several solution pathways as well as possible global adjustments to the dynamics of the system. The study of bifurcation theory focuses on differential equations that rely on a parameter. Pitchfork, transcritical, and saddle-node, hopf, backward bifurcations can all occur in a system. All of these are examples of local bifurcations, which explain how the bifurcation parameter affects the flow's structure close to a fixed point. The phenomenon of backward bifurcation, which has been observed in several disease models, is usually characterized by the co-existence of a stable disease free equilibrium and a stable endemic equilibrium when the associated reproduction number, R_0 of the model is less than unity. Mathematical co-infection models with control interventions such as vaccination and treatment often undergo bifurcation, which hampers the prevention and eradication of communicable diseases as illustrated in the study by Brauer et al. (2019). In this case, we use the center manifold theorem as used in the studies; Kotola, Teklu, and Abebaw (2023), Gitonga (2017) to determine the stability of the co-infection endemic equilibrium point and investigate the possibility of backward bifurcation. The following theorem 6 is stated.

Theorem 6. The HIV-HBV co-infection model exhibits a backward bifurcation at $R^{HB}_{0,S} = 1$

if the following prepositions are ascertained (Castillo-Chavez & Song, 2004).

i) The Jacobian of the model equations at the co-infection free equilibrium and bifurcation parameter are $J = D_y f(0,0) = \left(\frac{\partial f_i}{\partial y_i}(0,0)\right)$

ii) The remaining eigenvalues of A are in the left-hand of the complex plane, and matrix J has a real zero eigenvalue.

iii) The characteristic equation of matrix J has the zero eigenvalue, which is related to the right eigenvector, u and the left eigenvector, v.

iv) The bifurcation coefficients a and b define the local dynamics of the model around the stationary state of co-infection, which are defined as follows.

$a = \sum_{k=i=j=1}^{n} v_k u_i u_j \frac{\partial^2 f_k}{\partial y_i \partial y_j}(0,0)$

$b = \sum_{k=i=1}^{n} v_k u_i \frac{\partial^2 f_k}{\partial y_i \partial \beta^*}(0,0)$

where f_k is the kth component of F.

In particular when

a) $a > 0$ and $b > 0$, when $\beta^* < 0$ with $\|\beta^*\| \ll 1$, then (0,0) is locally asymptotically stable and there exists a positive unstable equilibrium and when $0 < \beta^* \ll 1$, then $(0,0)$ is unstable and there exists a negative and locally asymptotically stable equilibrium.

b) $a < 0$ and $b < 0$, when $\beta^* < 0$ with $\|\beta^*\| \ll 1$, then (0,0) is unstable and when $0 < \beta^* \ll 1$, then $(0,0)$ is asymptotically stable and there exists a positive unstable equilibrium.

c) $a < 0$ and $b > 0$, when $\beta^* < 0$ with $\|\beta^*\| \ll 1$, then (0,0) is unstable, there exists a negative and locally asymptotically stable equilibrium and when $0 < \beta^* \ll 1$, then $(0,0)$ is stable and there exists a positive unstable equilibrium.

d) $a > 0$ and $b < 0$, when β^* changes from negative to positive, (0,0) changes its stability from stable to unstable. Correspondingly a negative equilibrium becomes positive and locally asymptotically stable.

According to the study by Akinyi, Mugisha, Manyonge, Ouma, and Maseno (2013), If $a > 0$ and $b > 0$, then a backward bifurcation occurs at $\beta^* = 0$.

Proof. The method involves making the following simplifications and change of variables for the full model as follows;

$S = y_1, I_H = y_2, A = y_3, I_B = y_4, I_{HB} = y_5, I_{CB} = y_6, I_{HCB} = y_7, T_B = y_8, T_{HB} = y_9, V = y_{10}, V_H = y_{11}$ and $R = y_{12}$ such that $N = y_1 + y_2 + y_3 + y_4 + y_5 + y_6 + y_7 + y_8 + y_9 + y_{10} + y_{11} + y_{12}$

Further by vector notation $Y = \{y_1, y_2, y_3, y_4, y_5, y_6, y_7, y_8, y_9, y_{10}, y_{11}, y_{12}\}^T$ for which we rewrite the system 4.2.1 to 4.2.12 with the change of variables as $\frac{dY}{dt} = F(Y)$ where $F = \{f_1, f_2, f_3, f_4, f_5, f_6, f_7, f_8, f_9, f_{10}, f_{11}, f_{12}\}^T$ written as follows

$$
\begin{aligned}
\frac{dy_1}{dt} &= f_1 = \theta_5\pi - (\lambda_1 + \lambda_2 + \lambda_3 + \mu)\, y_1 + \omega y_{12} \\
\frac{dy_2}{dt} &= f_2 = \theta_1\pi + \lambda_1 y_1 + (1-\varepsilon_2)\,\sigma y_9 - (\lambda_4 + \mu + (1-\varepsilon_1)\, D_H)\, y_2 \\
\frac{dy_3}{dt} &= f_3 = (1-\varepsilon_1)\, D_H y_2 - (\delta_1 + \mu)\, y_3 \\
\frac{dy_4}{dt} &= f_4 = \theta_2\pi + \lambda_2 y_1 - (\mu + \lambda_5 + \alpha + \tau + \psi D_B)\, y_4 \\
\frac{dy_5}{dt} &= f_5 = (1-\rho)\pi + \lambda_3 y_1 + (y_2 + v)\,\lambda_4 + \lambda_5 y_4 - (\phi + \gamma + \mu) y_5 \\
\frac{dy_6}{dt} &= f_6 = \psi D_B y_4 - (\mu + \delta_2)\, y_6 \\
\frac{dy_7}{dt} &= f_7 = \gamma y_5 - (\mu + \delta_4)\, y_7 \\
\frac{dy_8}{dt} &= f_8 = \tau y_4 - (\mu + \delta_3 + (1-\varepsilon_2)\,\varphi)\, y_8 \\
\frac{dy_9}{dt} &= f_9 = \phi y_5 - (\mu + \delta_3 + (1-\varepsilon_2)\,\sigma)\, y_9 \\
\frac{dy_{10}}{dt} &= f_{10} = \theta_3\pi - (\mu + \Gamma\lambda_1)\, y_{10} \\
\frac{dy_{11}}{dt} &= f_{11} = \theta_4\pi + \Gamma\lambda_1 y_{10} - (\mu + v\lambda_4)\, y_{11} \\
\frac{dy_{12}}{dt} &= f_{12} = \alpha y_4 + (1-\varepsilon_2)\,\varphi y_8 - (\omega + \mu) y_{12}
\end{aligned}
\tag{4.2.51}
$$

with

$\lambda_1 = \frac{\beta_1(y_2+\eta_1 y_5+\eta_2 y_7+\eta_3 y_3+\eta_4 y_9)}{N}$,

where $\eta_1 \geq \eta_2 \geq \eta_3 \geq \eta_4 \geq 1$,

$\lambda_2 = \frac{\beta_2(y_4+\chi_1 y_6+\chi_2 y_5+\chi_3 y_7+\chi_4 y_8+\chi_5 y_9)}{N}$,

where $\chi_1 \geq \chi_2 \geq \chi_3 \geq \chi_4 \geq 1$,

$\lambda_3 = \frac{\beta_3(y_5+\Psi_1 y_7+\Psi_2 y_9)}{N}$, where, $\Psi_1 \geq \Psi_2 \geq 1$,

$\lambda_4 = \frac{\beta_4(y_2+\Lambda_1 y_5+\Lambda_2 y_7+\Lambda_3 y_3+\Lambda_4 y_9+\Lambda_5 y_{11})}{N}$,

where $\Lambda_1 > \Lambda_2 > \Lambda_3 > \Lambda_4 > \Lambda_5$ and

$\lambda_5 = \frac{\beta_5(y_4+\Upsilon_1 y_5+\Upsilon_2 y_6+\Upsilon_3 y_7+\Upsilon_4 y_8+\Upsilon_5 y_9)}{N}$,

where $\Upsilon_1 > \Upsilon_2 > \Upsilon_3 > \Upsilon_4 > \Upsilon_5$ and $\Gamma \leq 1$ and $\nu \leq 1$

We choose $\beta^* = \beta_2^*$ as the bifurcation parameter since it has a significant effect on the transmission dynamics and by making β_2 the subject in (4.2.28) at $R_{0,N}^B = 1$, we have

$\beta_2 = \beta^* = \frac{\mu(\mu+\delta_2)(\alpha+\mu+\psi D_B)}{\pi\theta_5(\mu+\delta_2+\chi_1\psi D_B)}$

Evaluating the Jacobian of (4.2.51) at E_{HB}^0 and the bifurcation parameter β^* we obtain

$J_{E_{HB}^0}(\beta_2 = \beta^*)$

$$= \begin{pmatrix} -\mu & -F_{12}^{*} & -F_{13}^{*} & -F_{14}^{*} & -F_{15}^{*} & -F16 & -F_{17}^{*} & -F_{18}^{*} & -F_{19}^{*} & 0 & 0 & \omega \\ 0 & F_{22} & F_{23} & 0 & F_{25} & 0 & F_{27} & 0 & F_{29} & 0 & 0 & 0 \\ 0 & F_{32} & -F_{33} & 0 & 0 & 0 & 0 & 0 & 0 & 0 & 0 & 0 \\ 0 & 0 & 0 & F_{44}^{*} & F_{45}^{*} & F_{46}^{*} & F_{47}^{*} & F_{48}^{*} & F_{49}^{*} & 0 & 0 & 0 \\ 0 & F_{52} & F_{53} & 0 & F_{55} & 0 & F_{57} & 0 & F_{59} & 0 & F_{511} & 0 \\ 0 & 0 & 0 & \psi D_B & 0 & -F_{66} & 0 & 0 & 0 & 0 & 0 & 0 \\ 0 & 0 & 0 & 0 & \gamma & 0 & -F_{77} & 0 & 0 & 0 & 0 & 0 \\ 0 & 0 & 0 & \tau & 0 & 0 & 0 & -F_{88} & 0 & 0 & 0 & 0 \\ 0 & 0 & 0 & 0 & \phi & 0 & 0 & 0 & -F_{99} & 0 & 0 & 0 \\ 0 & -F_{102} & -F_{103} & 0 & -F_{105} & 0 & -F_{107} & 0 & -F_{109} & -\mu & 0 & 0 \\ 0 & F_{112} & F_{113} & 0 & F_{115} & 0 & F_{117} & 0 & F_{119} & 0 & -\mu & 0 \\ 0 & 0 & 0 & \alpha & 0 & 0 & 0 & F_{128} & 0 & 0 & 0 & -F_{1212} \end{pmatrix} \tag{4.2.52}$$

where;

$$F_{12}^{*}=y_{1}^{0}\beta_{1},F_{12}^{*}=y_{1}^{0}\beta_{1}\eta_{3},F_{14}^{*}=y_{1}^{0}\beta_{2},F_{16}^{*}=y_{1}^{0}\beta_{2}\chi_{1},F_{18}^{*}=y_{1}^{0}\beta_{2}\chi_{4}$$

$$F_{15}^{*}=y_{1}^{0}\left(\beta_{3}+\beta_{1}\eta_{1}+\beta_{2}^{*}\chi_{1}\right),F_{17}^{*}=y_{1}^{0}\left(\beta_{1}\eta_{2}+\beta_{2}^{*}\chi_{3}+\beta_{3}\Psi_{1}\right)$$

$$F_{19}^{*}=y_{1}^{0}\left(\beta_{1}\eta_{4}+\beta_{2}^{*}\chi_{5}+\beta_{3}\Psi_{2}\right)$$

$$F_{22}=y_{1}^{0}\beta_{1}-\mu-D_{H}\left(1-\varepsilon_{1}\right),F_{23}=y_{1}^{0}\beta_{1}\eta_{3},F_{25}=y_{1}^{0}\beta_{1}\eta_{1},F_{27}=y_{1}^{0}\beta_{1}\eta_{2}$$

$$F_{29}=\sigma\left(1-\varepsilon_{2}\right)+y_{1}^{0}\beta_{1}\eta_{4}$$

$$F_{32}=D_{H}\left(1-\varepsilon_{1}\right),F_{33}=\mu+\delta_{1},F_{44}^{*}=y_{1}^{0}\beta_{2}^{*}-\left(\alpha+\mu+\tau+\psi D_{B}\right)-\beta_{5}$$

$$F_{45}^{*}=y_{1}^{0}\beta_{2}^{*}\chi_{2},F_{46}^{*}=y_{1}^{0}\beta_{2}^{*}\chi_{1}$$

$$F_{47}^{*}=y_{1}^{0}\beta_{2}^{*}\chi_{3},F_{48}^{*}=y_{1}^{0}\beta_{2}^{*}\chi_{4},F_{49}^{*}=y_{1}^{0}\beta_{2}^{*}\chi_{5},F_{52}=\nu\beta_{4},F_{53}=\nu\beta_{4}\Lambda_{3}$$

$$F_{55}=y_{1}^{0}\beta_{3}+\nu\beta_{4}\Lambda_{1}-\left(\gamma+\mu+\phi\right),F_{57}=\nu\beta_{4}\Lambda_{2}+y_{1}^{0}\beta_{3}\Psi_{1}$$

$$F_{59}=\nu\beta_{4}\Lambda_{4}+y_{1}^{0}\beta_{3}\Psi_{2},F_{511}=\nu\beta_{4}\Lambda_{5}$$

$$F_{66}=\mu+\delta_{2},F_{77}=\mu+\delta_{4},F_{88}=\mu+\delta_{3}+\varphi\left(1-\varepsilon_{2}\right),F_{99}=\mu+\delta_{3}+\sigma\left(1-\varepsilon_{2}\right)$$

$$F_{102}=y_{10}^{0}\Gamma\beta_{1},F_{103}=y_{10}^{0}\Gamma\beta_{1}\eta_{3},F_{105}=y_{10}^{0}\Gamma\beta_{1}\eta_{1},F_{107}=y_{10}^{0}\Gamma\beta_{1}\eta_{2}$$

$$F_{109}=y_{10}^{0}\Gamma\beta_{1}\eta_{4}$$

$$F_{112}=y_{10}^{0}\Gamma\beta_{1},F_{113}=y_{10}^{0}\Gamma\beta_{1}\eta_{3},F_{115}=y_{10}^{0}\Gamma\beta_{1}\eta_{1},F_{117}=y_{10}^{0}\Gamma\beta_{1}\eta_{2}$$

$$F_{119}=y_{10}^{0}\Gamma\beta_{1}\eta_{4},$$

$$F_{128}=\left(1-\varepsilon_{2}\right)\varphi,F_{1212}=\omega+\mu$$

Using mathematica software, we determined the eigenvalues of the Jacobian matrix 4.2.52 as

$$z_1 = z_2 = -\mu, z_3 = -(\omega + \mu), z_{10} = 0$$

$$z_4 = -\left(y_1^0 \beta_1 + \mu + D_H (1 - \varepsilon_1)\right)$$

$$z_5 = y_1^0 \beta_1 \eta_3 D_H (1 - \varepsilon_1) + \left(y_1^0 \beta_1 - \mu - D_H (1 - \varepsilon_1)\right)(\mu + \delta_1)$$

$$z_6 = y_1^0 \beta_2^* - (\alpha + \mu + \tau + \psi D_B) - \beta_5$$

$$z_7 = -(v\beta_4 F_5 - F_4 v\beta_4 \Lambda_3) F_9 F_6 + (F_5 F_9 + F_4 F_{10})(v\beta_4 F_6 - F_4 F_{17})$$

$$Z_8 = -((v\beta_4 F_5 - F_4 v\beta_4 \Lambda_3) F_9 F_6 - (F_5 F_9 + F_4 F_{10})(v\beta_4 F6 - F_4 F_{17}))$$

$$(\psi D_B F_{13}^* + F_{11}^* F_{20})$$

$$Z_9 = -\gamma((F_4 v\beta_4 \Lambda_3 - v\beta_4 F_5) F_9 F_7 + (F_5 F_9 + F_4 F_{10})(v\beta_4 F_7 - F_4 F_{18})) -$$

$$((v\beta_4 F_5 - F_4 v\beta_4 \Lambda_3) F_9 F_6 - (F_5 F_9 + F_4 F_{10})(v\beta_4 F6 - F_4 F_{17})) F_{21}$$

$$z_{11} = -(\gamma((v\beta_4 F_5 - F_4 v\beta_4 \Lambda_3) F_9 F_7 - (F_5 F_9 + F_4 F_{10})(v\beta_4 F_7 - F_4 F_{18})))$$

$$+ ((v\beta_4 F_5 - F_4 v\beta_4 \Lambda_3) F_9 F_6 - (F_5 F_9 + F_4 F_{10})(v\beta_4 F6 - F_4 F_{17})) F_{21})$$

$$((v\beta_4 F_5 - F_4 v\beta_4 \Lambda_3) F_9 F_6 - (F_5 F_9 + F_4 F_{10})(v\beta_4 F6 - F_4 F_{17}))$$

$$(\tau F_{13}^* ((v\beta_4 F_5 - F_4 v\beta_4 \Lambda_3) F_9 F_6 - (F_5 F_9 + F_4 F_{10})(v\beta_4 F6 - F_4 F_{17}))\psi D_B F_{15}^*)$$

$$- (\psi D_B F_{13}^* + F_{11}^* F_{20})(\tau F_{15}^* + F_{11}^* F_{22})$$

$$z_{12} = \phi\gamma F_{12}^* ((v\beta_4 F_5 - F_4 v\beta_4 \Lambda_3) F_9 F_7 - (F_5 F_9 + F_4 F_{10})(v\beta_4 F_7 - F_4 F_{18}))$$

$$((v\beta_4 F_5 - F_4 v\beta_4 \Lambda_3) F_9 F_8 - (F_5 F_9 + F_4 F_{10})(v\beta_4 F_8 - F_4 F_{19})) -$$

$$(\gamma((v\beta_4 F_5 - F_4 v\beta_4 \Lambda_3) F_9 F_7 - (F_5 F_9 + F_4 F_{10})(v\beta_4 F_7 - F_4 F_{18})))$$

$$+ ((v\beta_4 F_5 - F_4 v\beta_4 \Lambda_3) F_9 F_6 - (F_5 F_9 + F_4 F_{10})(v\beta_4 F_6 - F_4 F_{17})) F_{21}$$

$$(\phi F_{12}^* ((v\beta_4 F_5 - F_4 v\beta_4 \Lambda_3) F_9 F_8 - (F_5 F_9 + F_4 F_{10})(v\beta_4 F_8 - F_4 F_{19}))) +$$

$$((v\beta_4 F_5 - F_4 v\beta_4 \Lambda_3) F_9 F_6 - (F_5 F_9 + F_4 F_{10})(v\beta_4 F6 - F_4 F_{17})) F_{23}$$

The Jacobian matrix 4.2.52 has a simple zero eigenvalue, z_{10}. Thus, the concept of center manifold theorem by Carr (2012) is applied to investigate the possibility of bifurcation for

the full model near $\beta_2 = \beta^*$. The corresponding left and the right eigenvectors to the zero eigenvalue of the Jacobian matrix were obtained as follows;

We let the right eigenvector defined as a column vector by

$u = [u_1, u_2, u_3, u_4, u_5, u_6, u_7, u_8, u_9, u_{10}, u_{11}, u_{12}]^T$ satisfying $J_{E^0_{HB}}.u = 0$

Solving for $u_1, u_2, u_3, u_4, u_5, u_6, u_7, u_8, u_9, u_{10}, u_{11}$ and u_{12} we obtain

$$u_1 = -\frac{S\beta_1 F_{10}\left(\frac{F_8F_{21}\phi-\gamma F_7-F_6F_{21}}{\gamma(F_4F_{10}+F_5F_9)}\right)}{\mu}u_5 -$$

$$\frac{S\beta_1\eta_3 F_9\left(\frac{F_8F_{21}\phi-\gamma F_7-F_6F_{21}}{\gamma(F_4F_{10}+F_5F_9)}\right)}{\mu} - \frac{\frac{F_1F_{21}}{\gamma}u_5}{\mu} - \frac{F_2}{\mu}u_5 - \frac{F_3F_{21}\phi}{\gamma F_{23}\mu}u_5$$

$$u_2 = F_{10}\left(\frac{F_8F_{21}\phi-\gamma F_7-F_6F_{21}}{\gamma(F_4F_{10}+F_5F_9)}\right)u_5,$$

$$u_3 = F_9\left(\frac{F_8F_{21}\phi-\gamma F_7-F_6F_{21}}{\gamma(F_4F_{10}+F_5F_9)}\right)u_5,$$

$$u_4 = \frac{F_{21}}{\gamma}u_5$$

$$u_6 = \frac{F_{21}\phi}{\gamma F_{23}}u_5,$$

$$u_{12} = \frac{V^0\Gamma\beta_1 F_{10}\left(\frac{F_8F_{21}\phi-\gamma F_7-F_6F_{21}}{\gamma(F_4F_{10}+F_5F_9)}\right)}{\mu}u_5 + \frac{V^0\Gamma\beta_1\eta_1\frac{F_{21}}{\gamma}}{\mu}u_5 + \frac{V^0\Gamma\beta_1\eta_2}{\mu}u_5$$

$$V^0\Gamma\beta_1\eta_3 F_9\left(\frac{F_8F_{21}\phi-\gamma F_7-F_6F_{21}}{\gamma(F_4F_{10}+F_5F_9)}u_5 + \frac{V^0\Gamma\beta_1\eta_4\frac{F_{21}\phi}{\gamma F_{23}}}{\mu}u_5\right.$$

$$u_5 = u_5 > 0, u_7 = u_8 = u_9 = u_{10} = u_{11} = 0.$$

Similarly, the left eigenvector given as a row vector associated with the zero eigenvalue at $\beta_2 = \beta^*$ is denoted by

$v = [v_1, v_2, v_3, v_4, v_5, v_6, v_7, v_8, v_9, v_{10}, v_{11}, v_{12}]$

and satisfies the equation $v \cdot J_{E^0_{HB}} = 0$ with values

$v_1 = 0, v_2 = 0, v_6 = \left(\frac{F_{22}F^*_{14}+F^*_{16}\tau}{F_{22}\psi D_B}\right)v_4$

$v_3 = -\left(\left(v_5\left(\mu\phi F_5F_{19}F_{21}F_{24} + \gamma\mu F_5F_{18}F_{23}F_{24} + \mu F_5F_{17}F_{21}F_{23}F_{24} - \mu\phi F_4F_{19}F_{21}F_{25}\right)\right) -\right.$

$\gamma\mu F_4F_{18}F_{23}F_{25} - \mu F_4F_{17}F_{21}F_{23}F_{25} - \mu\phi F_8F_{21}F_{25}\nu\beta_4\Big)$

$v_7 = \left(v_5\left(-\mu F_6F_{18}F_{23}\left(F_{10}F_{24}+F_9F_{25}\right) + \left(F_5F_9+F_4F_{10}\right)\left(-\left(\phi F_{19}+F_{17}F_{23}\right)F_{27}+\right.\right.\right.$

$$F_{18}\left(F_{23}F_{26}+\phi F_{28}\right)))+\left(\left(F_5F_9+F_4F_{10}\right)V\Gamma\beta_1$$
$$\left(F_{23}\left(-\eta_1F_{27}+F_{26}\eta_2\right)+\phi\left(F_{28}\eta_2-F_{27}\eta_4\right)\right)\Lambda_3+F_{26}F_{23}\left(F_9\left(-F_{25}V\Gamma\beta_1\eta_2+\right.\right.$$
$$\left.\left.F_{27}\left(\mu+V\Gamma\beta_1\eta_3\right)\Lambda_3+F_{10}\left(\mu F_{27}+V\Gamma\beta_1\left(F_{27}-F_{24}\eta_2\right)\Lambda_3\right)\right)\right)\nu\beta_4+$$
$$\phi F_8\left(\gamma F_{18}\left(F_{10}F_{24}+F_9F_{25}\right)-\left(F_9\left(-F_{25}V\Gamma\beta_1\eta_2+F_{27}\left(\mu+V\Gamma\beta_1\eta_3\right)+\right.\right.\right.$$
$$\left.\left.\gamma\left(-F_{25}V\Gamma\beta_1\eta_2+F_{27}\left(\mu+V\Gamma\beta_1\eta_3\right)\right)\Lambda_3+F_{10}\left(\mu F_{27}+V\Gamma\beta_1\left(F_{27}-\eta_2F_{24}\right)\Lambda_3\right)\right)\nu\beta_4\right)+$$
$$F_7\left(\mu\left(\phi F_{19}+F_{17}F_{23}\right)\left(F_{10}F_{24}+F_9F_{25}\right)-F_9\left(\phi F_{28}\left(\mu+V\Gamma\beta_1\eta_3\right)+F_{23}\left(-F_{25}V\Gamma\beta_1\eta_1\right.\right.\right.$$
$$\left.\left.+F_{26}\left(\mu+V\Gamma\beta_1\eta_3\right)\right)-\phi F_{25}V\Gamma\beta_1\eta_4\right)\Lambda_3$$
$$\left.+F_{10}\left(\mu\left(F_{23}F_{26}+\phi F_{28}\right)+V\Gamma\beta_1\left(F_{23}\left(F_{26}-F_{24}\eta_1\right)+\phi\left(F_{28}-F_{24}\eta_2\right)\right)\Lambda_3\right)\nu\beta_4\right)\Big)\Big/$$
$$\left(\mu\left(\phi F_{28}F_{21}\left(F_{10}F_{24}+F_9F_{25}\right)+F_{23}\left(-\gamma F_7\left(F_{10}F24+F_9F_{25}\right)-F_6F_1\left(F_{10}F_{24}+\right.\right.\right.\right.$$
$$\left.\left.\left.\left.F_9F_{25}\right)\right.\right.$$
$$\left.+\left(F_5F_9+F_4F_{10}\right)\left(F_{21}F_{26}+\gamma F_{27}\right)+\phi\left(F_5F_9+F_4F_{10}\right)F_{21}F_{28}\right)\right)$$
$$-v_4\frac{\left(F_{12}^*+\frac{\left(-F_{10}F_{24}-F_9F_{25}\right)\left(F_7-\frac{\left(F_5F_9+F_4F_{10}\right)F_{27}}{F_{10}F_{24}+F_9F_{25}}\right)\left(-\gamma F_{23}F_{12}^*-F_{21}\left(F_{23}F_{11}^*+\phi F_{13}^*\right)\right)}{\left(-\phi F_{28}F_{21}+\left(\gamma F_7+F_6F_{21}\right)F_{23}\right)\left(F_{10}F_{24}+F_9F_{25}\right)-\left(F_5F_9+F_4F_{10}\right)\left(\gamma F_{23}F_{27}+F_{21}\left(F_{23}F_{26}+\phi F_{28}\right)\right)}\right)}{F_{21}}$$
$$v_8=-\frac{F_{16}}{F_{22}}v_4$$
$$v_9=\left(v_5\left(\mu F_{19}\left(-\gamma F_7\left(F_{10}F_{24}+F_9F_{25}\right)-F_6F_{21}\left(F_{10}F_{24}+F_9F_{25}\right)\right)\right.\right.$$
$$\left.+\left(F_5F_9+F_4F_{10}\right)\left(F_{21}F_{26}+\gamma F_{27}\right)\right)-$$
$$\mu\left(F_5F_9+F_4F_{10}\right)\left(\gamma F_{18}+F_{17}F_{21}\right)F_{28}+\left(\mu F_{10}\left(\gamma F_7+F_6F_{21}\right)F_{28}+\left(\left(F_5F_9+F_4F_{10}\right)V\Gamma\beta_1\right.\right.$$
$$\left(-F_{28}\left(\eta_1F_{21}+\gamma\eta_2\right)+\left(F_{21}F_{26}+\gamma F_{27}\right)\eta_4\right)+\gamma F_7\left(F_{28}\left(F_{10}V\Gamma\beta_1+F_9\left(\mu+V\Gamma\beta_1\eta_3\right)\right)-\right.$$
$$\left(F_{10}F_{24}+F_9F_{25}\right)V\Gamma\beta_1\eta_4\Big)+F_6F_{21}\left(F_{28}\left(F_{10}V\Gamma\beta_1+F_9\left(\mu+V\Gamma\beta_1\eta_3\right)\right)-\left(F_{10}F_{24}+\right.\right.$$
$$\left.\left.F_9F_{25}\right)V\Gamma\beta_1\eta_4\right)\Big)\nu\beta_4+$$
$$F_8\left(-\mu\left(\gamma F_{18}+F_{17}F_{21}\right)\left(F_{10}F_{24}+F_9F_{25}\right)+\left(F_9\left(F_{21}\left(-F_{25}V\Gamma\beta_1\eta_1+F_{26}\left(\mu+V\Gamma\beta_1\eta_3\right)+\right.\right.\right.\right.$$
$$\gamma\left(-F_{25}V\Gamma\beta_1\eta_2\right.$$
$$\left.\left.+F_{27}\left(\mu+V\Gamma\beta_1\eta_3\right)\right)\Lambda_3+F_{10}\left(\mu\left(F_{21}F_{26}+\gamma F_{27}\right)+V\Gamma\beta_1\left(F_{21}\left(F_{26}-\eta_1F_{24}\right)+\gamma\left(F27-\right.\right.\right.\right.$$
$$\left.\left.\left.\left.\eta\left(2F24\right)\right)\Lambda3\right)\right)\nu\beta_4\right)\Big)\Big/$$
$$\left(\mu\left(\phi F_{28}F_{21}\left(F_{10}F_{24}+F_9F_{25}\right)+F_{23}\left(-\gamma F_7\left(F_{10}F24+F_9F_{25}\right)-F_6F_1\left(F_{10}F_{24}+F_9F_{25}\right)+\right.\right.\right.$$
$$\left.\left.\left.\left(F_5F_9+F_4F_{10}\right)\left(F_{21}F_{26}+\gamma F_{27}\right)+\phi\left(F_5F_9+F_4F_{10}\right)F_{21}F_{28}\right)\right)\right.$$
$$-v_4\frac{\left(F_{13}^*+\frac{\left(-F_{10}F_{24}-F_9F_{25}\right)\left(F_8+\frac{\left(F_5F_9+F_4F_{10}\right)F_{28}}{F_{10}F_{24}+F_9F_{25}}\right)\left(-\gamma F_{23}F_{12}^*-F_{21}\left(F_{23}F_{11}^*+\phi F_{13}^*\right)\right)}{\left(-\phi F_{28}F_{21}+\left(\gamma F_7+F_6F_{21}\right)F_{23}\right)\left(F_{10}F_{24}+F_9F_{25}\right)-\left(F_5F_9+F_4F_{10}\right)\left(\gamma F_{23}F_{27}+F_{21}\left(F_{23}F_{26}+\phi F_{28}\right)\right)}\right)}{F_{23}}$$

$$v_{10} = \Bigg(\left(\phi F_8 F_{21} - (\gamma F_7 + F_6 F_{21}) F_{23}\right) v_5 x_4 F_9 - v_2 F_2^* + v_5 v \beta_4 + \frac{v \beta_4 \Lambda_5}{\mu} v_5 V^0 \Gamma \beta_1 /$$

$$(\mu \left(\phi F_{28} F_{21} \left(F_{10} F_{24} + F_9 F_{25}\right) + F_{23} \left(-\gamma F_7 \left(F_{10} F24 + F_9 F_{25}\right) - F_6 F_1 \left(F_{10} F_{24} + \right.\right.$$

$$\left. F_9 F_{25} \right)$$

$$\left. + \left(F_5 F_9 + F_4 F_{10}\right) \left(F_{21} F_{26} + \gamma F_{27}\right) + \phi \left(F_5 F_9 + F_4 F_{10}\right) F_{21} F_{28}\right))$$

$$v_{11} = \frac{v \beta_4 \Lambda_3}{\mu} v_5$$

$$v_{12} = \left(\frac{F_{14}^* F_{22} F_{20} + \tau F_{20} F_{16}^* + F_{22} \psi D_B F_{15}^*}{F_{22} \psi \alpha D_B} \right) v_4$$

$$v_4 = v_4 > 0 \text{ and } v_5 = v_5 > 0$$

According to the theorem, the bifurcation coefficients a and b were computed as follows;

$a = \sum_{k=i=j=1}^{12} v_k u_i u_j \frac{\partial^2 f_k}{\partial x_i \partial x_j}$

$= v_5 u_4 u_5 \frac{\partial^2 f_5}{\partial x_4 \partial x_5} + v_5 u_5 u_6 \frac{\partial^2 f_5}{\partial x_5 \partial x_6} = v_5 u_5 \left(u_4 \frac{\partial^2 f_5}{\partial x_4 \partial x_5} + u_6 \frac{\partial^2 f_5}{\partial x_5 \partial x_6} \right) = v_5 u_5 \left(u_4 \beta_5 \Upsilon_1\right)$

and

$b = \sum_{k=i=1}^{12} v_k u_i \frac{\partial^2 f_k}{\partial x_i \partial \beta^*} = v_4 u_5 \frac{\partial^2 f_4}{\partial x_5 \partial \beta^*} = v_4 u_5 \left(\beta y_1^0 \chi_2\right)$

since $v_4 > 0, v_5 > 0$ and $u_5 > 0$, it follows that $a > 0$ and $b > 0$ which conforms to condition (a).

According to theorem 6 , it follows that $(0,0)$ is locally asymptotically stable and there exists a positive unstable equilibrium and when $0 < \beta^* \ll 1$, then (0,0) is unstable and there exists a negative and locally asymptotically stable equilibrium. Hence, in the co-infection model, there is a backward bifurcation phenomena because a stable co-infection free equilibrium point co-exist with a stable co-infection endemic equilibrium point.

4.5 Numerical Simulation of Deterministic Co-infection Model

In this section, we use secondary data from the literature to demonstrate the numerical solution of the deterministic co-infection model. We show the dynamics of each population with time with respect to clinical and non-clinical control interventions. The deterministic model is solved by the fourth-order Runge-Kutta method implemented in MATLAB

(R2017a) with ode45 solver . This ode45 solver has an inbuilt numerical scheme, Runge-Kutta method.

The formula is implemented in Matlab for the deterministic and optimal control problem as given in appendix A and B. The Matlab codes for the co-infection are found in appendix A. The initial conditions in table 4.1 are chosen based on HIV/AIDS and HBV prevalence data in Sub-Saharan Africa, because it bears one of the highest burdens of HIV and viral Hepatitis according to Mohareb et al. (2021) and World Health Organization (2017). The table 4.1. below lists the estimated values of the parameters and initial conditions.

Table 4.1
Parameter values and initial conditions

Parameter	**Nominal Value/Range**	**Source**
N	1,257,334,259	https://www.worlddata.info/africa
S	1,131,600,833	https://www.ncbi.nlm.nih.gov
b	4.18-37.1% (2021)	https://www.worlddata.info/africa
μ	13.1%	https://www.worlddata.info/africa/niger

Parameter	Nominal Value/Range	Source
δ_1	1.62%-0.7114 (2022)	https://www.who.int/news-room/fact-sheet
δ_2	0.28%-15%	WHO (2019)
δ_3	2.84 per 100 persons/yr	Jia et al. (2022)
δ_4	42%	National Institutes of Health (2022)
τ	10.5%	WHO (2019)
ω	2-24 weeks	https://www.hepb.org
I_H	39.0 Million	WHO (2022)
A	29.8 Million	UNAIDS (2022), https://www.unaids.org
V_H	2/3 of people with HIV	Martins et al. (2015)
V	1 Billion people (2017)	https://www.hepb.org
I_B	1.704 Billion (2019)	https://www.hepb.org
I_{cB}	80 million	Feigin et al. (2021)

Parameter	Nominal Value/Range	Source
I_{HB}	2.7 Million (1%)	WHO (2019), https://www.who.int/fact-sheets/hepatitis-
I_{HcB}	$8-10\%$ of I_{HB}	Leumi et al. (2020)
T_B	6.6 Million (22%)	WHO (2019)
T_{HB}	$12-25\%$ of I_{HB}	NIH (2020)
R	1.5336 Billion (90%)	https://www.hepb.org
λ_1	9.0%	Goliber (2002)
λ_3	7.4-10%	WHO (2019), Thio (2009)
λ_2	3.2-7.5%	*Global Hepatitis report 2022* (n.d.)
λ_4	10%	World Health Organization (2022)
λ_5	5-10%	Okocha, Oguejiofor, Odenigbo, Okonkwo, and Asomugha (2012)
φ	2-24 weeks	https://www.hepb.org
β_3	10%	CDC, 2021

Parameter	Nominal Value/Range	Source
ψ	5-10%	Hyams (1995)
γ	20-25%	Bodsworth, Cooper, and Donovan (1991)
ϕ	17%	Hutin et al. (2018)
β_1	0.0257-0.0347	Nagelkerke et al. (2009), Han, Lou, Ruan, and Shao (2008)
v	8%	Mohareb and Kim (2021) & Kim (2020)
D_H	2.3-5	Chen, Xiao, et al. (2014), https://www.iapac.org
D_B	0.00008249	De Boer et al. (2001), Whalley et al. (2001)
α	94-98%	World Health Organization and others (2020), Gastanaduy et al. (2019)
Γ	22%	K. Allen et al. (2015)
θ_3	10-18%	Feldstein et al. (2017), CDC (2022)
ε_1	60-80%	Koethe et al. (2020)

Parameter	Nominal Value/Range	Source
ε_2	72-96%	Hadziyannis, Papatheodoridis, Dimou, Laras, and Papaioannou (2000)
β_4	5-20%	Singh et al. (2017)
β_2	0.1-20%	Inoue and Tanaka (2016) & Tanaka (2016)
ρ	0.7 to 11.6%	Landes et al. (2008)
θ_1	85-90%	Frigati et al. (2020)
θ_2	5.8-6%	Razavi-Shearer et al. (2018)
θ_4	15-45%	https://www.who.int/hepatitis/publications/global-hepatitis
σ	80.7%	Pappoe, Hagan, Obiri-Yeboah, and Nsiah (2019)

Source: Researcher (2025)

4.5.1 Local sensitivity analysis of model parameters

As evidenced by Siriprapaiwan, Moore, and Koonprasert (2018), Chitnis et al. (2008), and Samsuzzoha, Singh, and Lucy (2013), sensitivity analysis is useful because it assists in identifying the parameter (s) that is the most useful in moderating the intensity of the in-

fection. More than that, to realize how one should counteract the virus and cases, those aspects that influence the epidemic must be described. To achieve this, the incorporated data set is fitted to the model to estimate the basic reproduction number and the strength number. The specific method that is applied for quantification is the forward normalized sensitivity. The forward normalized sensitivity indices are calculated by the direct method of partial differentiation of R_0 with regard to the focal parameter as in the following equation

$$\Lambda_{\emptyset}^{R_0} = \frac{\partial R_0}{\partial \emptyset} \times \frac{\emptyset}{R_0} \tag{4.2.53}$$

where $\emptyset$ is the model parameter. The direct method gives the analytical expressions for each model parameter but then evaluated numerically using the estimated values in table 4.1. In addition to the direct method, Chitnis et al. (2008) proposed a method that linearized the model equations at the co-infection free equilibrium point and solves for the sensitivity indices of the resulting algebraic equations. The direct and Chitnis Method are used for local sensitivity analysis while Latin Hypercube Sampling method used in the study by Wang, Liu, and Liu (2016) is used for global uncertainties of the model parameters.

4.5.2 Local sensitivity analysis of basic reproduction and strength number

The sensitivity indices of basic reproduction determined using NGM, R_{0N}, survival function, $R_{0,S}$ and strength number A_0 are computed numerically from the expression 4.2.53 as tabulated in table 4.2. These indices are compared for each of the parameter.

Table 4.2

Normalized Sensitivity Indices for Model Parameters $R_{0,N}, R_{0,S}$ and A_0

Parameter ($\emptyset$)	Normalized Sensitivity Indices		
	$\frac{\partial A_0}{\partial \varnothing} \times \frac{\varnothing}{A_0}$	$\frac{\partial R_{0,S}}{\partial \emptyset} \times \frac{\emptyset}{R_{0,S}}$	$\frac{\partial R_{0,N}}{\partial \emptyset} \times \frac{\emptyset}{R_0^B}$
β_3	1.000000	1.000000	0.000000
γ	-0.458365	-0.187763	0.000000
μ	-1.121696	-1.281300	0.000000
π	1.000000	1.000000	1.000000
θ_5	1.000000	0.834363	1.000000
ϕ	-0.324675	-0.132999	0.000000
β_1	0.000000	0.232247	0.000000
α	0.000000	-0.292162	-0.821046
τ	0.000000	-0.031352	0.000000
D_B	0.000000	-0.000002	0.216701
D_H	0.000000	-0.060016	0.000000
Γ	0.000000	0.165637	0.000000
θ_3	0.000000	0.165637	0.000000
ν	0.000000	-0.014218	0.000000
β_2	0.000000	0.357892	1.000000
β_4	0.000000	-0.014218	0.000000
Λ_5	0.000000	-0.000006	0.000000
ε_1	0.000000	0.238750	0.000000
χ_1	0.000000	0.000000	0.300481
ψ	0.000000	0.000000	0.216701
δ_2	0.000000	0.000000	-0.007228

Note. Sensitivity indices are the normalized derivative (rates of change) of model outputs (A_0, $R_{0,S}$, $R^B_{0,N}$) with respect to parameter change. Potential sensitivity is indicated by the values and is proportional
Source: Researcher (2025)

From table 4.2 above, it is observed that the co-infection contact rate β_3, recruitment rate π and proportion of susceptible θ_5 have positive sensitivity indices while progression rate, natural death and treatment have negative sensitivity indices. It is also observed that HIV transmission rate, HIV-HBV transmission rate, birth rate, proportion of susceptible births, progression rate of vaccinated Hep B to HIV, proportion of births vaccinated with Hep B, Hepatitis B transmission rate and HIV ART efficacy have yielded highest sensitivity indices while acute hepatitis B recovery rate due to natural immunity, screening rate, Hep B saturation function, HIV saturation function, AHB to CHB progression rate in co-infected individuals, treatment rate of Hepatitis B infection, the proportion of HIV-positive indi-

viduals vaccinated against Hep B, the progression rate of Hep B-vaccinated individuals with HIV to HIV-HBV co-infected individuals, and the transmission rate of HIV-infected individuals becoming co-infected all have lower sensitivity indices.

The local sensitivity analyses of A_0 and $R_{0,s}$ above clearly show that the indices vary from -1 to 1 , with regard to each model parameter included in their explicit expressions. Moreover, the parameters with negative indices relate to the basic reproduction number, $R_{0,s}$ inversely while positive sensitivity indices are directly proportional. Positive sensitivity scores suggest that $R_{0,s}$ has a significant effect on the model parameters. Therefore, changing the value of the parameter while keeping the value of the other factors the same will result in changes in the $R_{0,s}$. On the other hand, an increase or decrease in $R_{0,s}$ has a negative significance, according to negative sensitivity indices. In other words, changes in the parameter's value will cause changes in the $R_{0,s}$ even if the values of the other parameters don't change. Thus, to reduce the infection spread, these parameters have to be monitored and controlled.

4.5.3 Latin hypercube sampling

Latin hypercube sampling (LHS) is a stratified form of Monte Carlo sampling without replacement introduced by Mc kay and others in 1979 (Ali, Means, Ho, & Heffernan, 2021). It is meant to provide samples of model input to examine the sensitivity of the effect of their input on their model outputs through the PRCC examination. To create the probability density sample of actual sample size N of each of the variables p, $X = [X_1, X_2, ...X_P]^T$. LHS follows the procedure below using an $f(X)$. The domain of each parameter is partitioned into N mutually exclusive unequal probability intervals with probability 1/N. At each interval one value is picked up in a random manner based on the probability density within the interval. The N values of X_1 are found and are randomly paired with the N values of X_2. The N pairs are then joined with N of X_3 making up N triplets and so on until a set of N p-tuples are made. In this way, (N!p) possible sets of combinations of intervals forming Latin hypercube sample exist which are assembled in a N x p matrix. The mathematical model is then simulated looping through the N parameter suites.

4.5.4 Partial rank correlation coefficient (PRCC)

The Partial rank correlation coefficient (PRCC) method is a sampling based sensitivity analysis technique to compute the rank correlation coefficients of the model inputs and outputs that are partials. In case of two variables, X_i (Input variable) and Y (Output variable), a normal correlation coefficient is calculated as given below:

$C(X_i, Y) = \frac{\text{Cov}(X_i, Y)}{\sqrt{\text{Var}(X_i) \cdot \text{Var}(Y)}}$

with Cov(Xi,Y) being the covariance of Xi and Y, Var (Xi) and Var (Y) the respective variances of X_i and Y; and and the sample means of X and Y respectively. The correlation coefficient is known as Pearson correlation coefficient (PCC). When the data are rank-transformed, the outcome is referred to as a rank correlation coefficient. LHS-PRCC can be used to make an important decision on reality, as well as significance of unknown parameters of interest in contributing towards the outputs of a given model (Ali et al., 2021). Description of the PRCC approach can be traced in various publications (Ali et al., 2021), (Gomero, 2012). The relative importance of the input parameters to the basic reproduction number, is shown in Figure 4.2 below. Meanwhile, the most influential parameters of locally applied interventions into the problem of co-infection control are determined. Table 4.3 below shows PRCC results for $R_{0,S}$;

Figure 4.2
Relative significance of Normalized indices of A_0 and $R_{0,S}$

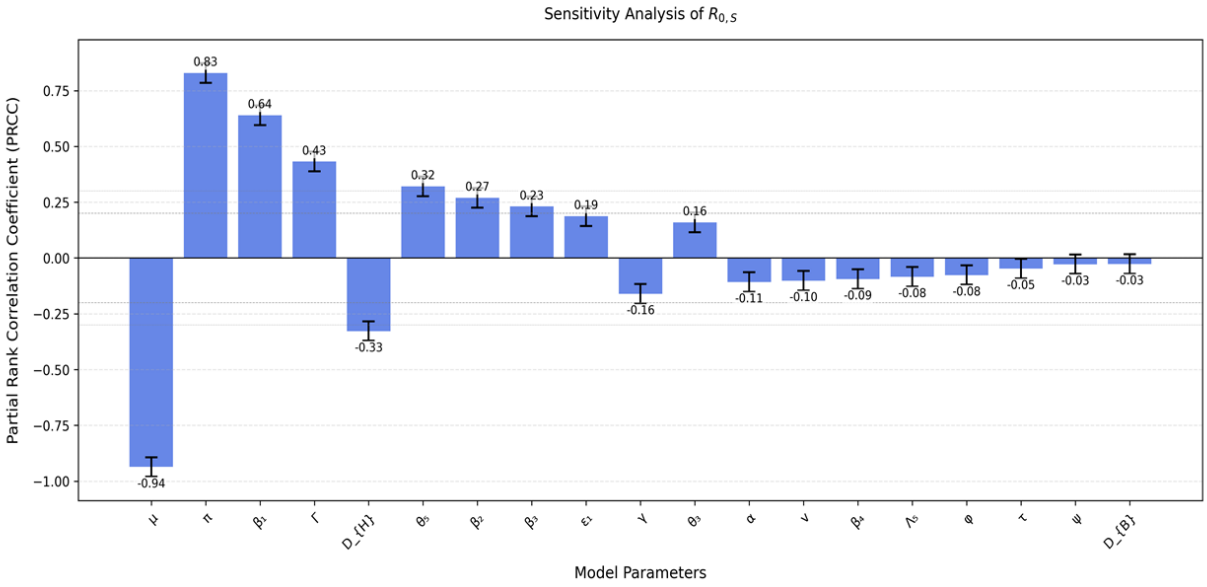

Source: Researcher (2025)

Table 4.3
Partial Rank Correlation Coefficients (PRCC) for $R_{0,S}$ Sensitivity Analysis

Parameter	PRCC [95% CI]	Influence	Effect
μ	-0.9374 ± 0.0439	Very strong	Decreases
π	0.8249 ± 0.0439	Very strong	Increases
β_1	0.5933 ± 0.0439	Very strong	Increases
Γ	0.4580 ± 0.0439	Strong	Increases
D_H	-0.2731 ± 0.0439	Moderate	Decreases
θ_5	0.2730 ± 0.0439	Moderate	Increases
β_2	0.2440 ± 0.0439	Moderate	Increases
β_3	0.2429 ± 0.0439	Moderate	Increases
ε_1	0.2054 ± 0.0439	Moderate	Increases
Λ_5	-0.1506 ± 0.0439	Weak	Decreases
θ_3	0.1452 ± 0.0439	Weak	Increases
α	-0.1357 ± 0.0439	Weak	Decreases
ν	-0.1049 ± 0.0439	Weak	Decreases
γ	-0.0902 ± 0.0439	Weak	Decreases
ϕ	-0.0796 ± 0.0439	Weak	Decreases
τ	-0.0794 ± 0.0439	Weak	Decreases
β_4	-0.0575 ± 0.0439	Weak	Decreases
D_B	-0.0431 ± 0.0439	Weak	Decreases
ψ	-0.0078 ± 0.0439	Weak	Decreases

Source: Researcher (2025)

4.5.5 Numerical computation of basic and control reproduction numbers

Substituting for the parameters into equations 4.2.27, 4.2.28, 4.2.29, 4.2.30 and 4.2.31, we therefore get the following numerical values for the reproduction number;

$R^H_{0,N} = 0.0000775277, R^B_{0,N} = 0.000422663, R^H_C = 0.000107824, R^B_C = 0.000404564$, $R_{0,S} = 0.011031$ and $R^{HB}_{0,N} = 1.00999 - 2.93127 \times 10^{-6} i$

It is evident from these values that $R^H_{0,N} < 1, R^B_{0,N} < 1, R^H_C < 1, R^B_C < 1$ and $R_{0,S} < 1$. It is also worth noting that $R_{0,S} > R^H_{0,N}, R_{0,S} > R^B_{0,N}, R_{0,S} > R^H_C$ and $R_{0,S} > R^B_C$. However, $R^B_{0,N}$ and R^B_C is more than that of HIV case. Subsequently,

$R^{HB}_{0,N}$ yields a complex number, whose magnitude is computed as follows;

$$\left|R^{HB}_{0,N}\right| = \sqrt{(1.00999)^2 + (-2.93127 \times 10^{-6})^2} = 1.00999 > 1$$

4.6 Numerical Simulations of Deterministic Population Dynamics

The deterministic co-infection model is numerically simulated in this section and is illustrated in the accompanying graphics. Considerations are made to assess the impact of both clinical and non-clinical control interventions on population dynamics. The initial conditions and parameter values in table 4.1 are used to simulate the model to predict the dynamics of co-infected populations. The ordinary differential equations in section 3.3.4 are coded in MATLAB (R2017a) as shown in appendix A and the corresponding numerical results are plotted.

4.6.1 Effect of varying natural immunity, α

Natural immunity also known as innate immunity, describes the body's general defensive systems against pathogens. Natural immunity is essential for the early response to the HBV in the event of an infection, prior to the emergence of adaptive immunity. The impact of varying natural immunity to the dynamics of co-infected populations is demonstrated in Figure 4.3. The values of α at interval of twenty percent are considered.

Figure 4.3

Effect of natural immunity

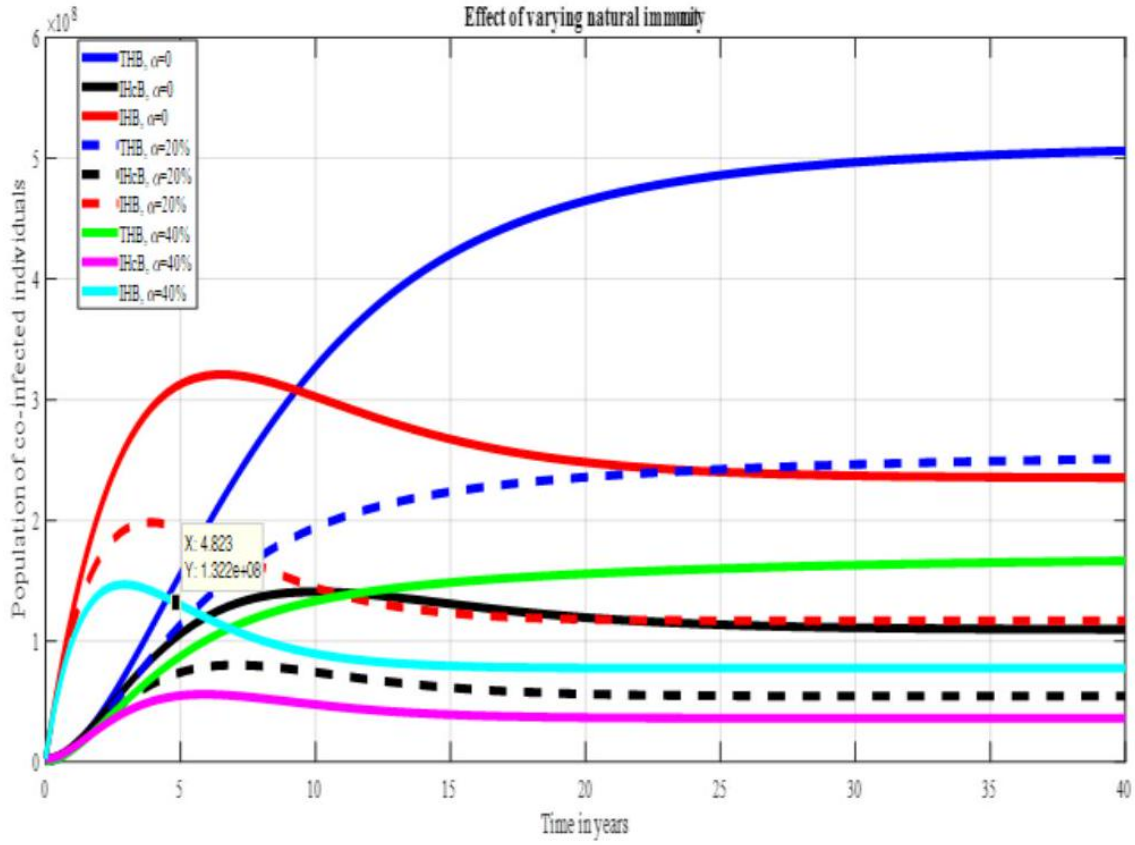

Source: Researcher (2025)

In Figure 4.3, initially the number of each co-infected case I_{HB}, I_{HcB}, T_{HB} increases in the absence of natural immunity. The increasing trend is attributed to comprised immunity to protect the host against the illness. On reaching maximum point, the number of co-infected cases starts to decline and becomes constant afterwards. On increasing the rate of natural immunity, the number of co-infected individuals I_{HB}, I_{HCB}, T_{HB} reduces with increase in rate of natural immunity. Increasing the natural immunity by 20% decreases the co-infection by at least 40% for each of the co-infected populations.

4.6.2 Effect of viral load on infection progression

HIV viral load, which is quantitatively defined by the amount of HIV RNA per millilitre of blood, is the amount of HIV RNA in blood. A high viral load indicates a high level of viral replication, indicating ongoing infection. Monitoring HIV viral load is crucial for HIV management and assessing the effectiveness of antiviral therapy. A continuous significant viral load is associated with faster progression to AIDS, as it indicates decreased immunity

and higher chances of opportunistic infections. Treatment aims to reduce viral load to an undetectable level, which is often fewer than 20 to 50 copies /ml. CD4 T-cell count is another crucial marker of HIV infection. HIV viral load is commonly reported on a logarithmic scale, but it is more manageable and easier to interpret. The HIV viral load saturation function is expressed by;

$$D_H = \log_{10} V_L \tag{4.2.54}$$

in which V_L denotes the viral load in copies/ml. However, one must understand that this logarithmic transformation is a common practice in virology and clinical laboratories in order to simplify data interpretation and analysis. The logarithmic scale simplifies the expression of viral load changes and the efficacy of treatment. Traditionally, the definition of a high HIV viral load is greater than 100,000 copies/ml of blood but it could be one million or more. The virus causes infection and the reproduction of the virus occurs with the progression of the disease. A HIV viral load that can be measured is considered to be less than 10,000 copies per milliliter of blood (Matthews, Geretti, Goulder, & Klenerman, 2014). The measurement of the HBV in the blood helps to determine the amount of virus activity and when to start treating chronic hepatitis B. Antivirals aid in lowering the HBV's rate of replication and thus decrease the viral load in the liver so that the disease does not progress. This saturation function of the viral-load, V , of Hepatitis B is represented by

$$D_B(V) = \frac{V}{l+V} \tag{4.2.55}$$

where l is the antigen needed to stimulate half-maximally. Less than $1cp/ml$ of the hepatitis B surface antigen (HBsAg) is considered negative, whereas more than $5cp/ml$ is considered positive (Ciupe, Ribeiro, Nelson, & Perelson, 2007). The HBV viral load lies between 0 to 1 billion according to Ribeiro et al. (2020), which can be classed as harmless and highly infectious. Substituting for D_H into equation (4.2.2) and (4.2.3), and solving numerically, we obtain figure 4.4 which shows the effect of HIV viral load on progression I_H to A at different values of V_L and D_H.

Figure 4.4
Effect of HIV viral load on co-infection

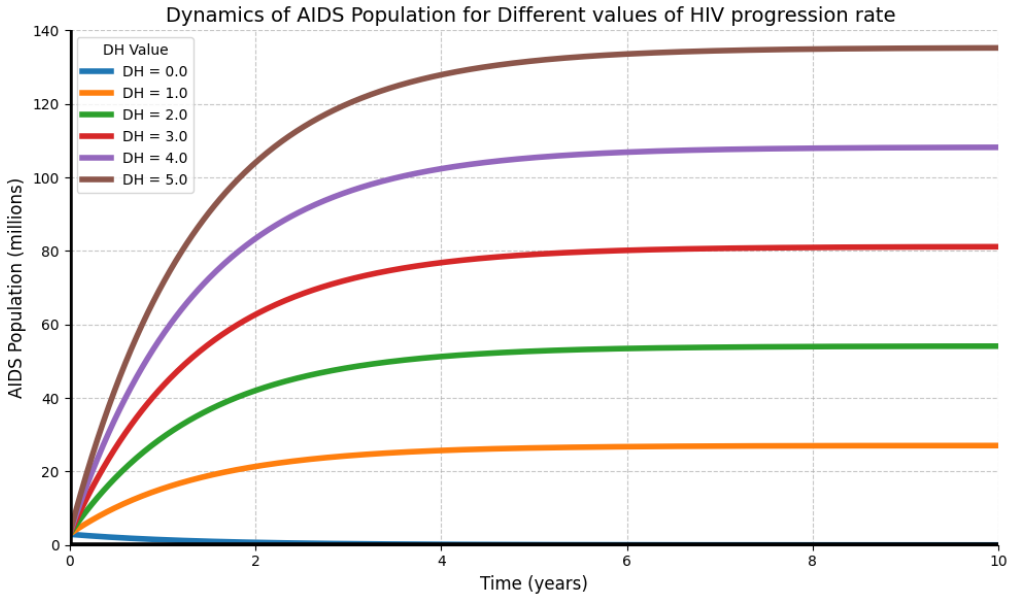

Source: Researcher (2025)

In Figure 4.4 above, at zero D_H, the number of AIDS infective reduces exponentially. This implies that there is no transition of HIV infective to AIDS population. At this instant, the progression rate of I_H to A is zero. Increasing HIV viral load by a multiple of 10 , and D_H increasing by 1 , the number of AIDS infective increases. This means that there are more HIV infected individuals, I_H moving to AIDS stage. Thus, a higher HIV progression rate. This trend continues for higher viral loads and the population tends to remain constant over time for each case. The increment of I_H is because during the acute stage, I_H, the viral load increases significantly characterized by a surge in viral replication as the virus multiplies within host cells, particularly CD4 + T cells. If the immune system cannot successfully stop the virus from replicating over time, then the HIV viral load will eventually start to rise once more. As the virus continues to multiply, the CD4 count, which is crucial for the immune system, declines steadily. A person is diagnosed with AIDS when their CD4+ T cell count falls below 200 copies/ml. The graph indicates a noticeable increase in viral load once more, which is followed by a slow decrease in CD4+ T cell count and the eventual development of AIDS. This is why I_H changes to A. Similarly, substituting for

D_B into (4.2.9), (4.2.10) respectively, the effect of HBV viral load on I_B progression to I_{cB} is demonstrated as follows

Figure 4.5

Effect of HBV viral load

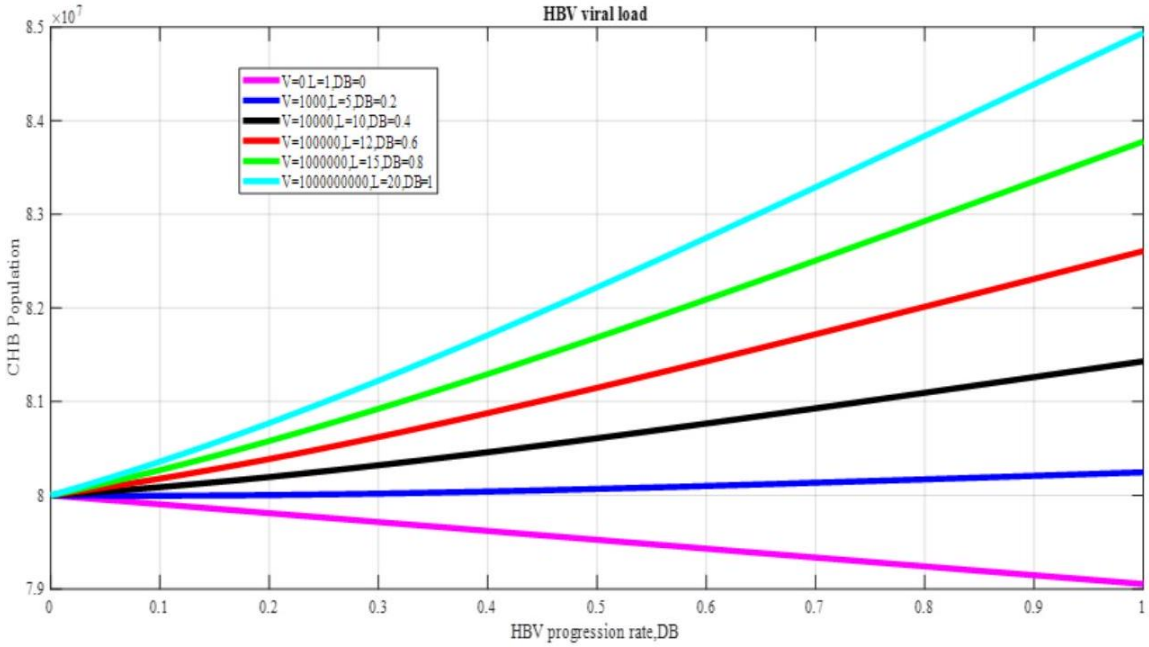

Source: Researcher (2025)

In Figure 4.5, the chronic Hepatitis B infected population declines at zero viral load while the population increases accordingly with increase in HBV viral load or HBV progression rate D_B. The reduction in the population with chronic hepatitis B at zero viral load is due to the effective antiviral therapy that inhibits viral multiplication, enhances liver function, and lowers the risk of transmission. On the other hand, a growth in the population with chronic hepatitis B is linked to greater viral loads and a faster course of the infection. This emphasizes the need of early screening, identification, close monitoring, and efficient antiviral treatments in the management of CHB

Figure 4.6
Effect of HIV and HBV viral load

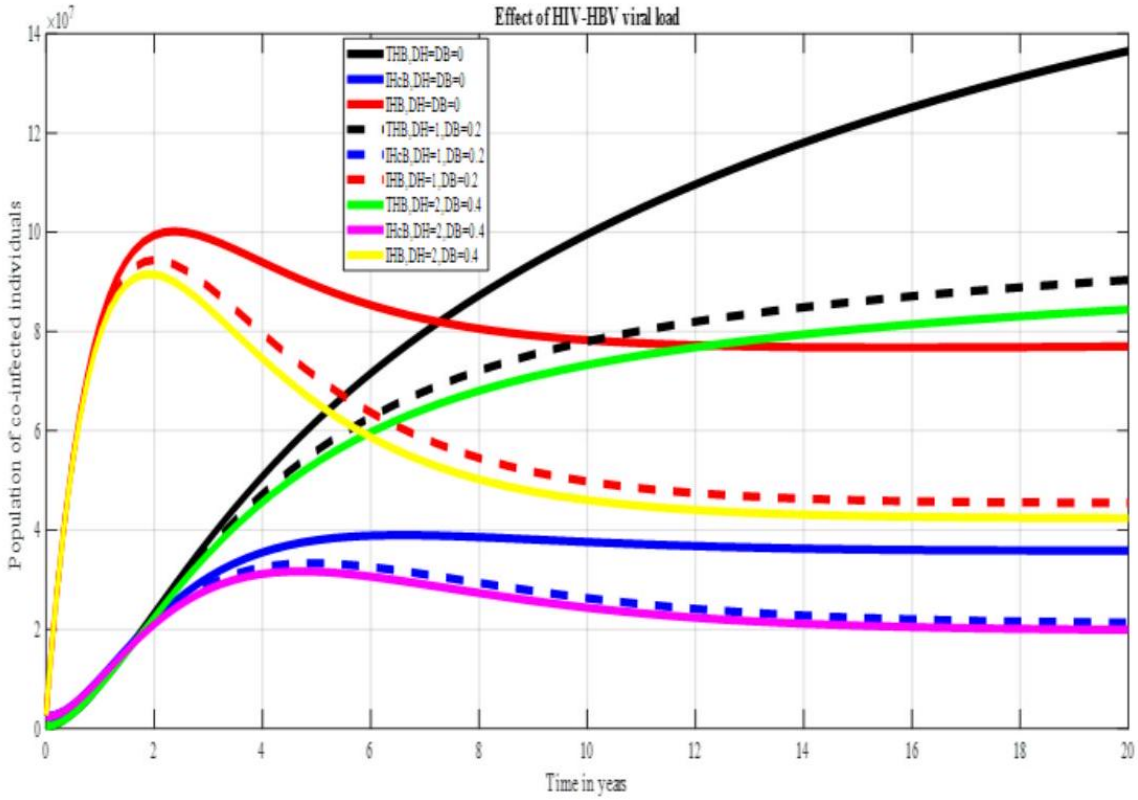

Source: Researcher (2025)

Figure 4.6 outlines the impact of changes of viral load HIV and HBV on dynamic of co-infection. At zero HIV and HBV viral load, $D_H = D_B = 0$, the population of HIV-HBV co-infected individuals increases rapidly for the first two years. On attaining the maximum value of 10×10^7, it starts to drop and continues to decline tending towards constant. Similarly, the population of treated co-infected individuals shows an upward trajectory. The chronic hepatitis B co-infected population increases slowly and for the first six years and then becomes constant afterwards at zero D_H and D_B. The population behaves in the same manner on increasing HIV viral loads, D_H by 1 and HBV viral load, D_B by 20% .

4.6.3 Effect of vertical transmission

This is the passing on of an infectious agent from an infected mother to her unborn child throughout her pregnancy or delivery, and breastfeeding. Vertical transmission is one of the ways that HIV and HBV can spread through which children become co-infected with both virus types from mothers who are chronically infected with either of the two viruses. The impact of vertical transmission is illustrated in Figure 4.7 below.

Figure 4.7

Effect of varying ρ on co-infection

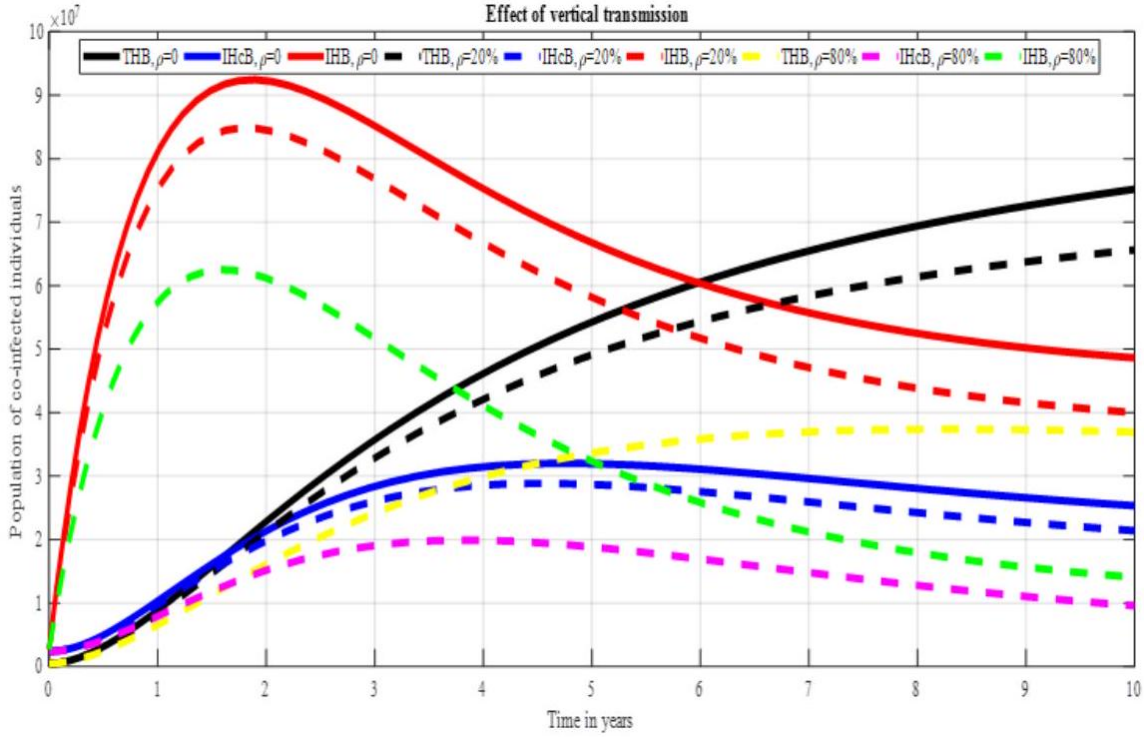

Source: Researcher (2025)

Figure 4.7 illustrates the dynamics of co-infected individuals on varying the proportion of HIV-HBV births, ρ. At $\rho = 0$, $(1-\rho)\pi = \pi$, so the whole recruitment goes to I_{HB} and ρ is the co-infected births, therefore, the population of co-infected HIV-HBV increases for the first two years and then decreases before tending to become constant. The treated co-infected population, T_{HB} increases steadily and chronic hepatitis co-infected population, I_{HCB} increases progressively and then shows a decreasing trend afterwards at $\rho = 0$. On increasing the proportion of co-infected births by 20%, the number of co-infected individuals decreases.

4.6.4 Effect of varying HIV infection rate on the dynamics of HIV and HBV co-infection

Figure 4.8 below demonstrates the effect of varying the rate of HIV co-infection, β_4 at an interval 20% on the dynamics of HIV-HBV population for a period of ten years, on the assumption that HBV co-infection rate, β_5 is kept constant.

Figure 4.8

Variation of HIV infection rate, β_4 at constant HBV infection rate, β_5

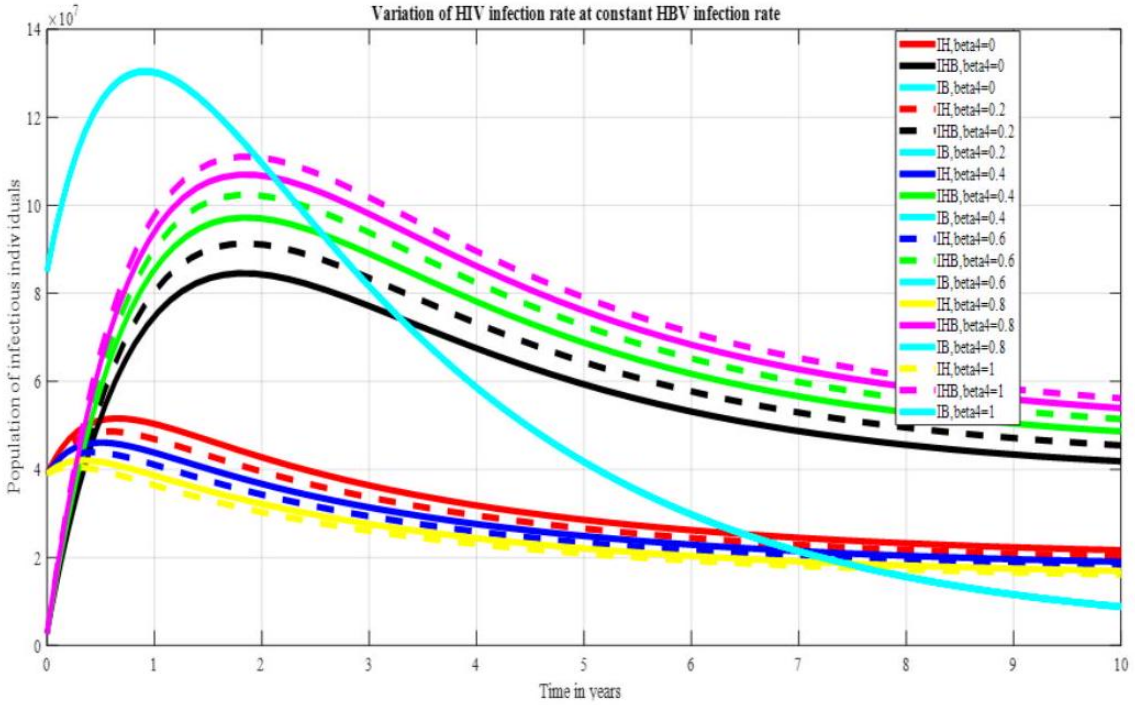

Source: Researcher (2025)

Similarly, Figure 4.9 illustrates the effect of varying HBV co-infection rate, β_5 at a interval of 30% on the population dynamics while maintaining the rate of HIV co-infection, β_4 constant during a ten year time span.

Figure 4.9

Variation of HIV infection rate, β_4 at constant HBV infection rate, β_5

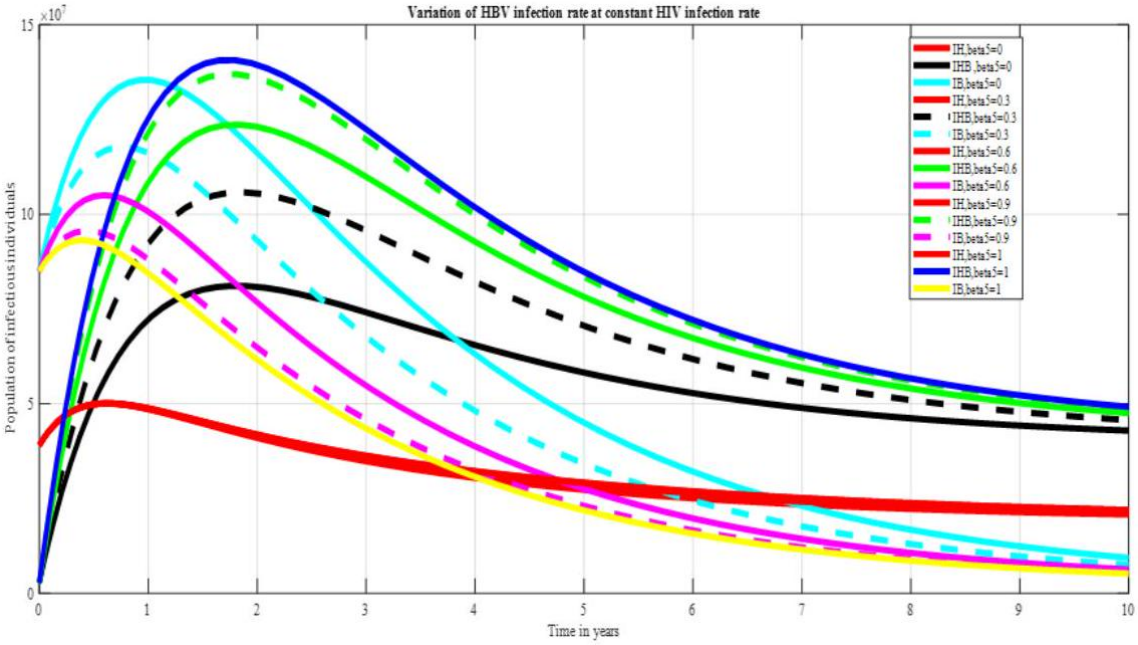

Source: Researcher (2025)

From Figure 4.8 and 4.9 above, it is observed that the population of I_H decreases with increase in HIV infection rate, β_4 after two years. The shift of HIV-positive individuals to the AIDS class and HIV-HBV co-infected compartment is a contributing factor to these declining rates. As the HIV infection rate rises, β_4, the population of co-infected individuals with HIV and HBV, I_{HB} also rises. For each value of HIV infection rate, the population of I_{HB} increases rapidly and on reaching the maximum value, the rate of change starts decreasing tending towards a constant level. This dynamic is as a result of high recruitment of HIV infective and constant supply of HBV infections into HIV-HBV co-infected compartment. Thus, a high percentage of co-infected individuals are sourced from HIV infections. The population of HBV infected individuals increases steadily and reaches the peak and then decreases for all values of HIV infection rate, β_4, at constant HBV infection rates, β_5. Similarly, the dynamics of the infectious populations at varying HBV infection rate at constant HIV infection rate follow the same trend and explanation as for the variation in HIV infection rate.

In the presence of both co-infection rates, β_4, β_5 and absence of control strategies, the dynamics of the co-infection is shown in figure 4.10. HIV co-infection rate, β_4 and HBV co-infection rate, β_5 are varied at a interval of 20%.

Figure 4.10

Variation of both β_4 and β_5 on HIV-HBV co-infection

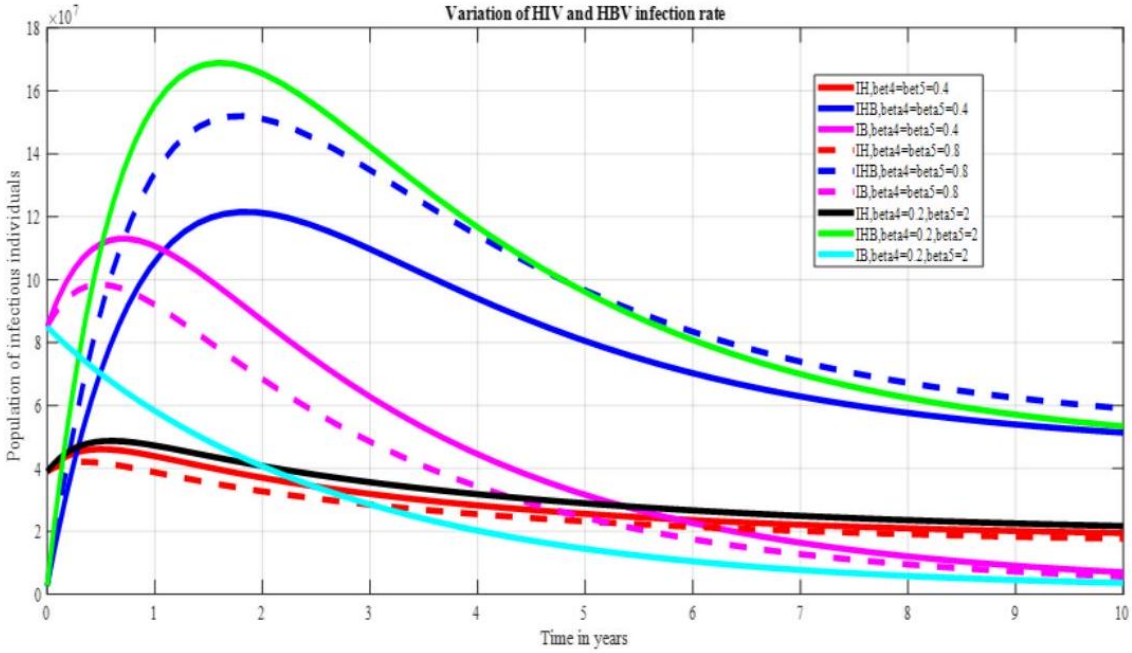

Source: Researcher (2025)

With the same and distinct values of HBV and HIV infection rates, the population of individuals infected with acute hepatitis B, I_B decreases exponentially, but decreases slowly with equal values of HBV and HBV infection rates after reaching the maximum point. Similarly the HIV individuals, I_H slightly increases and flatten faster for different and equal values of HIV and HBV infection rates. As a result, for various HIV and HBV infection rates, the number of co-infected individuals rises. This increase is the result of new HIV and HBV infections among the population that is co-infected. The population reaches the peak, and then decreases before stabilizing at a constant level, as a result of a balance between new co-infections and individuals transiting the co-infected state. This state of balance is brought about by the persistence of chronic hepatitis B and HIV infective progressing to AIDS.

4.6.5 Impact of clinical strategies on HIV-HBV co-infection

The impact of clinical control strategies on the dynamics of HIV-HBV co-infection is demonstrated graphically in the following sub-sections.

4.6.5.1 Effect of treatment and drug efficacy

The effect of treatment and vaccination on the dynamics of HIV-HBV co-infection is demonstrated in Figure 4.11.

Figure 4.11
Variation of treatment rates and HBV efficacy

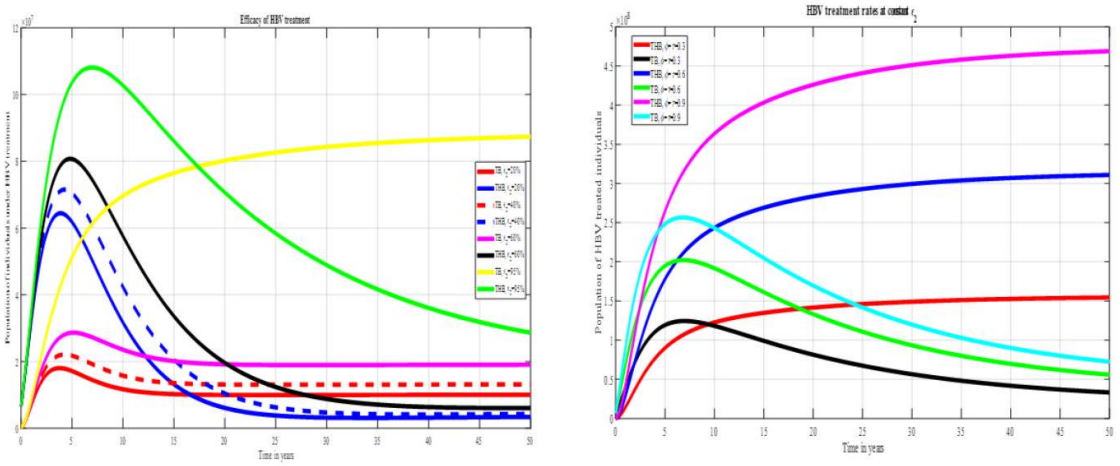

Source: Researcher (2025)

In Figure 4.11 above, we find that as HBV medication efficiency, ε_2 rises, the rate of T_B rises progressively at constant ϕ and τ. On reaching the peak the rate becomes zero and starts to decrease exponentially before becoming constant. Similarly, the rate of change of T_{HB}, follows the same trend but convergence to constant is faster than the case in T_B. However at 95% efficacy, the rate of T_{HB} grows gradually and tends towards constant rates. These dynamics can be explained by the expectation that treatment reduces viral loads, decreases transmission rates, and assists in co-infected persons' HBV management. The positive impact of HBV antiviral treatment on individuals with acute Hepatitis B influences the increase in the number of treated individuals. Treatment can suppress HBV replication, leading to a decrease in viral load and transmission. The continuous growth before reaching a constant level suggests ongoing treatment initiation for new co-infected cases, followed by a stabilization of the treated population. The steady increase in treated co-infected individuals with HIV and HBV, T_{HB}, is contributed by ongoing transmission and new HIV cases, while the constant rate suggests a balance between new co-infections and individuals recovering from acute HBV infection.

Figure 4.12 shows the effect of varying the treatment rate, ϕ at constant HBV drug efficacy,

ε_2.

Figure 4.12
Effect of varying treatment rate at constant drug efficacy

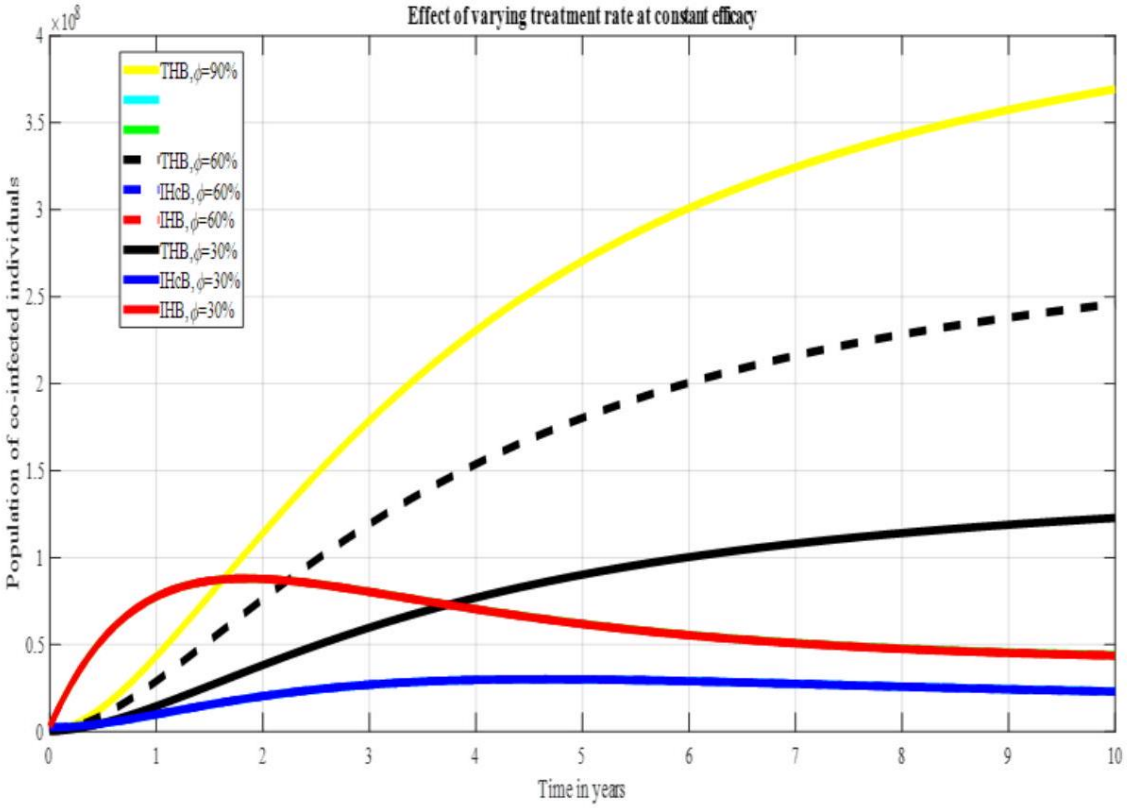

Source: Researcher (2025)

As seen in Figure 4.12, the population of T_B initially shows a rise followed by a decline at constant HBV efficacy of 95% and different treatment rates. The initial rise in the treated population is due to the effectiveness of treatment interventions, while the decline in treatment effectiveness over time causes the observed trend. In addition, this trend is influenced by factors such as treatment effectiveness, availability, and adherence to treatment regimens. Variations in these factors across different settings and populations can result in distinct patterns of population dynamics. On the other hand, the population of T_{HB} increases gradually with increasing treatment rates and stabilizes afterwards. These dynamics indicate the management of HBV infection in co-infected individuals.

4.6.5.2 Variation of HBV birth dose vaccination

Vaccination strategy targets the proportion of births vaccinated with HBV vaccine, V and HIV positive births given HBV vaccine, V_H. Figure 4.13 illustrates the variation of birth dose Hepatitis B vaccination on the dynamics of mono-infection and co-infection.

Figure 4.13
Variation of HBV-BD vaccination

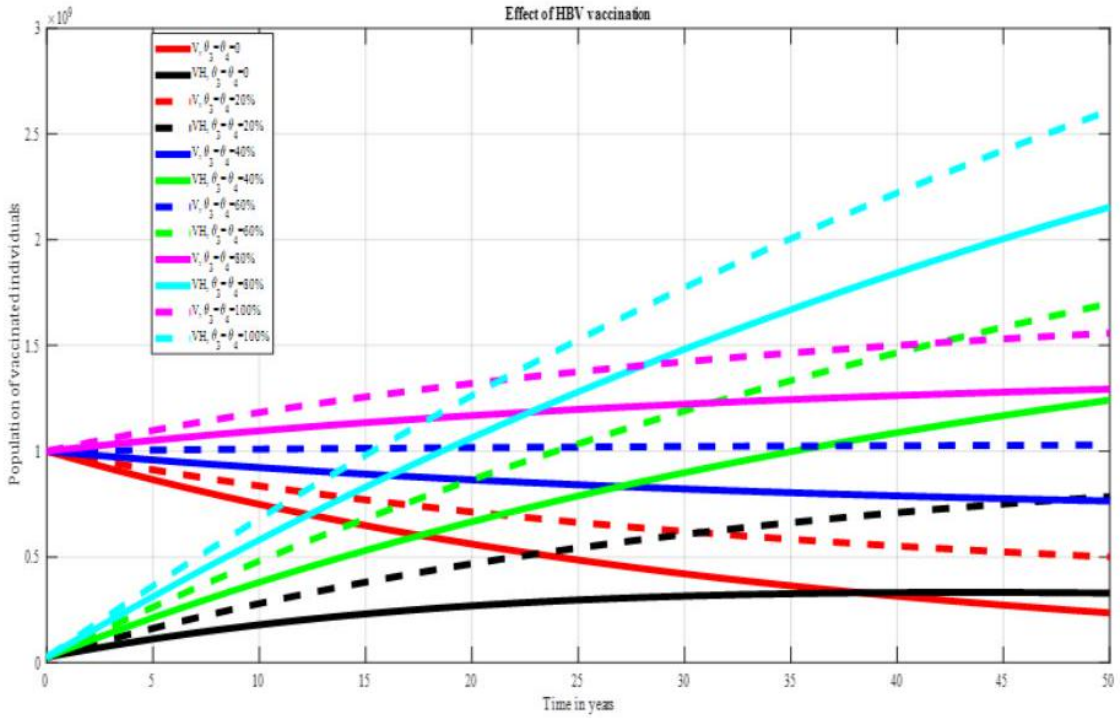

Source: Researcher (2025)

It is shown in Figure 4.13 that in the absence of Hepatitis B vaccination at birth, the proportion of births in I_B, I_H and I_{HB} increases leading to an equivalent rise in cases of co-infection. As a result, the number of people who have received vaccinations against Hepatitis B declines with time. This decline differs for different proportions but remains constant at 60%. As the birth dose vaccination is increased, the proportions of births to I_B, I_H and I_{HB} decreases while the population of vaccinated HBV infected increases at a slower rate. While the population of vaccinated HIV positive individuals increases as the proportions of HBV birth dose vaccination is increased. This increment is due to shortcoming of HBV vaccine efficiency as well as lack of HIV vaccination. The HBV vaccine wanes with time and the HBV vaccinated births become infected with HIV.

4.6.6 Effect of non-clinical strategies on HIV-HBV co-infection

Infection rate, β influences HIV and HBV transmission, which is related to non-clinical interventions such as mass campaigns geared towards reducing sexual contact, sexual partners, use of condom/protection, abstinence, media or health campaigns or sensitization programs among others.

Figure 4.14
Effect of infection rate, β

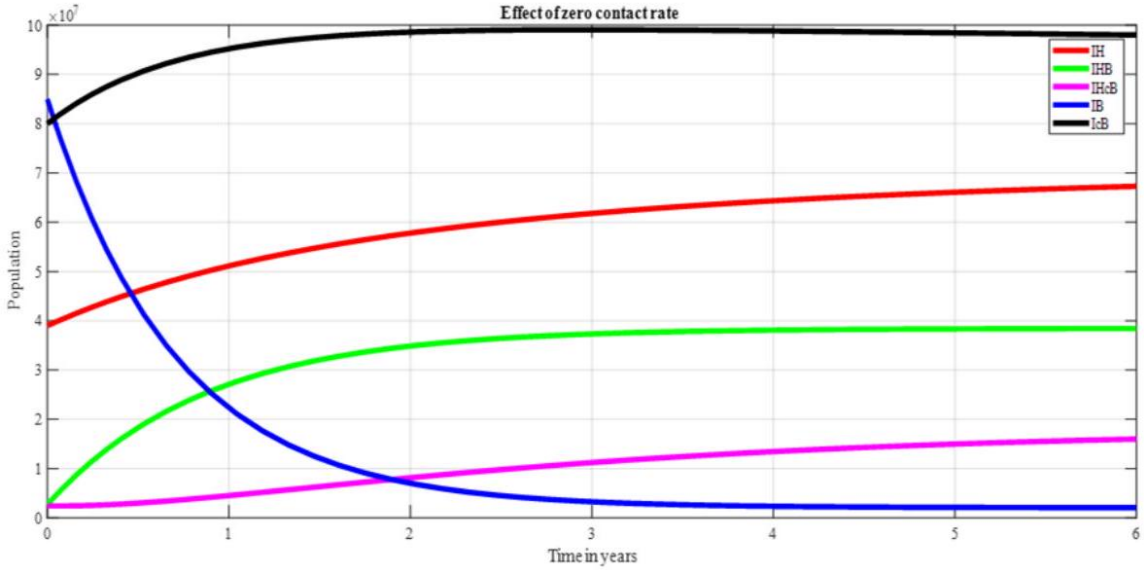

Source: Researcher (2025)

Figure 4.14 shows the effect of infection rate on dynamics of mono infection and co-infection. The number of I_H increases for five years and then tends to decrease with time. In the absence of sexual contact between susceptible and HIV infectious individuals, new cases of infection cannot occur. The existing HIV-infected individuals, I_H will continue to live with the virus, but the overall prevalence will not increase. Similarly, the population of HBV-infected individuals, I_B decreases exponentially. No increase is expected because there is no transmission, so the infection remains constant. The existing cases persist, but new infections cannot occur without any sexual interaction between vulnerable and HBV-positive people. The number of individuals infected with chronic hepatitis B increases slowly and after two years it reaches a constant state. The initial cases of acute hepatitis B progress to chronic stage. For co-infection, initially the number of co-infected individuals increases drastically and later becomes constant. This is because there are no new cases of HIV-HBV co-infection. The co-infection prevalence will not rise since those who are already co-infected remain in this state.

4.6.7 Effect of clinical and non-clinical control interventions on HIV-HBV co-infection

Figure 4.15 below shows the effect of both clinical and nonclinical control measures on the dynamics of HIV-HBV co-infection for a period of six years.

Figure 4.15

Combined effect of clinical and non-clinical strategies

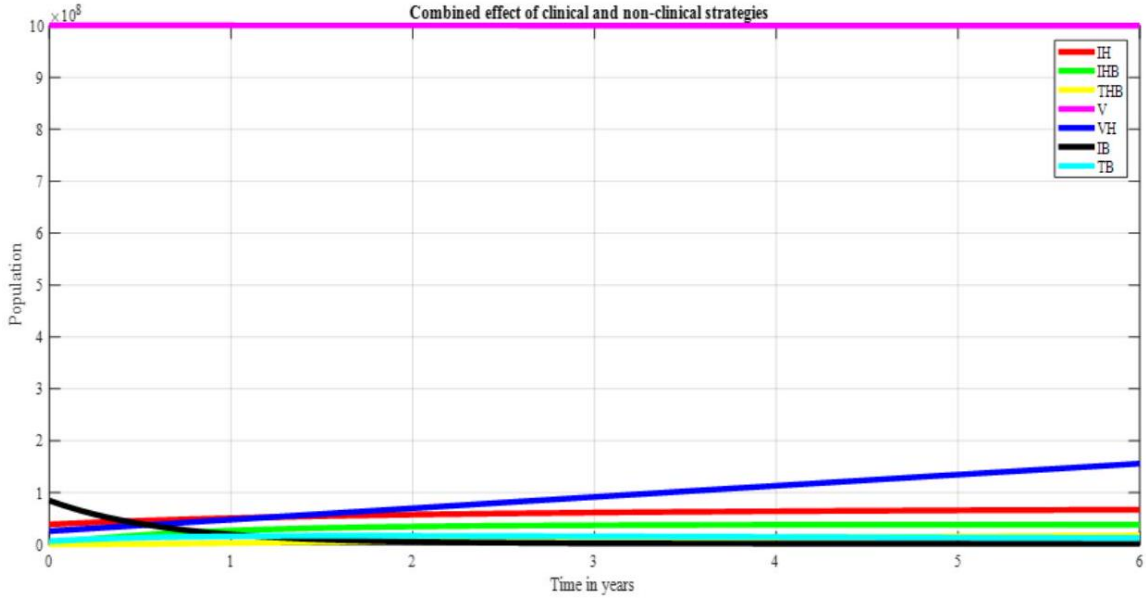

Source: Researcher (2025)

From Figure 4.15, it is observed that the number of hepatitis B vaccinated population infected with HIV, V_H increases steadily with time. The number of people living with HIV/AIDS, I_H rises gradually and then stays the same. The HBV vaccinated population, V remains constant throughout with constant birth dose vaccination, and the proportion of individuals born with HIV increases steadily. The number of people infected with acute hepatitis B, I_B declines quickly before becoming stable. The number of HIV-HBV co-infected individuals, I_{HB} increases drastically for a short duration and becomes constant after some time.

The number of treated co-infected individuals, T_{HB} are absorbed into an infection free state and remain entirely in this state. This point out that hepatitis B treatment can manage the co-infected individuals. Clinical strategies like ART and antiviral therapy reduce viral loads, leading to a decrease in HIV and HBV infected individuals. Non-clinical strategies like condom use, abstinence, health education and vaccination programs contribute to reducing new infections. The combined effect of these strategies results in decline in HIV, HBV, and co-infection prevalence with time.

4.7 Optimal Control Model Results

This section illustrates the effect of with and without control interventions on the dynamics of co-infected classes.The percentage reduction of the co-infected population is computed in each case.

4.7.1 Optimal control model framework

This model is obtained from the deterministic model as described in section 3.5. The optimal control model with controls variables u_1, u_2, u_3, u_4 and u_5 is as shown in Figure 4.16 below. u_1 represents the prevention control which targets the susceptible population from becoming infected with HIV, HBV and HIV-HBV co-infection. u_2 stands for the treatment control that targets the HBV infected and HIV-HBV co-infected individuals seeking HBV and combined antivirals. The viral load control, u_3 targets the Hiv infected patients and individuals infected with HBV at acute stage. This control intervention regulates the movement of patients from acute to chronic stage with the help of antiviral medication. u_4 denotes the HBV vaccination control, which protects the infants from HIV and HBV infection at the birth or during delivery. The recovery control, u_5 assesses the efficiency of HIV and HBV drug usage by the treated population.

Figure 4.16

Optimal control co-infection model of HIV-HBV with control set U

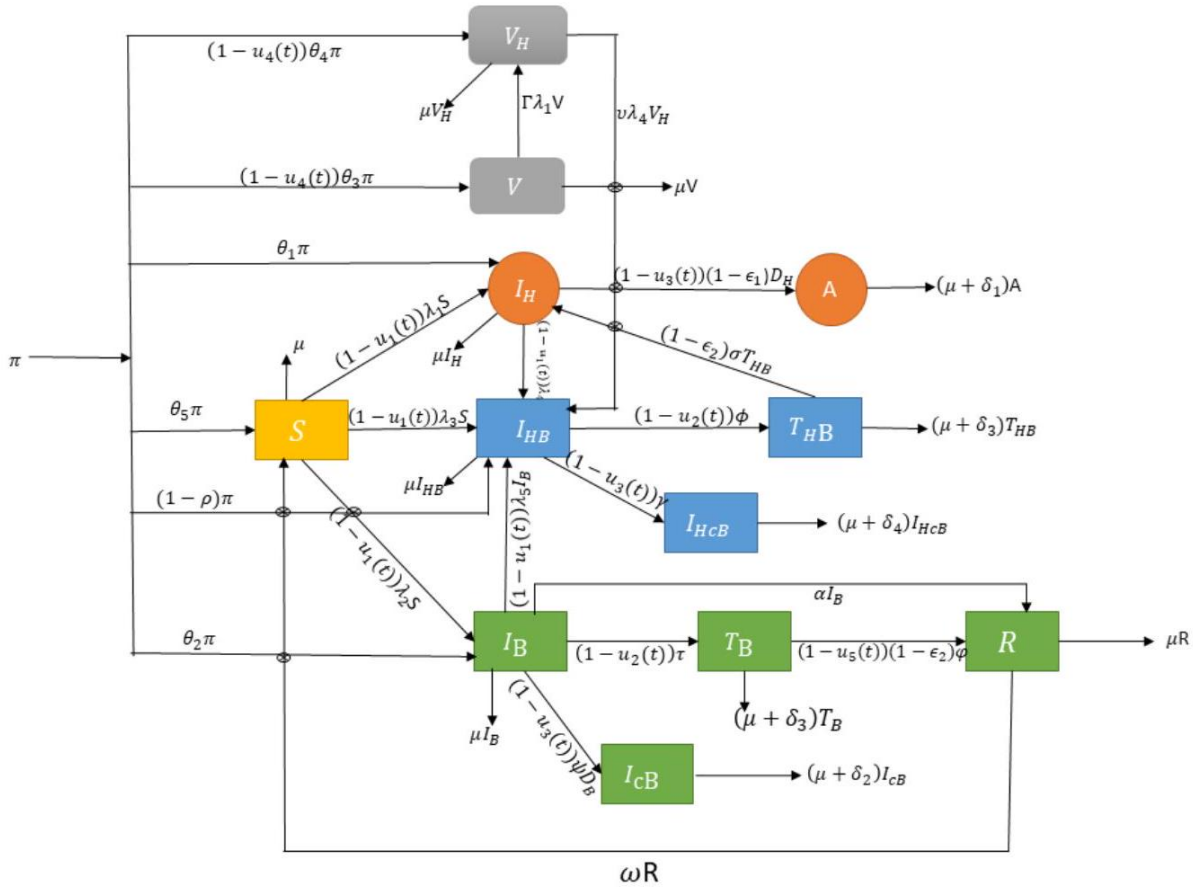

Source: Researcher (2025)

The following set of non-linear ordinary differential equations with control parameters governs the optimal control model

$$\frac{dS}{dt} = \theta_5\pi - [(1-u_1(t))(\lambda_1+\lambda_2+\lambda_3)+\mu]S + \omega R \tag{4.1}$$

$$\frac{dI_H}{dt} = \theta_1\pi + (1-u_1(t))\lambda_1 S + (1-\varepsilon_2)\sigma T_{HB} - (\lambda_4+\mu+(1-u_3(t))(1-\varepsilon_1)D_H)I_H \tag{4.2}$$

$$\frac{dA}{dt} = (1-u_3(t))(1-\varepsilon_1)D_H I_H - (\delta_1+\mu)A \tag{4.3}$$

$$\frac{dI_{HB}}{dt} = (1-\rho)\pi + (1-u_1(t))\lambda_3 S + [(1-u_1(t))I_H + vV_H]\lambda_4 + (1-u_1(t))\lambda_5 I_B - [(1-u_2(t))\phi + (1-u_3(t))\gamma + \mu]I_{HB} \tag{4.4}$$

$$\frac{dT_{HB}}{dt} = (1-u_2(t))\phi I_{HB} - (\mu+\delta_3+(1-\varepsilon_2)\sigma)T_{HB} \tag{4.5}$$

$$\frac{dI_{HcB}}{dt} = (1-u_3(t))\gamma I_{HB} - (\mu+\delta_4)I_{HcB} \tag{4.3.6}$$

$$\frac{dV}{dt} = (1-u_4(t))\theta_3\pi - (\mu+\Gamma\lambda_1)V \tag{4.6}$$

$$\frac{dV_H}{dt} = (1-u_4(t))\theta_4\pi + \Gamma\lambda_1 V - (\mu+v\lambda_4)V_H \tag{4.7}$$

$$\frac{dI_B}{dt} = \theta_2\pi + (1-u_1(t))\lambda_2 S - [\mu+(1-u_1(t))\lambda_5+\alpha+(1-u_2(t))\tau + (1-u_3(t))\psi D_B I_B \tag{4.8}$$

$$\frac{dI_{cB}}{dt} = (1-u_3(t))\psi D_B I_B - (\mu+\delta_2)I_{cB} \tag{4.9}$$

$$\frac{dT_B}{dt} = (1-u_2(t))\tau I_B - (\mu+\delta_3+(1-\varepsilon_2)\varphi)T_B \tag{4.10}$$

$$\frac{dR}{dt} = \alpha I_B + (1-u_5(t))(1-\varepsilon_2)\varphi T_B - (\omega+\mu)R \tag{4.11}$$

Subject to initial conditions;

$S_0 = S(0), I_{H0} = I_H(0), A_0 = A(0), I_{HB0} = I_{HB}(0), T_{HB0} = T_{HB}(0),$

$I_{HcB0} = I_{HcB}(0), V_0 = V(0), V_{H0} = V(0), I_{B0} = I_B(0), I_{cB0} = I_{cB}(0),$

$T_{B0} = T_B(0), R_0 = R(0)$

To study the optimal levels of the controls, the control set U is Lebesgue measurable and it is defined as

$$U = \left\{ u_1(t); u_2(t); u_3(t); u_4(t); u_5(t) : 0 \le u_1 < 1; 0 \le u_2 < 1; 0 \le u_3 < 1; 0 \le u_4 < 1; \right.$$
$$\left. 0 \le u_5 < 1; 0 \le t \le t_f \right\}$$

4.7.2 Analysis of optimal control model

It is challenging to effectively control both infections in the population since model 1 experienced a backward bifurcation. In known structures of disease dynamics, a phenomenon referred to as backward bifurcation emerges where there is coexistence of both a stable endemic and stable disease free equilibrium though the fundamental reproduction number R_0 is strikingly less than 1. Such observation makes the supposition that minimizing R_0 to 1 a major goal usually used to achieve disease eradication problematic as it seems to automatically straddle out the disease. Rather, the slow process of the lower R_0 equilibrium may serve to actually keep the infection going long past theoretical eradication level (Wangari, Davis, & Stone, 2016). In order to determine the best interventions for the management of the co-infection, the goal of this section is to integrate model (1) with time-dependent controls.

In this section, Pontryagin's Maximum Principle (PMP) is utilized to analyze the optimal control system that was established in section 4.3 and solved numerically using MATLAB. In order to identify the essential conditions to suggest a potential optimal control for the co-infection model, we use PMP in this case. The core objective of this part is to determine an optimal HIV-HBV co-infection prevention and control measures at the lowest implementation cost. To estimate the optimal states and controls, we seek to maximize the number of R, V, T_B, T_{HB}, V_H and minimize the number of $I_H, A, I_{HB}, I_{HcB}, I_B$ to concurrently lower the costs related to implementing each measure in place. Five controls are introduced, and the model (1) takes on the following form. In order to determine the best course of action, we incorporate time-dependent controls in the co-infection. HIV-HBV co-infection is controlled and decreased in a community by increasing the percentage of uninfected individuals and decreasing the number of infected and co-infected individuals. So we utilize a quadratic objective function in line with the literature by Aghdaoui et al.

(2021); Seidu, Makinde, et al. (2014) and Gao and Huang (2018) given in the form:

$$J(u_1,u_2,u_3,u_4,u_5) = \min_{(u_1,u_2,u_3,u_4,u_5)} \int_0^{t_f} \Bigg[L_1 I_H + L_2 A + L_3 I_{HB} + L_4 T_{HB} + L_5 I_{HcB} + L_6 V_H + L_7 I_B + L_8 I_{cB} + L_9 T_B + \frac{1}{2}\sum_{i=1}^{5} C_i u_i^2 \Bigg] dt \tag{4.12}$$

where $L_1, L_2, L_3, L_4, L_5, L_6, L_7, L_8, L_9, L_{10}, L_{11}, L_{12}$ and C_i are positive constants with $i = 1, \ldots\ldots 5$ and the term $\frac{1}{2}\sum_{i=1}^{i=5} C_i u_i^2$ denotes the cost function associated with each of the controls. The objective function J (4.12) for the end time t_f means the definite integral comprising of the states contributing to infections in proportions and corresponding costs. Finding the best control, $u_1^*, u_2^*, u_3^*, u_4^*, u_5^*$, is our goal.

$J\left(u_1^*, u_2^*, u_3^*, u_4^*, u_5^*\right) = \min\left\{J\left(u_1^*, u_2^*, u_3^*, u_4^*, u_5^*\right) \mid u_1, u_2, u_3, u_4, u_5 \in U\right\}$

where $U = \left\{\left(u_1^*, u_2^*, u_3^*, u_4^*, u_5^*\right)\right\}$ is the control set such that $u_1^*, u_2^*, u_3^*, u_4^*, u_5^*$ are Lebesgue measurable with $0 \leq u_1*, u_2*, u_3*, u_4*, u_5* \leq 1$ for $t \in \left[0, t_f\right]$.

4.7.3 The Hamiltonian and optimality system

By PMP, the necessary optimality condition is established using Lagrangian and Hamiltonian polynomials by Pontryagin (1987) and Lenhart and Workman (2007) as defined below;

$$\begin{aligned}\mathscr{L}\left(I_H, A, I_{HB}, T_{HB}, I_{HcB}, V_H, I_B, I_{CB}, T_B\right) &= L_1 I_H + L_2 A + L_3 I_{HB} + L_4 T_{HB} + L_5 I_{HcB} \\ &+ L_6 V_H + L_7 I_B + L_8 I_{cB} + L_9 T_B \\ &+ \frac{1}{2} C_1 u_1^2 + \frac{1}{2} C_2 u_2^2 + \frac{1}{2} C_3 u_3^2 \\ &+ \frac{1}{2} C_4 u_4^2 + \frac{1}{2} C_5 u_5^2\end{aligned} \tag{4.13}$$

and the corresponding Hamiltonian H is given by;

$$
\begin{aligned}
&H\big(I_H, A, I_{HB}, T_{HB}, I_{HcB}, V_H, I_B, I_{cB}, T_B, u_1, u_2, u_3, u_4, u_5,\\
&\quad P_1, P_2, P_3, P_4, P_5, P_6, P_7, P_8, P_9\big)\\
&= \mathscr{L}\big(I_H, A, I_{HB}, T_{HB}, I_{HCB}, V_H, I_B, I_{CB}, T_B, u_1, u_2, u_3, u_4, u_5\big)\\
&\quad + \frac{dI_H}{dt}P_1(t) + \frac{dA}{dt}P_2(t) + \frac{dI_{HB}}{dt}P_3(t) + \frac{dT_{HB}}{dt}P_4(t)\\
&\quad + \frac{dI_{HcB}}{dt}P_5(t) + \frac{dV_H}{dt}P_6(t) + \frac{dI_B}{dt}P_7(t)\\
&\quad + \frac{dI_{cB}}{dt}P_8(t) + \frac{dT_B}{dt}P_9(t)
\end{aligned}
\tag{4.14}
$$

where $P_1, P_2, P_3, P_4, P_5, P_6, P_7, P_8, P_9$ are the adjoint variables that will be determined. Using the normal control arguments with the limits on the controls, we write as follows:

$$
u_1^* = \begin{cases} \Phi_1 & \text{if } 0 < \Phi_1 < 1 \\ 0 & \text{if } \Phi_1 \leq 0 \\ 1 & \text{if } \Phi_1 \geq 1 \end{cases}
$$

$$
u_2^* = \begin{cases} \Phi_2 & \text{if } 0 < \Phi_2 < 1 \\ 0 & \text{if } \Phi_2 \leq 0 \\ 1 & \text{if } \Phi_2 \geq 1 \end{cases}
$$

$$u_3^* = \begin{cases} \Phi_3 & \text{if } 0 < \Phi_3 < 1 \\ 0 & \text{if } \Phi_3 \leq 0 \\ 1 & \text{if } \Phi_3 \geq 1 \end{cases}$$

$$u_4^* = \begin{cases} \Phi_4 & \text{if } 0 < \Phi_4 < 1 \\ 0 & \text{if } \Phi_4 \leq 0 \\ 1 & \text{if } \Phi_4 \geq 1 \end{cases}$$

$$u_5^* = \begin{cases} \Phi_5 & \text{if } 0 < \Phi_5 < 1 \\ 0 & \text{if } \Phi_5 \leq 0 \\ 1 & \text{if } \Phi_5 \geq 1 \end{cases}$$

The compactly defined control set $U = \left(u_1^*, u_2^*, u_3^*, u_4^*, u_5^*\right)$ is therefore Lebesgue integrable on the interval 0 to t_f, where t_f is the fixed time period to which the controls are applied. We further assume that

$u_1^*(t) = \max\left[0, \min\left(1, \Phi_1\right)\right]$

$u_2^*(t) = \max\left[0, \min\left(1, \Phi_2\right)\right]$

$u_3^*(t) = \max\left[0, \min\left(1, \Phi_3\right)\right]$

$u_4^*(t) = \max\left[0, \min\left(1, \Phi_4\right)\right]$

$u_5^*(t) = \max\left[0, \min\left(1, \Phi_5\right)\right]$

Thus, the formed optimality system consists of the optimal control system (state system) and the adjoint variable system by introducing the characterized control set, initial as well as, transversality condition, $I_H, A, I_{HB}, T_{HB}, I_{HcB}, V_H, I_B, I_{cB}, T_B\ \lambda_i\left(t_f\right) = 0, i = 1,2,3,4,5,$

$I_H(0) = I_H, I_{HB}(0) = I_{HB}, T_{HB}(0) = T_{HB}, I_{HcB}(0) = I_{HcB}, V_H(0) = V_H,$

$I_{CB}(0) = I_{CB}, T_B(0) = T_B$

4.7.4 Uniqueness of the optimality system

The optimality system's solutions are unique for the short time interval because of the state's prior boundedness, the adjoint functions, and the consequent Lipschitz structure of the ordinary differential equations. By partially differentiating the Hamiltonian with

regard to the state variables, the adjoint or co-state equations can be found through the use of Pontryagin's maximal principle. Therefore, we have

$$\dot{P}_1(t) = -\frac{\partial H}{\partial I_H} = [2\beta_4 I_H + (1-u_3)(1-\varepsilon_1)D_H - (\beta_1 S - u_1\beta_1 S)]\,P_1(t)$$
$$-(1-u_3(t))(1-\varepsilon_1)D_H P_2 - (2I_H(1-u_1)+v)\beta_4 P_3$$
$$+(v\beta_4 V_H - \Gamma\beta_1 V)P_6 - L_1$$
$$\dot{P}_2(t) = -\frac{\partial H}{\partial A} = (\beta_4\Lambda_3 I_H - (1-u_1)\beta_1\eta_3 S)P_1 + (\delta_1+\mu)P_2$$
$$-((1-u_1(t))I_H + v)\beta_4\Lambda_3 P_3 - (\Gamma\beta_1\eta_3 V - v\beta_4\Lambda_3 V_H)P_6 - L_2$$
$$\dot{P}_3(t) = -\frac{\partial H}{\partial I_{HB}} = (\beta_4\Lambda_1 I_H - (1-u_1)\beta_1\eta_1 S)P_1$$
$$-\big[(1-u_1)\beta_3 S + ((1-u_1)I_H + v)\beta_4\Lambda_1$$
$$-((1-u_2)\phi + (1-u_3)\gamma + \mu) + (1-u_1)\beta_5\Upsilon_1 I_B\big]P_3$$
$$-(1-u_2)\phi P_4 - (1-u_3(t))\gamma P_5$$
$$-(\Gamma\beta_1\eta_1 V - v\beta_4\Lambda_1 V_H)P_6$$
$$-((1-u_1(t))\beta_2\chi_2 S - (1-u_1)\beta_5\Upsilon_1 I_B)P_7 - L_3$$
$$\dot{P}_4(t) = -\frac{\partial H}{\partial T_{HB}} = -\left((1-u_1)\beta_1\eta_4 S + (1-\varepsilon_2)\sigma - \beta_4\Lambda_4 I_H\right)P_1$$
$$-\left((1-u_1)\beta_3\Psi_2 S + ((1-u_1)I_H + v)\beta_4\Lambda_4 + (1-u_1)\beta_5\Upsilon_5 I_B\right)P_3$$
$$+\left(\mu + \delta_3 + (1-\varepsilon_2)\sigma\right)P_4$$
$$-\left(\Gamma\beta_1\eta_4 V - v\beta_4\Lambda_4 V_H\right)P_6$$
$$-\left((1-u_1(t))\beta_2\chi_5 S - (1-u_1)\beta_5\Upsilon_5 I_B\right)P_7 - L_4$$
$$\dot{P}_5(t) = -\frac{\partial H}{\partial I_{HcB}} = -\left((1-u_1)\beta_1\eta_2 S - \beta_4\Lambda_2 I_H\right)P_1$$
$$-\left((1-u_1)\beta_3\Psi_1 S + ((1-u_1)I_H + v)\beta_4\Lambda_2 + (1-u_1)\beta_5\Upsilon_3 I_B\right)P_3$$
$$+\left(\mu + \delta_4\right)P_5 - \left(\Gamma\beta_1\eta_2 V - v\beta_4\Lambda_2 V_H\right)P_6$$
$$-\left((1-u_1)\beta_2\chi_3 S - (1-u_1)\beta_5\Upsilon_3 I_B\right)P_7 - L_5$$
$$\dot{P}_6(t) = -\frac{\partial H}{\partial V_H} = \beta_4\Lambda_5 P_1 - \left((1-u_1)I_H + v\right)\beta_4\Lambda_5 P_3$$
$$+\left(\mu + v\beta_4(I_H + \Lambda_1 I_{HB} + \Lambda_2 I_{HcB} + \Lambda_3 A + \Lambda_4 T_{HB} + 2\Lambda_5 V_H)\right)P_6$$
$$+\left(\mu + (1-u_1)\beta_5(2I_B + \Upsilon_1 I_{HB} + \Upsilon_2 I_{cB} + \Upsilon_3 I_{HcB} + \Upsilon_4 T_B + \Upsilon_5 T_{HB})\right.$$
$$\left.(\alpha + (1-u_3)\psi D_B)\right)P_7 + (1-u_2)\tau P_7 - L_6$$
$$\dot{P}_7(t) = -\frac{\partial H}{\partial I_B} = -\left(1-u_1\right)\beta_5\left(2I_B + \Upsilon_1 I_{HB} + \Upsilon_2 I_{cB} + \Upsilon_3 I_{HcB} + \Upsilon_4 T_B + \Upsilon_5 T_{HB}\right)P_3$$
$$-\left(\left(1-u_1\right)\beta_2 S\left(2I_B + \chi_1 I_{cB} + \chi_2 I_{HB} + \chi_3 I_{HcB} + \chi_4 T_B + \chi_5 T_{HB}\right)\right)P_7$$
$$-\left(1-u_3\right)\psi D_B P_8 - \left(1-u_2\right)\tau P_9 - L_7$$

$\dot{P}_8(t) = -\frac{\partial H}{\partial I_{cB}} = -(1-u_1)\beta_5\Upsilon_2 I_B P_3 - ((1-u_1)\beta_2\chi_2 S - (1-u_1)\beta_5\Upsilon_2 I_B)P_7$

$+(\mu+\delta_2)P_8 - L_8$

$\dot{P}_9(t) = -\frac{\partial H}{\partial T_B} = (\mu+\delta_3+(1-\varepsilon_2)\varphi)P_9 - (1-u_1)\beta_5\Upsilon_4 I_B P_3 -$

$((1-u_1)\beta_2\chi_4 S - (1-u_1)\beta_5\Upsilon_4 I_B)P_7 - L_9$

with the transversality conditions;

$P_1(t_f) = P_2(t_f) = P_3(t_f) = P_4(t_f) = P_5(t_f) = P_6(t_f) = P_7(t_f) = P_8(t_f) = P_9(t_f) = 0$

The optimality criteria are met since the Hamiltonian is minimized at the optimal controls, $\frac{\partial H}{\partial u_i} = 0$. These optimality requirements can be applied to typical control arguments using the bounds on the controls to generate formulas for u_i^*. Following the method by Pontryagin (1987) and Aghdaoui et al. (2021), for each i between 1 and 5, we solve the equation $\frac{\partial H}{\partial u_i} = 0$ to find the controls. Using the optimality conditions, at $(u_1(t), u_2(t), u_3(t), u_4(t), u_5(t)) = \left(u_1^*(t), u_2^*(t), u_3^*(t), u_4^*(t), u_5^*(t)\right)$ we have the following model

$$\frac{\partial H}{\partial u_1} = C_1 u_1 - \lambda_1 S P_1(t) - (\lambda_3 S + I_H\lambda_4 + \lambda_5 I_B)P_3(t) - (\lambda_2 S - \lambda_5 I_B)P_7(t) = 0$$

$$\frac{\partial H}{\partial u_2} = C_2 u_2 + \phi I_{HB} P_3(t) - \phi I_{HB} P_4(t) + \tau I_B P_7(t) - \tau I_B P_9(t) = 0$$

$$\frac{\partial H}{\partial u_3} = C_3 u_3 + (1-\varepsilon_1) D_H I_H P_1(t) - (1-\varepsilon_1) D_H I_H P_2(t) + \gamma I_{HB} P_3(t) -$$

$$\gamma I_{HB} P_5(t) + \psi D_B I_B P_7(t) - \psi D_B I_B P_8(t) = 0$$

$$\frac{\partial H}{\partial u_4} = C_4 u_4 - \theta_4 \pi P_6(t) = 0$$

$$\frac{\partial H}{\partial u_5} = C_5 u_5 = 0$$

which gives

$$u_1^* = \frac{\lambda_1 S P_1(t) + (\lambda_3 S + I_H\lambda_4 + \lambda_5 I_B)P_3(t) + (\lambda_2 S - \lambda_5 I_B)P_7(t)}{C_1}$$

$$u_2^* = \frac{\phi I_{HB} P_4(t) - \tau I_B P_7(t) + \tau I_B P_9(t) - \phi I_{HB} P_3(t)}{C_2}$$

$$u_3^* = \frac{(1-\varepsilon_1) D_H I_H P_2(t) - (1-\varepsilon_1) D_H I_H P_1(t) - \gamma I_{HB} P_3(t) + \gamma I_{HB} P_5(t) - u3_*}{C_3}$$

$$u_4^* = \frac{\theta_4 \pi P_6(t)}{C_4}$$

$$u_5^* = 0$$

where $u3_* = -\psi D_B I_B P_7(t) + \psi D_B I_B P_8(t)$

4.8 Numerical Simulations With and Without the Controls

By constructing a MATLAB code, numerical solutions are presented to analyze the results which also exhibits the nature of the solutions while considering the controls. In addition, the control profiles for u_1, u_2, u_3, u_4 and u_5 are displayed graphically. The numerical solution of the optimal system is performed using a fourth-order Runge-Kutta algorithm. A fourth-order Runge-Kutta technique is used to solve the state ordinary differential equations 4.3.1 to 4.3.12 forward in time given the initial conditions for the states and an initial estimate for the controls. Another fourth-order Runge-Kutta method is used to solve the adjoint system backward in time, using the transversality criteria and the state equations that are currently iterated in section 4.3. The two values used are state and adjoint values. The characterization is then used to update the controls and then the iteration process continues. This procedure is repeated continuously until current state, adjoint and controls have converged to the required level. Parameter values used for model simulations are tabulated below

Table 4.4
Parameter Values for Optimal Control Model Simulation

Parameter	Value Range	Source
$u_1^{\max}$	0.79–0.87	Hatcher et al. (2015)
$u_2^{\max}$	0.96	Lee, Amin, and Carr (2014)
$u_3^{\max}$	0.6–0.8	Lecher et al. (2021)
$u_4^{\max}$	0.5	Amponsah-Dacosta (2021)
$u_5^{\max}$	0.8–0.9	Spearman et al. (2017)

Source: Researcher (2025)

All parameters represent maximum implementation rates for co-infection control interventions. Value ranges indicate parameter sensitivity across studies.

The optimal control simulations is implemented in MATLAB to investigate the optimality of the control variables. Utilizing various combinations of the controls, like using a single control at a time, two controls at a time, three controls at a time, four controls at a time and also all controls at a time, we analyze and compare numerical results from simulations with the following scenarios.

4.9 Implementation of Control Interventions at Optimal Levels

The impact of both clinical and non-clinical control measures at optimal levels are illustrated graphically in the following sections.

4.9.1 Impact of implementing prevention strategy, u_1 on HIV-HBV co-infection

Figure 4.17 display the dynamics of co-infected individuals with and without the implementation of prevention strategy u_1 for a period of fifty years. In this case we consider $u_1 \neq 0$ but i the absence other control strategies, $u_2 = u_3 = u_4 = u_5 = 0$ in attempt to prevent sexual contact and vertical transmission. Thus, we simulate the model by prevention control intervention only.

Figure 4.17
Effect of using prevention control, u_1

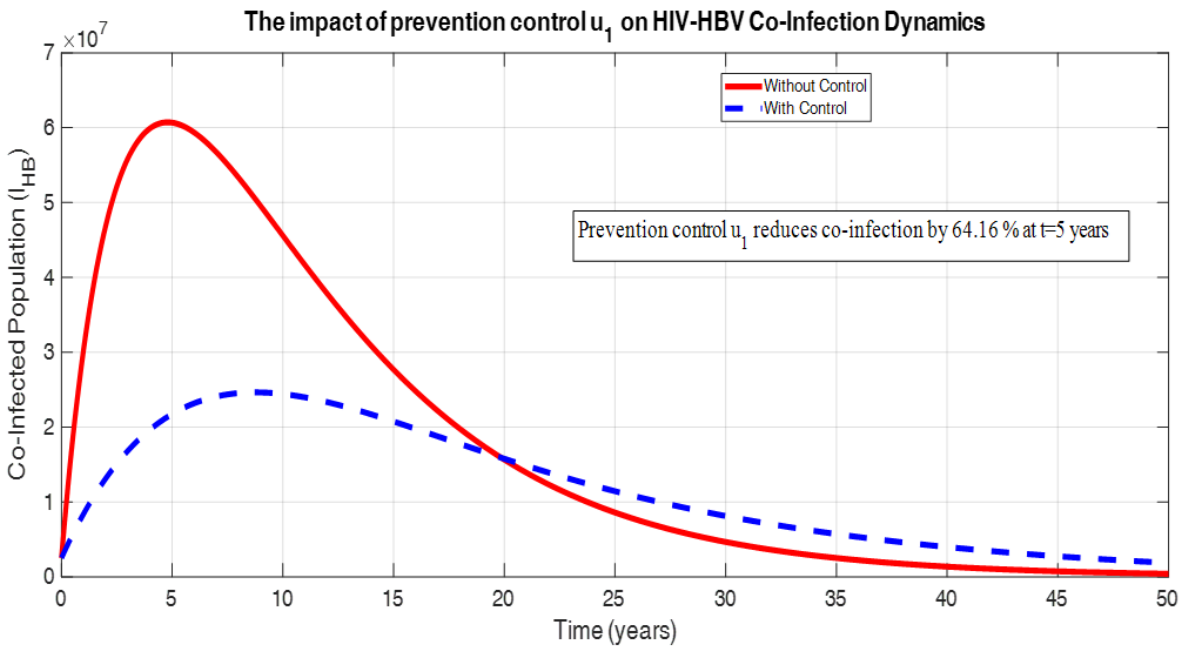

Source: Researcher (2025)

Figure 4.17 indicates the role of the prevention control, u_1 on the co-infected population within fifty years. It is seen that the curve is in the increasing pattern that is exponential at the beginning for five years and then saturates at the turning point with natural constraints. Without the introduction of prevention measures, co-infections spread incredibly fast, which increases the co-infection burden for $R_0 > 1$. Afterwards, the co-infected population decreases exponentially with time, approaching the co-infection free equilibrium

point for $R_0 < 1$. Under the controlled case, the curve lies lower than the baseline, with its beginning steeply increasing at a slower rate. The peak level is delayed by the prevention control until $t = 10$ years. Later the co-infected population reduces tending towards co-infection free equilibrium point. At $t = 5$ years, the effectiveness of prevention control is exhibited by 64.16% decrease, which may occur through a decrease in the transmission, making the individuals less susceptible, more recovery, or the decreased progression of the co-infection. The shape of the curve also shows the period in which one can expect the greatest benefits as well as the cost-effectivity of the intervention. This is realized at $t = 20$ years. The graph offers information on the dynamics of the co-infection to enable the planners in the field of public health to plan on the timing and magnitude of intervention. When prevention measures are first introduced, there is a backlog due to existing infections that are yet to be diagnosed or treated. This backlog combined with ongoing transmission before the preventive measures take full effect, can lead to an initial increase in the number of infected individuals. However, as time progresses and prevention measures become more effective, the number of affected people reduces as the rate of new infections declines. Additionally, with effective campaigns and care for those infected, the mortality rate among infected individuals decreases, contributing to a more stable or declining population of infected individuals over time. At a certain point, when prevention measures reach their optimal level of effectiveness, the transmission rates of the infections stabilize. This stabilization occurs when the rate of new infections is balanced by the rate of individuals recovering from the infections or being effectively treated, leading to a steady-state or constant population of infected individuals. In this case, the infected populations may fluctuate around a relatively constant level, reflecting the equilibrium reached between new infections and interventions that reduce transmission or improve health outcomes for those infected. This suggests that the burden of co-infection and mono-infection is lessened with optimal prevention.

4.9.2 Impact of implementing the treatment strategy, u_2 on HIV-HBV co-infection dynamics

Figure 4.18 exhibits the dynamics of co-infected population with and without the implementation of treatment intervention during twenty years. The treatment strategy, u_2 is implemented when other strategies $u_1 = u_3 = u_4 = u_5 = 0$.

Figure 4.18
Implementation of treatment strategy u_2

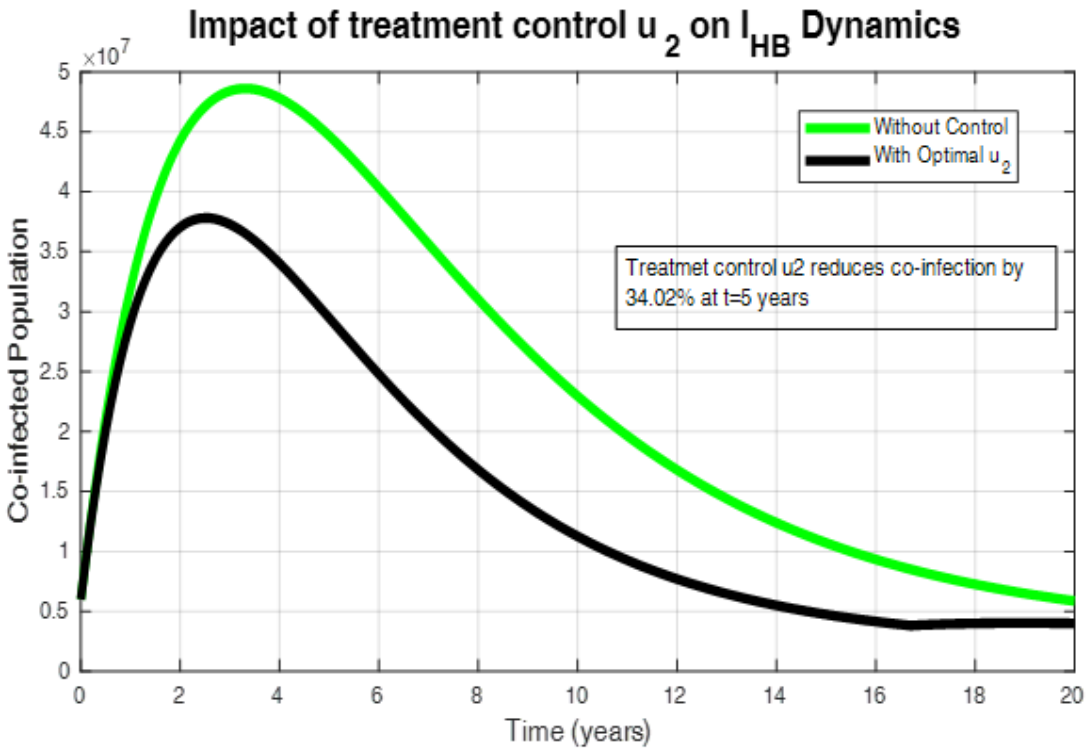

Source: Researcher (2025)

From Figure 4.18 above, the rate of change of co-infected population increases steadily with time without the treatment control. This rise is due to high HIV and HBV infection rate facilitating high susceptible population getting co-infected. As I_{HB} grows, the force of infection amplifies, accelerating new infections. in the absence of treatment , there is no suppression of transmission as well progression. After three years, the rate of change of the co-infected population reaches the maximum point. At this point the susceptible population decline significantly, thereby reducing the new infections. Later the rate of change decreases with time as it tends towards the infection free equilibrium point. This

exponential decay is attributed by increase in the rate of screening and treatment rate, with more co-infected individuals seeking diagnosis and treatment. Without the treatment control, the co-infected individuals die at a very high rate, high progression of HIV to AIDS, acute HBV to chronic HBV and there is no transition to recovery stage. This behavior necessitates introduction and the implementation of treatment strategy, u_2 .

When the treatment control is implemented, the rate of change of co-infected I_{HB} increases initially for two years before reaching the peak at $t = 2.5$ years. As compared to peak level when there is no treatment, the treatment response time is hastened by 50%. This is followed by a decreasing trend of the co-infected I_{HB} population with time. Afterwards, the rate of change of the co-infected I_{HB} population stabilizes at the co-infection free state. The impact of the treatment control u_2 is that it reduces the co-infection by 34.02% after five years.

4.9.3 The impact of implementing viral load control, u_3 on dynamics of HIV-HBV co-infection

Figure 4.19 reveals the dynamics of the co-infected population, I_{HB} with and without the implementation of viral load control strategy u_3 in a span of twenty years. In this case, the prevention control u_1, treatment control u_2, vaccination control u_4 and recovery control u_5 are absent. The implementation of the viral load control, u_3 is considered which targets the HIV, I_H and chronic HBV, I_{cB} classes. This strategy regulates the progression rate of the transition of I_H to AIDS as well as I_B to I_{cB} with and without the control.

Figure 4.19
Impact of viral load control, u_3

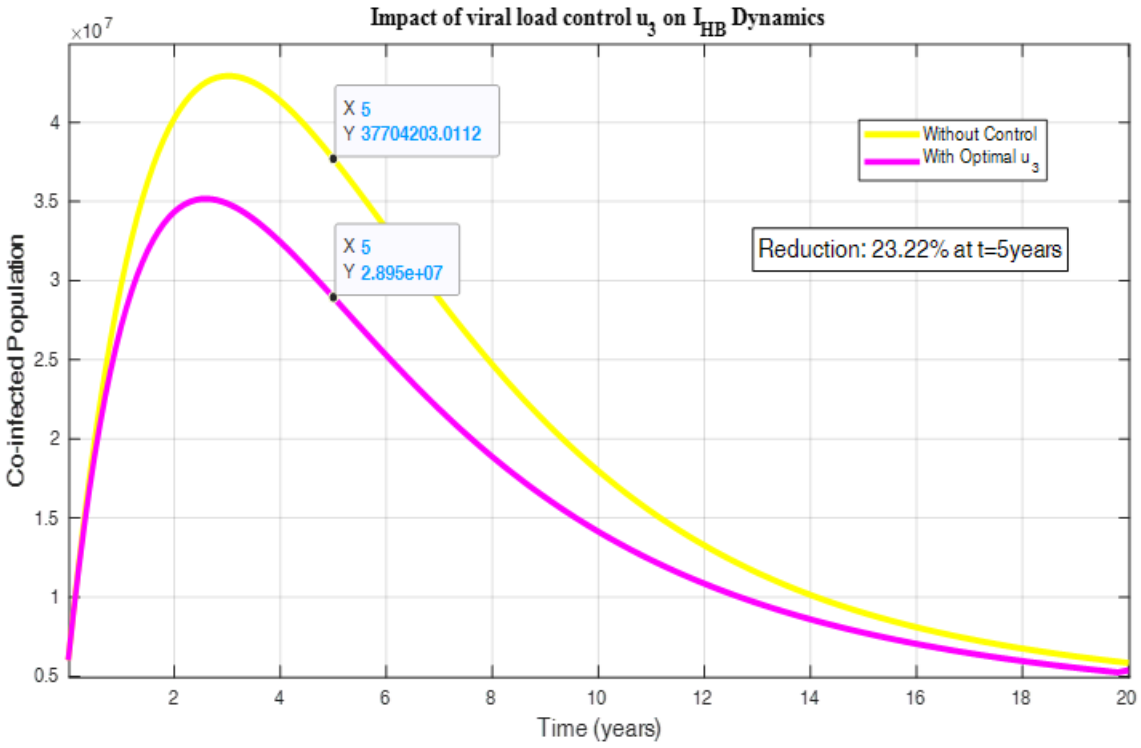

Source: Researcher (2025)

Figure 4.19 shows the implementation of viral load control strategy only when $u_1 = u_2, u_4 = u_5 = 0$. The population of I_B declines exponentially and after four years remain in steady state. I_H and A population decreases slowly over time moving towards infection free state. This implies that the related mechanisms to viral load reduction such as ART helps achieve viral suppression, delaying the progression of I_H to A or reducing the chances of infection to others. This slows down the spread of HIV, lowering the death rate among HIV-positive people and the quantity of new infections. Conversely, the population of co-infected, I_{HB} and I_{HCB} decreases and converges to the co-infection free state quickly. Strategies to further decrease HIV viral load include early identification, timely ART initiation, adherence to treatment, support programs, prevention strategies, and addressing stigma. Implementing condom use, PrEP, harm reduction programs, and targeted outreach can further reduce HIV transmission and viral load. Addressing HIV-related stigma and promoting comprehensive education can also contribute to viral load control efforts.

4.9.4 Impact of implementing vaccination strategy, u_4

When the vaccination control u_4 is implemented figure 4.20 is obtained together with the dynamics of co-infected population without the vaccination control for a period of twenty years. In this case, the vaccination control, $u_4 \neq 0$ is taken into consideration while other control strategies $u_1 = u_2 = u_3 = 0$.

Figure 4.20
Implementation of vaccination strategy, u_4

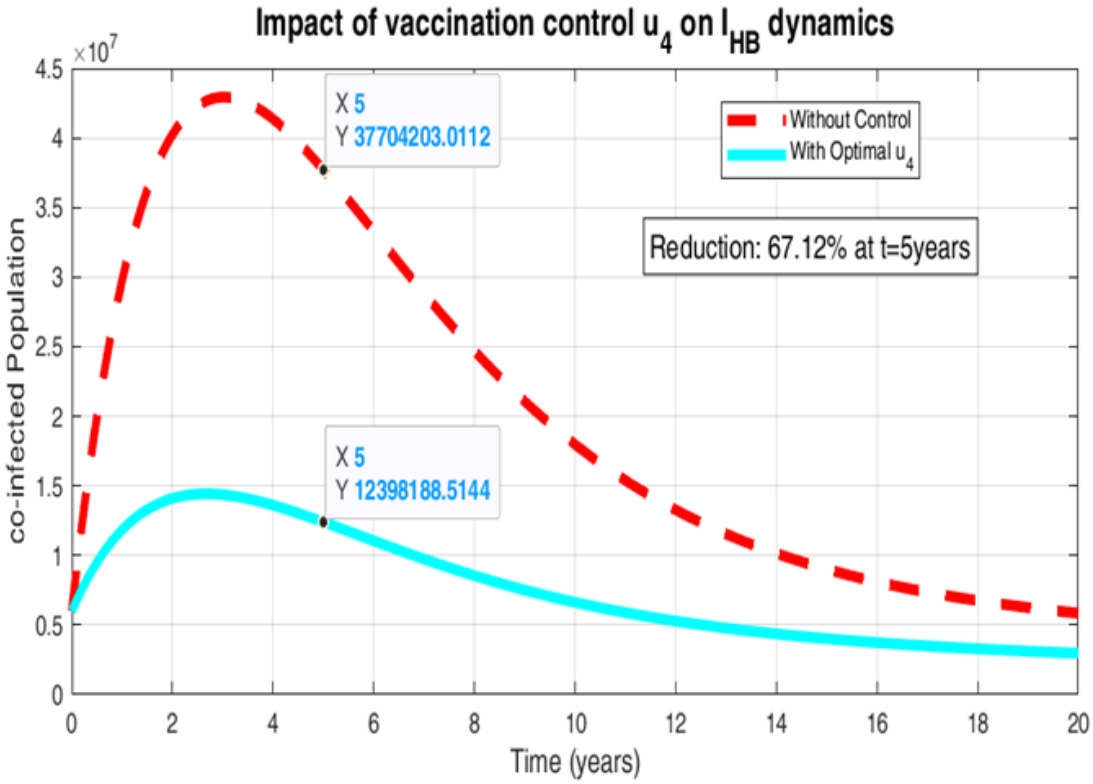

Source: Researcher (2025)

The number of vaccinated individuals, V and V_H increases continuously with time while the population of co-infected T_{HB}, I_{HB} and I_{HcB} increases marginally from the co-infection free state and maintains constant trajectory afterwards. The gradual increase in vaccinated individuals is due to increased awareness, integration of vaccination programs, improved coverage and adherence, as well as initiatives for mother-to-child transmission prevention.

4.9.5 Impact of implementing recovery or cure strategy, u_5

Figure 4.21 below demonstrates the dynamics of treated individuals when the recovery control, u_5 is implemented for a period of twenty years. The impact of the recovery control u_5 on treated individuals with and without the recovery control is compared.

Figure 4.21
Implementation of recovery control, u_5

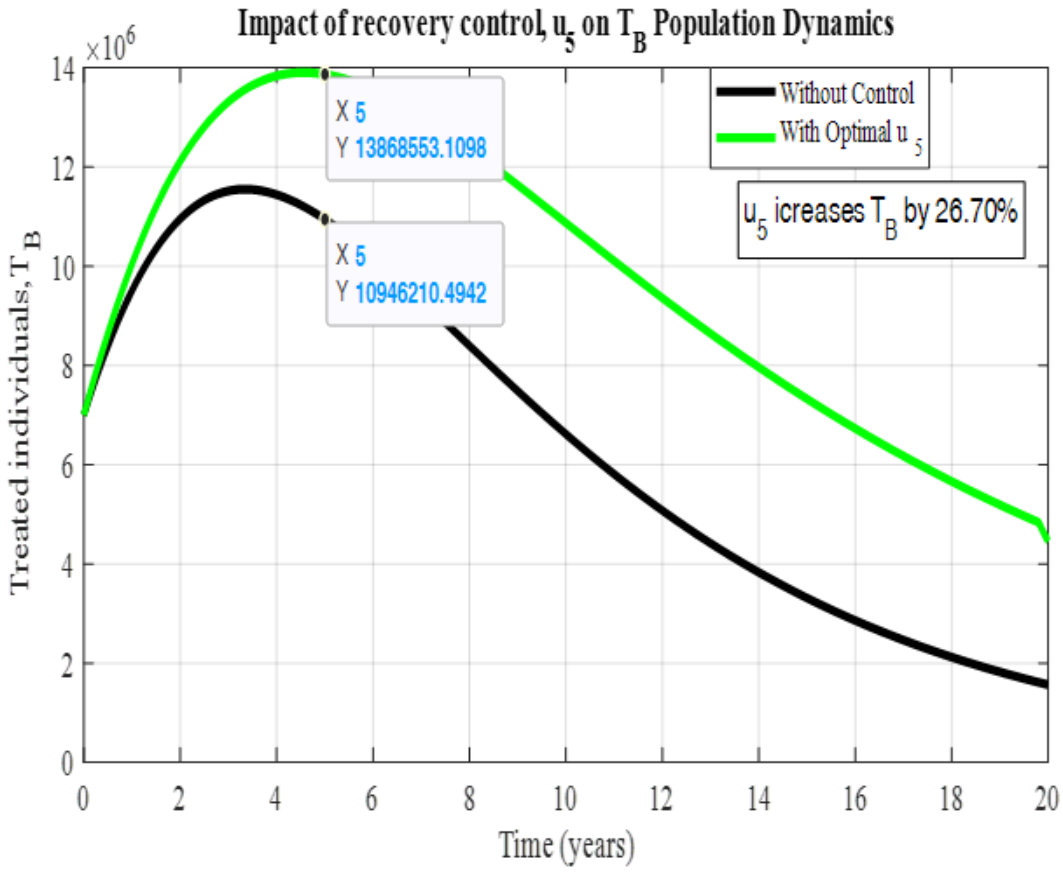

Source: Researcher(2025)

In addition, figure 4.22 illustrates the dynamics of treated co-infected individuals when the recovery control, u_5 is implemented for a period of twenty years. The impact of the recovery control u_5 on treated co-infected individuals with and without the recovery control is compared.

Figure 4.22
Implementation of recovery control, u_5

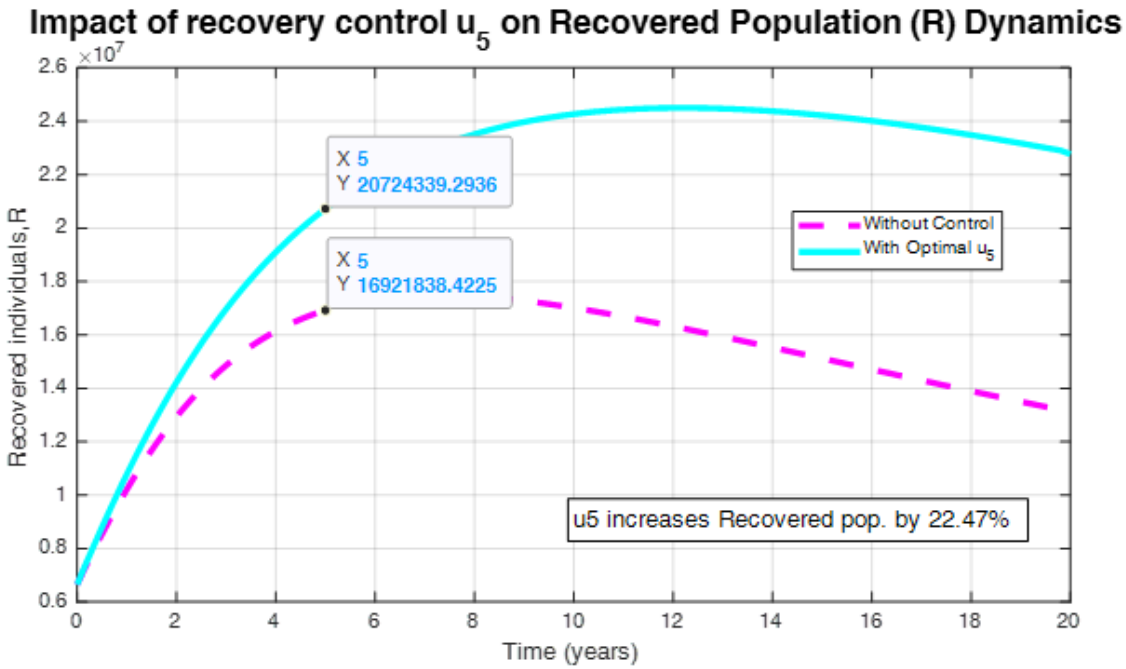

Source: Researcher (2025)

Figure 4.21 and 4.22 display the implementation of recovery control u_5 when $u_1 = u_2 = u_3 = u_4 = 0$. The number of treated acute hep b individuals, T_B showed slight increase and then steadily declines with the number of those who have recovered, R increases. Within a four-year period, the number of co-infected persons I_{HB} and T_{HB} gradually grows and afterwards maintains constant rate over time. The population of co-infected individuals with chronic hepatitis B, I_{HcB} increases with time.

Acute hepatitis B can be treated effectively by focusing on early diagnosis, supportive care, antiviral therapy, regular monitoring and follow-up. This approach allows for a more favorable outcome and reduces the number of individuals requiring active medical treatment. Early diagnosis, screening and treatment of T_B leads to a shorter duration of infection and faster symptom resolution. An increase in R means that many individuals experience spontaneous recovery, allowing for a significant number of T_B to recover with natural immunity and effective treatment. The duration of treatment is reduced, allowing T_B individuals to complete their treatment course and no longer require active medical management. Thus, the number of recovered individuals, R increases over time due to improved immune re-

sponse, effective treatment, and the natural history of HBV.

4.9.6 Impact of implementing combined control strategies u_1, u_2, u_3, u_4 and u_5

Figure 4.23 shows the impact of all the control strategies u_1, u_2, u_3, u_4 and u_5 on the dynamics of co-infected population for a period of 10 years. Under this consideration, the prevention control u_1, treatment control u_2, viral load control u_3, vaccination control u_4 and recovery control u_5 are not equal to zero, that is $u_1 \neq 0, u_2 \neq 0, u_3 \neq 0, u_4 \neq 0, u_5 \neq 0$.

Figure 4.23
Implementation of combined control strategies, $U = \{u_1, u_2, u_3, u_4, u_5\}$

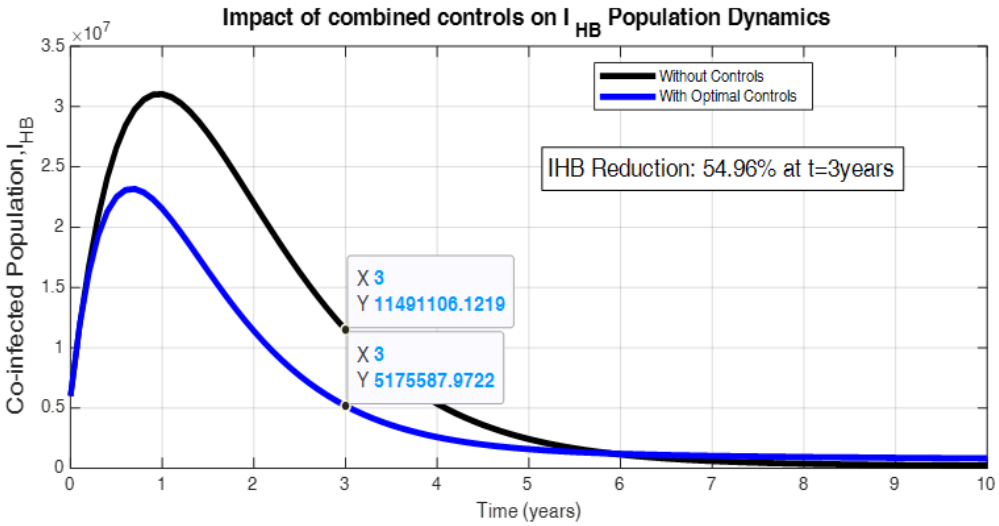

Source: Researcher (2025)

In Figure 4.23, we observe that the number of vulnerable people reduces exponentially and attains steady state as a result of implementing prevention control, u_1. The treatment control, u_2 ensures access to antiretroviral therapy by I_B, I_{HB}, leading to reduced transmission rates. The number of HIV-HBV co-infected individuals, I_{HB} increases steadily for few months and starts decreasing after one year until five years when they attain steady state where they remain over time. Similarly, the population of co-infected individuals with chronic hepatitis B, I_{HcB} increases continuously for three years and later decline approaching steady state afterwards. In the same manner, the number of treated co-infected individuals with chronic hepatitis B, T_{HB} increases for four years and later stabilizes with time.

Vaccinated individuals, V and V_H are targeted with vaccination control, u_4 ensuring hepati-

tis b vaccines at birth for susceptible infants and for those born with HIV. From the graph, it is seen that the population of V and V_H increases continuously with time. The population of I_H and I_B increases spontaneously with time for few months and decreases before being absorbed to infection free state. Difference in convergence to steady state is noted as I_B convergences earlier than I_H. These infections are aimed with prevention control, u_1.

The population of AIDS infective, A and chronic hepatitis B infective, IcB are targeted with viral load control strategy, u_3. This approach results in lowering the number of people infected with HIV and HBV and suppressing HIV and HBV viral loads, respectively. Consequently, the population of A and I_{CB} gradually grows for a short period of time before settling into a stable state. It is also observed that I_{cB} attains infection free state faster than A. This strategy also slows down infection progression and reduces mortality at the same time reducing the AIDS population. Recovery control, u_5 targets population of T_B and R. By implementation of this strategy, it is clear that T_B and R numbers rise for approximately four years and then maintains stabilization state over time. This strategy enhances the immune response to acute hepatitis B infection, leading to increased viral clearance and recovery.

4.10 Stochastic Model Results

This section demonstrate the stochastic model results.

4.10.1 Determination of transition probabilities, drift and diffusion coefficients

We symbolize the population in the states in each compartment by vector X and denote the potential change of X during the time Δt by ΔX, where vector

$X = \{S, I_H, A, I_{HB}, T_{HB}, I_{HcB}, V, V_H, I_B, I_{cB}, T_B, R\}^T$ and

$\Delta X = \{\Delta S, \Delta I_H, \Delta A, \Delta I_{HB}, \Delta T_{HB}, \Delta I_{HcB}, \Delta V, \Delta V_H, \Delta I_B, \Delta I_{cB}, \Delta T_B, \Delta R\}^T$ be n-dimensional stochastic vectors. The possible changes or transitions from the deterministic model in figure 1 and their corresponding probabilities in a small time-interval Δt are computed as shown in the table 4.5 below.

Table 4.5
Transition Probabilities

Possible change of state	Vector Representation	Probability
ΔX_1	$(1,0,0,0,0,0,0,0,0,0,0,0)^T$	$P_1 = \theta_5 \pi \Delta t$
ΔX_2	$(1,0,0,0,0,0,0,0,0,0,0,-1)^T$	$P_2 = \omega R \Delta t$
ΔX_3	$(-1,0,0,0,0,0,0,0,0,0,0,0)^T$	$P_3 = \mu S \Delta t$
ΔX_4	$(-1,1,0,0,0,0,0,0,0,0,0,0)^T$	$P_4 = \lambda_1 S \Delta t$
ΔX_5	$(-1,0,0,0,0,0,0,0,1,0,0,0)^T$	$P_5 = \lambda_2 S \Delta t$
ΔX_6	$(-1,0,0,1,0,0,0,0,0,0,0,0)^T$	$P_6 = \lambda_3 S \Delta t$
ΔX_7	$(0,1,0,0,0,0,0,0,0,0,0,0)^T$	$P_7 = \theta_1 \pi \Delta t$
ΔX_8	$(0,1,0,0,-1,0,0,0,0,0,0,0)^T$	$P_8 = (1-\varepsilon_2)\,\sigma T_{HB} \Delta t$
ΔX_9	$(0,-1,1,0,0,0,0,0,0,0,0,0)^T$	$P_9 = (1-\varepsilon_1)\,D_H I_H \Delta t$
ΔX_{10}	$(0,-1,0,0,0,0,0,0,0,0,0,0)^T$	$P_{10} = \mu I_H \Delta t$
ΔX_{11}	$(0,0,-1,0,0,0,0,0,0,0,0,0)^T$	$P_{11} = \delta_1 A \Delta t$
ΔX_{12}	$(0,0,-1,0,0,0,0,0,0,0,0,0)^T$	$P_{12} = \mu A \Delta t$
ΔX_{13}	$(0,0,0,1,0,0,0,0,-1,0,0,0)^T$	$P_{13} = \lambda_5 I_B \Delta t$
ΔX_{14}	$(0,0,0,1,0,0,0,0,0,0,0,0)^T$	$P_{14} = (1-\rho)\pi \Delta t$
ΔX_{15}	$(0,0,0,1,0,0,0,-1,0,0,0,0)^T$	$P_{15} = v\lambda_4 V_H \Delta t$
ΔX_{16}	$(0,0,0,-1,0,0,0,0,0,0,0,0)^T$	$P_{16} = \mu I_{HB} \Delta t$
ΔX_{17}	$(0,0,0,-1,1,0,0,0,0,0,0,0)^T$	$P_{17} = \phi I_{HB} \Delta t$
ΔX_{18}	$(0,0,0,-1,0,1,0,0,0,0,0,0)^T$	$P_{18} = \gamma I_{HB} \Delta t$
ΔX_{19}	$(0,0,0,0,-1,0,0,0,0,0,0,0)^T$	$P_{19} = \mu T_{HB} \Delta t$
ΔX_{20}	$(0,0,0,0,-1,0,0,0,0,0,0,0)^T$	$P_{20} = \delta_3 T_{HB} \Delta t$
ΔX_{21}	$(0,0,0,0,0,-1,0,0,0,0,0,0)^T$	$P_{21} = \mu I_{HcB} \Delta t$
ΔX_{22}	$(0,0,0,0,0,-1,0,0,0,0,0)^T$	$P_{22} = \delta_4 I_{HcB} \Delta t$
ΔX_{23}	$(0,0,0,0,0,0,1,0,0,0,0,0)^T$	$P_{23} = \theta_3 \pi \Delta t$
ΔX_{24}	$(0,0,0,0,0,0,-1,0,0,0,0,0)^T$	$P_{24} = \mu V \Delta t$
ΔX_{25}	$(0,0,0,0,0,0,-1,1,0,0,0,0)^T$	$P_{25} = \Gamma \lambda_1 V \Delta t$
ΔX_{26}	$(0,0,0,0,0,0,0,1,0,0,0,0)^T$	$P_{26} = \theta_4 \pi \Delta t$
ΔX_{27}	$(0,0,0,0,0,0,0,-1,0,0,0,0)^T$	$P_{27} = \mu V_H \Delta t$
ΔX_{28}	$(0,0,0,0,0,0,0,0,0,1,0,0)^T$	$P_{28} = \theta_2 \pi \Delta t$
ΔX_{29}	$(0,0,0,0,0,0,0,0,0,-1,1,0)^T$	$P_{29} = \psi D_B I_B \Delta t$
ΔX_{30}	$(0,0,0,0,0,0,0,0,-1,0,1,0)^T$	$P_{30} = \tau I_B \Delta t$
ΔX_{31}	$(0,0,0,0,0,0,0,0,-1,0,0,1)^T$	$P_{31} = \alpha I_B \Delta t$
ΔX_{32}	$(0,0,0,0,0,0,0,0,-1,0,0,0)^T$	$P_{32} = \mu I_B \Delta t$
ΔX_{33}	$(0,0,0,0,0,0,0,0,0,-1,0,0)^T$	$P_{33} = \mu I_{cB} \Delta t$
ΔX_{34}	$(0,0,0,0,0,0,0,0,0,-1,0,0)^T$	$P_{34} = \delta_2 I_{cB} \Delta t$
ΔX_{35}	$(0,0,0,0,0,0,0,0,0,0,-1,1)^T$	$P_{35} = (1-\varepsilon_2)\,\varphi T_B \Delta t$
ΔX_{36}	$(0,0,0,0,0,0,0,0,0,0,-1,0)^T$	$P_{36} = \mu T_B \Delta t$
ΔX_{37}	$(0,0,0,0,0,0,0,0,0,0,-1,0)^T$	$P_{37} = \delta_3 T_B \Delta t$
ΔX_{38}	$(0,0,0,0,0,0,0,0,0,0,0,-1)^T$	$P_{38} = \mu R \Delta t$

The related events to the changes in the state variables are described in table 4.6

Table 4.6
Description of event of possible change of states

Change of state variable	Event description
ΔX_1	Birth of a susceptible
ΔX_2	Recovered becomes re-infected with HBV
ΔX_3	Susceptible dies a natural death
ΔX_4	Susceptible becomes infected with HIV
ΔX_5	Susceptible becomes infected with HBV
ΔX_6	Susceptible becomes co-infected with HIV-HBV
ΔX_7	Birth of infected HIV infants
ΔX_8	Treated Co-infected persons becomes infected with HIV
ΔX_9	HIV infected persons progress to AIDS class
ΔX_{10}	HIV infected dies natural death
ΔX_{11}	AIDS infected persons dies due to HIV infection
ΔX_{12}	AIDS infected person dies naturally
ΔX_{13}	AHB infected person becomes co-infected
ΔX_{14}	Birth of co-infected infants
ΔX_{15}	HIV positive-vaccinated with Hep B becomes co-infected
ΔX_{16}	HIV-HBV co-infected person dies natural death
ΔX_{17}	Co-infected seeks Hep B treatment
ΔX_{18}	Co-infected becomes chronically infected with Hep B
ΔX_{19}	Treated co-infected person dies natural death
ΔX_{20}	Treated co-infected person dies due to effects of Hep B treatment
ΔX_{21}	HIV-CHB co-infected person dies naturally
ΔX_{22}	HIV-CHB co-infected person dies due to co-infection
ΔX_{23}	Birth of susceptible infants vaccinated with Hep B vaccine
ΔX_{24}	HIV positive -vaccinated with Hep B vaccine dies natural death
ΔX_{25}	Hep B vaccinated person becomes infected with HIV
ΔX_{26}	HIV positive births vaccinated with Hep B vaccine
ΔX_{27}	HIV-positive with Hep B vaccine dies natural death
ΔX_{28}	Births infected with Hep B
ΔX_{29}	Hep B infected person progresses to CHB
ΔX_{30}	AHB infected person seeks treatment
ΔX_{31}	AHB infected recovers by natural immunity
ΔX_{32}	AHB infected person dies natural death
ΔX_{33}	CHB infected person dies natural death
ΔX_{34}	CHB infected person dies due to Hep B infection
ΔX_{35}	Hep B treated person recovers
ΔX_{36}	Treated Hep B infected person dies natural death
ΔX_{37}	Treated Hep B person dies due to treatment effects
ΔX_{38}	Death of recovered individuals

The expectation matrix, $E(\Delta X)$, and the covariance matrix, $Cov = E\left[\Delta X(\Delta X)^T\right]$ are computed in order to formulate the SDEs as follows:

$$
\begin{aligned}
E(\Delta X) &= \sum_{i=1}^{38} P_i \Delta X_i \\
&= P_1\Delta X_1 + P_2\Delta X_2 + P_3\Delta X_3 + P_4\Delta X_4 + P_5\Delta X_5 + P_6\Delta X_6 + P_7\Delta X_7 + P_8\Delta X_8 + \\
&\quad P_9\Delta X_9 + P_{10}\Delta X_{10} + P_{11}\Delta X_{11} + P_{12}\Delta X_{12} + P_{13}\Delta X_{13} + P_{14}\Delta X_{14} + P_{15}\Delta X_{15} + \\
&\quad P_{16}\Delta X_{16} + P_{17}\Delta X_{17} + P_{18}\Delta X_{18} + P_{19}\Delta X_{19} + P_{20}\Delta X_{20} + P_{21}\Delta X_{21} + P_{22}\Delta X_{22} + \\
&\quad P_{23}\Delta X_{24} + P_{25}\Delta X_{25} + P_{26}\Delta X_{26} + P_{27}\Delta X_{27} + P_{28}\Delta X_{28} + P_{29}\Delta X_{29} + P_{30}\Delta X_{30} + \\
&\quad P_{31}\Delta X_{31} + P_{32}\Delta X_{32} + \\
&\quad P_{33}\Delta X_{33} + P_{34}\Delta X_{34} + P_{35}\Delta X_{35} + P_{36}\Delta X_{36} + P_{37}\Delta X_{37} + P_{38}X_{38}
\end{aligned}
\tag{4.4.1}
$$

substituting for $P_i\Delta X_i$ and
$\Delta X = \{\Delta S, \Delta I_H, \Delta A, \Delta I_{HB}, \Delta T_{HB}, \Delta I_{HcB}, \Delta V, \Delta V_H, \Delta I_B, \Delta I_{cB}, \Delta T_B, \Delta R\}^T$ into equation 4.4.1we have

$$
E(\Delta X) = \theta_5\pi\Delta t \begin{pmatrix} 1 \\ 0 \\ 0 \\ 0 \\ 0 \\ 0 \\ 0 \\ 0 \\ 0 \\ 0 \\ 0 \\ 0 \end{pmatrix} + \omega R\Delta t \begin{pmatrix} 1 \\ 0 \\ 0 \\ 0 \\ 0 \\ 0 \\ 0 \\ 0 \\ 0 \\ 0 \\ 0 \\ -1 \end{pmatrix} + \mu S\Delta t \begin{pmatrix} -1 \\ 0 \\ 0 \\ 0 \\ 0 \\ 0 \\ 0 \\ 0 \\ 0 \\ 0 \\ 0 \\ 0 \end{pmatrix} + \lambda_1 S\Delta t \begin{pmatrix} -1 \\ 1 \\ 0 \\ 0 \\ 0 \\ 0 \\ 0 \\ 0 \\ 0 \\ 0 \\ 0 \\ 0 \end{pmatrix} +
$$

$$\lambda_2 S\Delta t \begin{pmatrix} -1 \\ 0 \\ 0 \\ 0 \\ 0 \\ 0 \\ 0 \\ 0 \\ 1 \\ 0 \\ 0 \\ 0 \end{pmatrix} + \lambda_3 S\Delta t \begin{pmatrix} -1 \\ 0 \\ 0 \\ 0 \\ 0 \\ 0 \\ 0 \\ 0 \\ 1 \\ 0 \\ 0 \\ 0 \end{pmatrix} + \theta_1 \pi\Delta t \begin{pmatrix} 0 \\ 1 \\ 0 \\ 0 \\ 0 \\ 0 \\ 0 \\ 0 \\ 1 \\ 0 \\ 0 \\ 0 \end{pmatrix} + (1-\varepsilon_2)\,\sigma T_{HB}\Delta t \begin{pmatrix} 0 \\ 1 \\ 0 \\ 0 \\ -1 \\ 0 \\ 0 \\ 0 \\ 0 \\ 0 \\ 0 \\ 0 \end{pmatrix} +$$

$$(1-\varepsilon_1)\,D_H I_H \Delta t \begin{pmatrix} 0 \\ -1 \\ 1 \\ 0 \\ 0 \\ 0 \\ 0 \\ 0 \\ 0 \\ 0 \\ 0 \\ 0 \end{pmatrix} + \mu I_H \Delta t \begin{pmatrix} 0 \\ -1 \\ 0 \\ 0 \\ 0 \\ 0 \\ 0 \\ 0 \\ 0 \\ 0 \\ 0 \\ 0 \end{pmatrix} + \delta_1 A\Delta t \begin{pmatrix} 0 \\ 0 \\ -1 \\ 0 \\ 0 \\ 0 \\ 0 \\ 0 \\ 0 \\ 0 \\ 0 \\ 0 \end{pmatrix} + \mu A\Delta t \begin{pmatrix} 0 \\ 0 \\ -1 \\ 0 \\ 0 \\ 0 \\ 0 \\ 0 \\ 0 \\ 0 \\ 0 \\ 0 \end{pmatrix} +$$

$$\lambda_5 I_B \Delta t \begin{pmatrix} 0 \\ 0 \\ 0 \\ 1 \\ 0 \\ 0 \\ 0 \\ 0 \\ -1 \\ 0 \\ 0 \\ 0 \end{pmatrix} + (1-\rho)\pi\Delta t \begin{pmatrix} 0 \\ 0 \\ 0 \\ 1 \\ 0 \\ 0 \\ 0 \\ 0 \\ 0 \\ 0 \\ 0 \\ 0 \end{pmatrix} + v\lambda_4 V_H \Delta t \begin{pmatrix} 0 \\ 0 \\ 0 \\ 1 \\ 0 \\ 0 \\ -1 \\ 0 \\ 0 \\ 0 \\ 0 \\ 0 \end{pmatrix} + \mu I_{HB} \Delta t \begin{pmatrix} 0 \\ 0 \\ 0 \\ -1 \\ 0 \\ 0 \\ 0 \\ 0 \\ 0 \\ 0 \\ 0 \\ 0 \end{pmatrix} +$$

$$\phi I_{HB} \Delta t \begin{pmatrix} 0 \\ 0 \\ 0 \\ -1 \\ 1 \\ 0 \\ 0 \\ 0 \\ 0 \\ 0 \\ 0 \\ 0 \end{pmatrix} + \gamma I_{HB} \Delta t \begin{pmatrix} 0 \\ 0 \\ 0 \\ -1 \\ 0 \\ 1 \\ 0 \\ 0 \\ 0 \\ 0 \\ 0 \\ 0 \end{pmatrix} + \mu T_{HB} \Delta t \begin{pmatrix} 0 \\ 0 \\ 0 \\ 0 \\ -1 \\ 0 \\ 0 \\ 0 \\ 0 \\ 0 \\ 0 \\ 0 \end{pmatrix} + \delta_3 T_{HB} \Delta t \begin{pmatrix} 0 \\ 0 \\ 0 \\ 0 \\ -1 \\ 0 \\ 0 \\ 0 \\ 0 \\ 0 \\ 0 \\ 0 \end{pmatrix} +$$

$$\mu I_{HcB}\Delta t \begin{pmatrix} 0 \\ 0 \\ 0 \\ 0 \\ 0 \\ -1 \\ 0 \\ 0 \\ 0 \\ 0 \\ 0 \\ 0 \end{pmatrix} + \delta_4 I_{HcB}\Delta t \begin{pmatrix} 0 \\ 0 \\ 0 \\ 0 \\ 0 \\ -1 \\ 0 \\ 0 \\ 0 \\ 0 \\ 0 \\ 0 \end{pmatrix} + \theta_3 \pi \Delta t \begin{pmatrix} 0 \\ 0 \\ 0 \\ 0 \\ 0 \\ 0 \\ 1 \\ 0 \\ 0 \\ 0 \\ 0 \\ 0 \end{pmatrix} + \mu V \Delta t \begin{pmatrix} 0 \\ 0 \\ 0 \\ 0 \\ 0 \\ 0 \\ -1 \\ 0 \\ 0 \\ 0 \\ 0 \\ 0 \end{pmatrix} +$$

$$\Gamma\lambda_1 V\Delta t \begin{pmatrix} 0 \\ 0 \\ 0 \\ 0 \\ 0 \\ 0 \\ 0 \\ 1 \\ 0 \\ 0 \\ 0 \\ 0 \end{pmatrix} + \mu V_H \Delta t \begin{pmatrix} 0 \\ 0 \\ 0 \\ 0 \\ 0 \\ 0 \\ 0 \\ -1 \\ 0 \\ 0 \\ 0 \\ 0 \end{pmatrix} + \theta_2 \pi \Delta t \begin{pmatrix} 0 \\ 0 \\ 0 \\ 0 \\ 0 \\ 0 \\ 0 \\ 1 \\ 0 \\ 0 \\ 0 \\ 0 \end{pmatrix} +$$

$$\psi D_B I_B \Delta t \begin{pmatrix} 0 \\ 0 \\ 0 \\ 0 \\ 0 \\ 0 \\ 0 \\ 0 \\ -1 \\ 1 \\ 0 \\ 0 \end{pmatrix} + \tau I_B \Delta t \begin{pmatrix} 0 \\ 0 \\ 0 \\ 0 \\ 0 \\ 0 \\ 0 \\ -1 \\ 0 \\ 1 \\ 0 \end{pmatrix} + \alpha I_B \Delta t \begin{pmatrix} 0 \\ 0 \\ 0 \\ 0 \\ 0 \\ 0 \\ 0 \\ -1 \\ 0 \\ 0 \\ 1 \end{pmatrix} + \mu I_B \Delta t \begin{pmatrix} 0 \\ 0 \\ 0 \\ 0 \\ 0 \\ 0 \\ 0 \\ -1 \\ 0 \\ 0 \\ 0 \end{pmatrix} +$$

$$\mu I_{cB} \Delta t \begin{pmatrix} 0 \\ 0 \\ 0 \\ 0 \\ 0 \\ 0 \\ 0 \\ 0 \\ -1 \\ 0 \\ 0 \end{pmatrix} + \delta_2 I_{cB} \Delta t \begin{pmatrix} 0 \\ 0 \\ 0 \\ 0 \\ 0 \\ 0 \\ 0 \\ 0 \\ -1 \\ 0 \\ 0 \end{pmatrix} + (1 - \varepsilon_2) \varphi T_B \Delta t \begin{pmatrix} 0 \\ 0 \\ 0 \\ 0 \\ 0 \\ 0 \\ 0 \\ 0 \\ 0 \\ -1 \\ 1 \end{pmatrix} + \mu T_B \Delta t \begin{pmatrix} 0 \\ 0 \\ 0 \\ 0 \\ 0 \\ 0 \\ 0 \\ 0 \\ 0 \\ -1 \\ 0 \end{pmatrix}$$

$$+\delta_3 T_B \Delta t \begin{pmatrix} 0 \\ 0 \\ 0 \\ 0 \\ 0 \\ 0 \\ 0 \\ 0 \\ 0 \\ 0 \\ -1 \\ 0 \end{pmatrix} + \mu R \Delta t \begin{pmatrix} 0 \\ 0 \\ 0 \\ 0 \\ 0 \\ 0 \\ 0 \\ 0 \\ 0 \\ 0 \\ 0 \\ -1 \end{pmatrix} \tag{4.4.2}$$

Equation (4.4.2) simplifies to

$$E(\Delta X) = \begin{pmatrix} \theta_5\pi + \omega R - \mu S - \lambda_1 S - \lambda_2 S - \lambda_3 S \\ \lambda_1 S + \theta_1\pi - (1-\varepsilon_2)\,\sigma T_{HB} - (1-\varepsilon_1)\,D_H - \mu I_H \\ (1-\varepsilon_1)\,D_H I_H - \mu A - \delta_1 A \\ \lambda_5 I_B + (1-\rho)\pi + v\lambda_4 V_H - \mu I_{HB} - \phi I_{HB} - \gamma I_{HB} \\ \phi I_{HB} - \mu T_{HB} - \delta_3 T_{HB} \\ \gamma I_{HB} - \mu I_{HcB} - \delta_4 I_{HcB} \\ \theta_3\pi - \mu V - \Gamma\lambda_1 V \\ \theta_4\pi - \mu V_H - v\lambda_4 V_H \\ \lambda_2 S + \theta_2\pi - \alpha I_B - \mu I_B - \lambda_5 I_B - \psi D_B I_B \\ \psi D_B I_B - \mu I_{cB} - \delta_2 I_{cB} \\ \tau I_B - (1-\varepsilon_2)\,\varphi T_B - \mu T_B - \delta_3 T_B \\ \alpha I_B + (1-\varepsilon_2)\,\varphi T_B - \omega R - \mu R \end{pmatrix} \Delta t \tag{4.4.3}$$

similarly, the covariance is also computed as

$E\left[\Delta X(\Delta X)^T\right] = \sum_{i=1}^{38} P_i \Delta X(\Delta X)^T$

$$= \theta_5 \pi \Delta t \begin{pmatrix} 1 \\ 0 \\ 0 \\ 0 \\ 0 \\ 0 \\ 0 \\ 0 \\ 0 \\ 0 \\ 0 \\ 0 \end{pmatrix} (\Delta X_1)^T + \omega R \Delta t \begin{pmatrix} 1 \\ 0 \\ 0 \\ 0 \\ 0 \\ 0 \\ 0 \\ 0 \\ 0 \\ 0 \\ 0 \\ -1 \end{pmatrix} (\Delta X_2)^T +$$

$$\mu S \Delta t \begin{pmatrix} -1 \\ 0 \\ 0 \\ 0 \\ 0 \\ 0 \\ 0 \\ 0 \\ 0 \\ 0 \\ 0 \\ 0 \end{pmatrix} (\Delta X_3)^T + \lambda_1 S \Delta t \begin{pmatrix} -1 \\ 1 \\ 0 \\ 0 \\ 0 \\ 0 \\ 0 \\ 0 \\ 0 \\ 0 \\ 0 \\ 0 \end{pmatrix} (\Delta X_4)^T$$

$$+\lambda_2 S\Delta t \begin{pmatrix} -1 \\ 0 \\ 0 \\ 0 \\ 0 \\ 0 \\ 0 \\ 0 \\ 1 \\ 0 \\ 0 \\ 0 \end{pmatrix} (\Delta X_5)^T + \lambda_3 S\Delta t \begin{pmatrix} -1 \\ 0 \\ 0 \\ 0 \\ 0 \\ 0 \\ 0 \\ 0 \\ 1 \\ 0 \\ 0 \\ 0 \end{pmatrix} (\Delta X_6)^T +$$

$$\theta_1 \pi \Delta t \begin{pmatrix} 0 \\ 1 \\ 0 \\ 0 \\ 0 \\ 0 \\ 0 \\ 0 \\ 1 \\ 0 \\ 0 \\ 0 \end{pmatrix} (\Delta X_7)^T + (1-\varepsilon_2)\,\sigma T_{HB} \Delta t \begin{pmatrix} 0 \\ 1 \\ 0 \\ 0 \\ -1 \\ 0 \\ 0 \\ 0 \\ 0 \\ 0 \\ 0 \\ 0 \end{pmatrix} (\Delta X_8)^T$$

$$+(1-\varepsilon_1)\,D_H I_H \Delta t \begin{pmatrix} 0 \\ -1 \\ 1 \\ 0 \\ 0 \\ 0 \\ 0 \\ 0 \\ 0 \\ 0 \\ 0 \\ 0 \end{pmatrix} (\Delta X_9)^T + \mu I_H \Delta t \begin{pmatrix} 0 \\ -1 \\ 0 \\ 0 \\ 0 \\ 0 \\ 0 \\ 0 \\ 0 \\ 0 \\ 0 \\ 0 \end{pmatrix} (\Delta X_{10})^T +$$

$$\delta_1 A \Delta t \begin{pmatrix} 0 \\ 0 \\ -1 \\ 0 \\ 0 \\ 0 \\ 0 \\ 0 \\ 0 \\ 0 \\ 0 \\ 0 \end{pmatrix} (\Delta X_{11})^T + \mu A \Delta t \begin{pmatrix} 0 \\ 0 \\ -1 \\ 0 \\ 0 \\ 0 \\ 0 \\ 0 \\ 0 \\ 0 \\ 0 \\ 0 \end{pmatrix} (\Delta X_{12})^T$$

$$+\lambda_5 I_B \Delta t \begin{pmatrix} 0 \\ 0 \\ 0 \\ 1 \\ 0 \\ 0 \\ 0 \\ 0 \\ -1 \\ 0 \\ 0 \\ 0 \end{pmatrix} (\Delta X_{13})^T + (1-\rho)\pi\Delta t \begin{pmatrix} 0 \\ 0 \\ 0 \\ 1 \\ 0 \\ 0 \\ 0 \\ 0 \\ 0 \\ 0 \\ 0 \\ 0 \end{pmatrix} (\Delta X_{14})^T + v\lambda_4 V_H \Delta t \begin{pmatrix} 0 \\ 0 \\ 0 \\ 1 \\ 0 \\ 0 \\ -1 \\ 0 \\ 0 \\ 0 \\ 0 \\ 0 \end{pmatrix} (\Delta X_{15})^T$$

$$+\mu I_{HB} \Delta t \begin{pmatrix} 0 \\ 0 \\ 0 \\ -1 \\ 0 \\ 0 \\ 0 \\ 0 \\ 0 \\ 0 \\ 0 \\ 0 \end{pmatrix} (\Delta X_{16})^T + \phi I_{HB} \Delta t \begin{pmatrix} 0 \\ 0 \\ 0 \\ -1 \\ 1 \\ 0 \\ 0 \\ 0 \\ 0 \\ 0 \\ 0 \\ 0 \end{pmatrix} (\Delta X_{17})^T + \gamma I_{HB} \Delta t \begin{pmatrix} 0 \\ 0 \\ 0 \\ -1 \\ 0 \\ 1 \\ 0 \\ 0 \\ 0 \\ 0 \\ 0 \\ 0 \end{pmatrix} (\Delta X_{18})^T$$

$$+\mu T_{HB}\Delta t \begin{pmatrix} 0 \\ 0 \\ 0 \\ 0 \\ -1 \\ 0 \\ 0 \\ 0 \\ 0 \\ 0 \\ 0 \\ 0 \end{pmatrix} (\Delta X_{19})^T + \delta_3 T_{HB}\Delta t \begin{pmatrix} 0 \\ 0 \\ 0 \\ 0 \\ -1 \\ 0 \\ 0 \\ 0 \\ 0 \\ 0 \\ 0 \\ 0 \end{pmatrix} (\Delta X_{20})^T + \mu I_{HcB}\Delta t \begin{pmatrix} 0 \\ 0 \\ 0 \\ 0 \\ 0 \\ -1 \\ 0 \\ 0 \\ 0 \\ 0 \\ 0 \\ 0 \end{pmatrix} (\Delta X_{21})^T$$

$$+\delta_4 I_{HcB}\Delta t \begin{pmatrix} 0 \\ 0 \\ 0 \\ 0 \\ 0 \\ -1 \\ 0 \\ 0 \\ 0 \\ 0 \\ 0 \\ 0 \end{pmatrix} (\Delta X_{22})^T + \theta_3 \pi \Delta t \begin{pmatrix} 0 \\ 0 \\ 0 \\ 0 \\ 0 \\ 0 \\ 1 \\ 0 \\ 0 \\ 0 \\ 0 \\ 0 \end{pmatrix} (\Delta X_{23})^T + \mu V \Delta t \begin{pmatrix} 0 \\ 0 \\ 0 \\ 0 \\ 0 \\ 0 \\ -1 \\ 0 \\ 0 \\ 0 \\ 0 \\ 0 \end{pmatrix} (\Delta X_{24})^T$$

$$+\Gamma\lambda_1 V\Delta t \begin{pmatrix} 0 \\ 0 \\ 0 \\ 0 \\ 0 \\ 0 \\ -1 \\ 1 \\ 0 \\ 0 \\ 0 \\ 0 \end{pmatrix} (\Delta X_{25})^T + \theta_4\pi\Delta t \begin{pmatrix} 0 \\ 0 \\ 0 \\ 0 \\ 0 \\ 0 \\ 0 \\ 1 \\ 0 \\ 0 \\ 0 \\ 0 \end{pmatrix} (\Delta X_{26})^T + \mu V_H \Delta t \begin{pmatrix} 0 \\ 0 \\ 0 \\ 0 \\ 0 \\ 0 \\ 0 \\ -1 \\ 0 \\ 0 \\ 0 \\ 0 \end{pmatrix} (\Delta X_{27})^T$$

$$+\theta_2\pi\Delta t \begin{pmatrix} 0 \\ 0 \\ 0 \\ 0 \\ 0 \\ 0 \\ 0 \\ 0 \\ 1 \\ 0 \\ 0 \\ 0 \end{pmatrix} (\Delta X_{28})^T + \psi D_B I_B \Delta t \begin{pmatrix} 0 \\ 0 \\ 0 \\ 0 \\ 0 \\ 0 \\ 0 \\ 0 \\ -1 \\ 1 \\ 0 \\ 0 \end{pmatrix} (\Delta X_{29})^T + \tau I_B \Delta t \begin{pmatrix} 0 \\ 0 \\ 0 \\ 0 \\ 0 \\ 0 \\ 0 \\ 0 \\ -1 \\ 0 \\ 1 \\ 0 \end{pmatrix} (\Delta X_{30})^T$$

$$+\alpha I_B \Delta t \begin{pmatrix} 0 \\ 0 \\ 0 \\ 0 \\ 0 \\ 0 \\ 0 \\ 0 \\ -1 \\ 0 \\ 0 \\ 1 \end{pmatrix} (\Delta X_{31})^T + \mu I_B \Delta t \begin{pmatrix} 0 \\ 0 \\ 0 \\ 0 \\ 0 \\ 0 \\ 0 \\ 0 \\ -1 \\ 0 \\ 0 \\ 0 \end{pmatrix} (\Delta X_{32})^T + \mu I_{cB} \Delta t \begin{pmatrix} 0 \\ 0 \\ 0 \\ 0 \\ 0 \\ 0 \\ 0 \\ 0 \\ 0 \\ -1 \\ 0 \\ 0 \end{pmatrix} (\Delta X_{33})^T$$

$$+\delta_2 I_{cB} \Delta t \begin{pmatrix} 0 \\ 0 \\ 0 \\ 0 \\ 0 \\ 0 \\ 0 \\ 0 \\ 0 \\ -1 \\ 0 \\ 0 \end{pmatrix} (\Delta X_{34})^T + (1-\varepsilon_2)\, \varphi T_B \Delta t \begin{pmatrix} 0 \\ 0 \\ 0 \\ 0 \\ 0 \\ 0 \\ 0 \\ 0 \\ 0 \\ 0 \\ -1 \\ 1 \end{pmatrix} (\Delta X_{35})^T + \mu T_B \Delta t \begin{pmatrix} 0 \\ 0 \\ 0 \\ 0 \\ 0 \\ 0 \\ 0 \\ 0 \\ 0 \\ 0 \\ -1 \\ 0 \end{pmatrix} (\Delta X_{36})^T$$

$$+\delta_3 T_B \Delta t \begin{pmatrix} 0 \\ 0 \\ 0 \\ 0 \\ 0 \\ 0 \\ 0 \\ 0 \\ 0 \\ 0 \\ -1 \\ 0 \end{pmatrix} (\Delta X_{37})^T + \mu R \Delta t \begin{pmatrix} 0 \\ 0 \\ 0 \\ 0 \\ 0 \\ 0 \\ 0 \\ 0 \\ 0 \\ 0 \\ 0 \\ -1 \end{pmatrix} (\Delta X_{38})^T \quad (4.4.4)$$

Simplifying (4.4.4) yields

$$E\left[\Delta X(\Delta X)^T\right] = \begin{pmatrix} f_{11} & -\lambda_1 S & 0 & 0 & 0 & 0 & 0 & 0 & 0 & 0 & 0 & -\omega R \\ -\lambda_1 S & f_{22} & f_{12} & 0 & f_{13} & 0 & 0 & 0 & f_{14} & 0 & 0 & 0 \\ 0 & f_{15} & f_3 & 0 & 0 & 0 & 0 & 0 & 0 & 0 & 0 & 0 \\ 0 & 0 & 0 & f_4 & f_{16} & f_{17} & f_{18} & 0 & f_{19} & 0 & 0 & 0 \\ 0 & f_{20} & 0 & -\phi I_{HB} & f_5 & 0 & 0 & 0 & 0 & 0 & 0 & 0 \\ 0 & 0 & 0 & -\gamma I_{HB} & 0 & f_6 & 0 & 0 & 0 & 0 & 0 & 0 \\ 0 & 0 & 0 & -\nu\lambda_4 V_H & 0 & f_{76} & f_7 & 0 & 0 & 0 & 0 & 0 \\ 0 & 0 & 0 & 0 & 0 & -\Gamma\lambda_1 V & \Gamma\lambda_1 V & f_{88} & 0 & 0 & 0 & 0 \\ -\lambda_1 S - \lambda_3 S & \theta_1\pi & 0 & -\lambda_5 I_B & 0 & 0 & 0 & 0 & f_8 & -\psi D_B I_B & -\tau I_B & -\alpha I_B \\ 0 & 0 & 0 & 0 & 0 & 0 & 0 & 0 & -\psi D_B I_B & f_9 & 0 & 0 \\ 0 & 0 & 0 & 0 & 0 & 0 & 0 & 0 & -\tau I_B & 0 & f_{10} & f_{1112} \\ -\omega R & 0 & 0 & 0 & 0 & 0 & 0 & 0 & -\alpha I_B & 0 & f_{1211} & f_{11} \end{pmatrix} \Delta t \quad (4.4.5)$$

where;

$f_{11} = \theta_5\pi + \omega R + \mu S + \lambda_1 S + \lambda_2 S + \lambda_3 S$

$f_{22} = \lambda_1 S + \theta_1\pi + (1-\varepsilon_2)\sigma T_{HB} + \mu I_H + (1-\varepsilon_1) D_H I_H$

$f_3 = (1-\varepsilon_1) D_H I_H + \delta_1 A + \mu A$

$\mathrm{f}_4 = \lambda_5 I_B + (1-\rho)\pi + \nu\lambda_4 V_H + \mu I_{HB} + \phi I_{HB} + \gamma I_{HB}$

$$f_5 = (1-\varepsilon_2)\,\sigma T_{HB} + \phi I_{HB} + \mu T_{HB} + \delta_3 T_{HB}$$

$$f_6 = \gamma I_{HB} + \mu I_{HcB} + \delta_4 I_{HcB}$$

$$f_7 = v\lambda_4 V_H + \theta_3\pi - \Gamma\lambda_1 V$$

$$f_8 = \lambda_1 S + \lambda_3 S + \theta_1\pi + \lambda_5 I_B + \theta_2\pi + \psi D_B I_B + \tau I_B + \alpha I_B + \mu I_B$$

$$f_9 = \psi D_B I_B + \mu I_{cB} + \delta_2 I_{cB}$$

$$f_{10} = \tau I_B + (1-\varepsilon_2)\,\varphi T_B + \mu T_B + \delta_3 T_B$$

$$f_{11} = \omega R + \alpha I_B + (1-\varepsilon_2)\,\varphi T_B + \mu R$$

$$f_{12} = -(1-\varepsilon_1)\,D_H I_H$$

$$f_{13} = -(1-\varepsilon_2)\,\sigma T_{HB}$$

$$f_{14} = -\lambda_1 S - \lambda_3 S + \theta_1\pi$$

$$f_{15} = -(1-\varepsilon_1)\,D_H I_H$$

$$f_{16} = -\phi I_{HB}, f_{17} = -\gamma I_{HB}, f_{18} = -v\lambda_4 V_H, f_{19} = -\lambda_5 I_B,$$

$$f_{20} = -(1-\varepsilon_2)\,\sigma T_{HB}, f_{1112} = -(1-\varepsilon_2)\,\varphi T_B, f_{1211} = -(1-\varepsilon_2)\,\varphi T_B,$$

$$f_{88} = \theta_4\pi + \mu V_H, f_{76} = \mu V + \Gamma\lambda_1 V$$

By dividing Δt on both sides of equation (4.4.4) we get $f(X(t),t)$ as

$$\frac{E(\Delta X)}{\Delta t} = H(X(t),t) = \begin{pmatrix} \theta_5\pi + \omega R - \mu S - \lambda_1 S - \lambda_2 S - \lambda_3 S \\ \lambda_1 S + \theta_1\pi - (1-\varepsilon_2)\,\sigma T_{HB} - (1-\varepsilon_1)\,D_H - \mu I_H \\ (1-\varepsilon_1)\,D_H I_H - \mu A - \delta_1 A \\ \lambda_5 I_B + (1-\rho)\pi + v\lambda_4 V_H - \mu I_{HB} - \phi I_{HB} - \gamma I_{HB} \\ \phi I_{HB} - \mu T_{HB} - \delta_3 T_{HB} \\ \gamma I_{HB} - \mu I_{HcB} - \delta_4 I_{HcB} \\ \theta_3\pi - \mu V - \Gamma\lambda_1 V \\ \theta_4\pi - \mu V_H - v\lambda_4 V_H \\ \lambda_2 S + \theta_2\pi - \alpha I_B - \mu I_B - \lambda_5 I_B - \psi D_B I_B \\ \psi D_B I_B - \mu I_{cB} - \delta_2 I_{cB} \\ \tau I_B - (1-\varepsilon_2)\,\varphi T_B - \mu T_B - \delta_3 T_B \\ \alpha I_B + (1-\varepsilon_2)\,\varphi T_B - \omega R - \mu R \end{pmatrix} \tag{4.4.6}$$

and from equation (4.4.6) we obtain,

$$\frac{E\left[\Delta X(\Delta X)^T\right]}{\Delta t} = V(X(t),t)$$

$$= \begin{pmatrix} f_{11} & -\lambda_1 S & 0 & 0 & 0 & 0 & 0 & 0 & 0 & 0 & 0 & -\omega R \\ -\lambda_1 S & f_{22} & V_{23} & 0 & V_{25} & 0 & 0 & 0 & V_{29} & 0 & 0 & 0 \\ 0 & V_{32} & f_3 & 0 & 0 & 0 & 0 & 0 & 0 & 0 & 0 & 0 \\ 0 & 0 & 0 & f_4 & V_{45} & V_{46} & V_{47} & 0 & V_{49} & 0 & 0 & 0 \\ 0 & V_{52} & 0 & V_{54} & f_5 & 0 & 0 & 0 & 0 & 0 & 0 & 0 \\ 0 & 0 & 0 & V_{64} & 0 & f_6 & 0 & 0 & 0 & 0 & 0 & 0 \\ 0 & 0 & 0 & V_{74} & 0 & V_{76} & f_7 & 0 & 0 & 0 & 0 & 0 \\ 0 & 0 & 0 & 0 & 0 & V_{86} & V_{87} & V_{88} & 0 & 0 & 0 & 0 \\ V_{91} & V_{92} & 0 & V_{94} & 0 & 0 & 0 & 0 & f_8 & V_{910} & -\tau I_B & -\alpha I_B \\ 0 & 0 & 0 & 0 & 0 & 0 & 0 & 0 & V_{109} & f_9 & 0 & 0 \\ 0 & 0 & 0 & 0 & 0 & 0 & 0 & 0 & -\tau I_B & 0 & f_{10} & V_{1112} \\ -\omega R & 0 & 0 & 0 & 0 & 0 & 0 & 0 & -\alpha I_B & 0 & V_{1211} & f_{11} \end{pmatrix} \tag{4.4.7}$$

where;

$$V_{23} = -(1-\varepsilon_1) D_H I_H, V_{25} = -(1-\varepsilon_2) \sigma T_{HB}, V_{29} = -(\lambda_1 S + \lambda_3 S - \theta_1 \pi),$$

$$V32 = -(1-\varepsilon_1) D_H I_H, V_{45} = -\phi I_{HB}, V_{46} = -\gamma I_{HB}, V_{47} = -v\lambda_4 V_H,$$

$$V_{49} = -\lambda_5 I_B, V_{52} = -(1-\varepsilon_2) \sigma T_{HB}, V_{54} = -\phi I_{HB}, V_{64} = -\gamma I_{HB},$$

$$V_{74} = -v\lambda_4 V_H, V76 = \mu V + \Gamma\lambda_1 V, V_{86} = -\Gamma\lambda_1 V, V_{87} = \Gamma\lambda_1 V,$$

$$V88 = \theta_4 \pi + \mu V_H, V_{91} = -(\lambda_1 S + \lambda_3 S), V_{92} = \theta_1 \pi, V_{94} = -\lambda_5 I_B,$$

$$V_{910} = -\psi D_B I_B, V109 = -\psi D_B I_B, V_{1112} = -(1-\varepsilon_2) \varphi T_B,$$

$$V_{1211} = -(1-\varepsilon_2) \varphi T_B$$

Thus, $J(X(t),t) = \sqrt{V}$.

4.10.2 Stochastic differential equations

Therefore, HIV-HBV deterministic co-infection model is converted to a stochastic model to predict infection outcomes when uncertainties are incorporated in the transition rates.

Incorporating these stochastic effects and applying equation 3.6.2 to the deterministic model, the following system of non-linear SDEs are derived from the deterministic equations in section 4.2.2.

$$\begin{aligned} dS(t) &= (\theta_5\pi - (\lambda_1+\lambda_2+\lambda_3+\mu)S + \omega R)\,dt \\ &\quad + \sqrt{f_{11}}dW_1(t) - \sqrt{\lambda_1 S}dW_2(t) - \sqrt{\omega R}dW_3(t) \end{aligned} \tag{4.4.8}$$

$$\begin{aligned} dI_H(t) &= (\theta_1\pi + \lambda_1 S + (1-\varepsilon_2)\sigma T_{HB} - (\lambda_4+\mu+(1-\varepsilon_1)D_H)I_H)\,dt \\ &\quad - \sqrt{\lambda_1 S}dW_2(t) + \sqrt{f_{22}}dW_4(t) - \sqrt{(1-\varepsilon_1)D_H I_H}dW_5 \\ &\quad - \sqrt{(1-\varepsilon_2)\sigma T_{HB}}dW_6 - \sqrt{\lambda_1 S + \lambda_3 S - \theta_1\pi}dW_7 \end{aligned} \tag{4.4.9}$$

$$dA(t) = ((1-\varepsilon_1)D_H I_H - (\delta_1+\mu)A)\,dt - \sqrt{(1-\varepsilon_1)D_H I_H}dW_5 + \sqrt{f_3}dW_8 \tag{4.4.10}$$

$$\begin{aligned} dI_{HB}(t) &= ((1-\rho)\pi + \lambda_3 S + v\lambda_4 V_H + \lambda_4 I_H + \lambda_5 I_B - (\phi+\gamma+\mu)I_{HB})\,dt \\ &\quad + \sqrt{f_4}dW_9 - \sqrt{\phi I_{HB}}dW_{10} - \sqrt{\gamma I_{HB}}dW_{11} - \sqrt{v\lambda_4 V_H}dW_{12} - \sqrt{\lambda_5 I_B}dW_{13} \end{aligned} \tag{4.4.11}$$

$$\begin{aligned} dT_{HB}(t) &= (\phi I_{HB} - (\mu+\delta_3+(1-\varepsilon_2)\sigma)T_{HB})\,dt \\ &\quad - \sqrt{(1-\varepsilon_2)\sigma T_{HB}}dW_6 - \sqrt{\phi I_{HB}}dW_{10} + \sqrt{f_5}dW_{14} \end{aligned} \tag{4.4.12}$$

$$dI_{HcB}(t) = (\gamma I_{HB} - (\mu+\delta_4)I_{HcB})\,dt - \sqrt{\gamma I_{HB}}dW_{11} + \sqrt{f_6}dW_{15} \tag{4.4.13}$$

$$\begin{aligned} dV(t) &= (\theta_3\pi - (\mu+\Gamma\lambda_1)V)\,dt - \sqrt{v\lambda_4 V_H}dW_{12} \\ &\quad + \sqrt{\mu V + \Gamma\lambda_1 V}dW_{16} + \sqrt{f_7}dW_{17} \end{aligned} \tag{4.4.14}$$

(4.15)

$$dV_H(t) = (\theta_4\pi + \Gamma\lambda_1 V - (\mu + v\lambda_4)V_H)\,dt - \sqrt{\Gamma\lambda_1 V}dW_{18} + \sqrt{\Gamma\lambda_1 V}dW_{19} + \sqrt{\theta_4\pi + \mu V_H}dW_{20} \quad (4.4.15)$$

$$dI_B(t) = (\theta_2\pi + \lambda_2 S - (\mu + \lambda_5 + \alpha + \tau + \psi D_B)I_B)\,dt - \sqrt{\lambda_1 S + \lambda_3 S}dW_{21} + \sqrt{\theta_1\pi}dW_{22} - \sqrt{\lambda_5 I_B}dW_{13} + \sqrt{f_8}dW_{23} - \sqrt{\psi D_B I_B}dW_{24} - \sqrt{\tau I_B}dW_{25} - \sqrt{\alpha I_B}dW_{26} \quad (4.4.16)$$

$$dI_{cB}(t) = (\psi D_B I_B - (\mu + \delta_2)I_{cB})\,dt - \sqrt{\psi D_B I_B}dW_{24} + \sqrt{f_9}dW_{27} \quad (4.4.17)$$

$$dT_B(t) = (\tau I_B - (\mu + \delta_3 + (1-\varepsilon_2)\varphi)T_B)\,dt - \sqrt{\tau I_B}dW_{25} + \sqrt{f_{10}}dW_{28} - \sqrt{(1-\varepsilon_2)\varphi T_B}dW_{29} \quad (4.4.18)$$

$$dR(t) = (\alpha I_B + (1-\varepsilon_2)\varphi T_B - (\omega + \mu)R)\,dt - \sqrt{\omega R}dW_3 - \sqrt{\alpha I_B}dW_{26} - \sqrt{(1-\varepsilon_2)\varphi T_B}dW_{29} + \sqrt{f_{11}}dW_{30} \quad (4.4.19)$$

where the terms

$\sqrt{f_{11}}dW_1(t), \sqrt{\lambda_1 S}dW_2(t), \sqrt{\omega R}dW_3(t), \sqrt{\lambda_1 S}dW_2(t), \sqrt{f_{22}}dW_4(t),$
$\sqrt{(1-\varepsilon_1)D_H I_H}dW_5(t), \sqrt{(1-\varepsilon_2)\sigma T_{HB}}dW_6(t), \sqrt{\lambda_1 S + \lambda_3 S - \theta_1\pi}dW_7$
$\sqrt{(1-\varepsilon_1)D_H I_H}dW_5, \sqrt{f_3}dW_8, \sqrt{f_4}dW_9, \sqrt{\phi I_{HB}}dW_{10}, \sqrt{\gamma I_{HB}}dW_{11},$
$\sqrt{v\lambda_4 V_H}dW_{12}, \sqrt{\lambda_5 I_B}dW_{13}, \sqrt{(1-\varepsilon_2)\sigma T_{HB}}dW_6, \sqrt{\phi I_{HB}}dW_{10}, \sqrt{f_5}dW_{14}$
$\sqrt{\gamma I_{HB}}dW_{11}, \sqrt{f_6}dW_{15}, \sqrt{v\lambda_4 V_H}dW_{12}, \sqrt{\mu V + \Gamma\lambda_1 V}dW_{16}, \sqrt{f_7}dW_{17},$
$\sqrt{\Gamma\lambda_1 V}dW_{18}, \sqrt{\Gamma\lambda_1 V}dW_{19}, \sqrt{\theta_4\pi + \mu V_H}dW_{20}, \sqrt{\lambda_1 S + \lambda_3 S}dW_{21}, \sqrt{\theta_1\pi}dW_{22}$
$\sqrt{\lambda_5 I_B}dW_{13}, \sqrt{f_8}dW_{23}, \sqrt{\psi D_B I_B}dW_{24}, \sqrt{\tau I_B}dW_{25}, \sqrt{\alpha I_B}dW_{26},$
$\sqrt{\tau I_B}dW_{25}, \sqrt{f_{10}}dW_{28}, \sqrt{(1-\varepsilon_2)\varphi T_B}dW_{29}, \sqrt{\omega R}dW_3, \sqrt{\alpha I_B}dW_{26},$
$\sqrt{\psi D_B I_B}dW_{24}, \sqrt{f_9}dW_{27}, \sqrt{(1-\varepsilon_2)\varphi T_B}dW_{29}$, and $\sqrt{f_{11}}dW_{30}$

represent the stochastic components of the transitions between compartments. These stochastic terms introduce randomness into the model, capturing the variability in the transmission, progression and recovery processes. The corresponding change in Wiener processes are;

$dW_1, dW_2, dW_3, dW_4, dW_5, dW_6, dW_7, dW_8, dW_9, dW_{10}, dW_{11}, dW_{12}, dW_{13}, dW_{14}, dW_{15}, dW_{16},$
$dW_{17}, dW_{18}, dW_{19}, dW_{20}, dW_{21}, dW_{22}, dW_{23}, dW_{24}, dW_{25}, dW_{26}, dW_{28}, dW_{29}, dW_{30}$. This processes represent random fluctuations over time which are independent of each other.

4.10.3 Euler-Maruyama scheme

Based on SDEs from (4.4.8) to (4.4.19) and applying (3.6.3), the corresponding Euler-Maruyama numerical scheme is given by;

$$S(t+\Delta t) = S(t) + (\theta_5\pi - (\lambda_1+\lambda_2+\lambda_3+\mu)\,S + \omega R)\,\Delta t + S\text{stoch} \tag{4.4.20}$$

where $Sstoch = \sqrt{f_1}dW_1 - \sqrt{\lambda_1 S}dW_2 - \sqrt{\omega R}dW_3$

$$I_H(t+\Delta t) = I_H(t) + (\theta_1\pi + \lambda_1 S + (1-\varepsilon_2)\,\sigma T_{HB} - (\lambda_4+\mu+(1-\varepsilon_1)\,D_H)\,I_H)\,\Delta t + I_H \text{ stoch} \tag{4.4.21}$$

where

$I_H stoch = -\sqrt{\lambda_1 S}dW_2 + \sqrt{f_2}dW_4 - \sqrt{(1-\varepsilon_1)\,D_H I_H}dW_5 - \sqrt{(1-\varepsilon_2)\,\sigma T_{HB}}dW_6$
$- \sqrt{\lambda_1 S + \lambda_3 S - \theta_1\pi}dW_7$

$$A(t+\Delta t) = A(t) + ((1-\varepsilon_1)\,D_H I_H - (\delta_1+\mu)\,A)\,\Delta t - \sqrt{(1-\varepsilon_1)\,D_H I_H}dW_5 + \sqrt{f_3}dW_8 \tag{4.4.22}$$

$$I_{HB}(t+\Delta t) = I_{HB}(t) + ((1-\rho)\pi + \lambda_3 S + v\lambda_4 V_H + \lambda_4 I_H + \lambda_5 I_B - (\phi+\gamma+\mu)I_{HB})\,\Delta t + I_{HB}stoch \tag{4.4.23}$$

where

$I_{HB}stoch = \sqrt{f_4}dW_9 - \sqrt{\phi I_{HB}}dW_{10} - \sqrt{\gamma I_{HB}}dW_{11} - \sqrt{v\lambda_4 V_H}dW_{12} - \sqrt{\lambda_5 I_B}dW_{13}$

$$T_{HB}(t+\Delta t) = T_{HB}(t) + (\phi I_{HB} - (\mu+\delta_3+(1-\varepsilon_2)\,\sigma)\,T_{HB})\,\Delta t + T_{HB}stoch \tag{4.4.24}$$

where

$T_{HB}stoch = -\sqrt{(1-\varepsilon_2)\,\sigma T_{HB}}dW_6 - \sqrt{\phi I_{HB}}dW_{10} + \sqrt{f_5}dW_{14}$

$$I_{HcB}(t+\Delta t) = I_{HcB}(t) + (\gamma I_{HB} - \mu + \delta_4 I_{HcB})\,\Delta t + I_{HcB}stoch \tag{4.4.25}$$

where

$I_{HcB}stoch = -\sqrt{\gamma I_{HB}}dW_{11} + \sqrt{f_6}dW_{15}$

$$V(t+\Delta t) = V(t) + (\theta_3\pi - (\mu + \Gamma\lambda_1)V)\,\Delta t + V\text{stoch} \tag{4.4.26}$$

where

$Vstoch = -\sqrt{v\lambda_4 V_H}dW_{12} + \sqrt{\mu V + \Gamma\lambda_1 V}dW_{16} + \sqrt{f_7}dW_{17}$

$$V_H(t+\Delta t) = V_H(t) + (\theta_4\pi + \Gamma\lambda_1 V - (\mu + v\lambda_4)V_H)\,\Delta t + \text{ VHstoch} \tag{4.4.27}$$

where

$V_H \text{ stoch } = -\sqrt{\Gamma\lambda_1 V}dW_{18} + \sqrt{\Gamma\lambda_1 V}dW_{19} + \sqrt{\theta_4\pi + \mu V_H}dW_{20}$

$$I_B(t+\Delta t) = I_B(t) + (\theta_2\pi + \lambda_2 S - (\mu + \lambda_5 + \alpha + \tau + \psi D_B)I_B)\,\Delta t + I_B \text{ stoch} \tag{4.4.28}$$

where

$I_B stoch = -\sqrt{\lambda_1 S + \lambda_3 S}dW_{21} + \sqrt{\theta_1\pi}dW_{22} - \sqrt{\lambda_5 I_B}dW_{13} + \sqrt{f_8}dW_{23}$

$-\sqrt{\psi D_B I_B}dW_{24} - \sqrt{\tau I_B}dW_{25} - \sqrt{\alpha I_B}dW_{26}$

$$I_{cB}(t+\Delta t) = I_{cB}(t) + (\psi D_B I_B - (\mu + \delta_2)I_{cB})\,\Delta t + I_{cB} \text{ stoch} \tag{4.4.29}$$

where

$I_{cB} \text{ stoch } = -\sqrt{\psi D_B I_B}dW_{24} + \sqrt{f_9}dW_{27}$

$$T_B(t+\Delta t) = T_B(t) + (\tau I_B - (\mu + \delta_3 + (1-\varepsilon_2)\varphi)T_B)\,\Delta t + T_B \text{ stoch} \tag{4.4.30}$$

where

$T_B stoch = -\sqrt{\tau I_B}dW_{25} + \sqrt{f_{10}}dW_{28} - \sqrt{(1-\varepsilon_2)\varphi T_B}dW_{29}$

$$R(t+\Delta t) = R(t) + (\alpha I_B + (1-\varepsilon_2)\varphi T_B - (\omega + \mu)R)\,\Delta t + \text{ Rstoch} \tag{4.4.31}$$

where

$\text{Rstoch } = -\sqrt{\omega R}dW_3 - \sqrt{\alpha I_B}dW_{26} - \sqrt{(1-\varepsilon_2)\varphi T_B}dW_{29} + \sqrt{f11}dW_{30}$

In simulating these SDEs, we apply the Euler-Maruyama method, which takes into account the stochastic terms to approximate the system's behavior over time. These simulations

are helpful in studying the impact of stochasticity on co-infection dynamics and the uncertainty associated with model predictions. The same parameter values given in table 4.1 are used but the initial conditions are estimated for small populations.

4.10.4 Numerical simulation of SDEs

Both deterministic solution and sample paths of SDEs related to infectious classes I_H, A, I_B, I_{cB}, I_{HB}, and I_{HcB} are demonstrated in figure 4.24 to 4.30. Individual trajectories for each SDE are produced and compared to its deterministic trajectory. Three sample paths of the SDEs are obtained to illustrate the range of variability of infections. The sample paths follow a property of the Wiener process that despite not being differentiable, the sample paths are continuous. The discretizations of the SDEs using Euler-Maruyama are implemented in MATLAB (R2017a). The MATLAB program for simulating SDEs is found in appendix C.

Figure 4.24 below demonstrates the deterministic solution of $I_H(t)$ for a period of one year together with three sample paths of $I_H(t)$ for the same initial condition of $I_H(t)$, and parameter values remain constant.

Figure 4.24
Deterministic and stochastic solution of $I_H(t)$

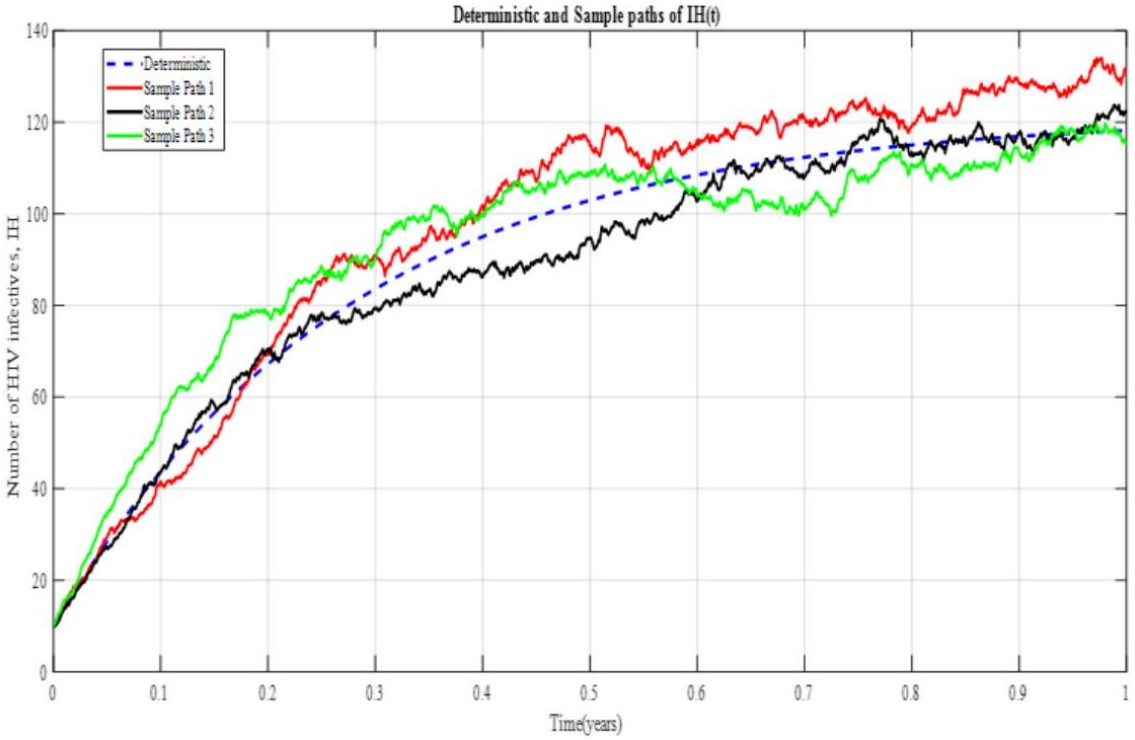

Source: Researcher (2025)

From figure 4.24 above, it is observed that the sample paths oscillate around the deterministic solution. The random fluctuations are as a result of diffusion terms associated with Wiener processes dW_2, dW_4, dW_5, dW_6 and dW_7. The range of volatility is shown by sample path 1 and 2. The variance between the deterministic and stochastic solution is close. Sample 3 shows the smallest variability in the infections while sample path 1 shows the highest variability of infections. The data statistics for each of the solution path is summarized in table 4.7 below;

Table 4.7
Data statistics for deterministic and sample paths of $I_H(t)$

Path	I_{Hin}	I_{Hmax}	Mean	Range
S1	10	134	97.62	124
S2	10	123.8	88.93	113.8
S3	10	119.7	93.63	109.7
Deterministic	10	118.2	91.27	108.2

Source: Researcher (2025)

Figure 4.25 shows the deterministic and stochastic solutions of $A(t)$ for a period of one year.

Figure 4.25

Deterministic and stochastic solution for $A(t)$

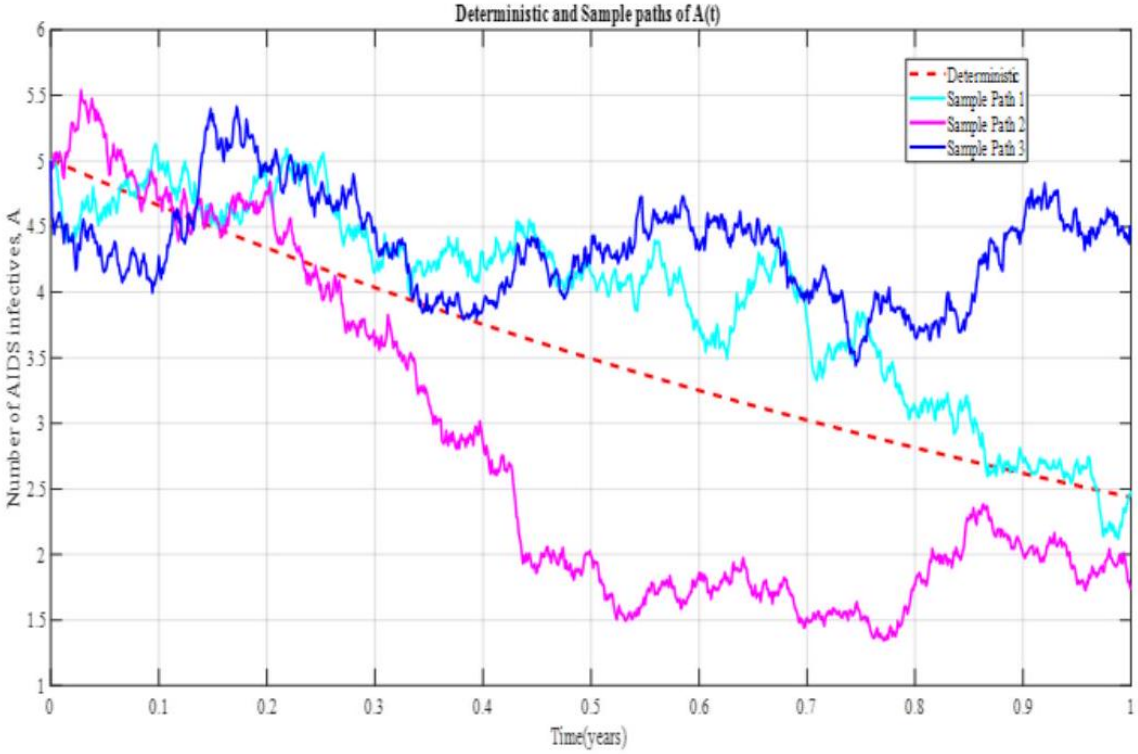

Source: Researcher (2025)

In deterministic solution, the AIDS infective drops gradually following a smooth trajectory assuming no random fluctuations over time. Because of regular ARVs usage and initiatives to lower the number of new infections, the viral load has decreased, resulting in this exponential decay. Each of the sample paths of $A(t)$ shows large variations from deterministic trajectory due to changes in random shocks dW_5 and dW_8. Sample path 2 shows the highest variability in infection outcomes while sample path 3 shows the lowest variations in infection outcomes as summarized in table 4.8 below;

Table 4.8

Data statistics for deterministic and sample paths of $A(t)$

Path	$A_{\min}$	$A_{\max}$	Mean	Range
S1	2.12	5.128	3.965	3.008
S2	1.347	5.539	2.815	4.291
S3	3.442	5.414	4.345	1.972
Deterministic	2.437	5.006	3.57	2.57

Source: Researcher (2025)

Figure 4.26 illustrates the dynamics of $I_B(t)$ over time in both deterministic and stochastic

perspectives. Three sample paths are considered for the stochastic case and data statistics compared in both cases.

Figure 4.26
Deterministic and stochastic solution for $I_B(t)$

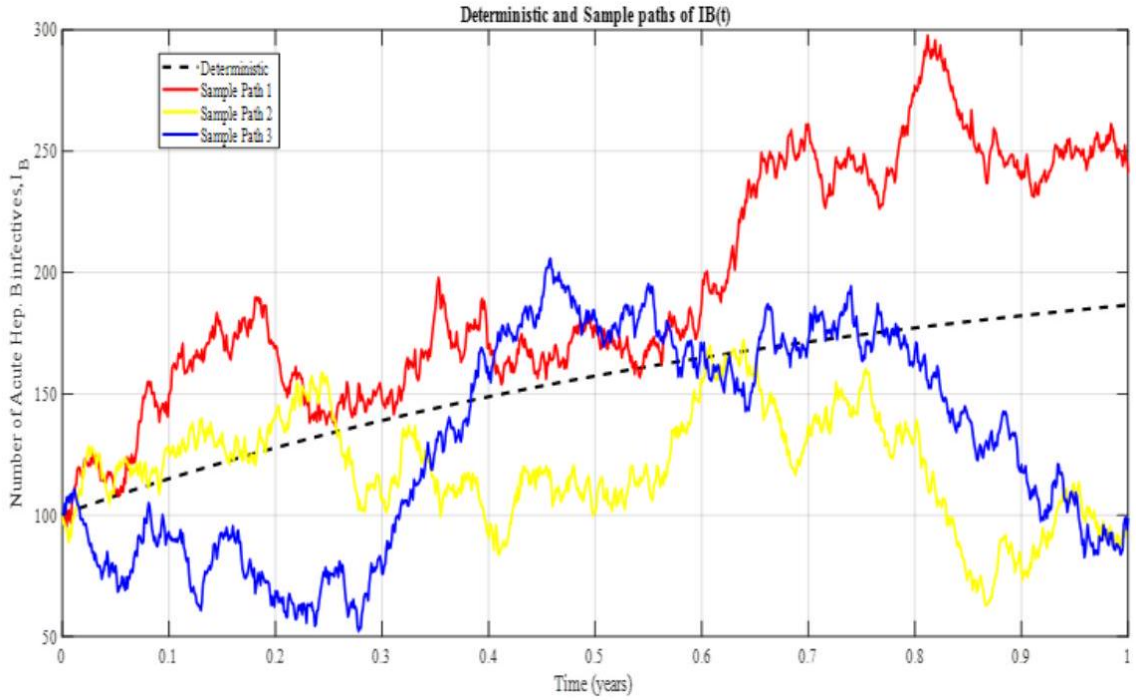

Source: Researcher (2025)

In deterministic case, $I_B(t)$ increases over time, indicating a growing population of $I_B(t)$ This trend is attributed by rate of new infections exceeding the rate of acute Hep B infective recovery or mortality. While in stochastic case, three sample paths display random fluctuations about the deterministic trajectory. Sample path 1 exhibit the largest variations in infections while sample path 2 shows the smallest variations in infections. These variations result from changes in Wiener processes $dW_{13}, dW_{21}, dW_{22}, dW_{23}, dW_{24}, dW_{25}$ and dW_{26}. The descriptive statistics for each of the sample paths of $I_B(t)$ are tabulated as follows;

Table 4.9
Data statistics for deterministic and sample paths of $I_B(t)$

Path	$IB_{\min}$	$IB_{\max}$	Mean	Range
S1	95.16	297.6	193.4	202.4
S2	62.8	172.1	119.7	109.3
S3	52.29	205.7	130.1	153.4
Deterministic	100	186.6	152.8	86.59

Source: Researcher (2025)

Figure 4.27 shows the deterministic and stochastic dynamic behaviour of $I_{HB}(t)$ with time.

Figure 4.27
Deterministic and stochastic solution for $I_{HB}(t)$

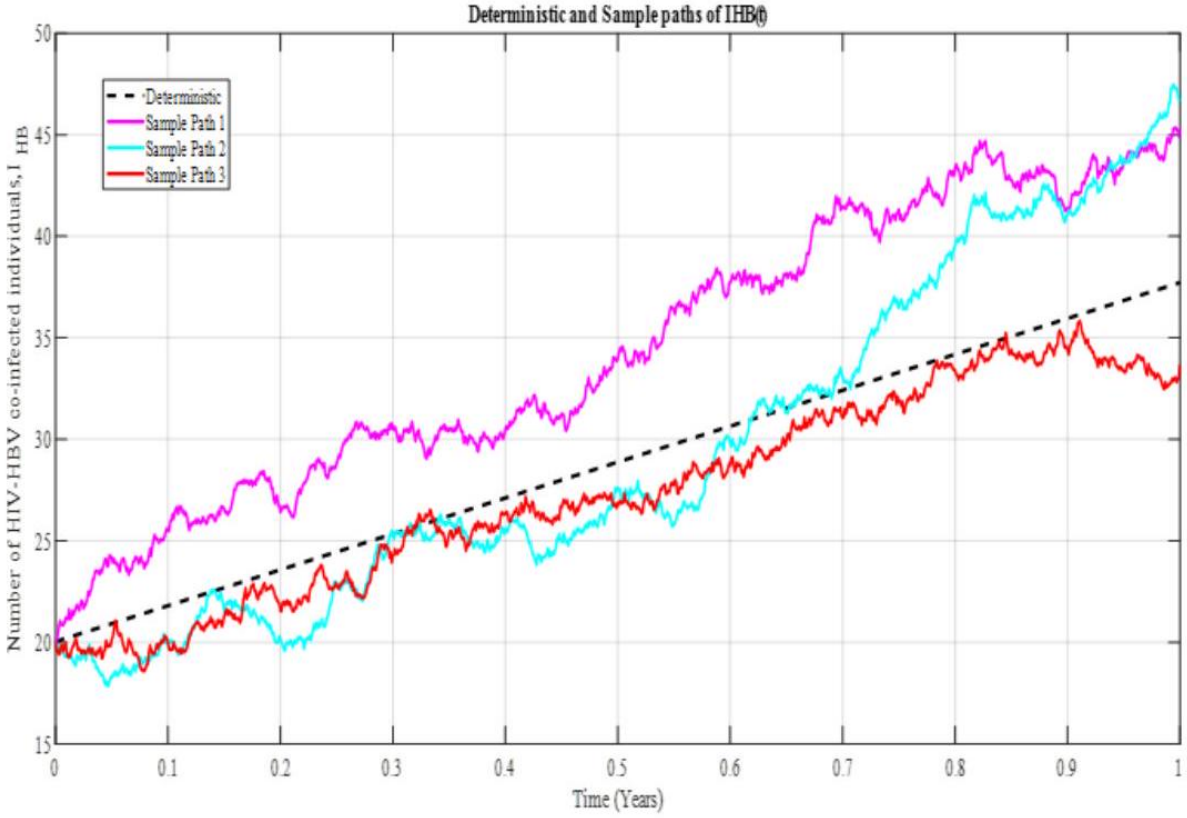

Source: Researcher (2025)

It is observed that $I_{HB}(t)$ grows linearly in deterministic case with time due to increase in transmission rates,progression rates and interactions between HIV and HBV infective. The stochastic solution is demonstrated by three different sample paths with different realization of infection outcomes around the deterministic path. Sample path 1 shows the largest variability while sample path 3 exhibits the smallest variability of infection outcomes.

Table 4.10
Data statistics for deterministic and sample paths of $I_{HB}(t)$

Path	I_{HBmin}	I_{HBmax}	Mean	Range
S1	19.97	45.35	34.41	25.37
S2	17.88	47.46	29.36	29.58
S3	18.6	35.81	27.38	17.21
Deterministic	20	37.72	28.88	17.72

Source: Researcher (2025)

Figure 4.28 shows the deterministic trajectory and stochastic sample paths for $I_{HcB}(t)$ for a period of one year.

Figure 4.28
Deterministic and stochastic solution for $I_{HCB}(t)$

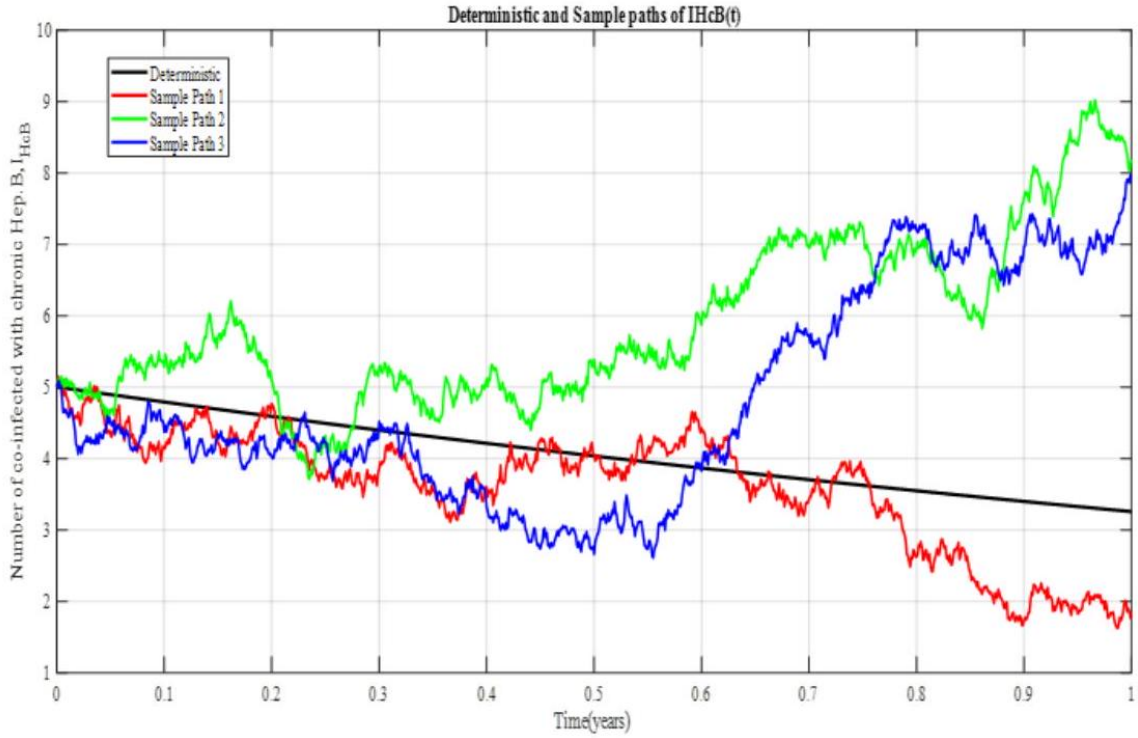

Source: Researcher (2025)

In figure 4.28, it is observed that the number of $I_{HcB}(t)$ infective declines with time in deterministic case. This trend is due to slow rate of new HIV and HBV infections as well as high treatment rates of people co-infected with HIV and HBV. In stochastic solution, the magnitude and direction of random fluctuations vary among the sample paths representing the Wiener processes dW_{11} and dW_{15}.

Figure 4.29 depicts the deterministic and sample paths of $I_{cB}(t)$ for a span of one year.

Table 4.11

Data statistics for deterministic and sample paths of $I_{HcB}(t)$

Path	I_{HcB} min	I_{HcB} max	Mean	Range
S1	1.625	5.147	3.604	3.522
S2	3.716	9.018	5.89	5.303
S3	2.614	7.971	4.82	5.357
Deterministic	3.256	5	4.067	1.744

Source: Researcher (2025)

Figure 4.29

Deterministic and sample paths for $IcB(t)$

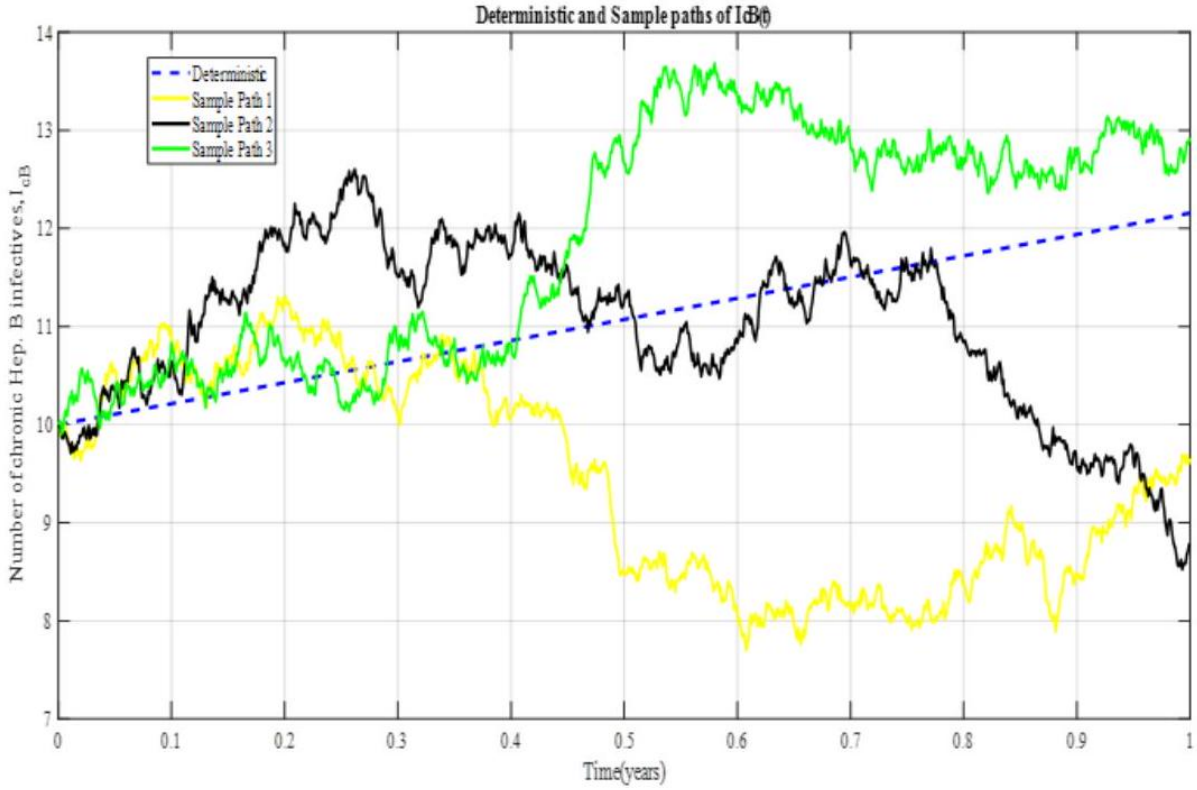

Source: Researcher (2025)

From figure 4.29 above, it is noted that the number of individuals with chronic viral hepatitis B increases with time due to increase in progression rate, compromised natural immunity, low treatment seeking behaviour of acute hepatitis B infective or even low transmission rates of HIV-HBV co-infection. The Wiener processes dW_{24} and dW_{27} influence the random fluctuations of infections around the deterministic smooth trajectory. The magnitude and direction of random fluctuations vary with the sample paths with sample path 1 exhibiting the largest variation in infection and sample path 3 showing the smallest variations.

Figure 4.30 illustrates the deterministic and stochastic sample paths of $T_{HB}(t)$ for one year.

Table 4.12

Data statistics for deterministic and sample paths of $IcB(t)$

Path	I_{cB} min	I_{cB} max	Mean	Range
S1	7.967	11.3	9.444	3.607
S2	8.525	12.6	11	4.074
S3	9.904	13.68	11.88	3.777
Deterministic	10	12.6	11.07	21.56

Source: Researcher (2025)

Figure 4.30

Deterministic and sample paths for $T_{HB}(t)$

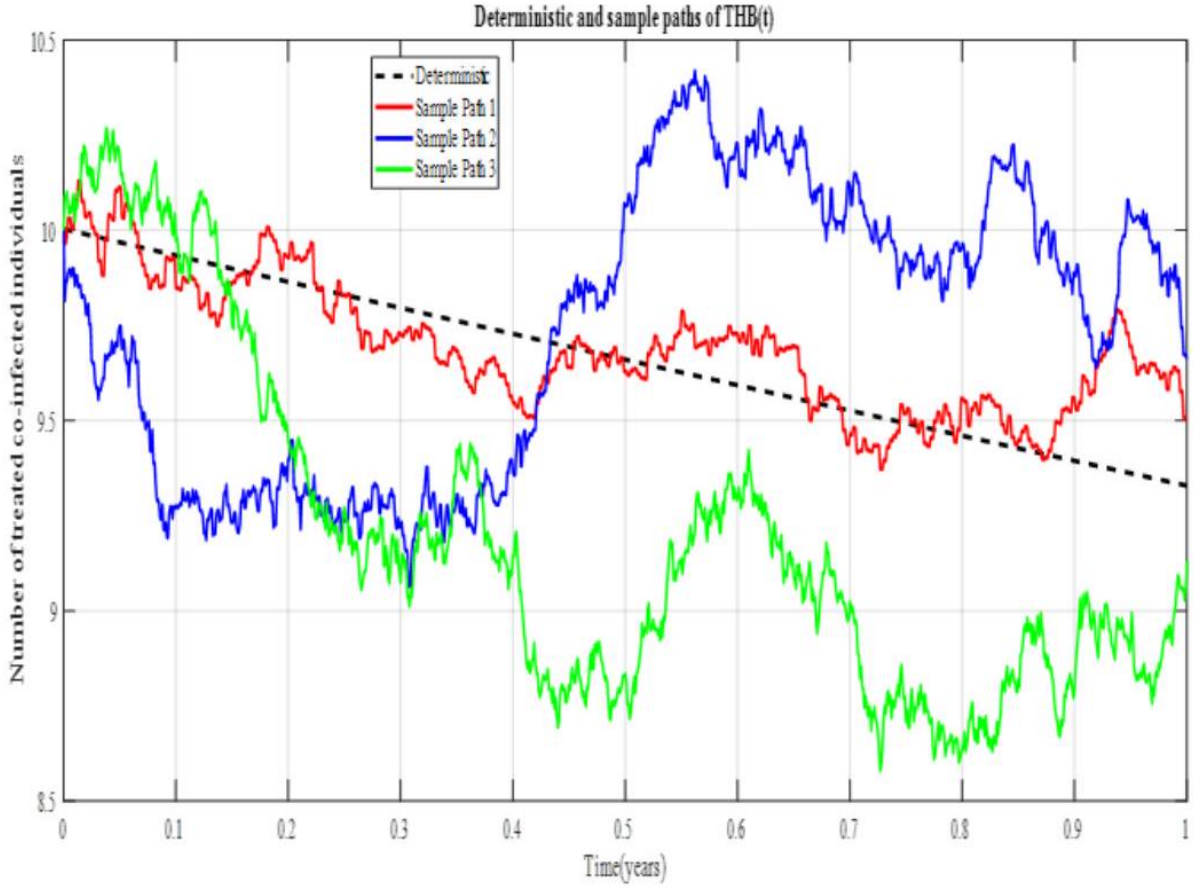

Source: Researcher(2025)

In deterministic case, the number of treated co-infected people decreases over time due to induced deaths due to adverse effects of HIV-HBV drugs, HIV reinfection, natural deaths as opposed to low treatment rates of co-infected individuals. However, the number of co-infected people receiving treatment fluctuates about the deterministic path for each of the sample paths. This demonstrates that the solution paths are not converging or absorbing to infection free equilibrium point. The variability is visualized from the following data statistics for the solution paths. Sample path 3 gives the highest variability while sample

path 1 gives the lowest.

Table 4.13
Data statistics for deterministic and sample paths of $T_{HB}(t)$

Path	T_{HB} min	T_{HB} max	Mean	Range
S1	9.373	10.13	9.689	0.7555
S2	9.064	10.42	9.742	1.354
S3	8.582	10.27	9.192	1.685
Deterministic	9.329	10	9.662	0.6737

Source: Researcher (2025)

CHAPTER FIVE: CONCLUSION, RECOMMENDATIONS AND PUBLICATIONS

5.1 Conclusion

This section highlight the conclusions drawn from the findings for each of the objectives.

5.1.1 Deterministic co-infection model

A deterministic co-infection model of HIV-HBV is first formulated in this study. The model incorporates vertical transmission of both HIV and HBV as risk factors, and the control measures such as treatment and vaccination. Effect of natural immunity and viral load saturation is also explored in the model. The model was analyzed based on reproduction numbers. The basic reproduction R_0 was computed using two methods; Next Generation matrix and survival function method. The methods yielded distinct values. Complexities in computing R_0 using NGM for a complex system such as a co-infection model involves a cumbersome process. In this case Gaussian Elimination method was employed to obtain the eigenvalues of the Jacobian matrix. Both techniques yielded a value less than unity an indication that the co-infection can be contained. However, in our case, the complex eigenvalues of the Jacobian matrix are ignored which depicts oscillations in co-infection about the equilibrium point. Moreover, the strength number A_0 was found to be negative depicting a possible complexity in the co-infection. This parameter has not be explored in many epidemic models, thus remains under investigation.

5.1.2 Stability analysis of co-infection free equilibrium point

Routh-Hurwitz criterion and numerical simulations showed that CFE point was locally asymptotically stable (LAS). This is an indication that in the presence of control interventions, the co-infection returns to co-infection -free equilibrium state. In addition, by use of Metzler matrix, the infection free equilibrium point was globally asymptotically stable.

This is an indication that across the entire feasible region, the population can be sustained at infection free state under both clinical and non-clinical control interventions. However, under varying control conditions, it was determined that there is a distinct and positive endemic co-infection equilibrium point, although explicit expressions of endemic states was not tenable. This reflects the persistence and complex nature of the co-infection in the population. By Center manifold theorem, it was found that the co-infection model exhibited a backward bifurcation suggesting that, in the absence of control efforts, eradicating the co-infection is impossible whenever $R_B^* < 1$.

Local sensitivity analysis of the model parameters yielded both positive and negative sensitivity indices. The sensitivity indices for R_{0N}, R_{0S} and A_0, revealed that an increase in co-infection rate, β_3 and recruitment rate, π, increases the basic reproduction and strength numbers. In the same breadth, an increase in the treatment rate, screening rate and natural immunity reduces the basic reproduction and strength numbers.

The effect of viral load saturation on HIV, HBV and co-infection outcomes was investigated. The three cases were considered independently. The impact of changing D_H and D_B as well as a case investigation of HIV viral load D_H and HBV viral load D_B was assessed. The relationship between increased infection outcomes and elevated HIV and HBV viral loads underscores the critical role of viral load management in the clinical care and prevention of HIV-HBV co-infection. Effective management strategies aimed at reducing viral loads can contribute to better disease control, improved quality of life, and reduced morbidity and mortality in infected individuals. The observed dynamics underscore the importance of both treatment and prevention strategies, including ART for HIV, antiviral treatment for HBV, and hepatitis B vaccination, in managing and controlling HIV-HBV co-infection. The findings of the study will inform public health policies and interven-

tions that will eventually lessen the global burden of co-infection and improve the overall well-being of people who are affected by the diseases. The impact of vertical transmission highlighted complex interplay in shaping the dynamics of HBV infection, HIV infection, and co-infection with HIV and HBV. The analysis i figure 4.7 showed that an increase in the proportion of co-infected births, ρ, leads to a decrease in the number of co-infected individuals. Developing and implementing effective prevention and control measures and understanding these dynamics is vital in mitigating the burden of these infections on public health. Without effective prevention measures targeting transmission routes, such as sexual behavior interventions and hepatitis B vaccination programs, the burden of these infections remains stable or decreases over time in populations where transmission is limited. The effect of treatment rates on co-infection dynamics showed that increasing the treatment rate, ϕ, increases the population of treated co-infected people at constant drug efficacy. Thus, increasing HIV and HBV drug efficacy, increases the number of treated co-infected individuals. The combination of clinical and non-clinical strategies, including ART, vaccination programs, health education, and stigma reduction, contributes to the decline in the prevalence of HIV, HBV, and co-infection over time. This suggests that comprehensive and integrated approaches are effective in controlling and preventing the spread of HIV, HBV, and co-infection, leading to improved public health outcomes.

The variation of natural immunity showed that increasing the natural immunity reduces the number of co-infected individuals. This because natural immunity plays a significant role in shaping the dynamics of HIV-HBV co-infection by influencing susceptibility, transmission dynamics, disease severity, vaccination strategies, and the effectiveness of public health interventions. Developing comprehensive strategies for the prevention, diagnosis, and treatment of co-infection is essential to understanding its effects on population dynam-

ics.

5.1.3 Optimal control model

Secondly, we formulated an optimal control problem using PMP by incorporating five controls related to clinical and non-clinical control interventions. From the numerical simulations, we found that effective preventative measures are essential for lowering the prevalence of HIV infection and co-infection in the general population, highlighting the importance of continued investment in prevention efforts. Optimal treatment control requires a comprehensive approach that includes early diagnosis, screening access to appropriate medical care, and ongoing treatment management. By addressing these factors, a stable or declining burden of both HIV-HBV co-infections and acute HBV infections over time can be achieved, enhancing public health outcomes in the long run and decreasing the population's exposure to these illnesses. The decrease in HIV-infected individuals and the AIDS population is attributed to the effectiveness of ART and comprehensive HIV management strategies. ART suppresses viral replication, slowing down HIV spread and reducing mortality rates. Strategies like early identification, ART initiation, treatment adherence, and support programs are crucial.

It is also evident from the results, that Increasing Hepatitis B dose vaccination increases the number of vaccinated births as well as treated co infected individuals. Thus, birth dose vaccination is an effective strategy for preventing mother-to-child transmission of hepatitis B, especially in HIV-exposed infants. In addition, increased awareness, integration of vaccination programs and improved coverage contribute to the gradual increase in vaccinated individuals. Effective management strategies for acute hepatitis B, including early diagnosis, supportive care, antiviral therapy, and regular monitoring, reduce the number of individuals requiring active treatment, promoting faster symptom resolution,

shorter infection duration, and increased spontaneous recovery rates. This approach reduces the burden of hepatitis B on affected individuals and healthcare systems. Integrated control measures targeting both HIV and HBO infections, including sexual contact control, vaccination control, treatment control, and recovery rate control, are highly effective in reducing the burden of HIV and HBV co-infections. The study suggests that integrated control measures targeting HIV and HBV infections, such as prevention control, vaccination, treatment, and recovery rate control, effectively reduce the burden of co-infections. These measures prevent new infections, suppress viral loads, enhance immune responses, and improve health outcomes. The gradual decrease in co-infection burden highlights the importance of comprehensive infection control.

5.1.4 Stochastic model

Finally, the deterministic model is converted to stochastic model by formulating SDEs. Numerical simulations using Euler-Maruyama method showed that stochastic processes introduce variability into the dynamics of infectious disease dynamics, leading to deviations from the deterministic solution. The sample paths oscillate around the deterministic solution over time, a characteristic behavior due to the interplay between deterministic and random forces. Sample paths showed varying levels of variability in each case. Stochastic models can incorporate parameter uncertainty, for instance, random variation in transmission rates, contact patterns, that deterministic models cannot. Thus, randomness in transmission of HIV-HBV co-infection cannot be ignored in mitigation measures.

5.2 Recommendations

This section state both policy and further research recommendations.

5.2.1 Policy recommendations

The study suggests the following recommendations; efforts towards maximizing combined clinical and non-clinical control interventions should be tailored to help lessen the rate of HIV and HBV infection, particularly in isolated areas. These include improved prevention strategies, including promoting safe sexual behaviors and campaigns geared towards Hepatitis B vaccination access, and comprehensive treatment approaches. Emphasizes should also be given to the importance of addressing HIV-related stigma and promoting health education in educational institutions, thereby reducing new infections among the teenagers and the youth. It also suggests enhanced public health policies informed by sensitivity analyses of most sensitive parameters to the model threshold parameter R_0 and optimization of control strategies; prevention, vaccination, treatment, and recovery rate control. In order to control and manage HIV-HBV co-infection, public health interventions and policy decisions should focus on efforts to reduce the co-infection and recruitment rates, while maximizing treatment seeking behaviour and screening the susceptible population. Knowing how different parameters affect the basic reproduction and strength number is an important consideration to policy makers that will create focused plans to stop further transmission of HIV and HBV infection and improve the well-being of communities. There is also need to develop a policy on prevention, treatment and control of dual infection. The implementation of the vaccination strategy yielded 67.12% reduction in co-infected population. Thus, the government through the Ministry of Health, should strengthen the implementation of universal Hepatitis birth dose vaccination for all newborns. Increase access to screening and treatment for HIV and HBV mono-infections should be encouraged. Moreover, knowledge on HIV-HBV co-infection should be enhanced especially among the populations at high risk. Further, efforts to mount strong natural immunity should be ad-

vocated for. Finally, stochasticity in infectious disease models cannot be ignored since it captures real-world variability and uncertainty. For this realization, regular research and monitoring of infection dynamics are also recommended.

5.2.2 Future research work

Future research work in this area may consider a triple co-infection with HIV, HBV and TB or malaria. Vaccination of adult population, mass screening of susceptible populations for hepatitis *B* infection and progression of chronic hepatitis *B* case to cancer stage may be included in the model. Population resistance to HIV and HBV antiretroviral therapy may also be considered. Higher order numerical schemes such as Milstein can be used to solve stochastic differential equations.

5.3 Publications

James, M. K., Ngari, C. G., Karanja, S., & Muriungi, R. (2025). Mathematical modeling and simulation of hepatitis B transmission dynamics with passive immunity and control strategies. Heliyon, 11(2), e41744. https://doi.org/10.1016/j.heliyon.2025.e41744.

James, M. K., Ngari, C. G., Karanja, S., & Muriungi, R. (2023). Stochastic Modelling, Analysis and Simulation of HIV-HBV Co-infection Using SDEs and Euler-Maruyama numerical Scheme. MUST Journal of ICT, 1(1).http://41.89.229.67/index.php/mustic/article/view/15.

James, M. K., Ngari, C. G., Karanja, S., & Muriungi, R. (2024). Modeling HIV-HBV Co-infection Dynamics: Stochastic Differential Equations and Matlab Simulation with Euler-Maruyama Numerical Method. Asian Research Journal of Mathematics, 20(7), 49–69. https://doi.org/10.9734/arjom/2024/v20i7811.

REFERENCES

Abatenh, E., Asmamaw, A., Hiluf, L., & Mohammed, N. (2018). Hepatitis b co-infection in hiv aids patients in woldia, ethiopia. *Biomedical Journal of Scientific & Technical Research*, *10*(3), 43–46.

Abbas, Z., & Abbas, M. (2021). Challenges in formulation and implementation of hepatitis b elimination programs. *Cureus*, *13*(4).

Agarwal, P., Nieto, J. J., Ruzhansky, M., Torres, D. F., et al. (2021). *Analysis of infectious disease problems (covid-19) and their global impact*. Springer.

Aghdaoui, H., Alaoui, A. L., Nisar, K. S., & Tilioua, M. (2021). On analysis and optimal control of a seiri epidemic model with general incidence rate. *Results in Physics*, *20*, 103681.

Akinsola, V. (2023). Numerical methods: Euler and runge-kutta. In *Qualitative and computational aspects of dynamical systems.* IntechOpen.

Akinyi, O. C., Mugisha, J., Manyonge, A., Ouma, C., & Maseno, K. (2013). Modelling the impact of misdiagnosis and treatment on the dynamics of malaria concurrent and co-infection with pneumonia. *Applied Mathematical Sciences*, *7*(126), 6275–6296.

Ali, M. A., Means, S., Ho, H., & Heffernan, J. (2021). Global sensitivity analysis of a single-cell hbv model for viral dynamics in the liver. *Infectious Disease Modelling*, *6*, 1220–1235.

Allen, E. (2007). *Modeling with itô stochastic differential equations* (Vol. 22). Springer Science & Business Media.

Allen, K., Mesner, O., Ganesan, A., O'Bryan, T. A., Deiss, R. G., Agan, B. K., & Okulicz, J. F. (2015). Association between hepatitis b vaccine antibody response and cd4 reconstitution after initiation of combination antiretroviral therapy in hiv-infected persons. *BMC Infectious Diseases*, *15*, 1–6.

Allen, L. J. (2010). *An introduction to stochastic processes with applications to biology*. CRC press.

Allen, L. J. (2017). A primer on stochastic epidemic models: Formulation, numerical simulation, and analysis. *Infectious Disease Modelling*, *2*(2), 128–142.

Amponsah-Dacosta, E. (2021). Hepatitis b virus infection and hepatocellular carcinoma in sub-saharan africa: Implications for elimination of viral hepatitis by 2030? *World journal of gastroenterology*, *27*(36), 6025.

Amwata, L. M. (2015). *Mathematical modeling of hiv and malaria co-infection dynamics* (Unpublished doctoral dissertation). University of Nairobi.

Anderson, R., Medley, G., May, R., & Johnson, A. (1986). A preliminary study of the transmission dynamics of the human immunodeficiency virus (hiv), the causative agent of aids. *Mathematical Medicine and Biology: a Journal of the IMA*, *3*(4), 229–263.

Anderson, R. M. (1991). Populations and infectious diseases: ecology or epidemiology? *Journal of Animal Ecology*, *60*(1), 1–50.

Atangana, A., & İğret Araz, S. (2021). Advanced analysis in epidemiological modeling: Detection of wave. *medRxiv*, 2021–09.

Ayele, T. K., Goufo, E. F. D., & Mugisha, S. (2021). Mathematical modeling of hiv/aids with optimal control: A case study in ethiopia. *Results in Physics*, *26*, 104263.

Banerjee, S. (2021). *Mathematical modeling: models, analysis and applications*. Chapman and Hall/CRC.

Bassey, B. E. (2020). Optimal control dynamics: Multi-therapies with dual immune response for treatment of dual delayed hiv-hbv infections. *infection*, *2*, 17.

Bellini, C., Keiser, O., Chave, J.-P., Evison, J. M., Fehr, J., Kaiser, L., ... others (2009). Liver enzyme elevation after lamivudine withdrawal in hiv–hepatitis b virus co-infected patients: the swiss hiv cohort study. *HIV medicine*, *10*(1), 12–18.

Bert, F., Gualano, M. R., Biancone, P., Brescia, V., Camussi, E., Martorana, M., ... Siliquini, R. (2018). Cost-effectiveness of hiv screening in high-income countries: a systematic review. *Health Policy*, *122*(5), 533–547.

Beyrer, C. (2021). A pandemic anniversary: 40 years of hiv/aids. *The Lancet*, *397*(10290), 2142–2143.

Bodsworth, N. J., Cooper, D. A., & Donovan, B. (1991). The influence of human immunodeficiency virus type 1 infection on the development of the hepatitis b virus carrier

state. *Journal of Infectious Diseases*, *163*(5), 1138–1140.

Bonnet, F. D. (2010). *Option pricing using path integrals.* (Unpublished doctoral dissertation).

Bowong, S., & Kurths, J. (2010). Modelling tuberculosis and hepatitis b co-infections. *Mathematical Modelling of Natural Phenomena*, *5*(6), 196–242.

Boyd, A., Melin, P., & Lacombe, K. (2022). Co-infection with hepatitis b and d viruses in people living with hiv. *Hépato-Gastro & Oncologie Digestive*, *29*(1), 35–43.

Brauer, F., Castillo-Chavez, C., & Feng, Z. (2019). *Mathematical models in epidemiology* (Vol. 32). Springer.

Bruchfeld, J., Correia-Neves, M., & Källenius, G. (2015). Tuberculosis and hiv coinfection. *Cold Spring Harbor perspectives in medicine*, *5*(7), a017871.

Campos, C., Silva, C. J., & Torres, D. F. (2019). Numerical optimal control of hiv transmission in octave/matlab. *Mathematical and computational applications*, *25*(1), 1.

Carr, J. (2012). *Applications of centre manifold theory* (Vol. 35). Springer Science & Business Media.

Castillo-Chavez, C., & Song, B. (2004). Dynamical models of tuberculosis and their applications. *Math. Biosci. Eng*, *1*(2), 361–404.

Chen, C., Xiao, Y., et al. (2014). Modeling saturated diagnosis and vaccination in reducing hiv/aids infection. In *Abstract and applied analysis* (Vol. 2014).

Cheng, D., Hu, X., & Shen, T. (2010). Linearization of nonlinear systems. In *Analysis and design of nonlinear control systems* (pp. 279–313). Springer.

Chevaliez, S., Roudot-Thoraval, F., Hezode, C., Pawlotsky, J.-M., & Njouom, R. (2021). Performance of rapid diagnostic tests for hepatitis b surface antigen detection in serum or plasma. *Diagnostic Microbiology and Infectious Disease*, *100*(2), 115353.

Chitnis, N., Hyman, J. M., & Cushing, J. M. (2008). Determining important parameters in the spread of malaria through the sensitivity analysis of a mathematical model. *Bulletin of mathematical biology*, *70*, 1272–1296.

Ciupe, S. M., Ribeiro, R. M., Nelson, P. W., & Perelson, A. S. (2007). Modeling the mechanisms of acute hepatitis b virus infection. *Journal of theoretical biology*, *247*(1),

23–35.

DeJesus, E. X., & Kaufman, C. (1987). Routh-hurwitz criterion in the examination of eigenvalues of a system of nonlinear ordinary differential equations. *Physical Review A*, *35*(12), 5288.

Derouin, F., Lacroix, C., Brun-Pascaud, M., Chau, F., Sinet, M., Maslo, C., & Girard, P.-M. (1998). Animal models of co-infection. *Clinical microbiology and infection*, *4*(10), 559–562.

Diekmann, O., & Heesterbeek, J. (2000). Wiley series in mathematical and computational biology. *Mathematical epidemiology of infectious diseases: model building, analysis and interpretation. United States: John Wiley and Sons*.

Diekmann, O., Heesterbeek, J., & Roberts, M. G. (2010). The construction of next-generation matrices for compartmental epidemic models. *Journal of the royal society interface*, *7*(47), 873–885.

Ditlevsen, S., & Samson, A. (2013). Introduction to stochastic models in biology. *Stochastic biomathematical models: with applications to neuronal modeling*, 3–35.

Dixit, R. K., Dixit, A. K., & Pindyck, R. S. (1994). *Investment under uncertainty*. Princeton university press.

Downs, L. O., Campbell, C., Yonga, P., Ansari, M. A., Matthews, P. C., & Etyang, A. O. (2022). A systematic review of hepatitis b virus (hbv) prevalence and genotypes in kenya: Data to inform clinical care and health policy. *medRxiv*.

Ecology, P. (2013). *Density-dependent vs. frequency-dependent disease transmission.*

Edelstein-Keshet, L. (1988). Mathematical models in biology (vol. 46). *Philadelphia, PA: SIAM*.

Endashaw, E. E., Gebru, D. M., Alemneh, H. T., et al. (2022). Coinfection dynamics of hbv-hiv/aids with mother-to-child transmission and medical interventions. *Computational and Mathematical Methods in Medicine*, *2022*.

Endashaw, E. E., & Mekonnen, T. T. (2022). Modeling the effect of vaccination and treatment on the transmission dynamics of hepatitis b virus and hiv/aids coinfection. *Journal of Applied Mathematics*, *2022*.

Farman, M., Shehzad, A., Akgül, A., Baleanu, D., & Sen, M. D. l. (2023). Modelling and analysis of a measles epidemic model with the constant proportional caputo operator. *Symmetry*, *15*(2), 468.

Farnoosh, R., & Parsamanesh, M. (2017). Stochastic differential equation systems for an sis epidemic model with vaccination and immigration. *Communications in Statistics-Theory and Methods*, *46*(17), 8723–8736.

Feigin, V. L., Stark, B. A., Johnson, C. O., Roth, G. A., Bisignano, C., Abady, G. G., ... others (2021). Global, regional, and national burden of stroke and its risk factors, 1990–2019: a systematic analysis for the global burden of disease study 2019. *The Lancet Neurology*, *20*(10), 795–820.

Feldstein, L. R., Mariat, S., Gacic-Dobo, M., Diallo, M. S., Conklin, L. M., & Wallace, A. S. (2017). Global routine vaccination coverage, 2016. *Morbidity and mortality weekly report*, *66*(45), 1252.

Frigati, L. J., Ameyan, W., Cotton, M. F., Gregson, C. L., Hoare, J., Jao, J., ... others (2020). Chronic comorbidities in children and adolescents with perinatally acquired hiv infection in sub-saharan africa in the era of antiretroviral therapy. *The Lancet Child & Adolescent Health*, *4*(9), 688–698.

Gaff, H., & Schaefer, E. (2009). Optimal control applied to vaccination and treatment strategies for various epidemiological models. *Mathematical biosciences & engineering*, *6*(3), 469.

Gao, D.-p., & Huang, N.-j. (2018). Optimal control analysis of a tuberculosis model. *Applied Mathematical Modelling*, *58*, 47–64.

Gastanaduy, P. A., Redd, S. B., Clemmons, N. S., Lee, A. D., Hickman, C. J., Rota, P. A., & Patel, M. (2019). Manual for the surveillance of vaccine-preventable diseases. *Center for Disease Control and Prevention. https://www. cdc. gov/vaccines/pubs/surv-manual/chpt07-measles. html*.

Gitonga, N. C. (2017). *Modelling childhood pneumonia and its implications regarding its control using kenyan data* (Unpublished doctoral dissertation). Moi University.

Global hepatitis report 2022. (n.d.).

Goliber, T. (2002). The status of the hiv/aids epidemic in sub-saharan africa. *Population Reference Bureau*.

Gomero, B. (2012). Latin hypercube sampling and partial rank correlation coefficient analysis applied to an optimal control problem.

Gopalappa, C., Farnham, P. G., Chen, Y.-H., & Sansom, S. L. (2017). Progression and transmission of hiv/aids (path 2.0) a new, agent-based model to estimate hiv transmissions in the united states. *Medical Decision Making*, *37*(2), 224–233.

Hadziyannis, S. J., Papatheodoridis, G. V., Dimou, E., Laras, A., & Papaioannou, C. (2000). Efficacy of long-term lamivudine monotherapy in patients with hepatitis b e antigen–negative chronic hepatitis b. *Hepatology*, *32*(4), 847–851.

Han, L., Lou, J., Ruan, Y., & Shao, Y. (2008). The analysis of the hiv/aids mathematical model for the injection drug use population. *J Biomath*, *23*(3), 429–434.

Hassard, B., & Wan, Y. H. (1978). Bifurcation formulae derived from center manifold theory. *Journal of Mathematical Analysis and Applications*, *63*(1), 297–312.

Hatcher, R. A., Trussell, J., Stewart, F. H., Stewart, G. K., Kowal, D., Guest, F., ... Policar, M. S. (2015). Contraceptive technology. In *Contraceptive technology* (pp. 730–730).

Hethcote, H. W. (1988). Optimal ages of vaccination for measles. *Mathematical Biosciences*, *89*(1), 29–52.

Hethcote, H. W., & Levin, S. (1989). *Applied mathematical ecology.* Springer-Verlag Berlin, Heidelberg.

Hirsch, M. W., Smale, S., & Devaney, R. L. (2013). *Differential equations, dynamical systems, and an introduction to chaos*. Academic press.

Hitzer, E. M. (2002). Imaginary eigenvalues and complex eigenvectors explained by real geometry. In *Applications of geometric algebra in computer science and engineering* (pp. 145–155). Springer.

Ho, D. D. (1995). *Time to hit hiv, early and hard* (Vol. 333) (No. 7). Mass Medical Soc.

Hussien, H. H., Genawi, K. R., Hagabdulla, N. H., & Ahmed, K. M. (2025). Understanding the basic reproduction number (r0): Calculation, applications, and limitations in

epidemiology. *Open Journal of Epidemiology*, *15*(2), 272–295.

Hutin, Y., Nasrullah, M., Easterbrook, P., Dongmo Nguimfack, B., Burrone, E., Averhoff, F., & Bulterys, M. (2018). *Access to treatment for hepatitis b virus infection—worldwide, 2016* (Vol. 18) (No. 10). Wiley Online Library.

Hyams, K. C. (1995). Risks of chronicity following acute hepatitis b virus infection: a review. *Clinical Infectious Diseases*, *20*(4), 992–1000.

Inoue, T., & Tanaka, Y. (2016). Hepatitis b virus and its sexually transmitted infection-an update. *Microbial cell*, *3*(9), 420.

James, J. Y., Garba, I. A.-k., Habila, M., & Bororo, A. (2022). A deterministic mathematical model and analysis of the transmission dynamics of hepatitis b virus in nigeria. *ResearchJet Journal of Analysis and Inventions*, *3*(03), 51–77.

James, M. (2019). Sustainable development in kenya. *Horizons: Journal of International Relations and Sustainable Development*(13), 172–183.

Joshi, H. R., Lenhart, S., Li, M. Y., & Wang, L. (2006). Optimal control methods applied to disease models. *Contemporary Mathematics*, *410*, 187–208.

Kamyad, A. V., Akbari, R., Heydari, A. A., & Heydari, A. (2014). Mathematical modeling of transmission dynamics and optimal control of vaccination and treatment for hepatitis b virus. *Computational and mathematical methods in medicine*, *2014*.

Kapur, J. N. (2023). Mathematical modeling.

Kenya, L. o. K. (2013). *The constitution of kenya: 2010*. Chief Registrar of the Judiciary.

Kermack, W. O., & McKendrick, A. G. (1927). A contribution to the mathematical theory of epidemics. *Proceedings of the royal society of london. Series A, Containing papers of a mathematical and physical character*, *115*(772), 700–721.

Kim, H. N. (2020). Chronic hepatitis b and hiv coinfection: a continuing challenge in the era of antiretroviral therapy. *Current hepatology reports*, *19*(4), 345–353.

Koethe, J. R., Lagathu, C., Lake, J. E., Domingo, P., Calmy, A., Falutz, J., ... Capeau, J. (2020). Hiv and antiretroviral therapy-related fat alterations. *Nature reviews Disease primers*, *6*(1), 48.

Kolokolnikov, T., & Iron, D. (2021). Law of mass action and saturation in sir model with

application to coronavirus modelling. *Infectious Disease Modelling*, *6*, 91–97.

Kotola, B. S., Teklu, S. W., & Abebaw, Y. F. (2023). Bifurcation and optimal control analysis of hiv/aids and covid-19 co-infection model with numerical simulation. *Plos one*, *18*(5), e0284759.

Kourtis, A. P., Bulterys, M., Hu, D. J., & Jamieson, D. J. (2012). Hiv–hbv coinfection—a global challenge. *New England Journal of Medicine*, *366*(19), 1749–1752.

Landes, M., Newell, M.-L., Barlow, P., Fiore, S., Malyuta, R., Martinelli, P., ... others (2008). Hepatitis b or hepatitis c coinfection in hiv-infected pregnant women in europe. *HIV medicine*, *9*(7), 526–534.

Lasisi, N. O. (2020). Effect of public awareness, behaviours and treatment on infection-age-structured of mathematical model for hiv/aids dynamics. *Mathematical Models in Engineering*, *6*(2), 103–121.

Lecher, S. L., Fonjungo, P., Ellenberger, D., Toure, C. A., Alemnji, G., Bowen, N., ... others (2021). Hiv viral load monitoring among patients receiving antiretroviral therapy—eight sub-saharan africa countries, 2013–2018. *Morbidity and Mortality Weekly Report*, *70*(21), 775.

Lee, F. J., Amin, J., & Carr, A. (2014). Efficacy of initial antiretroviral therapy for hiv-1 infection in adults: a systematic review and meta-analysis of 114 studies with up to 144 weeks' follow-up. *PloS one*, *9*(5), e97482.

Lenhart, S., & Workman, J. T. (2007). *Optimal control applied to biological models*. Chapman and Hall/CRC.

Leumi, S., Bigna, J. J., Amougou, M. A., Ngouo, A., Nyaga, U. F., & Noubiap, J. J. (2020). Global burden of hepatitis b infection in people living with human immunodeficiency virus: a systematic review and meta-analysis. *Clinical infectious diseases*, *71*(11), 2799–2806.

Li, J., Blakeley, D., et al. (2011). The failure of ** 0. *Computational and mathematical methods in medicine*, *2011*.

Li, Y.-J., Wang, H.-l., & Li, T.-S. (2012). Hepatitis b virus/human immunodeficiency virus coinfection: interaction among human immunodeficiency virus infection, chronic

hepatitis b virus infection, and host immunity. *Chinese Medical Journal*, *125*(13), 2371–2377.

Longini Jr, I. M., Ackerman, E., & Elveback, L. R. (1978). An optimization model for influenza a epidemics. *Mathematical Biosciences*, *38*(1-2), 141–157.

Ma, J. (2020). Estimating epidemic exponential growth rate and basic reproduction number. *Infectious Disease Modelling*, *5*, 129–141.

Macías-Díaz, J. (2017). Existence and uniqueness of positive and bounded solutions of a discrete population model with fractional dynamics. *Discrete Dynamics in Nature and Society*, *2017*.

MacIndoe, E. (2019). Analysis of deterministic and stochastic hiv models.

Maliyoni, M., Chirove, F., Gaff, H. D., & Govinder, K. S. (2017). A stochastic tick-borne disease model: Exploring the probability of pathogen persistence. *Bulletin of mathematical biology*, *79*, 1999–2021.

Martcheva, M. (2015). *An introduction to mathematical epidemiology* (Vol. 61). Springer.

Matthews, P. C., Geretti, A. M., Goulder, P. J., & Klenerman, P. (2014). Epidemiology and impact of hiv coinfection with hepatitis b and hepatitis c viruses in sub-saharan africa. *Journal of clinical virology*, *61*(1), 20–33.

Mayaphi, S. H., Rossouw, T. M., Martin, D. J., Masemola, D. P., Olorunju, S. A., & Mphahlele, M. J. (2012). Hbv/hiv co-infection: the dynamics of hbv in south african patients with aids. *South African Medical Journal*, *102*(3), 157–162.

Mohareb, A. M., & Kim, A. Y. (2021). Hepatitis b vaccination in people living with hiv—if at first you don't succeed, try again. *JAMA network open*, *4*(8), e2121281–e2121281.

Mohareb, A. M., Kouamé, G. M., Gabassi, A., Gabillard, D., Moh, R., Badje, A., ... others (2021). Mortality in relation to hepatitis b virus (hbv) infection status among hiv-hbv co-infected patients in sub-saharan africa after immediate initiation of antiretroviral therapy. *Journal of viral hepatitis*, *28*(4), 621–629.

Moyare, F. M. (2012). *Challenges of implementing the kenya vision 2030* (Unpublished doctoral dissertation). University of Nairobi.

Mukandavire, Z., Gumel, A. B., Garira, W., & Tchuenche, J. M. (2009). Mathematical analysis of a model for hiv-malaria co-infection. *Mathematical Biosciences & Engineering*, *6*(2), 333.

Musafili, N., Hadisaputro, S., & Sofro, M. A. (2022). *Influence of epidemiological risk factors for occurrence of hepatitis b virus (hbv) coinfection in hiv/aids patients:(study in dr. kariadi hospital, semarang, indonesia)* (Unpublished doctoral dissertation). School of Postgraduate Studies.

Mushayabasa, S., Tchuenche, J. M., Bhunu, C. P., & Ngarakana-Gwasira, E. (2011). Modeling gonorrhea and hiv co-interaction. *BioSystems*, *103*(1), 27–37.

Mwenzwa, E. M., & Misati, J. A. (2014). Kenya's social development proposals and challenges: review of kenya vision 2030 first medium-term plan, 2008-2012.

Nagelkerke, N. J., De Vlas, S. J., Jha, P., Luo, M., Plummer, F. A., & Kaul, R. (2009). Heterogeneity in host hiv susceptibility as a potential contributor to recent hiv prevalence declines in africa. *AIDS (London, England)*, *23*(1), 125.

Nampala, H., Jablonska-Sabuka, M., & Singull, M. (2021). Mathematical analysis of the role of hiv/hbv latency in hepatocytes. *Journal of Applied Mathematics*, *2021*.

Nampala, H., Luboobi, L. S., Mugisha, J. Y., Obua, C., & Jablonska-Sabuka, M. (2018). Modelling hepatotoxicity and antiretroviral therapeutic effect in hiv/hbv coinfection. *Mathematical biosciences*, *302*, 67–79.

Nannyonga, B., Mugisha, J., & Luboobi, L. (2011). The role of hiv positive immigrants and dual protection in a co-infection of malaria and hiv/aids. *Applied Mathematical Sciences*, *5*(59), 2919–2942.

Neilan, R. M., & Lenhart, S. (2010). An introduction to optimal control with an application in disease modeling. In *Modeling paradigms and analysis of disease trasmission models* (pp. 67–81).

Nowak, M. A., & May, R. M. (1992). Coexistence and competition in hiv infections. *Journal of Theoretical Biology*, *159*(3), 329-342. Retrieved from https://www.sciencedirect.com/science/article/pii/S0022519305807283 doi: https://doi.org/10.1016/S0022-5193(05)80728

-3

Nthiiri, J. K., Lavi, G., & Manyonge, A. (2015). Mathematical model of pneumonia and hiv/aids coinfection in the presence of protection.

Okocha, E., Oguejiofor, O., Odenigbo, C., Okonkwo, U., & Asomugha, L. (2012). Prevalence of hepatitis b surface antigen seropositivity among hiv-infected and non-infected individuals in nnewi, nigeria. *Nigerian Medical Journal: Journal of the Nigeria Medical Association*, *53*(4), 249.

Okongo, W., Okelo Abonyo, J., Kioi, D., Moore, S. E., & Nnaemeka Aguegboh, S. (2024). Mathematical modeling and optimal control analysis of monkeypox virus in contaminated environment. *Modeling Earth Systems and Environment*, 1–26.

Olabode, D., Culp, J., Fisher, A., Tower, A., Hull-Nye, D., & Wang, X. (2021). Deterministic and stochastic models for the epidemic dynamics of covid-19 in wuhan, china. *Mathematical Biosciences and Engineering*, *18*(1), 950–967.

Ouaro, S., Traoré, A., et al. (2013). Deterministic and stochastic schistosomiasis models with general incidence. *Applied Mathematics*, *4*(12), 1682.

Owusu-Ansah, F. E., Addae, A. A., Amoah, C., Raman, A. A., Adjei, V. D., & Ohenewa, E. (2023). Knowledge and sexual behaviors: A path towards hiv/aids prevention among university students. *African journal of reproductive health*, *27*(9), 117–126.

Packer, A., Forde, J., Hews, S., & Kuang, Y. (2014). Mathematical models of the interrelated dynamics of hepatitis d and b. *Mathematical Biosciences*, *247*, 38–46.

Pappoe, F., Hagan, C. K. O., Obiri-Yeboah, D., & Nsiah, P. (2019). Sero-prevalence of hepatitis b and c viral infections in ghanaian hiv positive cohort: a consideration for their health care. *BMC infectious diseases*, *19*(1), 1–8.

Patil, A. (2021). Routh-hurwitz criterion for stability: an overview and its implementation on characteristic equation vectors using matlab. *Emerging Technologies in Data Mining and Information Security: Proceedings of IEMIS 2020, Volume 1*, 319–329.

Pontryagin, L. S. (1987). *Mathematical theory of optimal processes*. CRC press.

Powell, D. R., Fair, J., LeClaire, R. J., Moore, L. M., & Thompson, D. (2005). Sensitivity analysis of an infectious disease model. In *Proceedings of the international system*

dynamics conference.

Prussing, C., Chan, C., Pinchoff, J., Kersanske, L., Bornschlegel, K., Balter, S., ... Fuld, J. (2015). Hiv and viral hepatitis co-infection in new york city, 2000–2010: prevalence and case characteristics. *Epidemiology & Infection*, *143*(7), 1408–1416.

Radix, A., Gonzalez, C. J., & Hoffmann, C. J. (2022). Hiv testing. *MEDICAL CARE*, *2*.

Razavi-Shearer, D., Gamkrelidze, I., Nguyen, M. H., Chen, D.-S., Van Damme, P., Abbas, Z., ... others (2018). Global prevalence, treatment, and prevention of hepatitis b virus infection in 2016: a modelling study. *The lancet Gastroenterology & hepatology*, *3*(6), 383–403.

Ribeiro, C. R. d. A., Martinelli, K. G., de Mello, V. d. M., Baptista, B. d. S., Dias, N. S. T., Paiva, I. A., ... de Paula, V. S. (2020). Cytokine, genotype, and viral load profile in the acute and chronic hepatitis b. *Viral Immunology*, *33*(10), 620–627.

Ringa, N., Diagne, M., Rwezaura, H., Omame, A., Tchoumi, S., & Tchuenche, J. (2022). Hiv and covid-19 co-infection: A mathematical model and optimal control. *Informatics in Medicine Unlocked*, 100978.

Roeger, L.-I. W., Feng, Z., & Castillo-Chavez, C. (2009). Modeling tb and hiv co-infections. *Mathematical Biosciences & Engineering*, *6*(4), 815.

Sachs, J., Kroll, C., Lafortune, G., Fuller, G., & Woelm, F. (2022). *Sustainable development report 2022*. Cambridge University Press.

Saha, S., & Samanta, G. (2019). Modelling and optimal control of hiv/aids prevention through prep and limited treatment. *Physica A: Statistical Mechanics and its Applications*, *516*, 280–307.

Samsuzzoha, M., Singh, M., & Lucy, D. (2013). Uncertainty and sensitivity analysis of the basic reproduction number of a vaccinated epidemic model of influenza. *Applied Mathematical Modelling*, *37*(3), 903–915.

Sauer, T. (2011). Numerical solution of stochastic differential equations in finance. In *Handbook of computational finance* (pp. 529–550). Springer.

Schillie, S., Vellozzi, C., Reingold, A., Harris, A., Haber, P., Ward, J. W., & Nelson, N. P. (2018). Prevention of hepatitis b virus infection in the united states: recommenda-

tions of the advisory committee on immunization practices. *MMWR Recommendations and Reports*, *67*(1), 1.

Seidu, B., Makinde, O. D., et al. (2014). Optimal control of hiv/aids in the workplace in the presence of careless individuals. *Computational and mathematical methods in medicine*, *2014*.

Selvan, T. T., & Kumar, M. (2023). Dynamics of a deterministic and a stochastic epidemic model combined with two distinct transmission mechanisms and saturated incidence rate. *Physica A: Statistical Mechanics and its Applications*, *619*, 128741.

Shahriar, S., Araf, Y., Ahmad, R., Kattel, P., Sah, G. S., Rahaman, T. I., ... others (2022). Insights into the coinfections of human immunodeficiency virus-hepatitis b virus, human immunodeficiency virus-hepatitis c virus, and hepatitis b virus-hepatitis c virus: prevalence, risk factors, pathogenesis, diagnosis, and treatment. *Frontiers in microbiology*, *12*, 780887.

Shaw, C. L., & Kennedy, D. A. (2021). What the reproductive number r0 can and cannot tell us about covid-19 dynamics. *Theoretical Population Biology*, *137*, 2–9.

Singh, K. P., Crane, M., Audsley, J., & Lewin, S. R. (2017). Hiv-hepatitis b virus coinfection: epidemiology, pathogenesis and treatment. *AIDS (London, England)*, *31*(15), 2035.

Singh, K. P., & Lewin, S. R. (2020). *Hepatitis b infection in people living with human immunodeficiency virus: A global challenge needing more research* (Vol. 71) (No. 11). Oxford University Press US.

Siriprapaiwan, S., Moore, E. J., & Koonprasert, S. (2018). Generalized reproduction numbers, sensitivity analysis and critical immunity levels of an seqijr disease model with immunization and varying total population size. *Mathematics and computers in simulation*, *146*, 70–89.

Soares, A. L. O., & Bassanezi, R. C. (2020). Stability analysis of epidemiological models incorporating heterogeneous infectivity. *Computational and Applied Mathematics*, *39*, 1–20.

Spearman, C. W., Afihene, M., Ally, R., Apica, B., Awuku, Y., Cunha, L., ... others

(2017). Hepatitis b in sub-saharan africa: strategies to achieve the 2030 elimination targets. *The lancet gastroenterology & hepatology*, *2*(12), 900–909.

Spradling, P., Richardson, J., Buchacz, K., Moorman, A., Brooks, J., & Investigators, H. O. S. H. (2010). Prevalence of chronic hepatitis b virus infection among patients in the hiv outpatient study, 1996–2007. *Journal of viral hepatitis*, *17*(12), 879–886.

Sun, H.-Y., Sheng, W.-H., Tsai, M.-S., Lee, K.-Y., Chang, S.-Y., & Hung, C.-C. (2014). Hepatitis b virus coinfection in human immunodeficiency virus-infected patients: a review. *World journal of gastroenterology: WJG*, *20*(40), 14598.

Teklu, S. W., & Mekonnen, T. T. (2021). Hiv/aids-pneumonia coinfection model with treatment at each infection stage: mathematical analysis and numerical simulation. *Journal of Applied Mathematics*, *2021*.

Thio, C. L. (2009). *Hepatitis b and human immunodeficiency virus coinfection.* LWW.

Van den Driessche, P., & Watmough, J. (2002). Reproduction numbers and sub-threshold endemic equilibria for compartmental models of disease transmission. *Mathematical biosciences*, *180*(1-2), 29–48.

Vinothini, P., & Kavitha, K. (2020). A review on fuzzy mathematical modeling in biology. *Adv. Math. Sci. J*, *9*(8), 5987–5996.

Volinsky, I. (2022). Mathematical model of hepatitis b virus treatment with support of immune system. *Mathematics*, *10*(15), 2821.

Wang, Y., Liu, J., & Liu, L. (2016). Viral dynamics of an hiv model with latent infection incorporating antiretroviral therapy. *Advances in Difference Equations*, *2016*, 1–15.

Wangari, I. M., Davis, S., & Stone, L. (2016). Backward bifurcation in epidemic models: Problems arising with aggregated bifurcation parameters. *Applied Mathematical Modelling*, *40*(2), 1669–1675.

Whalley, S. A., Murray, J. M., Brown, D., Webster, G. J., Emery, V. C., Dusheiko, G. M., & Perelson, A. S. (2001). Kinetics of acute hepatitis b virus infection in humans. *The Journal of experimental medicine*, *193*(7), 847–854.

World Health Organization. (2017). Prevention, control, and management of hepatitis b: Guidelines for healthcare providers. Retrieved from

https://www.who.int/hepatitis/publications/prevention-hepatitis-b-guidelines/en/

World Health Organization. (2022). Aids statistics—fact sheet| unaids (2021). *Dostopno na: https://www. unaids. org/en/resources/fact-sheet. Pridobljeno*.

World Health Organization. (2024). *Global hepatitis report 2024: Action for access in low- and middle-income countries*. World Health Organization.

World Health Organization and others. (2017). *Global hepatitis report 2017*. World Health Organization.

World Health Organization and others. (2020). Training modules on hepatitis b and c screening, diagnosis and treatment.

World Health Organization and others. (2021). Global progress report on hiv, viral hepatitis and sexually transmitted infections, 2021: accountability for the global health sector strategies 2016–2021: actions for impact: web annex 2: data methods.

Yu, S., Yu, C., Li, J., Liu, S., Wang, H., & Deng, M. (2020). Hepatitis b and hepatitis c prevalence among people living with hiv/aids in china: a systematic review and meta-analysis. *Virology journal*, *17*(1), 1–10.

Yusuf, T. T., & Idisi, O. I. (2020). Modelling the transmission dynamics of hiv and hbv coepidemics: analysis and simulation. *Mathematical Theory and Modeling*, *10*(2), 48–77.

Zaongo, S. D., Ouyang, J., Chen, Y., Jiao, Y.-M., & Wu, H. (2022). Hiv infection predisposes to increased chances of hbv infection: Current understanding of the mechanisms favoring hbv infection at each clinical stage of hiv infection. *Frontiers in Immunology*, *13*, 853346–853346.

APPENDICES

Appendix A: Matlab program for numerical solution of deterministic model

This appendix is related to section 4.2.3.1 to 4.2.3.17.

```
function dy=JAMES(t,y)
global pi mu psi delta1 delta2 delta3 delta4 alpha gamma rho
phi theta1 theta2 theta3 theta4 theta5 epsilon1 epsilon2 sigma
omega varphi tau Gamma nu lambda1 lambda2 lambda3 lambda4 lambda5
DH DB
% model parameters
pi=50000000;mu=0.00911;delta1=0.7114;delta2=0.0028;delta3=0.0284;
delta4=0.42;alpha=0.95; gamma=0.2;rho=0.116;phi=0.17;DH=5;DB=1;
Gamma = 0.22;theta1 = 0.875;theta2 = 0.058;theta3 = 0.18;
theta 4 = 0.45; theta5 = 0.14319; epsilon1=0.5; epsilon2=0.7;
tau=0.25; sigma=0.81; beta1=0.09; beta2=0.2; beta3=0.074;
beta4=0.1; beta5=0.075; varphi=0.2493; nu=0.08; omega=0.012;
psi=0.05;
%Model equations
%S=y(1),IH=y(2), A=y(3), IHB=y(4), THB=y(5), IHcB=y(6), V=y(7),
VH=y(8), IB=y(9), IcB=y(10), TB=y(11), R=y(12)
%N =y(1)+y(2)+y(3)+y(4)+y(5)+y(6)+y(7)+y(8)+y(9)+y(10)+y(11)+y(12)
pi=b*N,rho=theta1+theta2+theta3+theta4+theta5,
lambda1=beta1 *(IH+eta1IHB+eta2IHcB+eta3A+eta4THB),
lambda2=beta2*(IB+chi1IcB+chi2IHB+chi3IHcB+chi4TB+chi5THB),
lambda3=beta3*(IHB+Psi1IHcB+Psi2THB),
lambda4=beta5(IH+Lambda1IHB+Lambda2IHcB+Lambda3A
+Lambda4THB+Lambda5VH)
lambda5=beta5(IB+varepsilon1IHB+varepsilon2IcB
    +varepsilon3IHcB+varepsilon4TB+varepsilon5THB)
dy(1)=theta5*pi-(lambda1+lambda2+lambda3+mu)*y(1)-omega*y(12);
```

```
dy(2)=theta1 *pi+lambda1 *y(1)+(1-epsilon2)*sigma*y(5)
     -(lambda4 +mu+(1-epsilon1)*DH)*y(2);
dy(3)=(1-epsilon1)*DH*y(2)-(delta1+mu)*y(3);
dy(4)=(1-rho)*pi+lambda3*y(1)+(y(2)+nu)*lambda4
     +lambda5*y(9)-(alpha+gamma+mu)*y(4);
dy(5)=phi*y(4)-(mu+delta3+(1-epsilon2)*sigma)*y(5);
dy(6)=gamma*y(4)-(mu+delta4)*y(6);
dy(7)=theta3*pi-(mu+Gamma*lambda1)*y(7);
dy(8)=theta4*pi+Gamma*lambda1*y(7)-(mu+nu*lambda4)*y(8);
dy(9)=theta2*pi+lambda2*y(1)-(mu+lambda5+alpha+tau+psi*DB)*y(9);
dy(10)=psi*DB*y(9)-(mu+delta2)*y(10);
dy(11)=tau*y(9)-(mu+delta3+(1-epsilon2)*varphi)*y(11);
dy(12)=alpha*y(9)+(1-epsilon2)*varphi*y(11)-(omega+mu)*y(12);
    dy=dy';
    %This is a function file(Main file)
```

Appendix B: Matlab program for optimal control model

```
This appendix is related to section 4.3.3
function y=jamo(pi,mu,psi,delta1,delta2,delta3,delta4,alpha,gamma,
rho,phi,DH,DB, Gamma,theta1,theta2,theta3,theta4,epsilon1,epsilon2,
tau,sigma,lambda1,lambda2,lambda3,lambda4,lambda5,
varphi,nu,omega,Psi,u1,u2,u3,u4,u5, A1,A2,A3,A4,A5,A6,A7,A8,A9,B1,
B2,B3,B4,B5,S0,IH0,A0, IHB0,THB0,IHcB0,
V0,VH0,IB0,IcB0,TB0,R0,N,tfinal);
test = -1;
delta = 0.001;
M = 1000;
t=linspace(0,tfinal,M+1);
h=tfinal/M; %h=tfinal/M;
h2 = h/2;
% The initial guess for the state variables
S0=zeros(1,M+1);
IH0=zeros(1,M+1);
A0=zeros(1,M+1);
IHB0=zeros(1,M+1);
THB0 =zeros(1,M+1);
IHcB0=zeros(1,M+1);
V0=zeros(1,M+1);
VH0=zeros(1,M+1);
IB0=zeros(1,M+1);
IcB0=zeros(1,M+1);
TB0=zeros(1,M+1);
R0=zeros(1,M+1);
%======= The Initial conditions==========
S(1)=S0; IH(1)=IH0; A(1)=A0; IHB(1)=IHB0;
```

```
THB(1)=THB0; IHcB(1)=THB0; V(1)=V0;
VH(1)=VH0 ; IB(1)=IB0; IcB(1)=IcB0;
TB(1)=TB0; R(1)=R0;
%========== Non-trivial vector=========
P1=zeros(1,M+1);
P2=zeros(1,M+1);
    P3=zeros(1,M+1);
    P4=zeros(1,M+1);
    P5=zeros(1,M+1);
    P6=zeros(1,M+1);
    P7=zeros(1,M+1);
    P8=zeros(1,M+1);
    P9=zeros(1,M+1);
    %=============== The controls==========
    ul=zeros(1,M+1);
    u2=zeros(1,M+1);
    u3=zeros(1,M+1);
    u4=zeros(1,M+1);
    u5=zeros(1,M+1);
    while(test < 0)
    oldu1 = u1; oldu2 = u2; oldu3 = u3; oldu4 = u4; oldu5 = u5;
    oldS=S; oldIH=IH; oldA=A; oldIHB=IHB; oldTHB=THB; oldIHcB=IHcB;
    oldV=V; oldVH=VH; oldIB=IB; oldIcB=IcB; oldTB=TB; oldR=R;
    oldP1 = P1; oldP2 = P2; oldP3= P3; oldP4 = P4;
    oldP5 = P5; oldP6 = P6; oldP7 = P7; oldP8 = P8; oldP9 = P9;
    %========= Runge-Kutta Forward sweep solver ======
    for i = 1:M
    m11= theta5*pi-((1-u1(i))*(lambda1+lambda2+lambda3+mu))*S(i)
        -omega*R(i);
```

```
    m12= theta1 *pi+(1-u1(i))*lambda1 *S(i)
        +(1-epsilon2)*sigma*THB(i)
        -(lambda4+mu+(1-u3(i))*(1-epsilon1)*DH)*IH(i);
    m13=(1-u3(i))*(1-epsilon1)*DH*IH(i)-(delta1+mu)*A(i);
    m14=(1-rho)*pi+(1-u1(i))*lambda3*S(i)
        +((1-u1(i))*IH(i)+nu)*lambda4
        +(1-u1(i))*lambda5*TB(i)
-((1-u2(i))*phi+(1-u3(i))*gamma+mu)*IHB(i);
m15=(1-u2(i))*phi*IHB(i)-(mu+delta3+(1-epsilon2)*sigma)*THB(i);
m16=(1-u3(i))*gamma*IHB(i)-(mu+delta4)*IHcB(i);
m17=(1-u4(i))*theta3*pi-(mu+Gamma*lambda1)*V(i);
m18=(1-u4(i))*theta4*pi+Gamma*lambda1*V(i)-(mu+nu*lambda4)*VH(i);
m19=theta2*pi+(1-u1(i))*lambda2*S(i)-(mu+(1-u1(i))*lambda5+alpha+
(1-u2(i))*tau+(1-u3(i))*psi*DB)*IB(i);
m20=(1-u3(i))*psi*DB*IB(i)-(mu+delta2)*IcB(i);
m21=(1-u2(i))*tau*IB(i)-(mu+delta3+(1-epsilon2)*varphi)*TB(i);
m22=alpha*y(9)+(1-u5(i))*(1-epsilon2)*varphi*TB(i)-(omega+mu)*R(i);
%===============second forward sweep====================
m24=theta5*pi-((1-0.5*(u1(i)+u1(i+1))*(lambda1+lambda2
    +lambda3+mu)))*(S(i)+h2*m11)
    -omega*(R(i)+h2*m22);
m25= theta1 *pi+(1-0.5*(u1(i)+u1(i+1))*lambda1*(S(i)+h2*m11)
+(1-epsilon2)*sigma*(THB(i)+h2*m15))-(lambda4+mu+
(1-0.5*(u3(i)+u3(i+1)))*(1-epsilon1)*DH)*(IH(i)+h2*m12);
m26=(1-0.5*(u3(i)+u3(i+1))*(1-epsilon1)*DH*(IH(i)+h2*m12))-
(delta1+mu)*(A(i)+h2*m13);
m27=(1-rho)*pi+(1-0.5*(u1(i)+u1(i+1))*lambda3*(S(i)+h2*m11))+
((1-0.5*(u1(i)+u1(i+1))))*(IH(i)+h2*m12)+nu*lambda4
+(1-0.5*(u1(i)+u1(i+1))*lambda5*(TB(i)+h2*m21))-(1-u2(i)*phi+
```

```
(1-0.5*(u3(i)+u3(i+1))*gamma+mu))*(IHB(i)+h2*m14);
m28=(1-0.5*(u2(i)+u2(i+1))*phi*(IHB(i)+h2*m14))-
(mu+delta3+(1-epsilon2)*sigma)*(THB(i)+h2*m15);
m29=(1-0.5*(u3(i)+u3(i+1))*gamma*(IHB(i)+h2*m14))-
(mu+delta4)*(IHcB(i)+h2*m16);
m30=(1-0.5*(u4(i)+u4(i+1)))*theta3*pi
    -(mu+Gamma*lambda1)*(V(i)+h2*m17);
m31=(1-0.5*(u4(i)+u4(i+1)))*theta4*pi+Gamma*lambda1*(V(i)
    +h2*m17)-(mu+nu*lambda4)*(VH(i)+h2*m18);
m32=theta2*pi+(1-0.5*(u1(i)+u1(i+1)))*lambda2*(S(i)+h2*m11)
    -(mu+(1-0.5*(u1(i)+u1(i+1))))*lambda5
    +alpha+(1-0.5*(u2(i)+u2(i+1)))*tau
    +(1-0.5(u3(i)+u3(i+1))*psi*DB)*(IB(i)+h2*m19);
m33=(1-0.5*(u3(i)+u3(i+1)))*psi*DB*(IB(i)+h2*m19)
    -(mu+delta2)*(IcB(i)+h2*m20);
m34=(1-0.5*(u2(i)+u2(i+1)))*tau*(IB(i)+h2*m19)-
    (mu+delta3+(1-epsilon2)*varphi)*(TB(i)+h2*m21);
m35=alpha*(IB(i)+h2*m19)+(1-0.5*(u5(i)+u5(i+1)))*
    (1-epsilon2)*varphi*(TB(i)
    +h2*m21)-(omega+mu)*(R(i)+h2*m22);
%==================================================
m37=theta5*pi-(1-0.5(u1(i)+u1(i+1)))*lambda1+lambda2+lambda3+mu)*
    (S(i)+h2*m24)-omega*(R(i)+h2*m35);
m38= theta1 *pi+(1-0.5*(u1(i)+u1(i+1))*lambda1*(S(i)+h2*m24)+
    (1-epsilon2)*sigma*(THB(i)+h2*m28)-(lambda4+mu+
    (1-0.5*(u3(i)+u3(i+1)))*(1-epsilon1)*DH)*(IH(i)+h2*m25);
m39=(1-0.5*(u3(i)+u3(i+1))*(1-epsilon1)*DH*(IH(i)+h2*m25)-
    (delta1+mu)*(A(i)+h2*m26);
m40=(1-rho)*pi+(1-0.5*(u1(i)+u1(i+1))*lambda3*(S(i)+h2*m24)+
```

```
    ((1-0.5*(u1(i)+u1(i+1))*(IH(i)+h2*m25)+nu)*lambda4
    +(1-0.5*(u1(i)+u1(i+1))*lambda5*(TB(i)+h2*m34)-
    ((1-u2(i))*phi+(1-0.5*(u3(i)+u3(i+1))*gamma+mu)*(IHB(i)+h2*m27);
m41=(1-0.5*(u2(i)+u2(i+1))*phi*(IHB(i)+h2*m27)-
    (mu+delta3+(1-epsilon2)*sigma)*(THB(i)+h2*m28);
m42=(1-0.5*(u3(i)+u3(i+1))*gamma*(IHB(i)+h2*m27)-
    (mu+delta4)*(IHcB(i)+h2*m29);
m43=(1-0.5*(u4(i)+u4(i+1))*theta3*pi
    -(mu+Gamma*lambda1)*(V(i)+h2*m30);
m44=(1-0.5*(u4(i)+u4(i+1))*theta4*pi+Gamma*lambda1*(V(i)+h2*m30)
    -(mu+nu*lambda4)*(VH(i)+h2*m31);
m45=theta2*pi+(1-0.5*(u1(i)+u1(i+1))*lambda2*(S(i)+h2*m24)
    -(mu+(1-0.5*(u1(i)+u1(i+1))*lambda5
    +alpha+(1-0.5*(u2(i)+u2(i+1))*tau
    +(1-0.5*(u3(i)+u3(i+1))*psi*DB)*(IB(i)+h2*m32);
m46=(1-0.5*(u3(i)+u3(i+1))*psi*DB*(IB(i)+h2*m32)
    -(mu+delta2)*(IcB(i)+h2*m33);
m47=(1-0.5*(u2(i)+u2(i+1))*tau*(IB(i)+h2*m32)
    -(mu+delta3+(1-epsilon2)*varphi)*(TB(i)+h2*m34);
m48=alpha*(IB(i)+h2*m32)+(1-0.5*(u5(i)+u5(i+1))*
    (1-epsilon2)*varphi*(TB(i)
    +h2*m34)-(omega+mu)*(R(i)+h2*m35);
%===============Forth forward sweep=================
m50=theta5*pi-((1-0.5*(u1(i)
    +u1(i+1))*(lambda1+lambda2+lambda3+mu))*(S(i)
    +h2*m37)-omega*(R(i)+h2*m48);
m51= theta1 *pi+(1-0.5*(u1(i)+u1(i+1))*lambda1*(S(i)+h2*m37)
(1-epsilon2)*sigma*(THB(i)+h2*m41)-(lambda4+mu+
(1-0.5*(u3(i)+u3(i+1)))*(1-epsilon1)*DH)*(IH(i)+h2*m38);
```

```
m52=(1-0.5*(u3(i)+u3(i+1))*(1-epsilon1)*DH*(IH(i)+h2*m38)-
(delta1+mu)*(A(i)+h2*m39);
m53=(1-rho)*pi+(1-0.5*(u1(i)+u1(i+1))*lambda3*(S(i)+h2*m37)+
((1-0.5*(u1(i)+u1(i+1))*(IH(i)+h2*m38)+nu)*lambda4
+(1-0.5*(u1(i)+u1(i+1))*lambda5*(TB(i)+h2*m47)-((1-u2(i))*phi+
(1-0.5*(u3(i)+u3(i+1))*gamma+mu)*(IHB(i)+h2*m40);
m54=(1-0.5*(u2(i)+u2(i+1))*phi*(IHB(i)+h2*m40)-
(mu+delta3+(1-epsilon2)*sigma)*(THB(i)+h2*m41);
m55=(1-0.5*(u3(i)+u3(i+1))*gamma*(IHB(i)+h2*m40)-
(mu+delta4)*(IHcB(i)+h2*m42);
m56=(1-0.5*(u4(i)+u4(i+1))*theta3*pi
    -(mu+Gamma*lambda1)*(V(i)+h2*m43);
m57=(1-0.5*(u4(i)+u4(i+1))*theta4*pi+Gamma*lambda1*(V(i)
    +h2*m43)-(mu+nu*lambda4)*(VH(i)+h2*m44);
m58 &= \theta2 \pi + \left(1 - 0.5 \cdot (u1(i)
    + u1(i+1))\right) \cdot \text{lambda2} \cdot (S(i)
    + \text{h2} \cdot m37)  - \left( \mu
    + \left(1 - 0.5 \cdot (u1(i) + u1(i+1))\right)
    \cdot \text{lambda5} + \text{alpha}
    + \left(1 - 0.5 \cdot (u2(i) + u2(i+1))\right)
    \cdot \text{tau} \right \left + \left(1 - 0.5
    \cdot (u3(i) + u3(i+1))\right)
    \cdot \text{psi} \cdot \text{DB} \right)
    \cdot (IB(i) + \text{h2} \cdot m45); \\
m59 &= \left(1 - 0.5 \cdot (u3(i) + u3(i+1))\right)
    \cdot \text{psi} \cdot \text{DB}
    \cdot (IB(\text{h2} \cdot m45) \\&\quad
    - (\mu +\text{delta2}) \cdot (IcB(i)
    + \text{h2} \cdot m46); \\
```

```
m60 &= \left(1 - 0.5 \cdot (u2(i) + u2(i+1))\right)
    \cdot \text{tau} \cdot (IB(i) + \text{h2}
    \cdot m45) \\&\quad - \left( \mu + \text{delta3}
    +(1 - \text{epsilon2})\cdot \text{varphi} \right)
    \cdot (TB(i) + \text{h2} \cdot m47); \\
m61 &= \text{alpha} \cdot (IB(i) + \text{h2}
    \cdot m43) + \left(1 - 0.5 \cdot (u5(i) + u5(i+1))\right)
    \cdot (1 - \text{epsilon2})
    \cdot \text{varphi} \cdot (TB(i) +\text{h2}
    \cdot m47) - (\text{omega} + \mu)
    \cdot (R(i) + \text{h2} \cdot m48); \\
S(i+1) &= S(i) + (h/6) \cdot (m11 + 2
    \cdot m24 + 2 \cdot m37 + m50); \\
IH(i+1) &= IH(i) + (h/6) \cdot (m12 + 2
    \cdot m25 + 2 \cdot m38 + m51); \\
A(i+1) &= A(i) + (h/6) \cdot (m13 + 2
    \cdot m26 + 2 \cdot m39 + m52); \\
IHB(i+1) &= IHB(i) + (h/6) \cdot (m14 + 2
    \cdot m27 + 2 \cdot m40 + m53); \\
THB(i+1) &= THB(i) + (h/6) \cdot (m15 + 2
    \cdot m28 + 2 \cdot m41 + m54); \\
IHcB(i+1) &= IHcB(i) + (h/6) \cdot (m16 + 2
    \cdot m29 + 2 \cdot m42 + m55); \\
V(i+1) &= V(i) + (h/6) \cdot (m17 + 2
    \cdot m30 + 2 \cdot m43 + m56); \\
VH(i+1) &= VH(i) + (h/6) \cdot (m18 + 2
    \cdot m31 + 2 \cdot m44 + m57); \\
IB(i+1) &= IB(i) + (h/6) \cdot (m19 + 2
    \cdot m32 + 2 \cdot m45 + m58); \\
```

```
IcB(i+1) &= IcB(i) + (h/6) \cdot (m20 + 2
    \cdot m33 + 2 \cdot m46 + m59); \\
TB(i+1) &= TB(i) + (h/6) \cdot (m21 + 2
    \cdot m34 + 2 \cdot m47 + m60); \\
R(i+1) &= R(i) + (h/6) \cdot (m22 + 2
    \cdot m35 + 2 \cdot m48 + m61); \\
\end{aligned}
\begin{aligned}
&\text{\% ======= Runge-Kutta Backward sweep solver =====
&\text{for } i=1:M \\
&\quad j = M+2-i; \\
&\quad m11 = \left[ 2 \cdot \beta_{4} \cdot IH(j)
    + (1 - u3(j)) \cdot (1 - \epsilon_1) \cdot DH \right. \\
&\quad\quad - \left( \beta_{1} \cdot S(j) - u1(j)
    \cdot \beta_1 \cdot S(j) \right) \bigg] \cdot P1(j) \\
&\quad\quad - (1 - u3(j)) \cdot (1 - \epsilon_1)
    \cdot DH \cdot P2(j) \\
&\quad\quad - \left[ \left( 2 \cdot IH(j) \cdot (1 - u1(j))
+ \nu \right)\cdot \beta_4 \right]\cdot P3(j) \\
&\quad\quad + \left[ \nu \cdot \beta_4 \cdot VH(j)
    -\Gamma\cdot\beta_1\cdot V(j) \right]\cdot P6(j)- A_1;
m12 = (beta4*Lambda3*IH(j)-(1-u1(j))*beta1*eta3*S(j))*P1(j)
    +(delta1+mu)*P2(j)-((1-u1(j))*IH(j)+nu)*beta4*Lambda3*P3(j)
    -(Gamma*beta1*eta3*V(j)-nu*beta4*Lambda3*VH(j))*P6(j)-A2;
m13 =(beta4*Lambda1*IH(j)-(1-u1(j))*beta1*eta1*S(j))*P1(j)
    -((1-u1(j))*beta3*S(j)+((1-u1(j))*IH(j)+nu)*beta4*Lambda1
    -((1-u2(j))*phi+(1-u3(j))*gamma+mu)
    +(1-u1(j))*beta5*Upsilon1*IB(j))*P3(j)
    -(1-u2(j))*phi*P4(j)-(1-u3(j))*gamma*P5(j)
```

```
    -(Gamma*beta1*eta1*V(j)-nu*beta4*Lambda1*VH(j))*P6(j)
    -((1-u1(j))*beta2*chi2*S(j)
    -(1-u1(j))*beta5*Upsilon1*IB(j))*P7(j)-A3;
m14 = -((1-u1(j))*beta1 *eta4*S(j)+(1-epsilon2)*sigma
    -beta4*Lambda4*IH(j))*P1(j)
    -((1-u1(j))*beta3*Psi2*S(j)+((1-u1(j))*IH(j)+nu)*beta4
    *Lambda4+(1-u1(j))*beta5*Upsilon5*IB(j))*P3(j)
    +(mu+delta3+(1-epsilon2)*sigma)*P4(j)
    -(Gamma*beta1*eta4*V(j)-nu*beta4*Lambda4*VH(j))
    *P6(j)-((1-u1(j))*beta2*chi5*S(j)
    -(1-u1(j))*beta5*Upsilon5*IB(j))*P7(j)-A4;
m15 = -((1-u1)*beta1*eta2*S-beta4*Lambda2*IH)*P1
    -((1-u1)*beta3*Psi1 *S+((1-u1)*IH+nu)*beta4*Lambda2
    +(1-u1)*beta5*Upsilon3*IB)*P3+(mu+delta4)*P5
-(Gamma*beta1*eta2*V-nu*beta4*Lambda2*VH)*P6
    -((1-u1)*beta2*chi3*S-(1-u1)*beta5*Upsilon3*IB)*P7-A5;
m16 = beta4*Lambda5*P1-((1-u1)*IH +nu)*beta4*Lambda5*P3
    +(mu+nu*beta4*(IH+Lambda1*IHB+Lambda2*IHcB+Lambda3*A
    +Lambda4*THB+2*Lambda5*VH))*P6
    +(mu+(1-u1)*beta5*(2*IB+varUpsilon1*IHB+varUpsilon2*IcB
    +varUpsilon3*IHcB+varUpsilon4*TB+varUpsilon5*THB)
    +alpha+(1-u2)*tau+(1-u3)*psi*DB)*P7-A6;
m17 =-((1-u1)*beta2*S*(2*IB+chi1*IcB+chi2*IHB+chi3*IHcB+
chi4*TB+chi5*THB)-(mu+(1-u1)*beta5*(2*IB+varUpsilon1*IHB
+varUpsilon2*IcB+varUpsilon3*IHcB+varUpsilon4*TB
+varUpsilon5*THB)+alpha+(1-u2)*tau+(1-u3)*psi*DB))*P7
-(1-u1)*beta5(2*IB+varUpsilon1*IHB
+varUpsilon2*IcB+varUpsilon3*IHcB+varUpsilon4*TB
+varUpsilon5*THB)*P3-(1-u3)*psi*DB*P8
```

```
-(1-u2)*tau*P9-A7;
m18 =-(1-u1)*beta5*varUpsilon*2*IB*P3-((1-u1)*beta2*chi2*S
-(1-u1)*beta5*Upsilon2*IB)*P7+(mu+delta2)*P8-A8;
m19 =(mu+delta3+(1-epsilon2)*varphi)*P9
    -(1-u1)*beta5*varUpsilon4*IB*P3
    -((1-u1)*beta2*chi4*S-(1-u1)*beta5*Upsilon4*IB)*P7-A9;
%===============Second backward sweep=============
m21 =(2*beta4*IH(j)+(1-u3(j))*(1-epsilon1)*DH
    -(beta1*S(j)-u1(j)*beta1 *S(j)))*P1(j)
    -(1-u3(j))*(1-epsilon1)*DH*P2(j)
    -(2*IH(j)*(1-u1(j))+nu)*beta4*P3(j)
    +(nu*beta4*VH(j)-Gamma*beta1*V(j))*P6(j)-A1;
m22 = (beta4*Lambda3*IH(j)-(1u1(j))*beta1*eta3*S(j))*P1(j)
+(delta1+mu)*P2(j)-((1-u1(j))*IH(j)+nu)*beta4*Lambda3*P3(j)
-(Gamma*beta1*eta3*V(j)-nu*beta4*Lambda3*VH(j))*P6(j)-A2;
m23 =(beta4*Lambda1*IH(j)
    -(1-u1(j))*beta1*eta1*S(j))*P1(j)
    -((1-u1(j))*beta3*S(j)
    +((1-u1(j))*IH(j)+nu)*beta4*Lambda1
    -((1-u2(j))*phi+(1-u3(j))*gamma+mu)
    +(1-u1(j))*beta5*Upsilon1*IB(j))*P3(j)
    -(1-u2(j))*phi*P4(j)-(1-u3(j))*gamma*P5(j)
    -(Gamma*beta1*eta1*V(j)
    -nu*beta4*Lambda1*VH(j))*P6(j)
    -((1-u1(j))*beta2*chi2*S(j)
    -(1-u1(j))*beta5*Upsilon1 *IB(j))*P7(j)-A3;
m24 = -((1-u1(j))*beta1 *eta4*S(j)+(1-epsilon2)*sigma
    -beta4*Lambda4*IH(j))*P1(j)
    -((1-u1(j))*beta3*Psi2*S(j)
```

```
    +((1-u1(j))*IH(j)+nu)*beta4*Lambda4
    +(1-u1(j))*beta5*Upsilon5*IB(j))*P3(j)
    +(mu+delta3+(1-epsilon2)*sigma)*P4(j)
    -(Gamma*beta1*eta4*V(j)
    -nu*beta4*Lambda4*VH(j))*P6(j)
    -((1-u1(j))*beta2*chi5*S(j)
    -(1-u1(j))*beta5*Upsilon5*IB(j))*P7(j)-A4;
m25 = -((1-u1)*beta1*eta2*S-beta4*Lambda2*IH)*P1
    -((1-u1)*beta3*Psi1 *S
    +((1-u1)*IH+nu)*beta4*Lambda2
    +(1-u1)*beta5*Upsilon3*IB)*P3+(mu+delta4)*P5
    -(Gamma*beta1*eta2*V-nu*beta4*Lambda2*VH)*P6
-((1-u1)*beta2*chi3*S-(1-u1)*beta5*Upsilon3*IB)*P7-A5;
m26 = beta4*Lambda5*P1-((1-u1)*IH+nu)*beta4*Lambda5*P3
+(mu+nu*beta4*(IH+Lambda1*IHB+Lambda2*IHcB+Lambda3*A
+Lambda4*THB+2*Lambda5*VH))*P6+(mu+(1-u1)*beta5*(2*IB
+varUpsilon1*IHB+varUpsilon2*IcB+varUpsilon3*IHcB+
varUpsilon4*TB+varUpsilon5*THB)
+alpha+(1-u2)*tau+(1-u3)*psi*DB)*P7-A6;
m27 =-((1-u1)*beta2*S(2*IB+chi1*IcB+chi2*IHB+chi3*IHcB
+chi4*TB+chi5*THB)-(mu+(1-u1)*beta5(2*IB+varUpsilon1*IHB+
varUpsilon2*IcB+varUpsilon3*IHcB
+varUpsilon4*TB+varUpsilon5*THB)
+alpha+(1-u2)*tau
+(1-u3)*psi*DB))*P7-(1-u1)*beta5*(2*IB+varUpsilon1*IHB
+varUpsilon2*IcB
+varUpsilon3*IHcB+varUpsilon4*TB
+varUpsilon5*THB)*P3-(1-u3)*psi*DB*P8
-(1-u2)*tau*P9-A7;
```

```
m28 =-(1-u1)*beta5*varUpsilon*2*IB*P3-((1-u1)*beta2*chi2*S
-(1-u1)*beta5*Upsilon2*IB)*P7+(mu+delta2)*P8-A8;
m29 =(mu+delta3+(1-epsilon2)*varphi)*P9
    -(1-u1)*beta5*varUpsilon4*IB*P3
    -((1-u1)*beta2*chi4*S-(1-u1)*beta5*Upsilon4*IB)*P7-A9;
%===============Third backward sweep====================
m31 =(2*beta4*IH(j)+(1-u3(j))*(1-epsilon1)*DH-(beta1 *S(j)
    -u1(j)*beta1 *S(j)))*P1(j)-(1-u3(j))*(1-epsilon1)*DH*P2(j)
    -(2*IH(j)*(1-u1(j))+nu)*beta4*P3(j)+(nu*beta4*VH(j)
    -Gamma*beta1*V(j))*P6(j)-A1;
m32 = (beta4*Lambda3*IH(j)-(1-u1(j))*beta1*eta3*S(j))*P1(j)
+(delta1+mu)*P2(j)-((1-u1(j))*IH(j)+nu)*beta4*Lambda3*P3(j)
-(Gamma*beta1*eta3*V(j)-nu*beta4*Lambda3*VH(j))*P6(j)-A2;
m33 =(beta4*Lambda1*IH(j)-(1-u1(j))*beta1*eta1*S(j))*P1(j)
-((1-u1(j))*beta3*S(j)+((1-u1(j))*IH(j)+nu)*beta4*Lambda1
-((1-u2(j))*phi+(1-u3(j))*gamma+mu)
+(1-u1(j))*beta5*Upsilon1*IB(j))*P3(j)
-(1-u2(j))*phi*P4(j)-(1-u3(j))*gamma*P5(j)
-(Gamma*beta1*eta1*V(j)
-nu*beta4*Lambda1*VH(j))*P6(j)-((1-u1(j))*beta2*chi2*S(j)
-(1-u1(j))*beta5*Upsilon1 *IB(j))*P7(j)-A3;
\mathrm{m} 34=-\left((1-\mathrm{u} 1(\mathrm{j}))^{*}
    \text { beta1 }{ }^{*} \text { eta4 } *
    \mathrm{~S}(\mathrm{j})+(1-\text { epsilon2 })^{*}\right.
    \text { sigma-beta4*Lambda4*IH(j))*P1(j)}
    -\left((1-\mathrm{u} 1(\mathrm{j}))^{*}
    \text { beta3 }^{*} \text { Psi2 }^{*}
    \mathrm{~S}(\mathrm{j})+\left((1-\mathrm{u}
    1(\mathrm{j}))^{*}
```

```
\mathrm{IH}(\mathrm{j})+\mathrm{nu}\right)^{*}\right.
\text { beta4*Lambda4 } \left.+(1-\mathrm{u}
1(\mathrm{j}))^{*} \text { beta5*Upsilon5*IB}
(\mathrm{j})\right)^{*} \mathrm{P} 3(\mathrm{j})
+\left(\mathrm{mu}+\text{delta3}+(1-\text{epsilon2})
\text{sigma }{ }^{*} \mathrm{P} 4(\mathrm{j})\right
\text {-(Gamma*beta1*eta4*V(j)-nu*beta4*Lambda4*VH(j))
*P6(j)}-\left((1-\mathrm{u} 1(\mathrm{j}))^{*}
\text { beta2 }^{*}\text { chi5 }^{*} \mathrm{~S}
(\mathrm{j})-(1-\mathrm{u} 1(\mathrm{j}))^{*}
\text { beta5 }^{*} \text { Upsilon5 }{ }^{*}
\text { IB }(\mathrm{j})\right)^{*} \mathrm{P}7
(\mathrm{j})-\mathrm{A} 4 \text {; } \\
\mathrm{m}35=-\left((1-\mathrm{u} 1)^{*}
\text { beta1 }   { }^{*} \text { eta2 }{ }^{*}
\text { S-beta4 }{ }^{*} \text { Lambda2 }{ }
\mathrm{IH}\right){ }^{*} \mathrm{P}1
-\left((1-\mathrm{u} 1)^{*} \text { beta3*Psi1 }{ }
\mathrm{~S}\right \left.+\left((1-\mathrm{u} 1)^{*}
\mathrm{IH}+\mathrm{nu}\right)^{*} \text{beta4}^{*}
\text{Lambda2}+(1-\mathrm{u}1)^{*} \text{beta5}
\text { Upsilon3 }{ }^{*} \mathrm{IB}\right)^{*}
\mathrm{P}3 +(\mathrm{mu}+\mathrm{delta} 4)^{*}
\mathrm{P}5-\left(\mathrm{Gamma}^{*}\text{beta1}^{*}
\mathrm{eta2}^{*} \mathrm{~V}-\mathrm{nu}^{*}\right.
\text{beta4*Lambda2*VH)*P6}\text{-((1-u1)*beta2
*chi3*S-(1-u1)*beta5*Upsilon3*IB)*P7-A5; } \\
\mathrm{m}36=\text{beta4*Lambda5*P1-((1-u1)*IH+nu)*beta4*
Lambda5*P3}+\left(\mathrm{mu}
```

```
+\mathrm{nu}^{*}\text{ beta4}^{*}\left(\mathrm{IH}
+\mathrm{Lambda} 1^{*} \mathrm{IHB}+\mathrm{Lambda} 2^{*}
\mathrm{IHcB}+\mathrm{Lambda}3^{*} \mathrm{~A}\right.
\text{+Lambda4*THB+2*Lambda5*VH))*P6+(mu+(1-u1)*beta5*(2*IB}
\text{+varUpsilon1*IHB+varUpsilon2*IcB+varUpsilon3*IHcB
+varUpsilon4*TB}+\text{varUpsilon5*THB})
+\text{alpha}+(1-\mathrm{u}2)*\text{tau}+(1-\mathrm{u}3)*
\text { psi*DB)*P7-A6;} \\
\mathrm{m} 37=-\left((1-\mathrm{u}1)^{*}\text{beta2}^{*}
\mathrm{~S}^{*}\left(2*\mathrm{IB}+\mathrm{chi}1^{*}
\mathrm{IcB}+\mathrm{chi}2\mathrm{IHB}
+\mathrm{chi}3}\mathrm{IHcB}+
\mathrm{chi}4^{*}\mathrm{~TB}+
\mathrm{chi}5\mathrm{THB}\right)\right.
\text{-(mu+(1-u1)*beta5(2*IB+varUpsilon1
*IHB+varUpsilon2*IcB+varUpsilon3*IHcB}
\text{ +varUpsilon4*TB+varUpsilon5*THB)+alpha+(1-u2)*tau
+(1-u3)*psi*DB))*P7}\text{-(1-u1)*beta5(2*IB
+varUpsilon1*IHB+varUpsilon2*IcB+varUpsilon3*IHcB}
\text{varUpsilon4*TB+varUpsilon5*THB)*P3
-(1-u3)*psi*DB*P8-(1-u2)*tau*P9-A7;}
$\mathrm{m}38=-(1-\mathrm{u}1)*$beta5*varUpsilon*2*IB*P3
-((1-u1)*beta2*chi2*S-(1-u1)*beta5*Upsilon2*IB)*P7
+(mu+delta2)*P8-A8;
$\mathrm{m}39=(\mathrm{mu}+\mathrm{delta}3
+(1-\mathrm{epsilon} 2) *$ varphi $) * \mathrm{P}9
-(1-\mathrm{u} 1) *$ beta5 ${ }^{*}$ varUpsilon4
${ }^{*} \mathrm{IB} * \mathrm{P} 3$
-((1-u1)*beta2*chi4*S-(1-u1)*beta5*Upsilon4*IB)*P7-A9;
```

```
$\%==============$ Forth backward sweep============
\mathrm{m}41=\left(2^{*}\text{beta4}{}^{*}\mathrm{IH}
(\mathrm{j})+(1-\mathrm{u}3(\mathrm{j}))^{*}
(1-\text{epsilon1})^{*}\mathrm{DH}
-\left(\text{beta1}{}^{*}\mathrm{~S}(\mathrm{j})
-\mathrm{u}1(\mathrm{j})^{*}\text{beta1}{}^{*}\mathrm{~S}
(\mathrm{j})\right)\right)^{*} \mathrm{P} 1(\mathrm{j})
-(1-\mathrm{u} 3(\mathrm{j}))^{*}(1-\mathrm{epsilon1})^{*}
\mathrm{DH}^{*}\mathrm{P}2(\mathrm{j})-\left(2^{*}
\mathrm{IH}(\mathrm{j})^{*}(1-\mathrm{u}1(\mathrm{j}))
+\mathrm{nu}\right)^{*}$
beta4 $^{*} \mathrm{P} 3(\mathrm{j})$
+(nu*beta4*VH(j)-Gamma*beta1*V(j))*P6(j)-A1;
m42 =(beta4*Lambda3*IH(j)-(1-u1(j))*beta1*eta3*S(j))*P1(j)
+(delta1+mu)*P2(j)-((1-u1(j))*IH(j)+nu)*beta4*Lambda3*P3(j)
-(Gamma*beta1*eta3*V(j)
-nu*beta4*Lambda3*VH(j))*P6(j)-A2;
m43 =(beta4*Lambda1 *IH(j)-(1-u1(j))*beta1 *eta1 *S(j))*P1(j)
-((1-u1(j))*beta3*S(j)+((1-u1(j))*IH(j)+nu)*beta4*Lambda1
-((1-u2(j))*phi+(1-u3(j))*gamma+mu)
+(1-u1(j))*beta5*Upsilon1*IB(j))*P3(j)-(1-u2(j))*phi*P4(j)
-(1-u3(j))*gamma*P5(j)-(Gamma*beta1*eta1*V(j)
-nu*beta4*Lambda1*VH(j))*P6(j)-((1-u1(j))*beta2*chi2*S(j)
-(1-u1(j))*beta5*Upsilon1 *IB(j))*P7(j)-A3;
m44 = -((1-u1(j))*beta1*eta4*S(j)+(1-epsilon2)*sigma
-beta4*Lambda4*IH(j))*P1(j)-((1-u1(j))*beta3*Psi2*S(j)
+((1-u1(j))*IH(j)+nu)*beta4*Lambda4
+(1-u1(j))*beta5*Upsilon5*IB(j))*P3(j)+(mu+delta3
+(1-epsilon2)*sigma)*P4(j)-(Gamma*beta1*eta4*V(j)
```

```
-nu*beta4*Lambda4*VH(j))*P6(j)-((1-u1(j))*beta2*chi5*S(j)
-(1-u1(j))*beta5*Upsilon5*IB(j))*P7(j)-A4;
m45 = -((1-u1)*beta1*eta2*S-beta4*Lambda2*IH)*P1
-((1-u1)*beta3*Psi1*S+((1-u1)*IH+nu)*beta4*Lambda2
+(1-u1)*beta5*Upsilon3*IB)*P3+(mu+delta4)*P5
-(Gamma*beta1*eta2*V-nu*beta4*Lambda2*VH)*P6
-((1-u1)*beta2*chi3*S-(1-u1)*beta5*Upsilon3*IB)*P7-A5;
m46 = beta4*Lambda5*P1-((1-u1)*IH+nu)*beta4*Lambda5*P3
+(mu+nu*beta4*(IH+Lambda1*IHB+Lambda2*IHcB+ Lambda3*A
+Lambda4*THB+2*Lambda5*VH))*P6+(mu+(1-u1)*beta5*(2*IB
+varUpsilon1 *IHB+varUpsilon2*IcB
+varUpsilon3*IHcB+varUpsilon4*TB+varUpsilon5*THB)
+alpha+(1-u2)*tau+(1-u3)*psi*DB)*P7-A6;\\
m47 =-((1-u1)*beta2*S*(2*IB+chi1*IcB+chi2*IHB
+chi3*IHcB+chi4*TB+chi5*THB)
-(mu+(1-u1)*beta5(2*IB+varUpsilon1*IHB+varUpsilon2*IcB
+varUpsilon3*IHcB+varUpsilon4*TB+varUpsilon5*THB)
+alpha+(1-u2)*tau+(1-u3)*psi*DB))*P7
-(1-u1)*beta5(2*IB+varUpsilon1*IHB+varUpsilon2*IcB
+varUpsilon3*IHcB+varUpsilon4*TB+varUpsilon5*THB)*P3
-(1-u3)*psi*DB*P8-(1-u2)*tau*P9-A7;
 m48 =-(1-u1)*beta5*varUpsilon*2*IB*P3
 -((1-u1)*beta2*chi2*S-(1-u1)*beta5*Upsilon2*IB)*P7
 +(mu+delta2)*P8-A8;
m49 =(mu+delta3+(1-epsilon2)*varphi)*P9
-(1-u1)*beta5*varUpsilon4*IB*P3-((1-u1)*beta2*chi4*S
-(1-u1)*beta5*Upsilon4*IB)*P7-A9;
P1(j-1) = P1(j) - (h/6)*(m11 + 2*m21 + 2*m31 + m41);
P2(j-1) = P2(j) - (h/6)*(m12 + 2*m22 + 2*m32 + m42);
```

```
P3(j-1) = P3(j) - (h/6)*(m13 + 2*m23 + 2*m33 + m43);
P4(j-1) = P4(j) - (h/6)*(m14 + 2*m24 + 2*m34 + m44);
P5(j-1) = P5(j) - (h/6)*(m15 + 2*m25 + 2*m35 + m45);
P6(j-1) = P6(j) - (h/6)*(m16 + 2*m26 + 2*m36 + m46);
P7(j-1) = P7(j) - (h/6)*(m17 + 2*m27 + 2*m37 + m47);
P8(j-1) = P8(j) - (h/6)*(m18 + 2*m28 + 2*m38 + m48);
P9(j-1) = P9(j) - (h/6)*(m19 + 2*m29 + 2*m39 + m49);
end
```

Appendix C: Matlab code for stochastic differential equations

This appendix is related to section 4.3.4

Matlab program for $I_H(t)$

% Define the parameters

theta1 = 0.875; pi= 500 ; beta1 = 0.09; epsilon1 = 0.3; epsilon2 = 0.2; sigma = 0.81;

beta 4 = 0.1; mu = 0.00911; DH = 5; beta3 = 0.074; n = 1000;

% Define the time parameters

```
T=1; % Total time
dt = T / n; % Time step
N = n + 1;% Number of time steps
% set initial conditons and initialize arrays
to store stochastic process
IH_det = zeros(1, N);
IH_det(1) = 10;
S = zeros(1, N);
S(1) = 200;
THB = zeros(1, N);
THB(1) = 5;
num_sample_paths = 3;
IH_sto = zeros(num_sample_paths, N);
IH_sto(:, 1) = 10;
% Simulate the deterministic solution
using Euler method
for i = 2:N
IH_det(i) = IH_det(i - 1)+(theta1*pi+lambda1*S(i- 1)
+ (1 - epsilon2) *sigma * THB(i - 1)
-(lambda4+mu+(1-epsilon1)*DH)*IH_det(i-1))*dt;
end
%Simulate the stochastic solution
```

```
using Euler-Maruyama method
for j = 1:num_sample_paths
for i = 2:N
dW2 = sqrt(dt) * randn(1);
dW4 = sqrt(dt) * randn(1);
dW5 = sqrt(dt) * randn(1);
dW6 = sqrt(dt) * randn(1);
dW7 = sqrt(dt) * randn(1);
f2 =theta1*pi+lambda1*S(i-1)+(1-epsilon2)*sigma * THB(i-1)
+mu*IH_sto(j,i-1)+(1-epsilon1)*DH*IH_sto(j,i - 1);
IH_sto($\mathrm{j},\mathrm{i}$) = IH_sto( $\mathrm{j},
\mathrm{i}-1$ ) + (theta1 * pi+ lambda1 * S(i - 1)
+ (1 - epsilon2)*sigma*THB(i- 1)
- (lambda4+mu+(1-epsilon1)* DH) * IH_sto(j, i-1))*dt...
$-\operatorname{sqrt}(\max (0$, lambda1 $*
\mathrm{~S}(\mathrm{i}-1))*\mathrm{dW}2
+\operatorname{sqrt}(\mathrm{f} 2))*\mathrm{dW}4 \ldots
-\operatorname{sqrt}(\max (0,(1$- epsilon1)*DH *
IH_sto(j, i - 1))) * dW5
- sqrt(max(0, (1 - epsilon2) * sigma* THB(i - 1))) * dW6
- sqrt(max(0, lambda1 * S(i-1)
+ lambda3 * S(i-1) - theta1 * pi)) * dW7;
end
end
\% Plot the sample paths
time = 0:dt:T;
plot(time, IH_det, 'b--', 'LineWidth', 2);
hold on;
colors $=\{' \mathrm{r}$ ', 'k', 'g' $\}$;
```

```
for $\mathrm{j}=1$ :num_sample_paths
plot(time, IH_sto(j,:), colors $\{\mathrm{j}\}$,
'LineWidth', 2); \% Random color for each path
end
xlabel('Time'); ylabel('IH'); title('Deterministic and
Stochastic Solutions of SDE');
legend('Deterministic', 'Sample Path 1', 'Sample Path 2',
'Sample Path 3');
Matlab program for $I_{H B}(t)$
\% Define the parameters
rho $=0.116 ; \mathrm{pi}=20 ;$ beta $3=0.074;
\mathrm{nu}=0.008 ;$ beta $4=0.1 ;$ beta $5=0.075 ;$
phi $=0.17$; gamma $=0.2 ; \mathrm{mu}=0.00911 ;
\mathrm{n}=1000$;
\% Define the time parameters
$\mathrm{T}=1 ;$
\% Total time
dt = T / n;
% Time step
N = n + 1;
% Number of time steps
% Initialize arrays for S, VH, IH, and IB
S = zeros(1, N); VH = zeros(1, N); IH = zeros(1, N);
IB = zeros(1, N);
% Define the initial states with variability
S(1) = 500; IH(1) = 20; VH(1) = 10; IB(1) = 40;
% Set initial condition
IHB_det = zeros(1, N); IHB_det(1) = 20;
% Initial value of IHB for deterministic solution
```

```
    % Initialize arrays to store stochastic process
    num_sample_paths = 3;
    IHB_sto= zeros(num_sample_paths, N);
    IHB_sto(:, 1) = 20;
    % Initial value of IHB for stochastic solution
    % Simulate the deterministic solution
    using Euler method
    for i = 2:N
    IHB_det(i) = IHB_det(i-1) + ((1 - rho) * pi+
    lambda3 * S(i-1) + nu * lambda4* VH(i-1)
    +lambda4*IH(i-1)+lambda5*IB(i-1))*dt;
    end
    % Simulate the stochastic solution
    using Euler-Maruyama method
    for j = 1:num_sample_paths
    for i = 2:N
    dW9 = sqrt(dt) * randn(1);
    dW10 = sqrt(dt) * randn(1);
    dW11 = sqrt(dt) * randn(1);
    dW12 = sqrt(dt) * randn(1);
    dW13 = sqrt(dt) * randn(1);
$\mathrm{f}4=$lambda5$*\mathrm{IB}(\mathrm{i}-1)
+(1-\mathrm{rho})*\mathrm{pi}+\mathrm{nu}*$lambda4$*
\mathrm{VH}(\mathrm{i}-1)+\mathrm{mu} *$
IHB_sto(j, i-1) + phi * IHB_sto(j, i-1)
+ gamma * IHB_sto(j, i-1);
IHB_sto(j,i)$=$ IHB_sto(j,i-1)$+((1-$ rho $)*$pi
\\&+lambda3$*\mathrm{~S}(\mathrm{i}-1)+\mathrm{nu}*$
lambda4*VH(i-1)+lambda4*IH(i-1)+lambda5*IB(i-1))*dt ...
```

```
+sqrt(f4) * dW9 - sqrt(phi * IHB_sto(j, i-1)) * dW10
- sqrt(gamma * IHB_sto(j,i-1)) * dW11
- sqrt(nu * lambda4 * VH(i-1)) * dW12 ...
    - sqrt(lambda5 * IB(i-1)) * dW13;
end
end
\% Plot the results
time = 0:dt:T;
plot(time, IHB_det, 'k--', 'LineWidth', 2); hold on;
\% Plot stochastic solutions with different colors
colors $=\left\{\right.$ 'm ', $\left.{ }^{\prime}
\mathrm{c}^{\prime},{ }^{\prime}
\mathrm{r}^{\prime}\right\}$;
for $\mathrm{j}=1$ :num_sample_paths
plot(time, IHB_sto(j,:), colors $\{\mathrm{j}\}$,
'LineWidth', 2);
    end
xlabel('Time (Years)'); ylabel('I_\{HB\}');
title('Deterministic and Stochastic
Solutions of SDE');
legend('Deterministic', 'Sample Path 1', 'Sample Path 2',
'Sample Path 3');
Matlab program for $A(t)$
\% Define the parameters
epsilon1 = 0.8; DH = 5; mu = 0.00911; delta1 = 0.7114;
\% Define the time parameters
$\mathrm{T}=1 ;$
\% Total time
$\mathrm{n}=1000 ;$
```

```
\% Number of time steps
dt = T / n;
% Time step
N = n + 1;% Number of time steps
% Set initial condition
A_det = zeros(1, N); IH = zeros(1, N); A_det(1) = 5;
% Initial value of A for deterministic solution IH(1)= 10;
% Initialize arrays to store stochastic process
num_sample_paths = 3;
A_sto= zeros(num_sample_paths, N); A_sto(:,1) = 5;
% Initial value of A for stochastic solution
% Simulate the deterministic solution for i = 2:N
A_det(i) = A_det(i-1) + ((1
- epsilon1)*DH*IH(i-1) -(delta1 + mu)* A_det(i-1)) * dt;
end
% Simulate the stochastic solution
using Euler-Maruyama method
    for j = 1:num_sample_paths
    for i = 2:N
    dW5 = sqrt(dt) * randn(1);
    dW8 = sqrt(dt) * randn(1);
f3 = (1 - epsilon1)*DH*IH(i-1)+(delta1 + mu)*A_sto(j,i-1);
A_sto(j,i)= A_sto(j,i-1)+((1-epsilon1)*DH*IH(i-1)
-(delta1 + mu) * A_sto(j,i-1))*dt...
- sqrt((1 - epsilon1)* DH *IH(i-1))*dW5
+ sqrt(f3) * dW8;
end
end
% Plot the results
```

```
time = 0:dt:T; plot(time, A_det, 'r--', 'LineWidth', 2);
% Plot deterministic solution in black
hold on;
% Plot stochastic solutions with different colors
colors = { 'c', 'm', 'b' };
for j = 1:num_sample_paths
plot(time, A_sto(j,:), colors{j}, 'LineWidth', 2);
    end
xlabel('Time'); ylabel('A');
title('Deterministic and Stochastic Solutions of
    SDE');
legend('Deterministic', 'Sample Path 1', 'Sample Path 2',
'Sample Path 3');
Matlab program for IcB(t)
% Define the parameters
psi = 0.05; DB =0.9; mu = 0.00911; delta2 = 0.0028;
% Define the time parameters
T = 1; % Total time
n=1000;% Number of time steps
dt = T / n; % Time step
N = n + 1;% Number of time steps
% Initialize arrays to store stochastic process
IcB_det = zeros(1, N);
IB = zeros(1, N);
IcB_sto = zeros(num_sample_paths, N);
% Set initial condition
IcB_det(1) = 10;
IB(1) = 50;
num_sample_paths = 3;
```

```
IcB_sto(:,1) = 10;
% Simulate the deterministic solution
using Euler method
for i = 2:N
IB(i) = IB(i-1) + dt * (psi * DB * IB(i-1)
- (mu + delta2) * IB(i-1));
IcB_det(i) = IcB_det(i-1) + (psi * DB * IB(i-1)
- (mu + delta2) * IcB_det(i-1)) * dt;
end
% Simulate the stochastic solution
using Euler-Maruyama method
    for j = 1:num_sample_paths
    for i = 2:N
    dW24 = sqrt(dt) * randn(1);
    dW27 = sqrt(dt) * randn(1);
    % Update IB within the loop IB(i) = IB(i-1);
f9 = psi * DB * IB(i-1) + mu * IcB_sto(j,i-1)
+ delta2 * IcB_sto(j,i-1);
IcB_sto(j,i) = IcB_sto(j,i-1) + (psi * DB * IB(i-1)
- (mu + delta2) * IcB_sto(j,i-1)) * dt ...
- sqrt(psi * DB * IB(i-1)) * dW24 + sqrt(f9) * dW27;
    end
    end
    % Plot the deterministic results
time = 0:dt:T;
plot(time, IcB_det, 'b--','LineWidth',2);
hold on;
% Plot stochastic solutions with different colors
colors = {'y', 'k', 'g' };
```

```
for j = 1:num_sample_paths
plot(time, IcB_sto(j,:), colors{j}, 'LineWidth', 2);
end
xlabel('Time'); ylabel('I_{cB}');
title('Deterministic and Sample paths of
IcB(t)');
legend('Deterministic', 'Sample Path 1',
'Sample Path 2', 'Sample Path 3');
Matlab Program for I HcB (t)
% Define the parameters
gamma = 0.2; mu = 0.00911; delta4 = 0.42;
% Define the time parameters
T=1; % Total time
$\mathrm{n}=1000$; \% Number of time steps
$\mathrm{dt}=\mathrm{T} / \mathrm{n}$; \% Time step
$\mathrm{N}=\mathrm{n}+1$; \% Number of time steps
\% Set initial condition
IHcB_det = zeros(1, N);
$\mathrm{B}=\operatorname{zeros}(1, \mathrm{~N}) ;$
IHcB_det(1) =5;\\
% Initial value of IHcB for
deterministic solution
$\operatorname{IHB}(1)=10$;
\% Initialize arrays to store stochastic process
num_sample_paths = 3;
IHcB_sto = zeros(num_sample_paths, N);
IHcB_sto(:,1) =5;\\
\% Initial value of IHcB for
stochastic solution
```

```
\% Simulate the deterministic solution using Euler method
for $\mathrm{i}=2: \mathrm{N}$
IHcB_det(i)$=$ IHcB_det(i-1) $+($ gamma $*$ IHB(i-1)$
-($ mu + delta4 $) *$ IHcB_det(i-1)) * dt;
end
\% Simulate the stochastic solution
using Euler-Maruyama method
for $\mathrm{j}=1$ :num_sample_paths
for $\mathrm{i}=2: \mathrm{N}$
$\mathrm{dW}11=\operatorname{sqrt}(\mathrm{dt}) *
\operatorname{randn}(1);
$dW15 $=\operatorname{sqrt}(\mathrm{dt})$ * randn(1);
\% Update IHB within the loop
$\mathrm{IHB}(\mathrm{i})=\mathrm{IHB}(\mathrm{i}-1)$;
\% For this example, IHB is not changing
f6 $=$ gamma $^{*}$ IHB(i-1) +mu * IHcB_sto(j,i-1)
+delta4 * IHcB_sto(j,i-1);
IHcB_sto( $\mathrm{j}, \mathrm{i}$ ) $=$ IHcB_sto( $\mathrm{j},
\mathrm{i}-1$ ) $+($ gamma $*$ IHB(i-1) $
-(\mathrm{mu}+$ delta4) $*$ IHcB_det(i-1))*dt ...
- sqrt(gamma * IHB(i-1)) * dW11 + sqrt(f6) * dW15;
end
    end
% Plot the results
time = 0:dt:T; plot(time, IHcB_det, 'k', 'LineWidth', 2);
% Plot deterministic solution in black
    hold on;
% Plot stochastic solutions with different colors colors
    = {'r', 'g', 'b' };
```

```
for j = 1:num_sample_paths plot(time, IHcB_sto(j,:),
colors{j}, 'LineWidth',2);
end
xlabel('Time'); ylabel('I_{HcB}');
title('Deterministic and Stochastic Solu-
tions of SDE');
legend('Deterministic', 'Sample Path 1',
'Sample Path 2', 'Sample Path 3');
Matlab program for }\mp@subsup{I}{B}{}(t
% Define the parameters
    theta2 = 0.058; pi = 5000; beta2 = 0.2; mu = 0.00911;
    beta = 0.075; alpha=0.95; tau = 0.25;
psi = 0.05; DB =1; beta1 = 0.09; beta3 = 0.074; theta 1 = 0.875;
n = 1000;
% Define the time parameters
T=1;% Total time
dt = T / n; % Time step
N = n + 1;% Number of time steps
% Initialize arrays for S and IB
S = zeros(1, N);
% Define the initial state with variability
S(1) = 2000;
% Set initial condition
IB_det = zeros(1, N);
IB_det(1) = 100;
% Initial value of IB for deterministic solution
% Initialize arrays to store stochastic process
    num_sample_paths = 3;
    IB_sto = zeros(num_sample_paths, N);
```

```
    IB_sto(:, 1) = 100; % Initial value of
IB for stochastic solution
% Simulate the deterministic solution
    for i = 2:N
IB_det(i) = IB_det(i-1) + (theta2*pi_val + lambda2*S(i-1)
-(mu+lambda5+alpha+tau+psi*DB)*IB_det(i-1))* dt;
    end
% Simulate the stochastic solution
using Euler-Maruyama method
    for j = 1:num_sample_paths
    for i = 2:N
    dW13 = sqrt(dt) * randn(1);
    dW21 = sqrt(dt) * randn(1);
    dW22 = sqrt(dt) * randn(1);
    dW23 = sqrt(dt) * randn(1);
    dW24 = sqrt(dt) * randn(1);
    dW25 = sqrt(dt) * randn(1);
    dW26 = sqrt(dt) * randn(1);
f8 = (lambda1 + lambda3) * S(i-1)+(theta1 + theta2)*pi
+ (lambda5 + psi* DB + tau + alpha + mu) * IB_sto(j, i-1);
IB_sto(j, i) = IB_sto(j, i-1) + (theta2*pi+ lambda2*S(i-1)
-(mu + lambda5 +alpha + tau + psi *DB)*IB_sto(j, i-1))* dt ...
- sqrt(lambda1*S(i-1)+lambda3*S(i-1))*dW21
+ sqrt(theta1*pi_val)*dW22
-sqrt(max(0,lambda5*IB_sto(j,i-1)))*dW13+sqrt(f8)*dW23 ...
- sqrt(max(0,psi * DB * IB_sto(j, i-1)))*dW24
- sqrt(max(0,tau * IB_sto(j,i-1)))*dW25
-sqrt(max(0,alpha * IB_sto(j, i-1))) * dW26;
end
```

```
    end
% Plot the deterministic results
    time = 0:dt:T;
plot(time, IB_det, 'k--', 'LineWidth', 2);
    hold on;
% Plot stochastic solutions with different colors
    colors = {'r', 'y', 'b'};
    for j = 1:num_sample_paths
plot(time, IB_sto(j,:), colors {j}, 'LineWidth', 2);
    end
xlabel('Time (years)'); ylabel('I_B');
title('Deterministic and Stochastic So-
lutions of SDE');
legend('Deterministic', 'Sample Path 1',
'Sample Path 2', 'Sample Path 3');
Matlab Program for THB(t)
% Define the parameters
phi=0.17; epsilon2 = 0.96; sigma = 0.807; mu = 0.00911;
delta3 =0.0284;
% Define the time parameters
    T = 1; % Total time
    n=1000;% Number of time steps
    dt = T / n; % Time step
    N = n + 1;% Number of time steps
% Set initial condition
    THB_det = zeros(1, N); IHB=zeros(1, N); THB_det(1) =10;
% Initial value of THB for deterministic solution
IHB(1) = 20;
% Initialize arrays to store stochastic process
```

```
    num_sample_paths = 3;
THB_sto = zeros(num_sample_paths, N);
THB_sto(:,1)=10;
% Initial value of A for stochastic solution
% Simulate the deterministic solution
for i = 2:N
THB_det(i) = THB_det(i-1)+(phi*IHB(i-1)
-(mu+delta3+(1-epsilon2)*sigma)*THB_det(i-1))*dt;
end
% Simulate the stochastic solution
using Euler-Maruyama method
for j = 1:num_sample_paths
for i = 2:N
dW6 = sqrt(dt) * randn(1);
dW10 = sqrt(dt) * randn(1);
dW14 = sqrt(dt) * randn(1);
f5 = (1 - epsilon2)*sigma * THB_sto(i-1) + phi*IHB(i-1)+
(mu+delta3)*THB_sto(i-1);
THB_sto(j,i) = THB_sto(j,i-1) + (phi*IHB(i-1)-(mu+delta3+
(1-epsilon2)*sigma)*THB_det(i-1))*dt ...
+sqrt((1 - epsilon2)*sigma *THB_sto(i-1))*dW6
-sqrt(phi*IHB(i-1))*dW10+sqrt(f5)*dW14;
end
end
% Plot the deterministic results using Euler method
time = 0:dt:T;
plot(time, THB_det, 'k--', 'LineWidth', 2);
hold on;
% Plot stochastic solutions with different colors
```

```
colors = {’r’, ’b’, ’g’ }; for j = 1:num_sample_paths
plot(time, THB_sto(j,:), colors{j}, ’LineWidth’, 2);
end
xlabel(’Time’);
ylabel(’Number of treated co-infected individuals’);
title(’Deterministic and sample paths of THB(t)’);
legend(’Deterministic’, ’Sample Path 1’,
’Sample Path 2’, ’Sample Path 3’);
```

Appendix D: Python code for PRCC/LHS results

```
# Install required packages
!pip install SALib numpy matplotlib scipy
import numpy as np
from SALib.sample import latin
import matplotlib.pyplot as plt
from scipy import stats
# Set global font to Times New Roman size 12
plt.rcParams.update({
    'font.family': 'serif',
    'font.serif': 'Times New Roman',
    'font.size': 12,
    'axes.titlesize': 12,
    'axes.labelsize': 12,
    'xtick.labelsize': 10,
    'ytick.labelsize': 10,
    'figure.titlesize': 12
})

# 1. Define the epidemic model with the complex R0 expression
def calculate_R0(params):
    """
    Calculates R0,S using the complex expression:\\
    R0,S = (pi/mu) * [
        (beta1*theta5)/(mu + (1-epsilon1)D_H) +
        (beta2*theta5)/(mu+alpha + tau + varphi*D_B) +
        (beta3*theta5)/(phi + gamma + mu) +
        (Gamma*beta1*theta3)/(mu + v*beta4*Lambda5)
    ]
```

```
    """    \\
    # Unpack parameters in the correct order
    pi, mu, beta1, theta5, epsilon1, D_H, beta2, alpha, tau,
    psi, D_B, beta3, phi, gamma, Gamma, theta3, v, beta4,
    Lambda5 = params\\
    # Calculate each term separately\\
    term1=(beta1*theta5)/(mu+(1-epsilon1)*D_H)\\
    term2=(beta2*theta5)/(mu+alpha+tau+psi*D_B)\\
    term3=(beta3*theta5)/(phi+gamma+mu)\\
    term4=(Gamma*beta1*theta3)/(mu+v*beta4*Lambda5)\\
# Calculate R0,S\\
    R0 = (pi / mu) * (term1 + term2 + term3 + term4)\\

    return R0

# 2. Setup sensitivity analysis problem with realistic ranges\\
problem = {
    'num_vars': 19,\\
    'names': [
        'pi', 'mu', 'beta_{1}', 'theta_{5}',
        'epsilon_{1}', 'D_{H}', 'beta_{2}','alpha',
        'tau', 'varphi','D_{B}', 'beta_{3}',
        'phi', 'gamma', 'Gamma', 'theta_{3}',
        'v','beta_{4}', 'Lambda_{5}'
    ],\\
    'bounds': [
    [0.1, 1.0],     \pi: Birth rate\\
    [0.001, 0.1],   \mu: Natural death rate\\
    [0.1, 0.9],     \beta_{1}: Transmission rate 1\\
```

```
    [0.5, 1.0],     \theta_{5}: Probability factor\\
    [0.1, 0.9],     \epsilon_{1}: Intervention efficacy\\
    [0.01, 1.0],     D_H: HIV-related mortality\\
    [0.1, 0.9],      \beta_{2}: Transmission rate 2\\
    [0.01, 0.2],     \alpha: Disease-induced mortality\\
    [0.01, 0.1],     \tau: Treatment rate\\
    [0.01, 0.1],     \varphi: Mortality modifier\\
    [0.01, 0.9],     D_B: HBV-related mortality\\
    [0.1, 0.9],      \beta_{3}: Transmission rate 3\\
    [0.01, 0.1],    \phi: Recovery rate\\
    [0.05, 0.3],    \gamma: Recovery rate\\
    [0.1, 1.0],     \Gamma: Population fraction\\
    [0.5, 1.0],     \beta_{3}: Probability factor\\
    [0.1, 0.9],     v: Vaccination rate\\
    [0.1, 0.9],     \beta_{4}: Transmission rate 4\\
    [0.01, 0.1]     \Lambda_{5}: Mortality rate
    ]
}
#3.Generate parameter samples using Latin Hypercube Sampling\\
param_values = latin.sample(problem, 2000)
# Increased samples for better accuracy
# 4. Run model for all parameter sets\\
R0_values = np.array([calculate_R0(params)
for params in param_values])
# 5. Calculate PRCC manually
def calculate_prcc(parameters, output):
    """Compute Partial Rank Correlation Coefficients"""
# Rank transform all parameters and output
ranked_params = np.apply_along_axis(stats.rankdata, 0,
```

```
parameters)
ranked_output = stats.rankdata(output)
    prcc_results = []
    conf_intervals = []
for i in range(parameters.shape[1]):
        # Partial out other parameters
        other_params = np.delete(ranked_params, i, axis=1)
# Add constant term for regression
X = np.column_stack([np.ones(len(other_params)),
other_params])
# Regress current parameter against others
coeffs_param = np.linalg.lstsq(X, ranked_params[:, i],
rcond=None)[0]
residuals_param = ranked_params[:, i] - X.dot(coeffs_param)
# Regress output against others
coeffs_out = np.linalg.lstsq(X, ranked_output, rcond=None)[0]
        residuals_out = ranked_output - X.dot(coeffs_out)
# Calculate correlation between residuals
prcc, p_value = stats.pearsonr(residuals_param, residuals_out)
prcc_results.append(prcc)
# Calculate 95% confidence interval
        n = len(residuals_param)
        se = 1 / np.sqrt(n - 3)
        # Standard error using Fisher transformation
        z = stats.norm.ppf(0.975)  # 1.96 for 95% CI
        conf_intervals.append(z * se)
    return np.array(prcc_results), np.array(conf_intervals)
# 6. Perform sensitivity analysis
prcc, conf_intervals = calculate_prcc(param_values, R0_values)
```

```
# 7. Sort results by absolute PRCC value
sorted_idx = np.argsort(np.abs(prcc))[::-1]
sorted_names = [problem['names'][i] for i in sorted_idx]
sorted_prcc = prcc[sorted_idx]
sorted_conf = conf_intervals[sorted_idx]
# 8. Create the plot with parameters on x-axis
plt.figure(figsize=(14, 7), dpi=300)
# Create positions for bars
x_pos = np.arange(len(sorted_names))
# Plot PRCC values with error bars
bars = plt.bar(x_pos, sorted_prcc, yerr=sorted_conf,
        capsize=5, alpha=0.8, color='royalblue',
        error_kw={'elinewidth': 1.5, 'capthick': 1.5})
# Add horizontal lines at significance thresholds
plt.axhline(0, color='black', linewidth=0.8, linestyle='-')
plt.axhline(0.2, color='gray', linewidth=0.5, linestyle='--',
alpha=0.7)
plt.axhline(-0.2, color='gray', linewidth=0.5, linestyle='--',
alpha=0.7)
plt.axhline(0.3, color='gray', linewidth=0.5, linestyle=':',
alpha=0.7)
plt.axhline(-0.3, color='gray', linewidth=0.5, linestyle=':',
alpha=0.7)
# Set axis labels
plt.xlabel('Model Parameters', fontsize=12, labelpad=10)
plt.ylabel('Partial Rank Correlation Coefficient (PRCC)',
fontsize=12, labelpad=10)
# Customize plot appearance
plt.xticks(x_pos, sorted_names, rotation=45, ha='right',
```

```
rotation_mode='anchor')
plt.title('Sensitivity Analysis of $R_{0,S}$',
fontsize=12, pad=15)
plt.grid(axis='y', linestyle='--', alpha=0.3)
# Set axis limits with padding
plt.ylim(min(sorted_prcc) - 0.15, max(sorted_prcc) + 0.15)
# Add values above/below bars
for i, v in enumerate(sorted_prcc):
    y_pos = v + 0.02 if v >= 0 else v - 0.05
    va = 'bottom' if v >= 0 else 'top'
    plt.text(i, y_pos, f'{v:.2f}',
        ha='center', va=va,
        fontsize=9, rotation=0,
        bbox=dict(facecolor='white', alpha=0.7,
        edgecolor='none', boxstyle='round,pad=0.1'))
# Adjust layout to prevent clipping
plt.tight_layout()
plt.subplots_adjust(top=0.92, bottom=0.25)
# 9. Print parameter significance
print("\nTop influential parameters for $R_{0,S}$:")
print("| PRCC | > 0.5: Very strong influence")
print("| PRCC | > 0.3: Strong influence")
print("| PRCC | > 0.2: Moderate influence\n")
for i in range(len(sorted_names)):
    influence = ""
    abs_prcc = abs(sorted_prcc[i])
    if abs_prcc > 0.5:
        influence = "***** VERY STRONG"
    elif abs_prcc > 0.3:
```

```
        influence = "**** STRONG"
    elif abs_prcc > 0.2:
        influence = "*** MODERATE"
    else:
        influence = "** WEAK"
direction = "increases R0" if sorted_prcc[i] > 0 else
"decreases R0"
print(f"{sorted_names[i]}: {sorted_prcc[i]:.4f} ±
{sorted_conf[i]:.4f} - {influence} ({direction})")
# Save as high-quality PDF
plt.savefig('R0_Sensitivity_Analysis.pdf', dpi=300,
bbox_inches='tight'), plt.show()
```

Appendix E: Research permits/licences

REPUBLIC OF KENYA

NATIONAL COMMISSION FOR SCIENCE,TECHNOLOGY & INNOVATION

Ref No: **254974**

Date of Issue: **05/April/2024**

RESEARCH LICENSE

This is to Certify that Mr.. Mirgichan KHOBOCHA JAMES of Meru University of Science and Technology, has been licensed to conduct research as per the provision of the Science, Technology and Innovation Act, 2013 (Rev.2014) in Meru on the topic: MODELLING THE IMPACT OF CLINICAL AND NON-CLINICAL OPTIMAL CONTROL STRATEGIES ON DYNAMICS OF HIV AND HBV CO-INFECTION for the period ending : 05/April/2025.

License No: **NACOSTI/P/24/34055**

254974

Applicant Identification Number

Director General
NATIONAL COMMISSION FOR SCIENCE,TECHNOLOGY & INNOVATION

Verification QR Code

NOTE: This is a computer generated License. To verify the authenticity of this document, Scan the QR Code using QR scanner application.

See overleaf for conditions

Appendix F: MIRERC Clearance

MERU UNIVERSITY INSTITUTIONAL RESEARCH & ETHICS REVIEW COMMITTEE
(MIRERC)
Email: mirerc@must.ac.ke ***Website:*** ***https://research.must.ac.ke/research-ethics/***

REF: MU/1/39/28 Vol.3 (033) Date: 20th May, 2024

TO: **Mirgichan Khobocha James**, (PhD. Applied Mathematics)
Dr. Stephen Karanja, Dr.Robert Muriungi, Dr. Cyrus Gitonga Ngari

Dear Sir/madam

RE: Modeling The Impact of Clinical and Non-Clinical Optimal Control Strategies On Dynamics of HIV and HBV Co-Infection

This is to inform you that ***MIRERC*** has reviewed and approved your above research proposal. Your application approval number is ***MIRERC012/2024.*** The approval period is ***20th May, 2024– 19th May, 2025.***

This approval is subject to compliance with the following requirements;

i. Only approved documents including (informed consents, study instruments, MTA) will be used
ii. All changes including (amendments, deviations, and violations) are submitted for review and approval by ***MIRERC***.
iii. Death and life-threatening problems and serious adverse events or unexpected adverse events whether related or unrelated to the study must be reported to ***MIRERC*** within 72 hours of notification
iv. Any changes, anticipated or otherwise that may increase the risks or affected safety or welfare of study participants and others or affect the integrity of the research must be reported to ***MIRERC*** within 72 hours
v. Clearance for export of biological specimens must be obtained from relevant institutions.
vi. Submission of a request for renewal of approval at least 60 days prior to expiry of the approval period. Attach a comprehensive progress report to support the renewal.
vii. Submission of an executive summary report within 90 days upon completion of the study to ***MIRERC***.

You may also be required to obtain a research license from National Commission for Science, Technology and Innovation (NACOSTI), visit: https://research-portal.nacosti.go.ke and also obtain any other clearances needed for your study.

Yours sincerely

Prof. Peter Masinde, Ph.D.
Chairman, MIRERC

MUST IS ISO 9001:2015 and ISO/IEC 27001:2013 CERTIFIED

Appendix G: Publication One

Heliyon 11 (2025) e41744

Contents lists available at ScienceDirect

Heliyon

journal homepage: www.cell.com/heliyon

Research article

Mathematical modeling and simulation of hepatitis B transmission dynamics with passive immunity and control strategies

James Khobocha Mirgichan [a,*], Cyrus Gitonga Ngari [b], Stephen Karanja [c], Robert Muriungi [c]

[a] Meru University of Science and Technology, P.O.BOX 26, Marsabit, Kenya
[b] Kirinyaga University, P.O.BOX 143-10300, Kerugoya, Kenya
[c] Meru University of Science and Technology, P.O.BOX 972-60200, Meru, Kenya

ARTICLE INFO

Keywords:
Hepatitis B transmission dynamics
Passive immunity
Control strategies
Mathematical modeling
Vaccination impact
Reproduction number

ABSTRACT

Hepatitis B Virus (HBV) is a continued threat to mankind's health killing hundreds of thousands of people every year and thus calls for control and prevention measures to be put in place. This research constructs a deterministic mathematical model to capture the transmission dynamics of HBV and embracing the control measures including universal immunization of the infants at birth, screening, as well as treatment of the both the acute and chronic cases. We employ the NGM technique to estimate the control reproduction number Rc and also study the stability of the IFE. The study findings revealed the fact that the IFE is both locally and globally asymptotic stability if $Rc < 1$. The results derived from analytical and numerical analysis revealed that having higher vaccination coverage, better screening and more efforts invested in the treatment active reduce HBV cases. Also, exposure to past immunities through passive action on the part of newborns has a significant responsibility to bear concerning the management of HBV transference. Therefore, our research findings indicate that multiple interventions can go a long way towards eliminating the ravages of HBV in the general population and consequently enhancing the general wellbeing of the population. The future work includes taking co-infections, different degrees of compliance, and age structured models into account for the elaboration of the study. Some of the limitations include: A Constant mixing volume is assumed while this may not be true throughout the entire volume Mixing parameters are also assumed to be constant while in reality they may not be so.

1. Introduction

Hepatitis B remains an enormous concern for the world's health with millions of people affected by this viral infection. Understanding the intricate dynamics of Hepatitis B transmission is crucial for developing effective clinical control interventions and evaluating the potential impact of passive immunity strategies. This study delves into the intricate world of Hepatitis B transmission, employing mathematical modeling and simulation to uncover valuable insights. Hepatitis B virus (HBV) is a highly contagious pathogen transmitted mainly through coming into contact with infected blood or bodily fluids. The virus can lead to acute or chronic infections, and its effects may vary from minor sickness to serious liver damage, including cirrhosis and hepatocellular carcinoma.

* Corresponding author.
E-mail addresses: Kaks.mirgichan@gmail.com (J.K. Mirgichan), ngaricyrus15@gmail.com (C.G. Ngari), skaranja@must.ac.ke (S. Karanja), rgitunga@must.ac.ke (R. Muriungi).

https://doi.org/10.1016/j.heliyon.2025.e41744
Received 20 January 2024; Received in revised form 3 January 2025; Accepted 6 January 2025
Available online 7 January 2025

Appendix H: Publication Two

Asian Research Journal of Mathematics

Volume 20, Issue 7, Page 49-69, 2024; Article no.ARJOM.119562
ISSN: 2456-477X

Modeling HIV-HBV Co-infection Dynamics: Stochastic Differential Equations and Matlab Simulation with Euler-Maruyama Numerical Method

Mirgichan Khobocha James [a*], Cyrus Gitonga Ngari [b], Stephen Karanja [a] and Robert Muriungi [a]

[a] Department of Mathematics, School of Pure and Applied Sciences, Meru University of Science and Technology, P.O.BOX 972-60200, Meru, Kenya.
[b] Department of pure and Applied Sciences, Kirinyaga University, Kerugoya, Kenya.

Authors' contributions

This work was carried out in collaboration among all authors. All authors read and approved the final manuscript.

Article Information

DOI: https://doi.org/10.9734/arjom/2024/v20i7811

Open Peer Review History:
This journal follows the Advanced Open Peer Review policy. Identity of the Reviewers, Editor(s) and additional Reviewers, peer review comments, different versions of the manuscript, comments of the editors, etc are available here: https://www.sdiarticle5.com/review-history/119562

Original Research Article

Received: 05/05/2024
Accepted: 07/07/2024
Published: 11/07/2024

Abstract

HIV/AIDS and Hepatitis B co-infection complicates population dynamics and brings forth a wide range of clinical outcomes which makes it a difficult situation for public health. In particular designing treatment plans for the co-infection. A Stochastic Differential Equation (SDE) model is a special class of a stochastic model with continuous parameter space and continuous state space. Deterministic model lacks randomness while an

**Corresponding author: Email: kaks.mirgichan@gmail.com;*

Cite as: *James, Mirgichan Khobocha, Cyrus Gitonga Ngari, Stephen Karanja, and Robert Muriungi. 2024. "Modeling HIV-HBV Co-Infection Dynamics: Stochastic Differential Equations and Matlab Simulation With Euler-Maruyama Numerical Method". Asian Research Journal of Mathematics 20 (7):49-69. https://doi.org/10.9734/arjom/2024/v20i7811.*

Appendix I : Plagiarism Report

DrillBit

The Report is Generated by DrillBit Plagiarism Detection Software

Submission Information

Author Name	MIRGICHAN KHOBOCHA JAMES
Title	DETERMINISTIC AND STOCHASTIC MODELING OF CLINICAL AND NON-CLINICAL DYNAMICS OF HIV-HBV CO-INFECTION WITH OPTIMALITY
Paper/Submission ID	4364105
Submitted by	mmusungu@must.ac.ke
Submission Date	2025-09-15 15:11:32
Total Pages, Total Words	283, 76045
Document type	Dissertation

Result Information

Similarity **4 %**

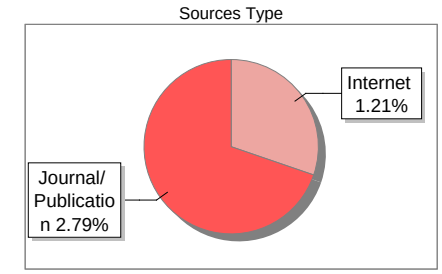

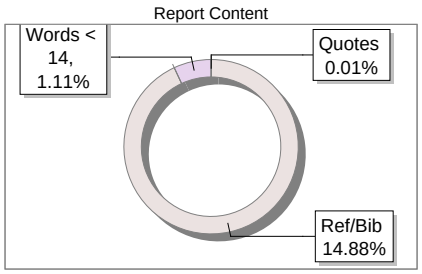

Exclude Information

Quotes	Not Excluded
References/Bibliography	Excluded
Source: Excluded < 14 Words	Not Excluded
Excluded Source	**0 %**
Excluded Phrases	Not Excluded

Database Selection

Language	English
Student Papers	Yes
Journals & publishers	Yes
Internet or Web	Yes
Institution Repository	Yes

A Unique QR Code use to View/Download/Share Pdf File